

CENTRE FOR COLD OCEAN RESOURCES ENGINEERING

Inversion of Electrical Resistivity
Data to Identify Granular
Resources in Arctic Waters. A

Contract Report

Prepared for
Supply and Services Canada

Prepared by
C-CORE - Centre for Cold Ocean Resources Engineering



C-CORE Contract 94 - C5
March 1994



Centre for Cold Ocean Resources Engineering
Memorial University of Newfoundland
St. John's, NF, A1B 3X5, Canada
Tel. (709) 737-8354 Fax. 709-737-4706

The correct citation for this report is :

Scott, W.J., English, G.M., and Smyth, S.J., 1994, Inversion of Electrical Resistivity Data to Identify Granular Resources in Arctic Waters. Contract report prepared for Supply and Services Canada, C-CORE Contract 94 - C5.

Table of Contents

INTRODUCTION	1
RESISTIVITY MEASUREMENT	2
INTERPRETATION OF RESISTIVITY SOUNDING DATA	3
INVERSION	4
1D Inversion	5
Iterative Inversion	6
Inversion with Ridge Regression	6
Monte Carlo Inversion	9
Direct Interpretation	10
Direct Interpretation (Basokur)	10
Direct Calculation (Zohdy)	11
Error of Fit of Inversion	12
Reliability of Inverted Models	13
Equivalence	14
Example of Equivalence (Scott and MacKay, 1977)	14
APPRAISAL OF INVERSION ROUTINES	18
COMPARISON OF PERFORMANCE OF INVERSION ROUTINES	22
Running inversions, Beaufort Sea Data	24
Fiducial marks	24
Line 10D	25
Line 22A	26
Line 44A	30
Line 45A	34
Running Inversions, Bay of Fundy Data	38
Line J1S	40
Line J2N	41
Line J2S	43
Running Inversions, Conception Bay Data	44
Discussion of Running Inversions	47
Influence of Starting Models	47
Inversions with Fixed Layer Thicknesses	51
Test 1	51
Test 2	53
Test 3	54
Test 4a	54
Test 4b	55
Trials on Theoretical Models	56
SUMMARY AND DISCUSSION	62
REFERENCES	66
APPENDIX A	
APPENDIX B	

LIST OF FIGURES

(Figures marked with * are in pocket).

- Figure 1: Common arrays for measuring electrical resistivity.
- Figure 2: Schematic illustration of the inversion process.
- Figure 3: Resistivity sounding and interpreted resistivity-depth curve, Atkinson Point, Tuktoyaktuk Peninsula, NWT.
- Figure 4: Resistivity sounding and interpreted resistivity-depth curves, Banook Lake, Tuktoyaktuk Peninsula, NWT.
- Figure 5: Resistivity sounding and resistivity-depth curve, IOL Lake, Tuktoyaktuk Peninsula, NWT.
- Figure 6: Location of survey lines, 1991 MICRO-WIP survey, Richards Island, Beaufort Sea, NWT.
- Figure 7: Fitting errors on Line 10D for three inversion routines.
- Figure 8: Fitting errors on Line 22A for three inversion routines.
- Figure 9: Fitting errors on Line 44A, for three inversion routines.
- Figure 10: Fitting errors on Line 45A, for three inversion routines.
- Figure 11: Location of survey lines, Bay of Fundy.
- Figure 12*: Results of inversions on Line J1S.
- Figure 13: Fitting errors on Line J1S, for three inversion routines.
- Figure 14*: Results of inversions on Line J2N.
- Figure 15: Fitting errors on Line J2N, for three inversion routines.
- Figure 16*: Results of inversions on Line J3S.
- Figure 17: Fitting errors on Line J3S, for three inversion routines.
- Figure 18: Location of survey line, Conception Bay.
- Figure 19*: Results of inversions on survey line, Conception Bay.
- Figure 20: Fitting errors on Conception Bay line.
- Figure 21: Fitting errors on Line 45A for Davis run with and without correction of the error at Fid 5253.
- Figure 22: Sounding curves on Line 45A from beginning, middle and end of line.
- Figure 23: Distribution of fitting errors along Line 10D, for various approaches to multi-set inversion with the Davis routine.

LIST OF TABLES

Table I: Dimensions of the Hardy logarithmic cable.

Table II: Average fitting errors for Beaufort Sea lines.

Table III: Comparison of inversions, Beaufort Sea Data, Line 10D, 10 m dipole spacing.

Table IV: Comparison of inversions, Beaufort Sea Data, Line 22A, 25 m dipole spacing.

Table V: Comparison of inversions, Beaufort Sea Data, Line 44A, 25 m dipole spacing.

Table VI: Comparison of inversions, Beaufort Sea Data, Line 45A, 25 m dipole spacing.

Table VII: Average Fitting errors for Bay of Fundy lines.

Table VIII: Starting models and first fits, Davis routine, Lines 22A and Line 45A.

Table IX: Summary of tests with 7 fixed layers, Davis and ResixIP.

Table X: Fitting errors on Line 10D, for seven-layer inversions with Davis and ResixIP, with the three-layer ResixIP errors shown for comparison.

Table XI: Schlumberger sounding from Basokur.

Table XII: Inversion with ResixIP of solution by Basokur of sounding of Table XI.

Table XIIIa: Inversion with ResixIP, all layers free.

Table XIIIb: Inversion with ResixIP, first layer fixed.'

Table XIV: Inversion with ResixIP with all layers free.

INTRODUCTION

The purpose of this report is to describe the results of a study of inversion of resistivity data obtained with the MICRO-WIP marine electrical survey system. In the Beaufort Sea there is a requirement to process marine electrical resistivity data continuously during survey to determine the resistivity of shallow sub-surface layers. Resistivity values can be used to indicate whether coarse-grained materials are present, and whether permafrost lies within the depths of interest. Since such surveys are often done just before sampling and/or dredging of aggregate, there is a need for a method which gives a rapid interpretation.

The approach taken in interpretation of resistivity data in general is to invert the data in terms of a layered sub-surface. Interpretation is usually a two-step process. First an automated inversion is performed, then the inverted model is adjusted to improve the fit, and finally the interpreted model is appraised for the range of equivalent models which could fit the data with the same error. This is generally a slow process because of the number of soundings to be interpreted.

Rapid analysis of survey data on board the vessel during survey requires automated inversion with no intervention by the operator. This requirement is unique to marine survey, as it is rare in terrestrial work to obtain sounding data at a rate which precludes interactive interpretation. While an automated inversion may not yield the final interpretation, it should provide reasonably reliable interpreted models.

This study was supported by the Atlantic Canada Opportunities Agency, and by the Atlantic Geoscience Centre, Natural Resources Canada (AGC). Preparation of this report for Indian and Northern Affairs Canada (INAC) was authorised by R. Gowan of INAC. Field work in support of this study was carried out in the Bay of Fundy, New Brunswick and in Conception Bay in Newfoundland.

Originally it was planned to collect MICRO-WIP data from an area in the Bay of Fundy at high tide, and then to return at low tide to measure the resistivity of the exposed sediments. Unfortunately the field program in Fundy was complete before authorisation for the additional work at low tide was received. However acoustic data from the Bay of Fundy indicated that the bottom was either rock or sand and gravel, so that at least a minimum of control is available. In addition, data collected in the Beaufort Sea in the summer of 1991 was used, with the permission of S. Solomon of AGC.

The study described in this report was carried out to find the best approach to real-time inversion. The report discusses the process of obtaining a set of data to interpret, and then the approaches taken to produce an interpretation of this data set. The problem of equivalence is outlined as well. Several schemes are appraised in terms of automated inversion of data from the Beaufort Sea, the Bay of Fundy in New Brunswick, and Conception Bay in Newfoundland. Finally the report describes an approach which is considered to be optimum.

RESISTIVITY MEASUREMENT

A value of apparent resistivity is determined by measurement of the potential established as a result of the flow of electric current in the sub-surface. The apparent resistivity is calculated as follows:

$$\rho_a = G * V/I \quad (1)$$

where ρ_a = apparent resistivity in ohm-metres,
 G = geometric factor (depends on array type and spacing),
 V = potential measured across receiver electrode pair,
 and I = current injected through current electrodes.

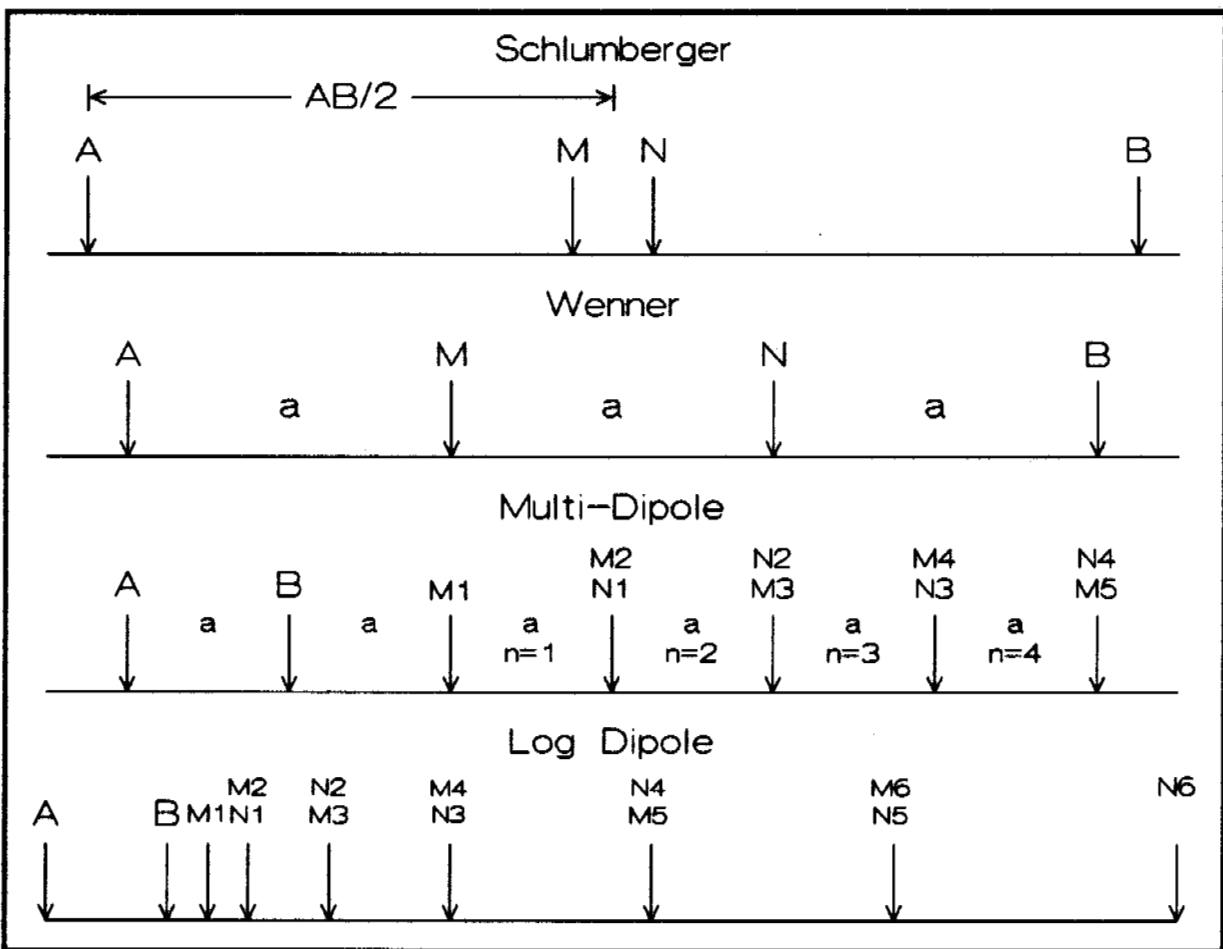


Figure 1: Electrode arrays.

To establish a depth dependence of apparent resistivity values, the scale of the electrode array is increased in steps; the resulting data set is called a sounding. Figure 1 shows the common electrode arrays used to obtain resistivity soundings. In Figure 1, following common practice in electrical geophysics, the potential electrodes are called M and N, and the current electrodes A and B.

work, the model electrical properties of interest are resistivity and sometimes chargeability, or induced polarization (IP).

IP is generally modelled in terms of percent frequency effect (PFE), by running the resistivity model a second time with resistivity values changed to reflect the model PFE values, and then comparing the two sets of calculated apparent resistivities to calculate apparent PFE values. Since there is a general equivalence between PFE and time-domain chargeability values, the apparent PFE values can be converted to apparent chargeabilities.

This report will discuss resistivity alone. In the earth, the resistivity may vary sharply at well-defined interfaces, or may change gradually with position. Generally, a model is made to include sharp interfaces, in the hopes that if variations are not step-wise, they are at least confined to narrow zones which can be modelled as well-defined layers. The interpretation process then involves determining the values of the parameters which define the model. Once the values of the parameters that describe the model are determined, the final step in the interpretation process involves drawing conclusions about the geology of the sub-surface from the model values.

A model may be one-dimensional (1D), two-dimensional (2D), or three-dimensional (3D). A 1D model is one in which the variation is in only one dimension, usually vertical, with the assumption that there are no variations in the other two directions (parallel to profile direction, and perpendicular to the profile plane). In a 2D model variation is confined to the two dimensions in the plane of the profile. A 3D model allows variation in all three dimensions.

When field data are to be interpreted, the first step is to examine the graphs of apparent resistivity as a function of spacing. A 1D interpretation is only valid if the layering under the sounding is essentially horizontal over the general dimensions of the sounding.

Before the advent of computer modelling routines, the common approach was to compare the field data with standard curves prepared for a range of 1D layered models. If the field curves resembled the standard ones in slopes and smoothness, then the assumption of a 1D case was considered justified, and a search was made for the family of standard curves which most closely resembled the field data. Once a reasonable fit to one of the family was obtained, the model parameters for the standard curve would be accepted as the basis for geological correlation. In simple cases this approach was quite useful, but as the number of layers increased beyond two or three, the number of standard curves required to offer a reasonable choice became extremely large, and the process of finding an appropriate fit became unwieldy.

INVERSION

Recent developments allow calculation of model parameters in terms of the field data, a process known as inversion. There are two general approaches to inversion. The first is the process of iterative solution, and the second is direct calculation of model parameters from the field data. This discussion will first cover iterative techniques, and then direct interpretation.

At present, inversion is generally limited to 1D models, although forward calculations can be made for 2D models, and some 2D inversion routines have been published (e.g., Narayan, S., 1990). Forward calculations can be made in some limited cases for 3D models as well.

1D Inversion

Several approaches to 1D inversion have been embodied in iterative computer routines. Those to be discussed are listed below, with the bold face indicating the name by which each will be identified in this report:

ResixIP	a commercial software package available on the open market,
Hardy BBT	(Scott, 1992), a routine developed to run on HP computers for INAC,
Davis	1979, Minnesota Geological Survey, a routine in the public domain,
Basokur	(1992), a routine which is in the public domain,
Zohdy	(1990), an Open File Release from the USGS.

All five routines are based on the concept of 1D models whose parameters are layer thickness and layer resistivity values. They incorporate a number of such layers lying on a half-space, which is in effect an infinitely deep layer. In practice, the number of layers in the model is limited by the number of apparent resistivity values available for the inversion. Thus in a sounding taken with a multi-dipole array of $n = 1$ to 6, only two layers on a half-space, with two thicknesses and three resistivities or a total of 5 parameters, can be reliably inverted. Three layers would involve four resistivities and three thickness, for a total of 7 parameters, too many to resolve with six apparent resistivity readings. Inversion of such a model will still yield a set of model parameters, but the uncertainty of the interpretation will be great. However, additional layers can be inserted without degrading the reliability of the inversion if their resistivity and thickness are known. For example, if the water depth and resistivity are known, then a water layer can be inserted without penalty. Furthermore, if a layer thickness can be determined by other means such as shallow acoustic profiling or drilling, and if the interface correlates with a change in resistivity, then the reliability of the interpretation will be improved by forcing one layer boundary to fit the known depth.

It should be noted that using inversion routines with the MICRO-WIP is working at the limits of the technique. All inversion schemes work best when the problem is well overdetermined; that is, when there are many more sounding values than layer thicknesses and resistivities to determine. The physical limitations of a towed streamer limits the system to a small number (six at present) of apparent resistivity values. At the same time models must include several layers so that the sub-bottom conditions can be adequately approximated. Thus the MICRO-WIP soundings are not really overdetermined, as the usual model incorporates five unknown parameters (two thicknesses and three resistivity values), with only six apparent resistivity values to work with. It is surprising how much of the time it is possible to achieve a reasonable solution with inversion.

ResixIP, Davis and Hardy are all examples of iterative techniques, while Basokur and Zohdy are direct interpretation routines, although Zohdy also makes

use of an iterative approach. Zohdy was developed to handle Schlumberger routines only. The approach in Zohdy could be adapted to other arrays, but only with considerable programming effort. At this stage it appears that Zohdy depends more than the others on the shape of the sounding curve, and thus requires that the sounding be greatly overdetermined to achieve reasonable accuracy. All of the others will handle apparent resistivity values from a variety of arrays, including multi-dipole. Only the Hardy routine, however, will handle the log dipole array, although in principle, the others could be modified to handle log dipole arrays.

Iterative Inversion

The iterative approach is shown schematically in Figure 2. It involves an iterative cycle of calculations, comparisons and corrections. To start, an estimate is made of the model parameter values. In what is known as a forward calculation, the parameter estimates are used to calculate model sounding data. These data are compared to the field data, and a set of error values is calculated. The standard deviation of the errors (or some other equivalent quantity) is used to evaluate the goodness of fit of the model to the field data. If the fitting error is within some acceptable limit then the model is said to fit the field data. If the fitting error is too large, then equations are constructed to calculate corrections to the model parameters in terms of the set of errors between model and field data. The core of the inversion process is the determination of the coefficients of this equation set, a process which is carried out by forming matrices to include the error equations, and then inverting the matrix equation to determine the values of the coefficients. The resulting corrections are applied to the model parameters. This process is called the inverse calculation. The new model parameters are then used in a new forward calculation, and the cycle is repeated, until the fitting error is reduced to a minimum, or to the predetermined limit.

Both ResixIP and Davis use ridge regression to determine the corrections to the model parameters. Hardy uses a method known as Monte Carlo or Random Walk, and is thus somewhat different from the other two. The ridge regression approach will be discussed first.

Inversion with Ridge Regression

The following discussion is based on Meju (1992). The inversion of electrical or electromagnetic sounding data for sub-surface resistivity distribution is a nonlinear and nonunique problem. Practical data are by their nature inaccurate, inconsistent and limited in bandwidth or spacing, and consequently an infinite number of models exists that can satisfy a given set of data. The goal of inversion is to determine some model that adequately explains our observations and also satisfies any constraints imposed by the physics of the problem, or any external control. A variety of methods has been developed for addressing such problems, (e. g. Inman, 1975; Jupp and Vozoff, 1975; Johansen, 1977; Meju, 1988). The mathematically robust least-squares formalism generally is adopted, and nonlinearity usually is addressed via an iterative procedure. However, most iterative procedures require a good initial guess at the true model in order to converge, and even so, there is no guarantee that any particular scheme will converge to the true model.

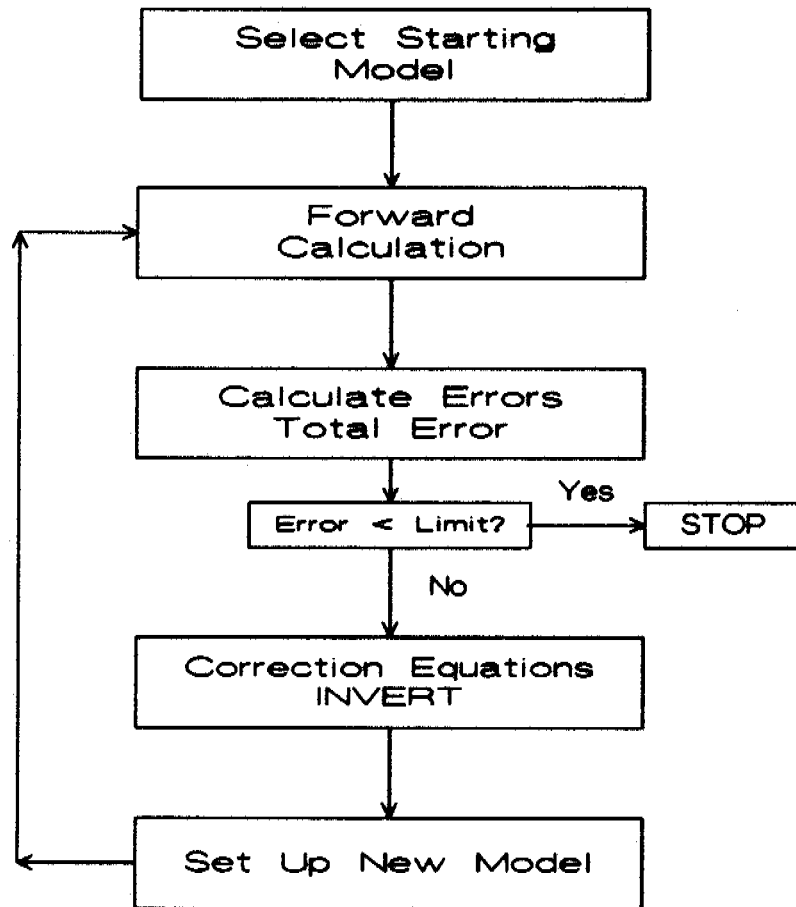


Figure 2: Typical iterative inversion flow chart.

In nonlinear problems such as resistivity inversion, the experimental data d are related to the model parameters m through a nonlinear function f (known as the forward model) as follows:

$$d = f(m) + e \quad (2)$$

where e is a vector of additive noise. Our goal is to determine a hypothetical earth model whose responses $f(m)$ are identical to the recorded data d .

Experimental errors also can be included in the inversion process. This is particularly important if some of the values in d are less reliable than others. If the n experimental errors e_i are Gaussian and statistically independent, then we may define a diagonal weighting matrix W as:

$$W = \text{diag}(1/\sigma_1, 1/\sigma_2, \dots, 1/\sigma_n).$$

This is used to scale the observed data to prevent undue importance being given to poorly-estimated data, but is not necessary if all data are equally reliable.

The differences between the forward model and the data are expressed as:

$$e = d - f(m) \quad (3)$$

or, with the experimental errors included:

$$e = Wd - Wf(m). \quad (3e)$$

To use least-squares to produce a fit between model and field data, it is necessary to adjust the model $f(m)$ to minimise the quadratic measure of fitting error:

$$\text{ssq} = e^T e = (d - f(m))^T (d - f(m)) \quad (4)$$

$$= (Wd - Wf(m))^T (Wd - Wf(m)) \text{ including errors.} \quad (4e)$$

where e^T signifies the transpose of e . This kind of problem is generally linearised so that the standard least-squares method can be used iteratively to refine an initial guess model (see Lines and Treitel, 1984, and references therein). To do this, we assume that the model is linear for some small interval around an initial guess m^0 , and perform the first-order Taylor's expansion:

$$f(m) = f(m^0) + (\partial f(m^0) / \partial m)(m - m^0), \quad (5)$$

or

$$f(m) = f(m^0) + Ax, \quad (6)$$

where $A = \partial f(m^0) / \partial m$ is the set of partial derivatives of $f(m)$ with respect to m at m^0 , and $x = (m - m^0)$ is the vector containing the corrections to be determined. This equation says that if m^0 is close to m then a correction to $f(m^0)$ in terms of partial derivatives at m^0 can be used to refine the estimate of $f(m)$.

Equation (2) may then be written

$$ssq = (y - Ax)^T(y - Ax) \quad (7)$$

or

$$ssq = (Wy - WAx)^T(Wy - WAx) \quad (7e)$$

To determine the corrections, it is necessary to determine the values of the model parameter corrections x which reduce ssq to a minimum. This is accomplished by setting to zero the derivatives of ssq with respect to each of the corrections x . This results in a set of equations which can be solved iteratively to determine the values of x . The iteration involves progressively smaller changes in trial values for x , and as the best values are approached, the sizes of the corrections become so small that in inverting the matrix of corrections, the process becomes unstable. To avoid this problem, ridge regression (Marquardt, 1970, Inman, 1975), controls the step length of the corrections to x by imposing a constraint on Equation (6) by minimising the combined function

$$\phi = (Wy - WAx)^T(Wy - WAx) + \lambda(x^T x - L^2), \quad (8)$$

where L^2 is a limit on the energy of the parameter corrections, and λ is called the damping factor.

Minimisation is then achieved by setting to zero the partial derivatives of ϕ with respect to each of the model parameter corrections x . This results in the least-squares normal equations

$$((WA)^T WA + \lambda I)x = (WA)^T Wy, \quad (9)$$

where I is the identity matrix. These equations may be solved for the model parameter corrections

$$x = (WA)^T WA + \lambda I)^{-1} (WA)^T Wy. \quad (10)$$

In ridge regression, the iterative formula is

$$m^{k+1} = m^k + (WA)^T WA + \lambda I)^{-1} (WA)^T Wy, \quad (11)$$

where m^k is the refined model at iteration k and A and y are evaluated at m^k .

Monte Carlo Inversion

Monte Carlo inversion, used by the Hardy routine, does not formally calculate the set of corrections for the model parameters. Instead, a starting model is proposed, a forward model is calculated, and then each parameter is varied in turn by a fixed percentage.

One parameter is increased first, and a new forward model is calculated. If the new error is smaller than the starting error, then the parameter

correction is accepted. If the new error is larger, then the parameter is reduced from the starting value by the same percentage, and another error is calculated. If this error is smaller than the starting error, then the new parameter value is accepted, otherwise the starting parameter value is kept.

The program moves to each parameter in succession, and goes through the same process. The end result is a set of modified or unmodified parameters, which now becomes the next starting set. A new forward model and a new error are calculated. The correction process is then repeated, but with a smaller percentage of parameter change. Three iterations are allowed in Hardy if required to reduce the error below the criterion. More iterations could be allowed if required, but the permitted ranges of parameter change would also require change for more iterations.

The advantage of the Hardy approach is that it is not necessary to calculate the partial derivatives A of the forward model $f(m)$, and then to solve for the corrections x . The main disadvantage is the need to calculate many forward models for each iteration. For example, with 5 parameters, all of which are too large, 10 forward calculations and 10 error calculations must be made in a single iteration. The Monte Carlo approach may be faster than the ridge regression approach for small data sets, but as the number of sounding values increases, the relative computation time increases.

Monte Carlo inversion also depends on a relatively close estimate for the starting model. If the initial estimates are too far from the best fit, the range of corrections allowed in the iteration series may not be large enough to bring the model into the range of minimum error. Furthermore, there may be local minima in the distribution of error, away from the true minimum error, which may stop the process before the ultimate best fit is achieved. This is a problem with many other inversion techniques as well..

Direct Interpretation

Basokur and Zohdy both offer direct interpretation approaches. Interpretation of apparent resistivity data can be carried out in either the apparent resistivity or the resistivity transform domain. Basokur operates in the resistivity transform domain, while Zohdy operates in the apparent resistivity domain. Each routine uses a different concept, and will be discussed separately.

Direct Interpretation (Basokur)

Basokur depends on a two-step approach; this discussion is based on Basokur (1984 and 1990). In these two papers, the theory of the method is outlined. Only an outline of the technique will be given here. The first step involves the calculation of the resistivity transform from the field apparent resistivity data. The second step involves calculation of the model parameters from the resistivity transform.

The first step in the direct interpretation method is to obtain the sample values of the resistivity transform function from the sample values of the measured apparent resistivity data. This is done with a technique described by

Santini and Zambrano (1981) and amplified in Basokur (1990). To obtain the resistivity transform function from the apparent resistivity data, it is necessary to develop a set of fitting functions. These act as a kind of filter applied to the apparent resistivity data to obtain the resistivity transform values. There is one resistivity transform value for each apparent resistivity value. Basokur (1990) gives fitting functions for a variety of arrays, including multi-dipole; these are incorporated in his computer program.

The second step in the process is to use recursive relations to determine the parameters of the model. The process starts by assuming that the early part of the resistivity transform curve is influenced only by the first and second layers. The resistivity and thickness of the first layer are computed. Once these are determined, the influence of the first layer is removed from the resistivity transform by means of the Pekeris recurrence equation. If more than two layers are present, the process is repeated on the next part of the resistivity transform curve. When all layers are accounted for, the final calculation gives the resistivity of the substratum.

When the program is run in its published form, the operator is asked how much of the resistivity transform curve reflects only the first two layers. Similar judgements are requested for each successive step until the substratum is identified. For automated operation of the program, this interaction must be removed. There is no simple method to calculate the part of the resistivity transform curve that reflects the influence of a given layer. In this study, the ranges of influence of each layer were fixed at the outset, and the program run in this way. Several passes were run with different ranges, and the arrangement with the minimum error of fit was chosen as the most appropriate. Good fits are obtained only when the prejudgements are at least approximately correct. This situation is probably not satisfactory for an automated inversion scheme. An additional disadvantage of Basokur is that the approach works best with a large number of closely-spaced apparent resistivity values, so that there are several values reflecting the influence of each layer. This is the condition of overdetermination mentioned above.

Direct Calculation (Zohdy)

Zohdy offers a direct calculation which is based on the characteristics of a sounding curve. Any sounding curve is a muted copy of the resistivity-depth curve of the model from which it is derived. Apparent resistivity excursions are always less than the corresponding true resistivity changes. Any change in true resistivity at a given depth is reflected by a change in apparent resistivity, but at a spacing which is somewhat greater than the depth of the corresponding interface in the model.

Zohdy points out that in most cases the resistivity-depth curve is not stepped, but is rather a curve with inflection points. He suggests that if the right reducing factor for depth and amplifying factor for resistivity can be determined, then the model resistivity-depth curve can be calculated from the apparent resistivity sounding curve.

Although the program offers a direct calculation from the sounding curve, it also depends on an iterative search for the appropriate depth-reducing and

resistivity-amplifying factors. A first estimate of the factors is embedded in the program, and the first resistivity-depth curve is determined. A forward calculation is made for this model, and the results compared with the field data. Changes to the factors are made to reflect differences between the two curves, a new resistivity-depth curve is determined, and a new forward calculation is made. When the fit between calculated and observed sounding curves meets the criterion, the process is terminated.

Zohdy's technique is particularly attractive because calculation is reduced to a minimum. As published, however, the program is set up for Schlumberger data only. Furthermore, it, like Basokur, is most effective when there are many apparent resistivity values in the curve, yet only a few layers in the model. The sounding of Figure 3a below is a good example of an overdetermined case, in which this program would give reliable results, if the top of permafrost could be represented as a gradational zone rather than a sharp interface.

In the present study, some effort was directed to automating the transformation of multi-dipole data to Schlumberger data to allow the use of the Zohdy routine. After some effort, however, we have decided that accurate transformation requires the use of judgement in each case, and is thus not well suited to inclusion in an automated routine.

Error of Fit of Inversion

To determine an acceptable error within which a model fits the field data, it is important first to determine the error associated with the measurement of apparent resistivity values. An inversion which fits the field data with a lower error than that associated with the field data could represent a fit to part of the inherent noise as well.

Error may arise from calibration errors such as the precision to which the array constants are known, or uncertainty in the value of the resistor across which the voltage is measured to calculate the transmitter current, but such errors are constant and will not affect the relative error associated with individual apparent resistivity values. The resolution of the digitizer, 16 bits plus sign, is adequate to ensure that no significant error is contributed.

The most significant source of error in the MICRO-WIP is the presence of noise. There are three principal sources of noise in the signal. The first is the presence of 60 Hz noise from the motor-generators used to supply operating power for the systems used in the survey. Measurements from experiments in the fall of 1992 (Scott et al., 1993) show that for signals of 1 millivolt, the 60 Hz content of the digitised signal is less than 0.1 percent of the input value.

The second noise type is long-term drift, or DC offset. The operator monitors this while the system is in operation, and corrections are applied if necessary. Over periods of a minute, this drift is in the range of microvolts, and appears to be linear; it is cancelled by working in terms of peak-to-peak values of successive cycles of the transmitter signal.

The third noise type is that associated with the motion of electrodes in the water. This noise is considered to be the limiting factor in the precision

with which apparent resistivity values are calculated. Research into the causes of this noise is continuing. At the time of the survey described in this report, a reasonable limit for motion-induced noise was a few tens of microvolts peak-to-peak, over periods of about one minute. This noise is most significant for the lowest measured apparent resistivity values. In the most extreme case, with an apparent resistivity of one ohm-metre and a transmitter current of 8 amperes, the motion-related noise on the farthest ($n = 6$) dipole is about 10 per cent of the signal. In an 8-cycle average, about 1400 such values are stacked, and the noise reduction thus achieved should reduce the error to less than 1 percent. In most of the survey, apparent resistivity values, even on $n = 6$ were significantly larger than one $\Omega\text{-m}$ and the associated errors were thus less than 1 percent. In evaluating inversions for the work described in this report, therefore, it was decided to use 1 per cent as the criterion for acceptable goodness of fit. When a model fit produced an error of less than 1 percent, the sounding was considered adequately fitted.

The reliability of the inversion was appraised by calculating, as part of the inversion, the standard deviation of the percentage differences between corresponding apparent resistivity values in the field and model data sets.

If the error of fit was larger than about 1.5 percent, then adjustments were made manually to the model values, and a new model data set was calculated. By such cut-and-try procedures, it was possible in all but a few cases to reduce the error of fit to about 1 percent.

Once the data sets for a line were inverted, a profile was plotted for the line, and the various sub-surface regions assigned a tentative geological correlation. The horizontal scale for the profile was kept the same as that of the plot of the vessel survey path. The vertical scale was chosen to allow good resolution of the near-surface features as well as adequate representation of deeper features.

Reliability of Inverted Models

There are three main sources of possible error in this process of interpretation. The first arises from lateral variations in the electrical properties of the sub-bottom materials. The second arises from bends in the streamer. The third is related to a condition known as equivalence.

The 1-D inversion process assumes that model parameters (layer thickness and resistivity) are laterally invariant to infinity. In practice this condition is approximately met if the values change slowly over horizontal distances of several dipole lengths, but the 1-D inversion process breaks down in areas where thicknesses or resistivities change rapidly along the survey line. In such cases it may not be possible to obtain a 1-D model with acceptable error, and consideration should be given to further interpretation in terms of two-dimensional models. It is also possible that a good fit may be obtained to the data in an area of rapid lateral variation; even if the error of fit is low, the interpretation in such an area should be viewed with caution. The soundings inverted for this report were chosen primarily from regions of limited lateral variation in apparent resistivity values.

The calculations of apparent resistivity values are based on the assumption that the potentials are measured with the streamer in a straight line. If the survey vessel holds a straight course during the time the MICRO-WIP is recording, then the streamer is also straight, and the condition is met. If, on the other hand, the vessel turns, then the streamer will have a kink in it until it has all passed the point at which the vessel turned. The apparent resistivity calculations will be in error, and there will be no indication of the error in the data. During survey the streamer position was monitored, and recording was undertaken only when the streamer was straight. It is possible, however, that some bends in the cable went undetected. The consequent errors would now be in the data, and could be neither identified nor removed.

Equivalence

In many cases more than one appropriate model can be determined for which the fit between field and model data sets is acceptable. These models are said to be equivalent. Equivalence arises most frequently when one of the layers in the model is thin in comparison to its depth of burial. If such a buried layer is more resistive than those surrounding it, and its thickness is less than or comparable to its depth of burial, then the inversion determines the product of thickness and resistivity, but does not yield a reliable indication of the values of resistivity and thickness. If the buried layer is less resistive than those surrounding it, then the inversion determines the ratio of thickness to resistivity, but cannot separate the two parameters (Lasfargues, 1957, p. 108-112). In such cases, a variety of sets of thicknesses and resistivities can be found such that the product of, or the ratio of thickness and resistivity for all the sets is the same. Equivalent models can vary quite widely in the thicknesses of a given layer, and unless independent evidence, such as depths from seismic profiles, can be obtained, all equivalent models may be equally acceptable in terms of error of fit.

It should be emphasised that the problem of equivalence is inherent in electrical soundings and is not a limitation of the chosen inversion technique, or of the array chosen for the field measurements. It arises equally in the interpretation of electromagnetic sounding results (e.g., Verma and Mallik, 1979). Equivalence in electrical sounding interpretations is discussed by a number of authors; see for example Lasfargues (1957), Keller and Frischknecht (1966), Koefoed (1969), Inman (1975), Rocroi (1975), Scott and MacKay (1977), and Szaraniec (1982). The examples presented here are taken from Scott and MacKay because they deal specifically with permafrost.

Example of Equivalence (Scott and MacKay, 1977)

Figures 3a, 4a, and 5a show three Schlumberger soundings taken on the Tuktoyaktuk Peninsula, across Kugmallit Bay from the survey area discussed in this report.

These soundings were interpreted by 1-D inversion, followed by adjustment in the same manner as in the present study; the computer program was written specifically for Schlumberger soundings by Zohdy (1974). Zohdy assumes initially that the number of layers is equal to the number of apparent resistivity values in the sounding. Inversion in terms of this model determines the resistivity

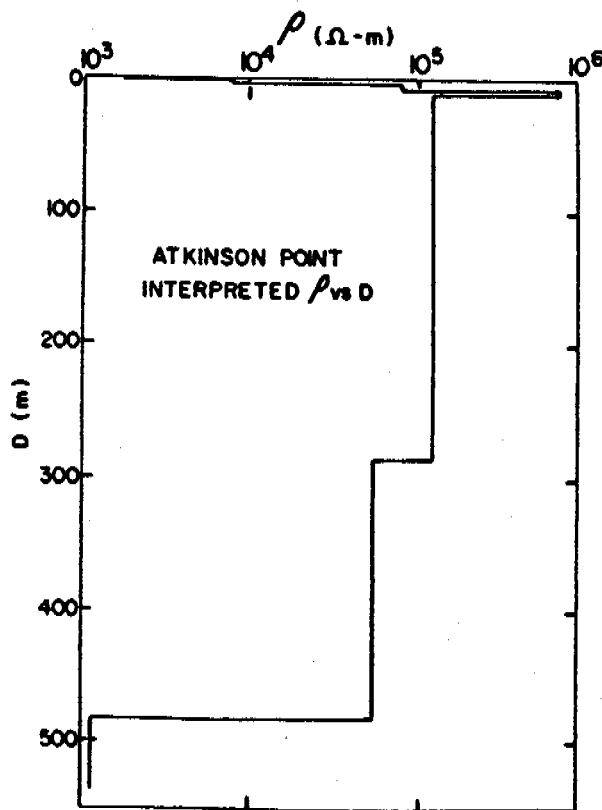
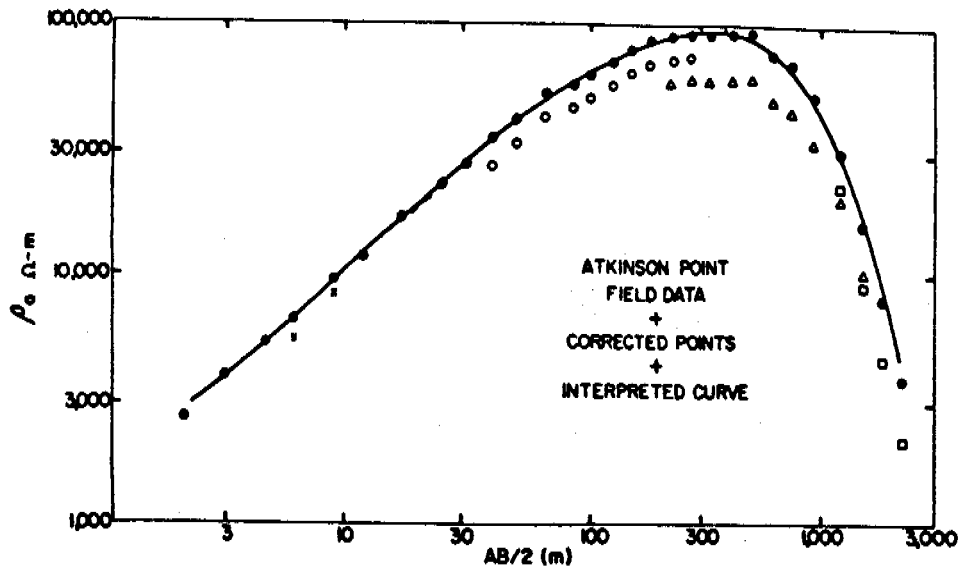


Figure 3: Top - Corrected field data and theoretical sounding curve for Schlumberger sounding south-east of Atkinson Point, after Scott and MacKay, 1977.
Bottom - Interpreted resistivity-depth function, after Scott and MacKay, 1977.

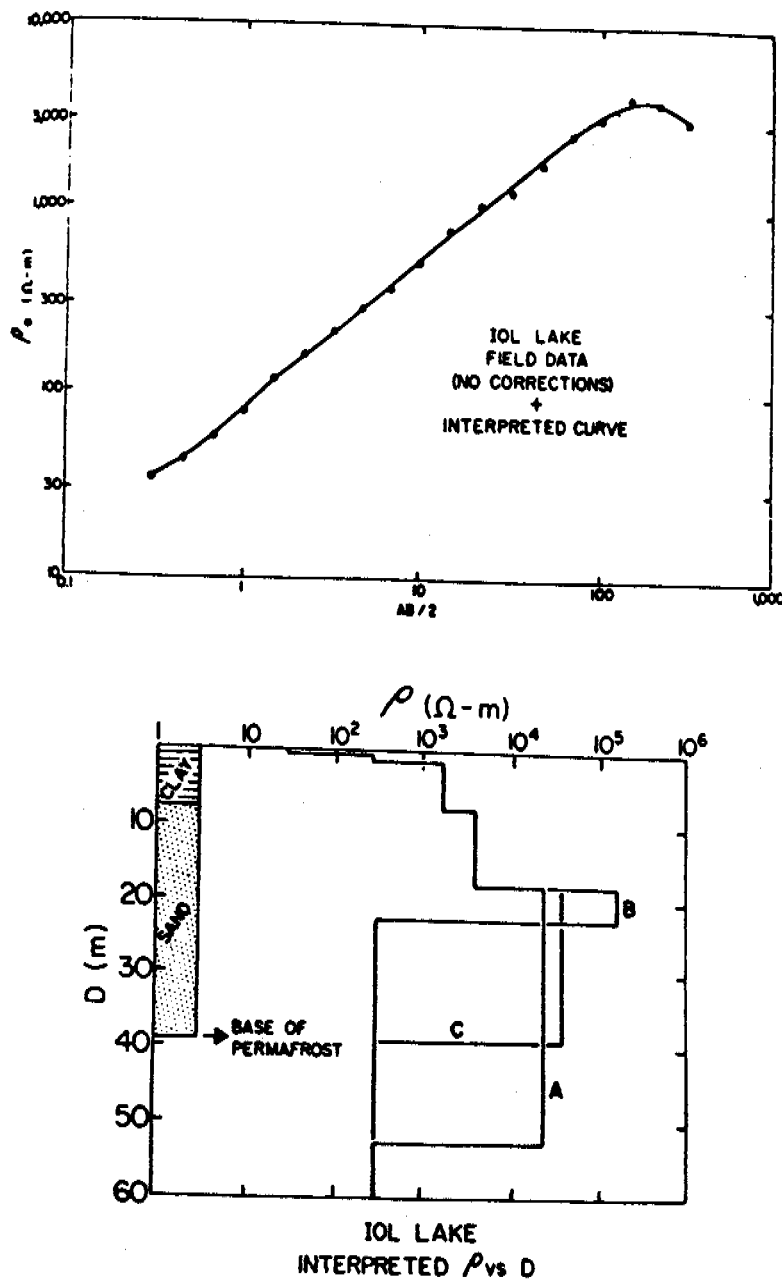


Figure 4: Top - Field data and theoretical sounding curve for Schlumberger sounding in drained basin of IOL Lake, after Scott and MacKay, 1977.
 Bottom - Resistivity-depth functions for IOL Lake sounding, after Scott and MacKay, 1977.
 A - maximum permafrost thickness interpretable for 2% increase in sum of squared residuals of theoretical fit to field data.
 B - Minimum interpretable permafrost thickness with the same error.
 C - interpretation chosen to match known permafrost thickness.

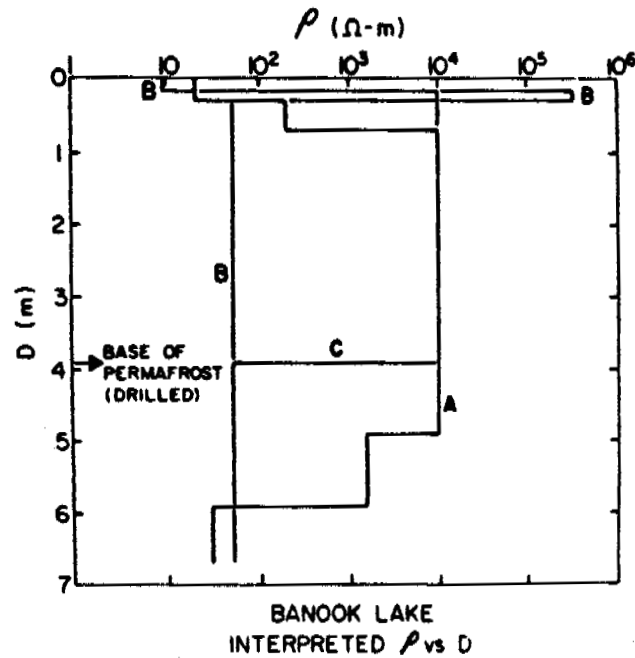
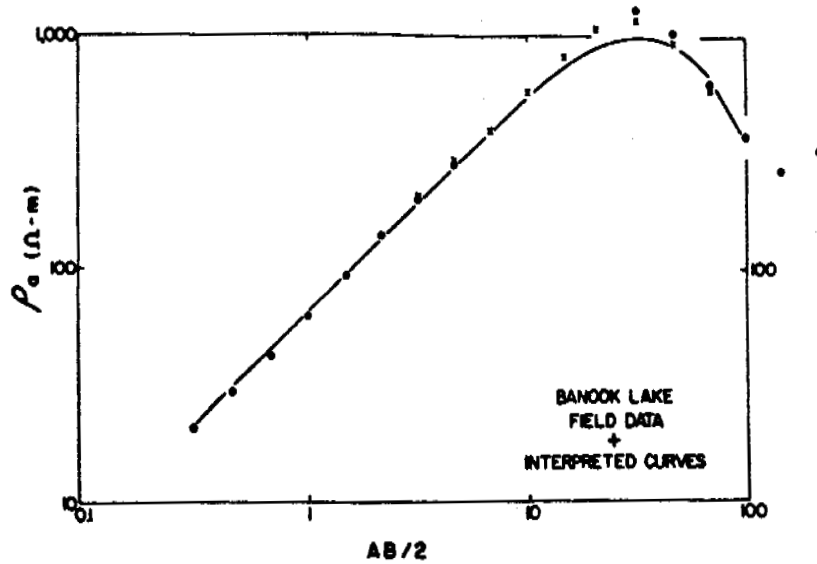


Figure 5: Top - Field data and theoretical curve for Schlumberger sounding in drained bed of Banook Lake. Points for $AB/2$ greater than 100 are influenced by the shore of the lake. After Scott and MacKay, 1977.
Bottom - Resistivity-depth functions interpreted for the sounding in Banook Lake. A, B, and C are as in Figure 4. After Scott and MacKay, 1977.

values of the layers. Once a reasonable fit is achieved, the number of layers is reduced in steps and forward calculations are made with the reduced model; reduction stops when the error of fit for the reduced model increases beyond some predetermined percentage of the error of fit for the original inversion.

Figure 3b shows the resistivity-depth curve determined for the sounding of Figure 3a. No other models with layers of differing thickness and resistivity can be found which can produce as low an error of fit as the model of Figure 3b, which gives rise to the theoretical sounding shown as a solid line in Figure 3a. Drill control in the area is consistent with the interpreted permafrost thickness of 480 metres.

Figure 4b shows some possible resistivity-depth curves for the sounding of Figure 4a, all of which fit the same theoretical sounding curve, shown in Figure 4a as a solid line, within 2 percent. Figure 4b also shows the log of a hole drilled at the centre of the sounding. The base of permafrost indicated by the drilling is consistent with the resistivity-depth curve in which the deepest high-resistivity layer is marked C. Layers A and B, however, represent extremes that give rise to the same error of fit. The layers A, B and C are said to be equivalent. They all have approximately the same product of resistivity and thickness, between 6.5×10^5 and 8×10^5 . Note that many other equivalent curves exist, whose resistivity-thickness products are comparable. There is no internal evidence in the sounding data to indicate that C or any other equivalent layer is the most accurate choice. Once some independent information on thickness is incorporated, however, the resistivity of the layer is well determined.

Figure 5b shows three equivalent resistivity-depth curves, all of which give rise to the same theoretical sounding curve, shown as a solid line in Figure 5a. Curves A and B represent the extremes of variation in the model for which the error of fit is the same; curve C was chosen to fit the known thickness of permafrost determined by jet-drilling.

Equivalent layers in a resistivity sounding cannot be resolved unless there is independent information on either thickness or resistivity. It is possible, however, to identify the presence of equivalence, and to analyse its limits. Plots of equivalent models which embody this analysis can be prepared to accompany the sounding interpretations.

APPRAISAL OF INVERSION ROUTINES

The appraisal of inversion routines concentrated on those described above. After the initial evaluation, the Zhody approach was not included in the set for appraisal, and efforts were directed to the others. Data available at the start of the study had been collected primarily with multi-dipole arrays; most of the appraisal therefore was done on the three routines written for that array.

A comparison of the Hardy routine with multi-dipole inversions was the last part of this study. Considerable effort was spent in trying to find the logarithmic array developed at Hardy BBT, but unfortunately it appears to have been discarded after the departure of W.J. Scott. It was one of a series of

streamers made in one run. There had been a problem with the multi-dipole streamers made at the same time, which led to frequent breakage of the signal-carrying conductors. While there is no record of the fate of the logarithmic array, it must have been discarded with the other faulty streamers. Within the budget constraints of this program, fabrication of a new log-array streamer was not feasible, but the 25-metre multi-dipole streamer was modified to a logarithmic spacing for the trials described in this report. Several attempts were necessary before a successful modification was achieved.

All of the inversion routines were examined for their suitability for incorporation into our operating system. Their performance was tested by converting the source code to the Microsoft QUICKBASIC language, where possible, and simulating real time operation using the apparent resistivity data collected in the Beaufort Sea in 1991.

The MICRO-WIP operating system executes on a 486 computer with a 33 MHz clock speed. The operating system is timed so that resistivity and chargeability values are computed every 16 seconds. Of this 16 seconds, approximately 6 seconds are required for the processing of the digitized data. This leaves approximately 10 seconds of CPU time for other operations such as a routine to perform an inversion on the data and plot the results along with a pseudo-depth section. Therefore, a suitable inversion routine would have to be capable of running in Microsoft QUICKBASIC 4.5 and giving a reasonable answer in less than 10 seconds. If future changes to the operating system make it necessary to use more of the free time for data collection, file handling, navigation and other operations, it would be possible to transfer the raw data (apparent resistivities and chargeabilities) to a second computer over a serial communications line and allow the second PC to perform the inversion on the data and to plot the pseudo-depth section and inverted model data on the printer.

1. Basokur

The Basokur program offers "direct interpretation of resistivity sounding curves measured with the two-electrode Wenner, Schlumberger or dipole arrays...The parameters of the first layer are determined from the early part of the resistivity transform curve. The top layer is removed by the Perkeris recurrence equation. This method operates on a modified kernel function. The successive application of the proposed method and the recurrence equation on each part of the resistivity transform curve determines all the layer parameters."

The original source code was written so that inversions were performed in an interactive manner between the software and the person processing the data. While running in real time, with only 10 seconds to carry out the inversion, the only interaction that we can offer is the resistivity and depth of the water layer (measured automatically) as well as the previous model parameters. Therefore the source code was modified so that these parameters were input automatically by the calling program each time the inversion routine was initiated.

The Basokur routine performed inversions most rapidly of all the routines tested. However, during testing it was determined that the results obtained with

much of our data was not reliable. The reason for this is that the program looks for inflection points in the apparent resistivity data and uses these points to determine the thickness of the layers. Because our data contains just six apparent resistivities which have subtle inflection points the program tends to fit a single layer on an infinite half space. When the inversion routine was tested with artificial data with well defined inflection points it gave reliable answers.

2. Davis

The Davis inversion program "finds the theoretical model whose apparent resistivity curve matches the field data to reasonable accuracy. The program accomplishes this using Marquardt's algorithm (Marquardt, 1963) which is an optimized combination of the Newton-Gauss and the gradient inversion methods. A set of field apparent resistivities and initial model parameters are input. Theoretical apparent resistivity values are computed for the trial model. In addition, derivatives of apparent resistivity with respect to each layer parameter are computed. Corrections to each parameter are determined from a generalized inversion of the derivative matrix. These corrections are then applied to the old model to give a new set of apparent resistivity values. The process is repeated until the root-mean-square error falls below a chosen cutoff value."

The original source code for this inversion routine was written in FORTRAN 77. It was translated to Microsoft QUICKBASIC to evaluate its performance.

3. Hardy

The Hardy inversion routine was originally written in HP BASIC for use with an earlier version of the MICRO-WIP operating system. This program takes a starting model and uses the Monte Carlo approach to fit the model to the data. The forward calculations used in this program are based on linear filter theory.

The filters used in this version of the program were for the calculation of apparent resistivities for an array with logarithmical spaced electrodes. In order to test this inversion routine an array with logarithmically-spaced dipoles was constructed. The spacings used matched those for which the program was written and are shown in Table I.

Distance (metres)	Identification	Electrode
0	Start of Cable	-
25	Current Dipole	C1
50		C2
60	Potential Channel 1	P1
70		P2
85.75	Potential Channel 2	P3
107.75	Potential Channel 3	P4
141.75	Potential Channel 4	P5
189.25	Potential Channel 5	P6
260.50	Potential Channel 6	P7

Table I: Design of Hardy Logarithmic Cable.

4. ResixIP

ResixIP uses ridge regression (Inman, 1975) to adjust in an iterative manner the parameters of a starting model supplied by the user. This allows the best fit model (in a least squares sense) to be obtained from the data.

We have used ResixIP in the past to model data for reports and papers. When given a reasonably good starting model the program quickly converges on the model which best fits the data. ResixIP also gives the range of equivalent models which fit the data within a specified error range. ResixIP is supplied in executable form only, therefore the source code is not available to the user. Because of the way the software is structured it cannot be called as a subprogram and passed raw data to be inverted. It can only be used in an interactive session with the operator supplying the necessary information. For a fee, Interpex, the vendor of ResixIP, would be prepared to develop a version which could be included in the MICRO-WIP operating system. In view of the initial review of inversion routines, it was felt that there would be little advantage in requesting such a development.

With these limitations, ResixIP is not suitable for use as an automated inversion routine. Because it has been the C-CORE standard method of interpreting data for some years, it was used on a subset of the field data on each line for comparison with the other inversion routines.

5. Zohdy

Zohdy, a direct interpretation scheme, was assessed but not used for the MICRO-WIP data because of the problems involved in changing the multi dipole values to equivalent ones which would have been read with a Schlumberger array. Zohdy is set up for Schlumberger data only, and significant effort would be needed to alter it to accept other arrays. Zohdy operates on the shape of the sounding curve, and would thus be more dependent on having many apparent resistivity values.

COMPARISON OF PERFORMANCE OF INVERSION ROUTINES

To appraise the performance of the various inversion schemes, data from three sources have been used. The first tests were carried out on apparent resistivity data sets from the 1991 Beaufort Sea survey. Subsequent comparisons were made on the set collected on three lines in the mouth of Passamaquoddy Bay in the Bay of Fundy. Finally, data sets collected in Conception Bay with both dipole and logarithmic arrays were processed. However, most of the appraisal effort was expended on the Beaufort Sea data sets. In addition to the running inversions, tests were made on the effect of inverting with fixed layer thicknesses, and on the influence of using different starting models on the ultimate fit.

The operation of three of the most promising inversion routines was compared. Two of the inversion routines, Basokur and Davis, were incorporated into the MICRO-WIP operating system. The routines were fed the raw data; the results were presented in the form of printer plots containing pseudo-depth sections and the models obtained from the inversion. The third inversion routine ResixIP was used as a benchmark to check the other results obtained from the other routines. ResixIP was used as the benchmark because it had proven itself to give reliable results in the past and had the capability to provide equivalence information with the models it produced. The results of the other two inversion routines were then compared to the equivalence range to determine the degree of agreement of the models and the reliability of the routines.

The appraisal process thus started with a running inversion of the Beaufort Sea data with Davis and Basokur, and comparison of selected inverted models with the results from ResixIP. This appraisal indicated that there were frequently great differences between the results obtained with Davis and with Basokur. Similar running inversions were performed on the data from the Bay of Fundy. Running inversions were also carried out on the data from the line in Conception Bay. Each set of results is discussed below. The final step was to investigate the approach of fixing the thicknesses of five sub-bottom layers and inverting in terms of the resistivities of the layers. Several sets of thicknesses were tried to see if a generally reliable set could be found.

Running Inversions, Beaufort Sea data

The three dipole routines were compared with data collected using 10m and 25m multi-dipole arrays with $n = 1$ to 6, on Line 10D (10m) and on Lines 22A, 44A, and 45A (25m), from the 1991 field program conducted for Atlantic Geoscience Centre. Figure 6 shows the location of the survey lines.

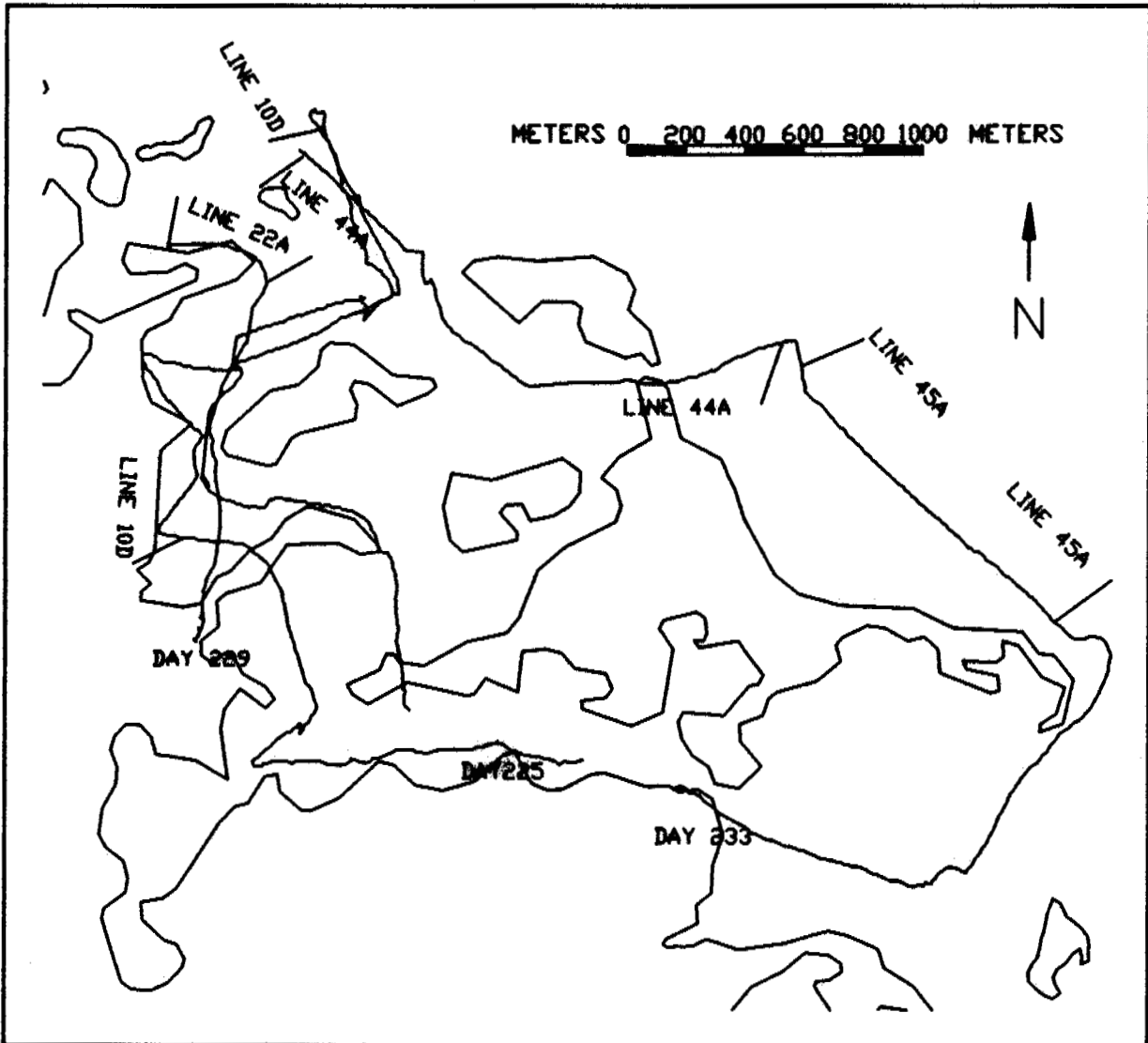


Figure 6: Location of survey lines, 1991 MICRO-WIP survey, Richards Island, Beaufort Sea, NWT.

All three of the inversion programs were given the values of thickness and resistivity for the first layer (the water layer), since these were measured independently in the field. With the values for the first layer held fixed, the inversion routines were left to find values for the thickness and resistivity of the second layer, and the value for the resistivity of the halfspace below this

layer. The performance of the routines was appraised in terms of the fitting error of the interpreted model. Table II summarises the average fitting errors observed for the four lines.

Line	ResixIP	Davis	Basokur
10D	4.53	64.2	2.61
22A	3.97	52.4	2.56
44A	3.90	74.3	4.64
45A	4.23	55.1	8.02

Table II: Average fitting errors for Beaufort Sea lines.

In many cases the sub-bottom conditions may offer greater complications than a simple layer on a half-space, and the continuous inversion routine may not offer the best ultimate solution. The inversion routines tested (and most other routines as well) start with a model with a fixed number of layers, and fit the model parameters. Most inversion routines are thus not capable of deciding how many layers to include; for a first pass the most efficient approach is to limit the number of layers. If the inversion fits a model with fewer than the specified number of layers, then the fitted model will have successive layers with the same resistivity value, or layers with zero thickness. If there are more layers implied in the data than have been fitted, then the half-space resistivity will include variations in deeper layers.

The results of the running inversions with Davis and Basokur are presented in Appendix A. These listings show the apparent resistivity pseudosection obtained in the field, and the results of the inversions with each routine plotted as layered models, with the values of thickness and resistivity displayed below each model.

Fiducial Marks

In order to correlate the position of the vessel with the position of a sounding, and with positions of other data, use is made of Fiducial Marks, known as fids. In MICRO-WIP surveys, fids are used to correlate positions between different measurements. At selected intervals either in time or in distance, a simultaneous mark is put on all geophysical records, and the position of the survey vessel is determined at that time. When the vessel track is recovered and plotted on a map the positions of the fids are shown. For the MICRO-WIP there is an offset between the vessel position at any fid, and the position of the centre of the sounding represented by the array. The size of this offset depends on the dipole spacing of the array.

In the Beaufort Sea inversion data presented in Appendix A, the fids have been corrected for this offset, and each fid appears on the profile directly over the centre of its associated sounding.

Line 10D

Figure 7 shows the fitting errors for the inversions on Line 10D. Errors in the values of apparent resistivity at Fids 1160-1162 and at Fid 1208 produce the two spikes at the right hand end of Figure 7. Table III compares the

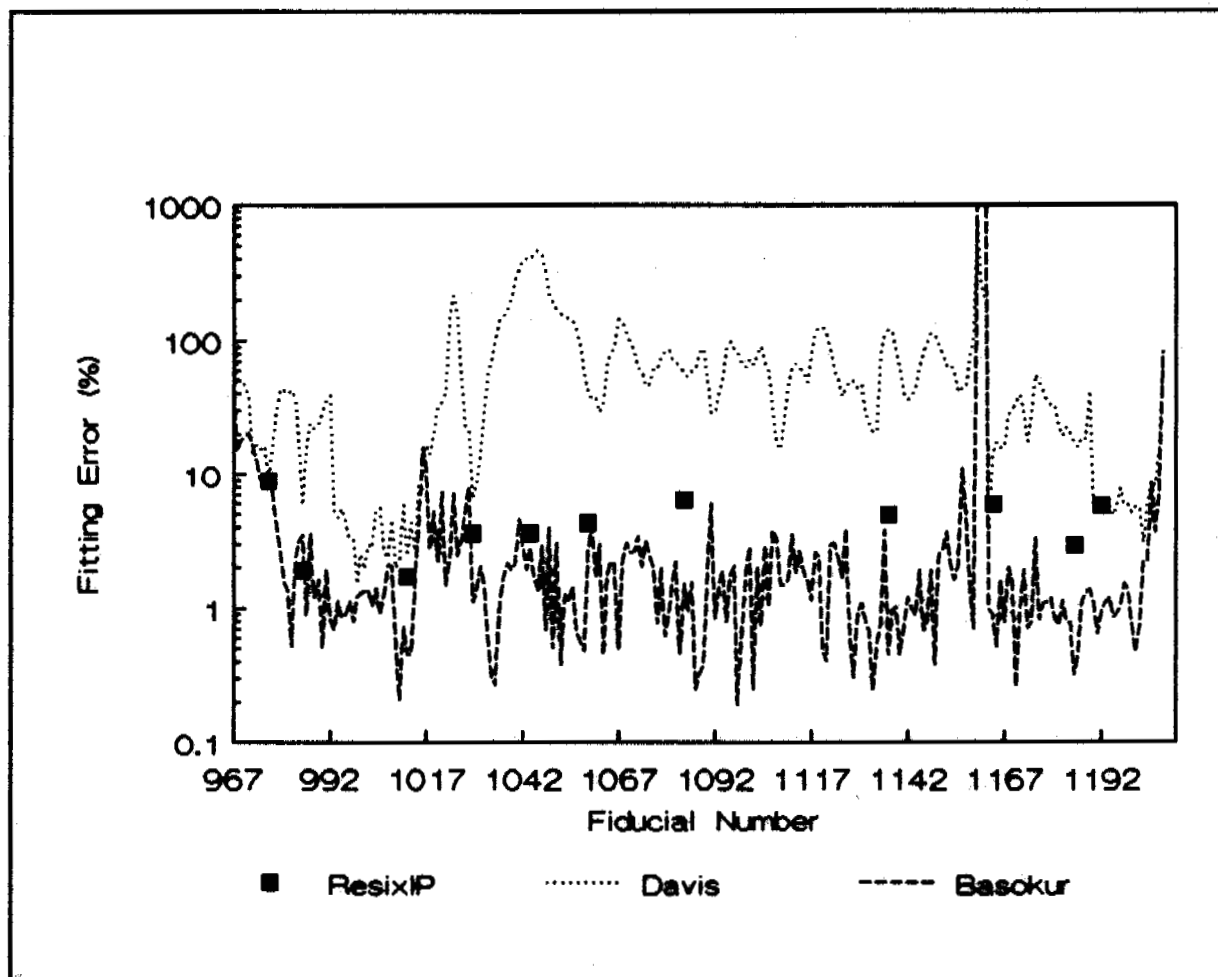


Figure 7: Fitting errors on Line 10D for three inversion routines.

inversion results at selected fids on this line. Printouts A-1 and A-2 (Appendix A) show the results of running inversions on Line 10D with Davis and Basokur respectively.

On Line 10D, the Basokur routine gives the best fit to the apparent resistivity values and thus the lowest errors. Average fitting errors, excluding the fids with data errors, (Table II) are 4.53 for ResixIP, 64.2 for Davis, and 2.61 for Basokur. Except at the left end, ResixIP assigns very high resistivity values to the half-space, even though most of the apparent resistivity values at $n = 6$ are less than 20 $\Omega\text{-m}$. The range of equivalent resistivity values appears to be much more limited than the shape of the sounding curve would justify. At $n = 6$ the apparent resistivity values are rising sharply, but are only in the 10

to 20 Ω -m range. It is surprising, then, that the equivalence range does not include lower final-layer resistivity values.

Davis gives 100 Ω -m for the half-space at the left end of the line, drops abruptly to about 2.5 Ω -m at Fid 993, and rises rapidly to about 38.5 k Ω -m between Fids 1009 and 1016. This resistivity is given for all fids up to Fid 1189, after which the value drops to about 4 k Ω -m and then rises to over 12 k Ω -m after Fid 1198. The high final resistivity values appear to contribute to the high fitting error on this line. Most of the high values fall in the range of equivalence given by ResixIP. For most of the line, Davis assigns to the second layer a thickness of from 10 to 20 m, which increases to nearly 30 m towards the right end of the line.

Basokur gives half-space resistivity values which are generally about twice the value of apparent resistivity at $n = 6$, or from 6 to 20 Ω -m, and rarely much greater than 40 Ω -m. For the central part of the line, Basokur reduces the thickness of the second layer to zero, although there are finite thicknesses assigned to it for short segments near both ends of the line.

For this line, Davis and ResixIP fit a similar model (2 layers on a high-resistivity half-space) to the apparent resistivity data, although ResixIP has much lower average fitting error (4.53%) and a lower half-space resistivity. Basokur, on the other hand, fits one layer on a much lower resistivity half-space, with the lowest average fitting error. This line is in an area with shallow water, a bottom which must be unfrozen at least in the top few metres, and relic permafrost at depth. It is thus unlikely that the model interpreted by Basokur is correct. The uncertainty could probably be better resolved if more dipole spacings had been measured.

Line 22A

Line 22A was a short segment which was run in shallow water near a spit. It was surveyed with 25 m dipoles and $n = 1$ to 6. Figure 8 shows the distribution of fitting errors for Line 22A, and Table IV shows the fitted models for selected fids. Printouts A-3 and A-4 (Appendix A) show the results of running inversions on the apparent resistivity data on Line 22A for Davis and Basokur respectively.

On this line, ResixIP has fitted two layers above the half-space. The thickness of the second layer ranged from 3 to 35 m, and the resistivity from 1.3 to 5.1 Ω -m. Half-space resistivity values varied from 10 Ω -m to 30 k Ω -m.

Davis also fitted two layers above the half-space. Thicknesses varied from 30 to 47 m, considerably greater than those of ResixIP, and resistivity values ranged from 6 to 31 Ω -m. The half-space resistivity was constant at 41.6 k Ω -m all along the line. Both second-layer and half-space resistivity values were consistently higher than those interpreted by ResixIP, and the fitting errors were consequently much higher.

Table III: Comparison of inversions, Beaufort Sea Data, Line 10D, 10 m dipole spacing.

Fid Time	Field Data	ResixIP				Davis				Basokur			
	Rho, n = 1 to 6	Bottom Layer		Half Space	Error	Bottom Layer		Half Space	Error	Bottom Layer		Half Space	Error
	Ω -m	Thickness m	Rho Ω -m	Rho Ω -m	%	T m	Rho Ω -m	Rho Ω -m	%	T m	Rho Ω -m	Rho Ω -m	%
976 19:13:33	.52, .69 .83, .99 1.2, 1.3	.13 - 3.35	.001 - .2	2.6 - 6.5	8.9	.03	.002	100	8.5	.1	.01	1.8	4.0
985 19:18:21	2.3, 3.5 4.9, 6.7 8.4, 9.6	9.2 - 9.7	4.1 - 4.3	17.8k - 19.2k	1.9	.04	.01	100	5.9	.02	.01	19.6	3.1
1012 19:32:44	2.7, 3.6 4.0, 4.7 5.5, 6.2	21.2 - 22.3	5.9 - 6.1	11.4k - 13.0k	1.7	0	n/a	2.8	40	.02	.01	9.6	4.6
1029 19:41:48	5.3, 9.1 11.9, 15.2 18.5, 21.7	13.0 - 16.3	17.6 - 25.3	45.4k - 72.9k	3.6	5.9	7.0	16.3k	3.3	.01	.01	39.5	5.5
1044 19:49:48	2.1, 2.3 2.2, 2.6 3.2, 3.9	21.2 - 23.2	3.0 - 3.6	12.0k - 23.6k	3.6	23.1	8.3	16.3k	161	12.1	8.3	6.3	8.5
1059 19:57:48	4.7, 7.9 10.6, 14.2 19.0, 23.6	10.2 - 11.7	13.9 - 16.8	77.2k - 100k	4.3	23.4	17.3	16.3k	43.6	.01	.01	54.6	11.2
1084 20:11:08	4.2, 7.2 9.2, 11.2 13.1, 14.4	4.6 - 9.0	2.8 - 5.6	96 - 10.7k	6.4	23.3	17.3	16.3k	51.7	.01	.01	21.9	3.0

Table III Continued: Comparison of inversions, Beaufort Sea Data, Line 10D, 10 m dipole spacing.

Fid Time	Field Data	ResixIP				Davis				Basokur			
		Bottom Layer		Half Space	Error	Bottom Layer		Half Space	Error	Bottom Layer		Half Space	Error
	ρ_{a} n = 1 to 6	Thickness m	ρ_{a} $\Omega\text{-m}$	ρ_{a} $\Omega\text{-m}$	%	T m	ρ_{a} $\Omega\text{-m}$	ρ_{a} $\Omega\text{-m}$	%	T m	ρ_{a} $\Omega\text{-m}$	ρ_{a} $\Omega\text{-m}$	%
1137 20:39:24	1.7, 2.6 3.3, 4.1 4.9, 5.7	9.2 - 12.4	1.9 - 2.8	3.0k - 9.5k	4.9	31.6	14.1	16.3	140	.03	.01	9.4	4.3
1164 20:54:52	2.4, 2.9 3.1, 3.3 3.6, 3.8	25.5 - 31.5	3.9 - 4.3	6.9k - 15.4k	5.9	>50	3.4	16.3k	12.1	5.7	1.5	4.4	2.7
1185 21:06:03	2.5, 3.1 3.4, 4.1 4.9, 5.7	19.0 - 20.8	4.5 - 5.7	15.9k - 28.7k	2.9	>50	4.4	16.8k	24.2	3.8	.7	9.4	5.2
1192 21:09:47	1.9, 2.4 2.4, 2.6 2.8, 2.9	24.9 - 32.5	2.5 - 3.2	2.3k - 10k	5.7	>50	2.6	100K	10.1	6.0	1.3	3.2	2.4

Table IV: Comparison of inversions, Beaufort Sea Data, Line 22A, 25 m dipole spacing.

Fid Time	Field Data	ResidP				Davis				Basokur			
		Bottom Layer		Half Space	Error	Bottom Layer		Half Space	Error	Bottom Layer		Half Space	Error
	ρ_{H} n = 1 to 6	Thickness m	Rho Ω -m	Rho Ω -m	%	T m	Rho Ω -m	Rho Ω -m	%	T m	Rho Ω -m	Rho Ω -m	%
3292 20:19:31	3.9, 5.1 5.8, 6.2 8.6, 11.6	1.9 - 41	3.0 - 6.0	290 - 100k	6.9	31.3	6.0	41.6k	14.5	0	n/a	21.0	11.5
3303 20:25:23	6.4, 12.1 17.8, 24.3 31.0, 38.8	1.8 - 2.7	1.8 - 2.1	45k - 90k	3.5	46.5	30.7	41.6k	35.4	0	n/a	92.3	8.6
3314 20:31:15	4.0, 6.5 8.5, 10.8 13.0, 15.2	10.7 - 16.7	2.9 - 3.5	78 - 210	1.5	46.5	30.7	41.6k	125	0	n/a	27.2	5.1

Basokur fitted the soundings with one layer on the half-space throughout the line, and assigned relatively low values to the resistivity of the half-space. Fitting errors (Table II) were lower than for either of the other two inversions, but again, the geology of the area suggests that there should be an

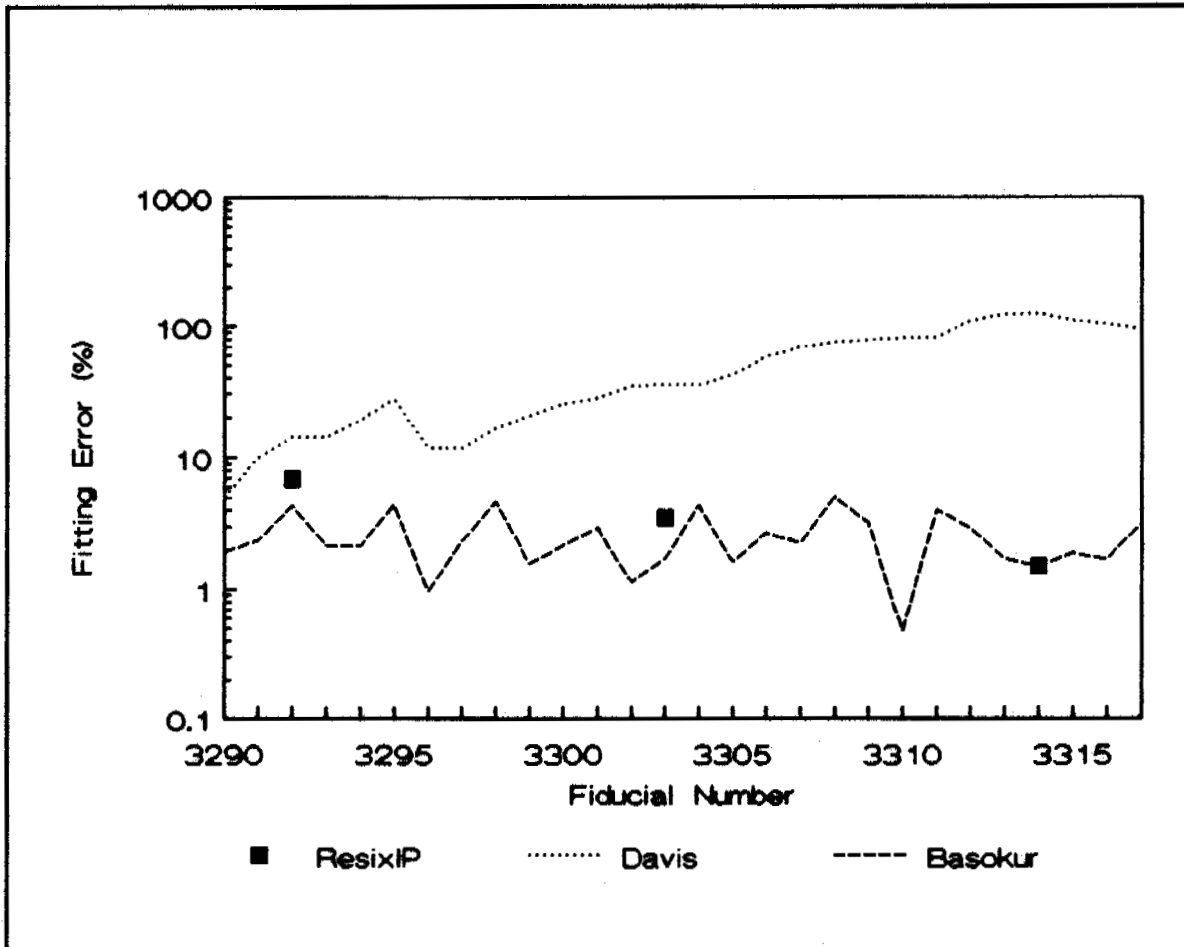


Figure 8: Fitting errors on Line 22A for three inversion routines.

unfrozen layer above the permafrost which almost certainly underlies the line.

Line 44A

Line 44A runs from west to east along the front of Richards Island, and crosses shallow water in a narrow zone between two islands. Printouts A-5 and A-6 (Appendix A) show the results of running inversions on the data of Line 44A, for Davis and Basokur respectively. The pseudosections in the complete inversion record in Appendix A shows very high apparent

Table V: Comparison of inversions, Beaufort Sea Data, Line 44A, 25 m dipole spacing.

Fid Time	Field Data	ResixIP				Davis				Basokur			
	Rho, n = 1 to 6	Bottom Layer		Half Space	Error	Bottom Layer		Half Space	Error	Bottom Layer		Half Space	Error
	Ω -m	Thickness m	Rho Ω -m	Rho Ω -m	%	T m	Rho Ω -m	Rho Ω -m	%	T m	Rho Ω -m	Rho Ω -m	%
5102 20:19:25	5.8, 9.8 14.2, 18.6 22.8, 26.9	3.7 - 10	1.3 - 3.7	1.9k - 30k	1.8	.58	.33	14.5k	2.61	0.1	0	54	4.0
5109 20:23:09	3.8, 4.4 4.9, 5.6 6.3, 6.9	30.4 - 35.9	3.8 - 4.0	10.9 - 14.1	1.4	2.1	1.39	14.5k	152	.04	0	9.5	1.7
5123 20:30:37	3.7, 6.1 9.0, 12.6 16.0, 18.8	.7 - 11.2	2 - 2.7	14k - 29.2k	5.7	70.1	20.6	14.5k	78.6	0	n/a	42.7	4.5
5133 20:35:58	8.1, 13.0 16.9, 20.5 23.5, 27.4	.3 - 6.6	2 - 5.1	285 - 9.0k	1.1	72.6	28.8	14.5k	16.9	0	n/a	43.4	3.6
5147 20:43:25	6.3, 9.4 12.3, 15.3 17.5, 21.1	15.0 - 19.7	5.8 - 7.1	65.9 - 121	1.6	61.0	78.2	14.5k	1505	0	n/a	31.8	3.40
5166 20:53:33	10.6, 15.9 19.0, 22.0 25.0, 29.0	9.5 - 21.5	10.4 - 16.2	43.2 - 64.6	2.59	61.0	78.2	14.5k	72.7	0	n/a	45.7	2.11

Table V continued: Comparison of inversions, Beaufort Sea Data, Line 44A, 25 m dipole spacing.

Fid Time	Field Data	ResixIP				Davis				Basokur			
		Bottom Layer		Half Space	Error	Bottom Layer		Half Space	Error	Bottom Layer		Half Space	Error
		Thickness m	Rho Ω -m	Rho Ω -m	%	T m	Rho Ω -m	Rho Ω -m	%	T m	Rho Ω -m	Rho Ω -m	%
5184 21:03:37	Rho, n = 1 to 6 13.5, 25.8 36.5, 42.8 44.6, 47.7	.043 - 12.5	.12 - 45.4	93.6 - 280	9.60	138	103	14.5k	15.1	4.3	471	61.2	6.33
5200 21:12:09	7.5, 12.1 16.8, 23.0 29.9, 35.9	.088 - 16.9	.083 - 16.8	221 - 3930	8.65	0.0	99999	99999	32.9	15.2	332	66.1	2.10
5216 21:20:41	3.8, 6.3 8.8, 10.8 12.3, 13.9	3.0 - 10.7	.77 - 2.8	46.3 - 78.6	2.61	2.3	1.43	9.7k	61.5	0	n/a	19.4	4.05

resistivity values at Fids 5177 and 5178, which correspond to passage through the narrows. Apparent resistivity values change so rapidly with position in this

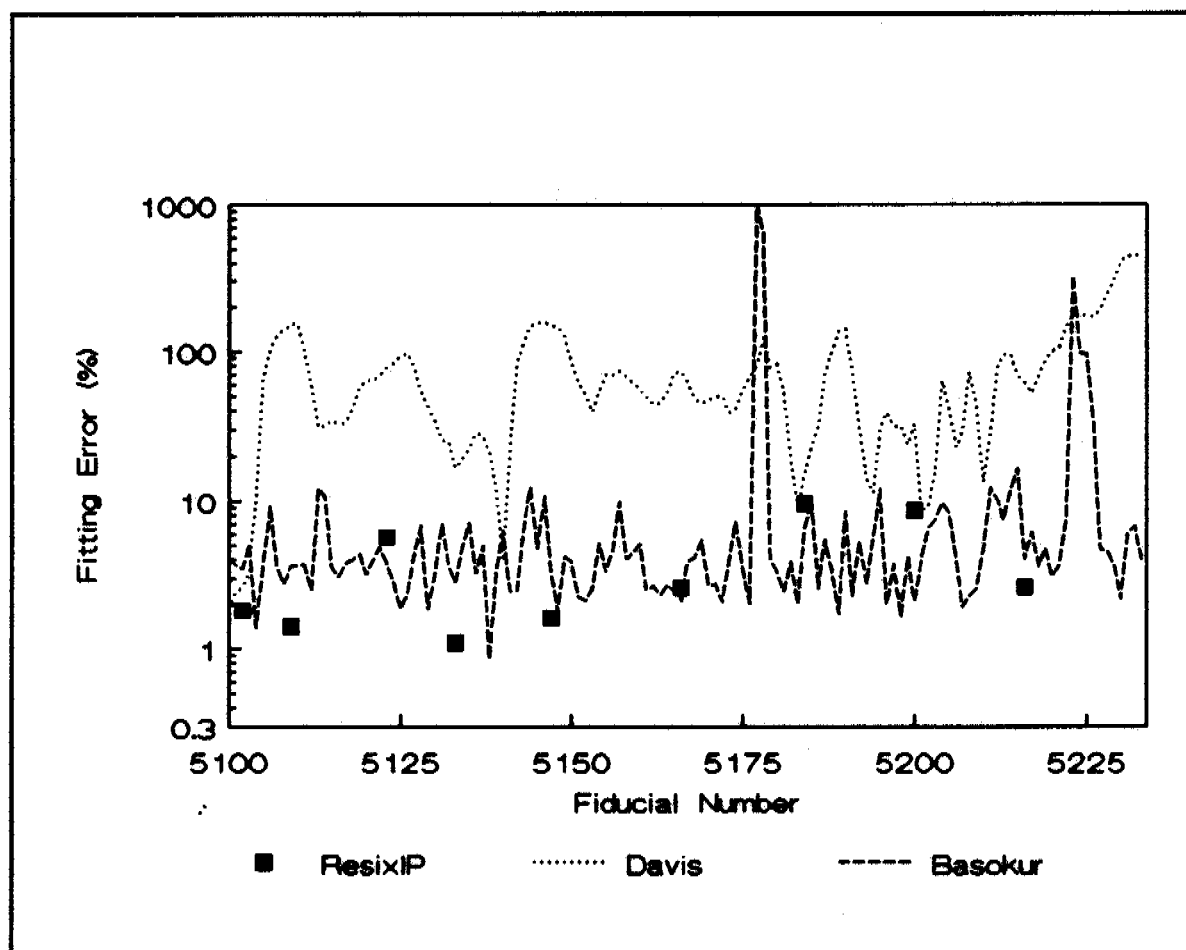


Figure 9: Fitting errors on Line 44A for three inversion routines.

area that it is doubtful that the lateral uniformity needed for one-dimensional inversion exists. It too is underlain by relic permafrost along most but not all of its length. Figure 9 shows the distribution of fitting errors along Line 44A, and Table V shows the fitted models for some selected fids. Conditions along Line 44A are quite variable, and the results of the inversions are similarly variable. Average fitting errors (Table II) are reasonably low for ResixIP and Basokur, but much higher for Davis. With the exception of two areas where the apparent resistivities are very high or unreliable (Fids 5177 and 5178, and 5222 to 5227), the fitting errors for ResixIP and Basokur are generally less than 10 percent.

ResixIP on this line supports the inclusion of a second layer above the half-space. At five of the nine fids in Table V, ResixIP produces a second layer which has a well-defined thickness and resistivity. At Fids 5123, 5133, 5184 and 5200, however, the thickness of the second layer is less well defined, and ranges from just over 0 to between 6 and 16 metres. At the same fids, the range of resistivity values for the second layer is similarly wide, ranging from a low of 0.08 to a high of 45 Ω -m. At these fids the fitting error is higher, and the

range of equivalence is consequently wider. The resistivity of the half-space is high enough to indicate the presence of sub-seabed permafrost at six of the nine fids, and is moderately high at two others. Only at Fid 5109 is the half-space resistivity low enough to rule out the presence of permafrost within the top 50 metres.

On this line, Davis starts out with a thin second layer, a high resistivity for the half-space and a fitting error comparable to ResixIP. When the apparent resistivity values drop rapidly after Fid 5103, however, Davis cannot track the change, and the fitting error rises rapidly. The only low fitting error after the beginning is at Fid 5140, where the apparent resistivity at high values of n rises enough to match the values calculated by the Davis inversion. It appears that once the fit is bad enough, Davis cannot find out how to improve it. By Fid 5115, Davis has locked onto an unsuitable model which, despite the high fitting error, is not changed again until high apparent resistivity values are encountered at Fid 5132. Drops in apparent resistivity after Fid 5140 again lose the routine, which locks onto another unsuitable model and carries it on to Fid 5178. Although the model changes at higher fid numbers, there is no satisfactory fit achieved for the rest of the line.

On almost all of Line 44A, Basokur reduces the effect of the second layer by finding a thickness which is either 0 or very close to 0. At Fid 5109 ResixIP shows a 3.9 Ω -m second layer with a thickness of between 30 and 35 m, and a half-space of between 2 and 30 k Ω -m, and Basokur a 2.5 Ω -m layer 9.2 m thick lying on a 12.3 Ω -m half-space. The fitting error for ResixIP at Fid 5109 (1.4%) is considerably lower than that for Basokur (3.71%). At Fid 5111, Basokur also provides a 4.1 Ω -m second layer 11.9 m thick.

Occasionally on this line Basokur substitutes a very thick second layer for a thin second layer over a half-space. At Fid 5102, for example, Basokur fits a 51.1 Ω -m second layer with a thickness of 2670 metres. For a 25 m array, this is effectively an infinite thickness, and the value assigned to the half-space (0 Ω -m) is not really relevant. The same situation exists at Fid 5171. Basokur gives similar fits for Fids 5162 to 5165, although the thicknesses are only in the range of 160 to 300 m. The half-space resistivity values are more realistic but equally unreliable, because they are not within the depth range of the array.

Line 45A

Line 45A runs from north-west to south-east along the eastern edge of Richards Island, off Reindeer Island. It was surveyed with the 25 m array and $n = 1$ to 6. Water depths range from 1.9 to 3 m, and the north-west part of the line may not be underlain by permafrost within the range of the array. To the south-east, the line passes close to Reindeer Spit, and permafrost is almost certainly present in the sub-seabed. Towards the south-east end of the line, apparent resistivity values change rapidly with position; the change may be too rapid to allow reliable inversion in one dimension, although the inversions were carried out anyway.

Figure 10 shows the distribution of fitting errors along Line 45A for the three inversion routines, and Table VI shows the fitted models for some selected fids. Printouts A-7 and A-8 (Appendix A) show the results of running inversions with Davis and Basokur respectively. High errors at Fids 5238 and 5253 indicate

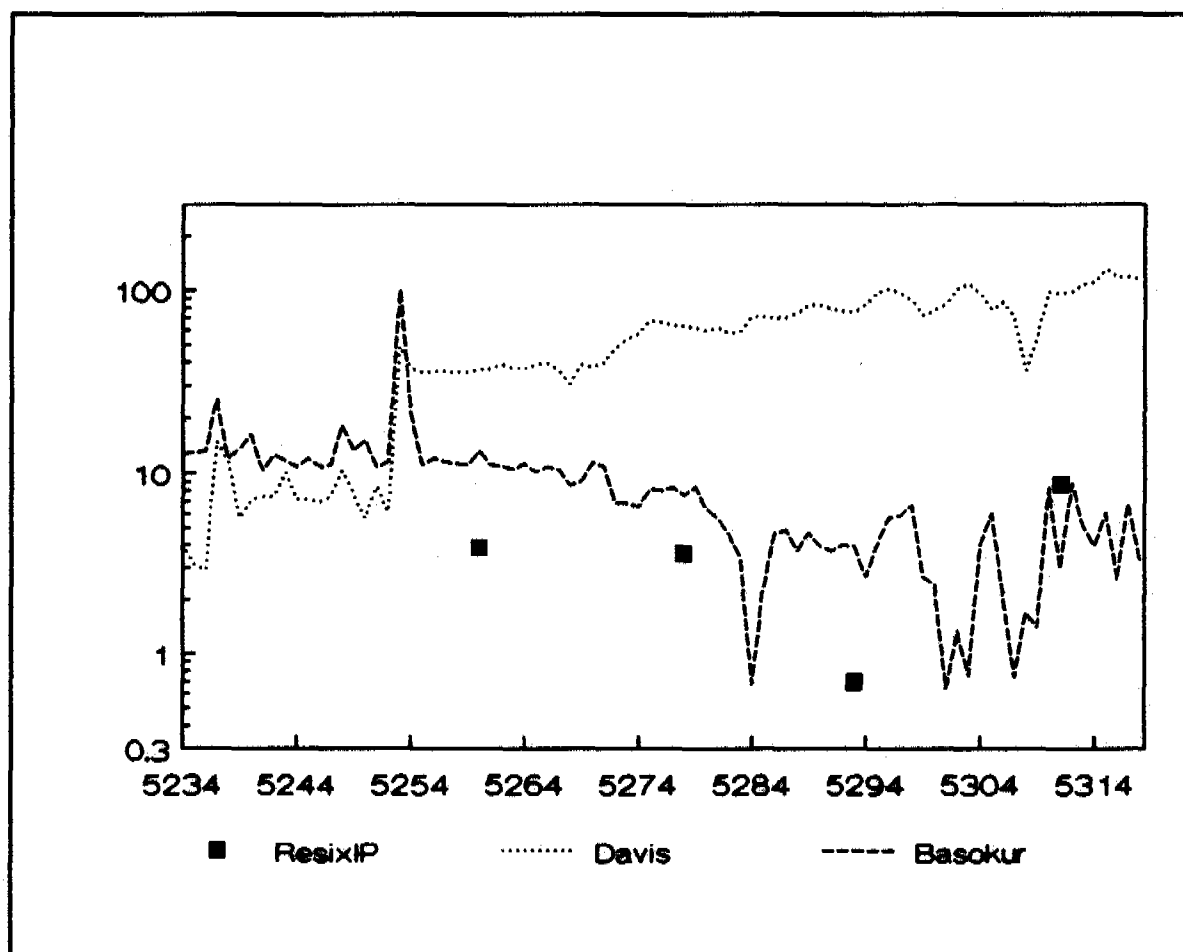


Figure 10: Fitting errors on Line 45A for three inversion routines.

problems with the apparent resistivity data, and have been excluded from the means shown in Table II. ResixIP has a low average fitting error, but Basokur has errors which are twice as large, and Davis has an average error an order of magnitude higher than ResixIP.

Along Line 45A, ResixIP gives reasonably well-defined values for both resistivity and thickness of the second layer, and the models have low fitting errors. Because the resistivity values are well constrained, it would be possible to use them to determine areas with coarse-grained material. Half-space resistivity values increase from north-east to south-west, but permafrost resistivity values are indicated only in the south-east. At the time

Table VI: Comparison of inversions, Beaufort Sea Data, Line 45A, 25 m dipole spacing.

Fid Time	Field Data	ResixIP				Davis				Basokur			
	Rho _n n = 1 to 6	Bottom Layer		Half Space	Error	Bottom Layer		Half Space	Error	Bottom Layer		Half Space	Error
	Ω-m	Thickness m	Rho Ω-m	Rho Ω-m	%	T m	Rho Ω-m	Rho Ω-m	%	T m	Rho Ω-m	Rho Ω-m	%
5260 21:47:13	2.0, 1.8 1.8, 1.7 1.7, 1.9	2.8 - 12.7	2.0 - 4.3	1.6 - 1.8	3.9	34.9	9.58	100k	36.6	95.5	1.81	0.0	13.3
5278 21:56:49	2.9, 2.6 2.8, 3.1 3.3, 3.6	42.6 - 59.8	2.6 - 2.8	5.0 - 10.2	3.6	45.2	15.2	100k	62.6	65.0	3.49	2.43	7.6
5293 22:04:49	2.9, 3.3 4.1, 4.8 5.4, 6.0	27.5 - 30.0	2.8 - 2.85	11.5 - 13.0	0.7	47.8	19.5	100k	75.9	13.4	3.23	7.1	3.97
5311 21:14:25	4.8, 7.8 11.0, 15.8 22.1, 25.4	0.8 - 17.3	0.3 - 6.1	20.2k - 49.3k	8.7	58.1	48.7	100k	0 96.1	0	n/a	51.5	3.01

of the survey, water resistivity values were between 4.7 and 6.5 Ω -m, reflecting the influence of the plume from the Mackenzie River. As a result, all the sounding curves start with a high apparent resistivity at $n = 1$ and have negative slopes. This situation holds until Fid 5273, after which the overall slope becomes positive.

For the first three fids on the line, Davis manages a good fit with thicknesses and resistivities comparable to those determined by ResixIP at Fid 5260. At Fid 5237 a momentary rise in apparent resistivity at $n=6$ forces Davis to raise the half-space resistivity. At subsequent fids, Davis holds the half-space resistivity constant, and manipulates the second layer to obtain a fit with errors somewhat lower than those of Basokur. At Fid 5252, the apparent resistivity at $n = 6$ is too high to be believable. In attempting to fit this, Davis sets the half-space resistivity to 100 $k\Omega$ -m, and never recovers on the rest of the line. The sensitivity of the Davis routine to sudden changes is considered below.

With a few exceptions, Basokur fits a resistivity of 0 to the half-space on the north-west end of the line. Basokur's second-layer thicknesses are generally in the hundreds of metres; the second layer is essentially the half-space because its base is below the range of influence of the array. After the change in slope of the sounding curves (Fid 5273), Basokur raises the half-space resistivity gradually along the line, ultimately reaching values as high as 51.5 Ω -m. After Fid 5300, however, the second layer thickness is set to zero, and from there to the end of the line, the interpretation is in terms of the water layer and a half-space.

Running Inversions, Bay of Fundy Data.

In the fall of 1992, a series of experiments was carried out near Deer Island, in the southern part of the Bay of Fundy, among the string of islands in the mouth of Passamaquoddy Bay. Most of the work was directed towards reduction of electrical noise associated with towing of the array in salt water (Scott et al., 1993). On the final day, however, three lines were run to obtain data for inversion with different schemes. In addition to the MICRO-WIP, a Raytheon RTT-1000 sub-bottom profiler was also used. As in the Beaufort Sea, a salinometer was used to obtain the conductivity of the seawater along the line, to use in defining the parameters of the first layer.

Originally it had been intended to carry out real-time inversions, and to run each line several times. However, time was limited, and navigation was complicated by the need to intersperse the runs with the passage of the ferry to Deer Island, so that it was not clear that exactly the same line could be covered on each pass. It was decided instead to collect one set of data on each line and to run the inversions afterwards. The results are equivalent to running the same line three times with three different inversions, and in addition there is assurance that the data sets really did come from the same line.

Figure 11 shows the location of the three lines. The ferry route is shown by the dashed line which crosses the three survey lines near 56'2" W. No path-recovery system was used, but the lines were reliably positioned by reference to the surrounding shore and islands. Note that Line J2N was run in the opposite direction to the other two, and has been plotted in the direction in which it was run so that the analogue record from the sub-bottom profiler can be shown in proper relationship to the line. Measurements were taken with 10 m dipoles and $n = 1$ to 6. In view of water depths which ranged up to 9 m, the 25 metre array would have been preferable, but would have led to complications with the passing ferry.

Line	ResixIP	Davis	Basokur
J1S (all fids) (5 fids)	4.01	3.91 4.49	4.3 4.39
J2N (all fids) (3 fids)	3.16	3.92 5.71	3.99 4.88
J3S (all fids) (5 fids)	2.62	4.46 4.76	5.27 3.96

Table VII: Average fitting errors for Bay of Fundy lines.

Because these lines were shorter than the Beaufort Sea lines, it was possible to compile on a single sheet the results of all the inversions for each line. The raw data from each of these three lines are plotted with the inverted values and the sub-bottom profile in Figures 12, 14 and 16. Inversion results from Davis and Basokur have been plotted above the centre of the appropriate sounding. The spot ResixIP inversions have also been plotted over the centres

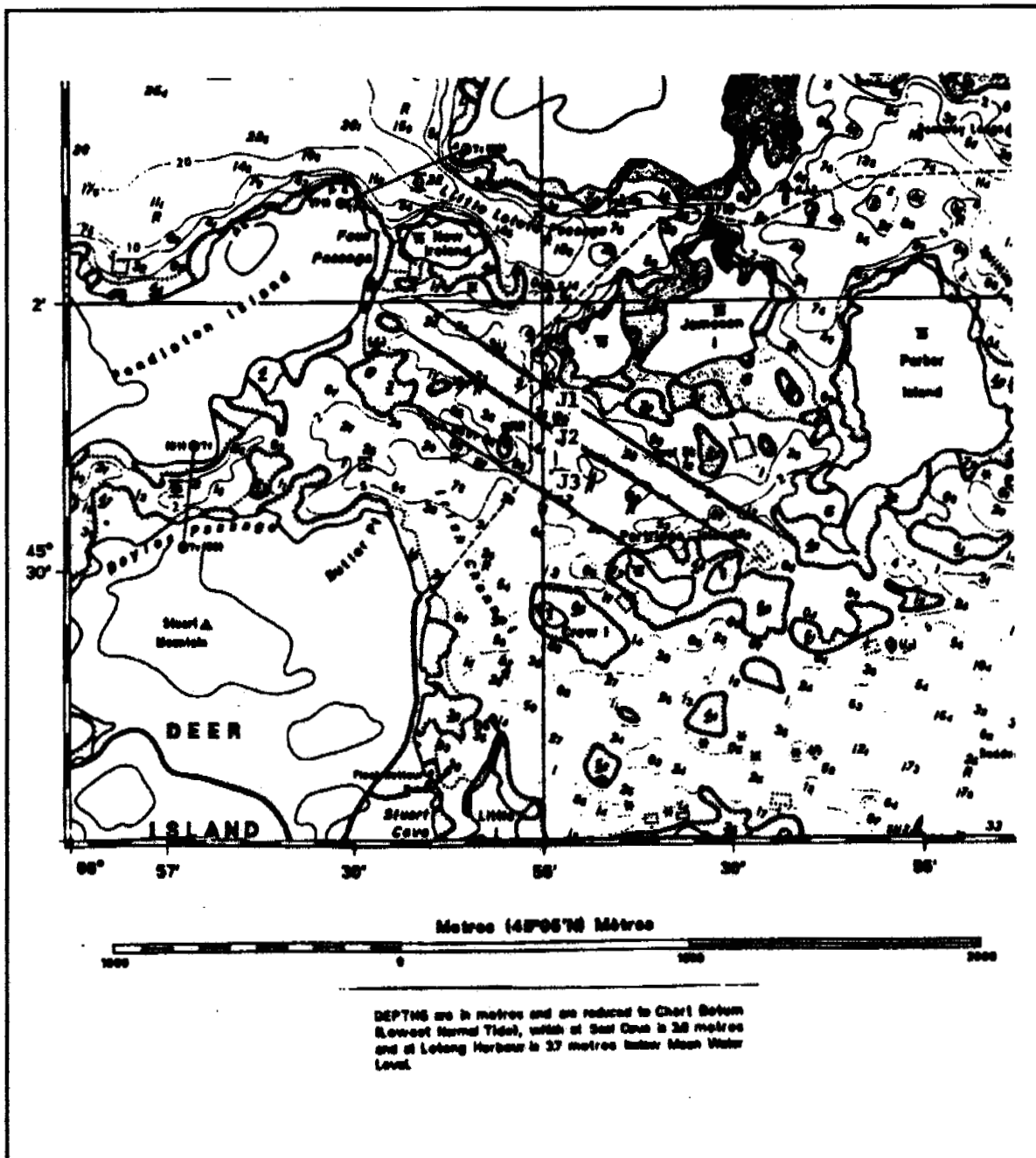


Figure 11: Location of survey lines, Bay of Fundy.

of their associated soundings. In Figures 12, 14 and 16, the bottom and sub-bottom profiles interpreted from the RTT-1000 analogue record have been displayed at the top. Below these are the interpreted profiles from the inversions, with the values for each model displayed below the depth point. At the bottom of each sheet is the pseudosection of apparent resistivity. The small graphs below the pseudosection show the range of equivalence calculated by ResixIP at the fids identified.

Line J1S

Figure 12 (in pocket) shows the results for Line J1S, and Figure 13 shows the distribution of fitting errors. Note that on this line the profile was run

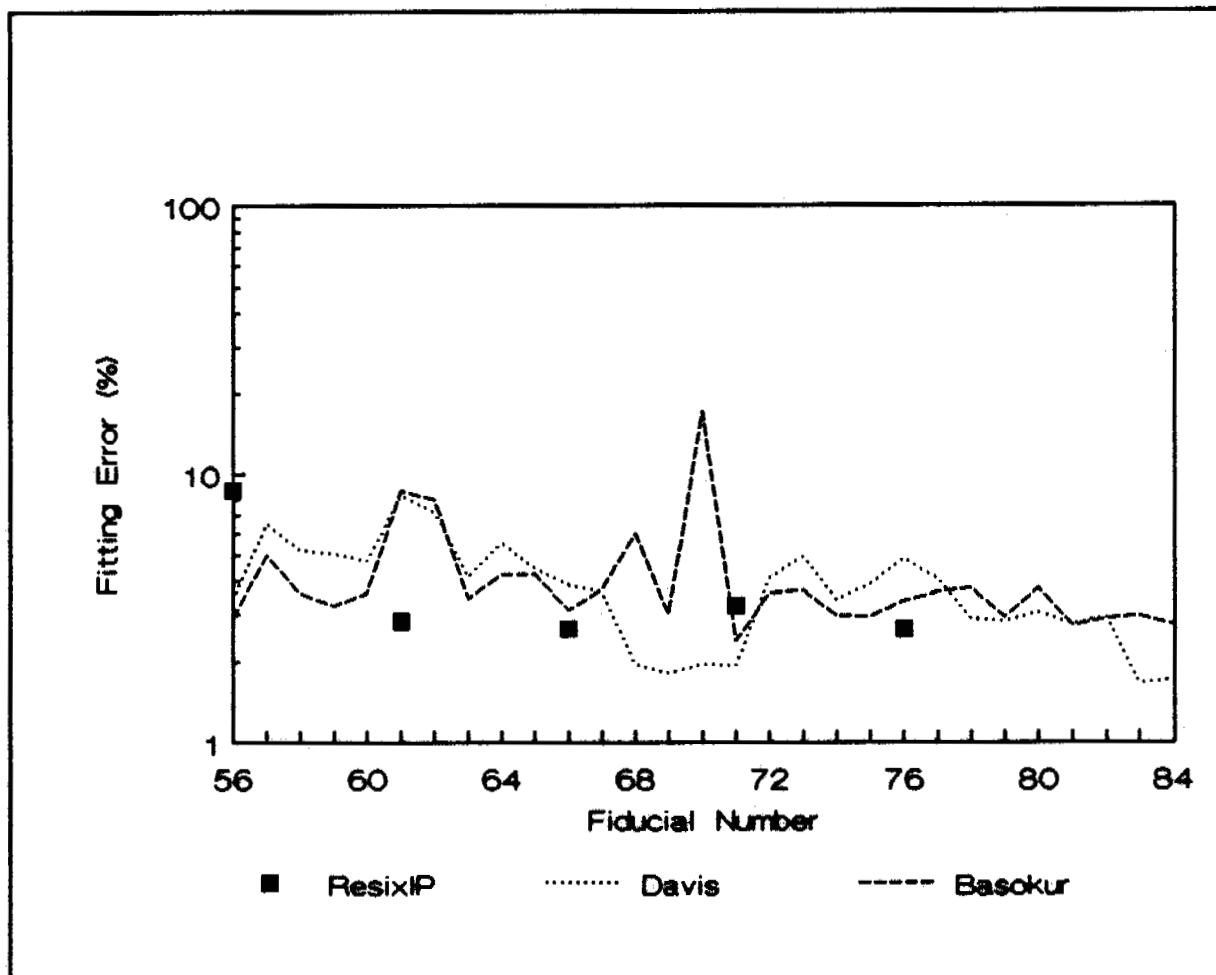


Figure 15: Fitting errors on Line J1S for three inversion routines.

from north to south, and North is shown on the left side of the profile. From the RTT-1000 record it appears that for much of Line J1S rock is exposed on the bottom. The only exceptions are the area from Fid 56 south to about Fid 63, which has sands and gravels varying in thickness from 0 to about 7 metres, and the area from Fid 75 to Fid 79, which has 1 to 2 metres of sand and gravel. Both bottom and bedrock surface are quite irregular, and probably too uneven to allow a perfect one-dimensional inversion.

Inversions with ResixIP were run at every fifth fid. All results indicated the presence of a layer on the bottom with resistivity values from 1.8 to 4.7 Ω -m, and thicknesses from 14 to 27 metres. Half-space resistivity values range from 940 to 6300 Ω -m, and are probably appropriate for the bedrock. The ResixIP inversions show the gravel layer as continuous along the line, despite the acoustic evidence to the contrary. If the inversions were not carried out on an automated basis, the starting model for the inversion could be adjusted to

reflect water lying on rock outcrop. With automated inversion, however, the starting model for each inversion is the finished model for the previous inversion, so known changes in the sub-bottom conditions are difficult to incorporate. Note that the average fitting error (Table VII) is not high enough to indicate a gross misfit, so that there is no internal indication that the model is not always correct. In fact, the highest error is found when ResixIP fits a two-layer model where gravel is present above the bedrock.

Inversions with the Davis routine (top of figure) show a gravel layer which is interpreted as almost continuous along the line, but variable in thickness. Where well-defined, it has resistivities from 1.5 to 5.5 Ω -m. At Fid 57, the intermediate layer is reduced in thickness to almost nothing, thus converting the interpretation to one layer on a half-space. At Fids 63 to 65, the second layer is assigned a thickness of over 1000 m, so that it in fact becomes the half-space. The most improbable inversion is at Fid 70, where the second layer is very thin, the resistivity of the third layer is 0 Ω -m, and the fitting error is very high. In the other inversions the half-space resistivity values are greater than 1000 Ω -m.

The results of the Basokur inversion are quite different from the other two. Along most of the line, Basokur shows only one layer on the half-space, and that is the water. The resistivity of the half-space, however, is very low. The Basokur inversion represents the most conservative interpretation, which assigns the half-space the minimum possible resistivity which will generate a fit to the sounding curve. The average fitting error is hardly different from those of ResixIP and Davis.

Line J2N

Figure 14 (in pocket) shows the raw data and the results of inversions on Line J2N, laid out in the same manner as in Figure 12. It is important to remember that this line was run in the opposite direction to J1S and J3S, so that the ends of the plot are reversed with respect to the ends of the other lines, with North on the right. Figure 15 shows the distribution of fitting errors on the same line. The sub-bottom profile indicates that the only area of sand and gravel is towards the north end of the line, and that the thickness probably does not exceed 3 metres.

Average fitting errors are very similar for all three inversion routines (Table VII). On Line J2N all five of the ResixIP inversions show a layer between the water and the bedrock, despite the acoustic indication of outcrop along most of the line. The overburden layer ranges in resistivity from 2.4 to 7.1 Ω -m, and in thickness from 13 to 34 metres, even though the acoustic shows no greater thicknesses than 3 m. The half-space resistivity ranges from 780 to 4800 Ω -m.

Davis shows a layer of overburden on the rock which is present except at Fids 104 and 108. At Fid 98, the second layer is effectively infinite, even though the second-layer resistivity is only 13 Ω -m. On the rest of the line, Davis shows overburden thicknesses from 18 to 24 m with occasional excursions to 90 m. Most resistivity values are between 1 and 3 Ω -m, with a few higher and lower values. The half-space resistivity is in the thousands.

Basokur again fits a model which is more in keeping with the data than with the expected situation. Over considerable parts of the line, Basokur also brings

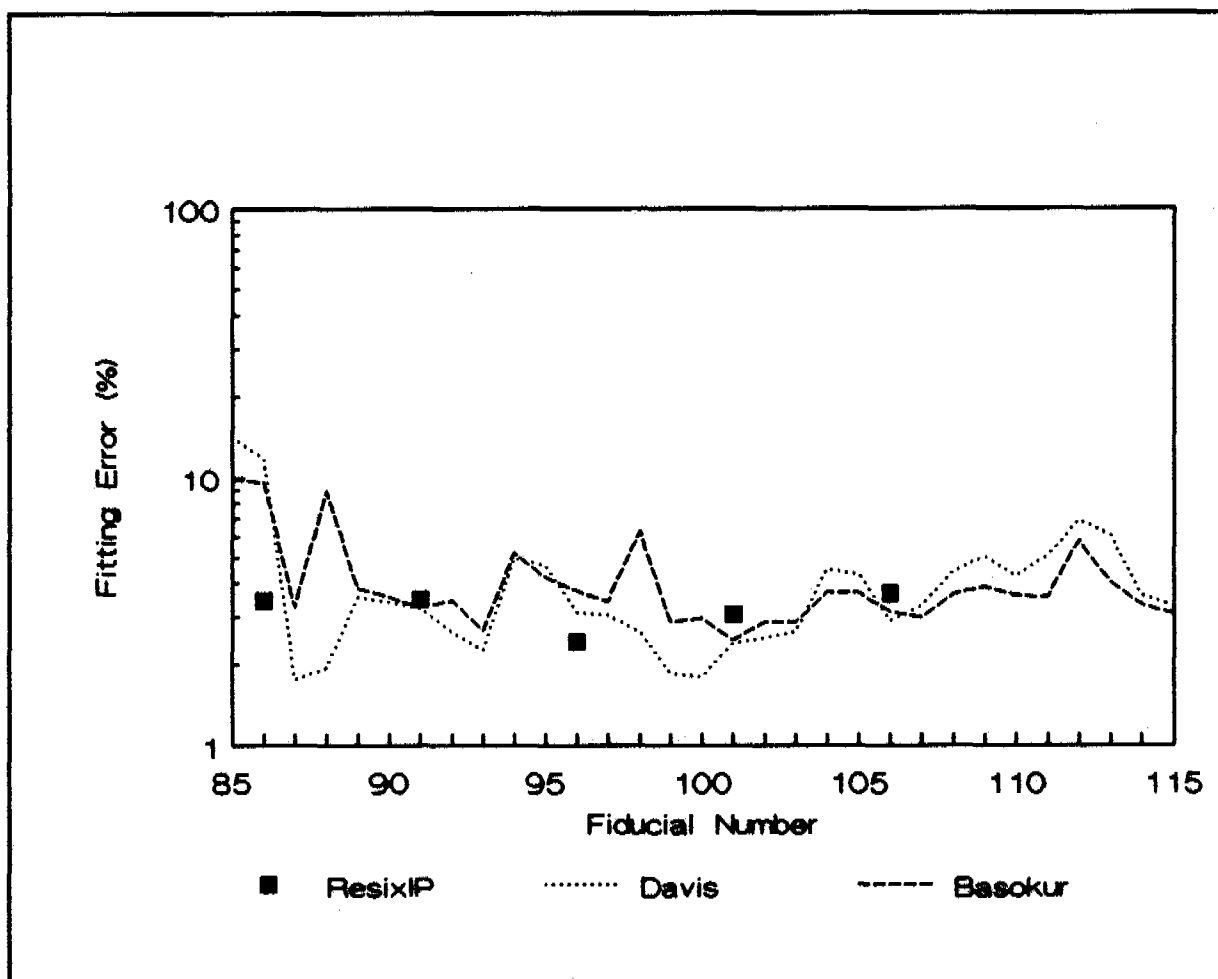


Figure 15: Fitting errors on Line J2N for three inversion routines.

the overburden layer to zero. Half-space resistivity values are quite low, ranging from 2 to 5 Ω -m. No decrease in error sets Basokur apart from the other inversions in terms of goodness of fit. An interpreter having no prior knowledge of a model to work with would find Basokur's inverted models quite acceptable.

Line J3S

Figure 16 (in pocket) shows the raw data and the results of inversions on Line J3S, laid out in the same manner as Figures 12 and 14. Note that this line was run from north to south, and North has thus been plotted on the left hand side of the profile. The only place which appears from the acoustic records to have any overburden is the north end of the line. Outcrop is present for most of the rest of the line.

Figure 17 shows the distribution of fitting errors on the same line. Average fitting errors are slightly higher than those for lines J1S and J2N. When the comparison is based on the same fids, ResixIP appears to have a lower fitting error.

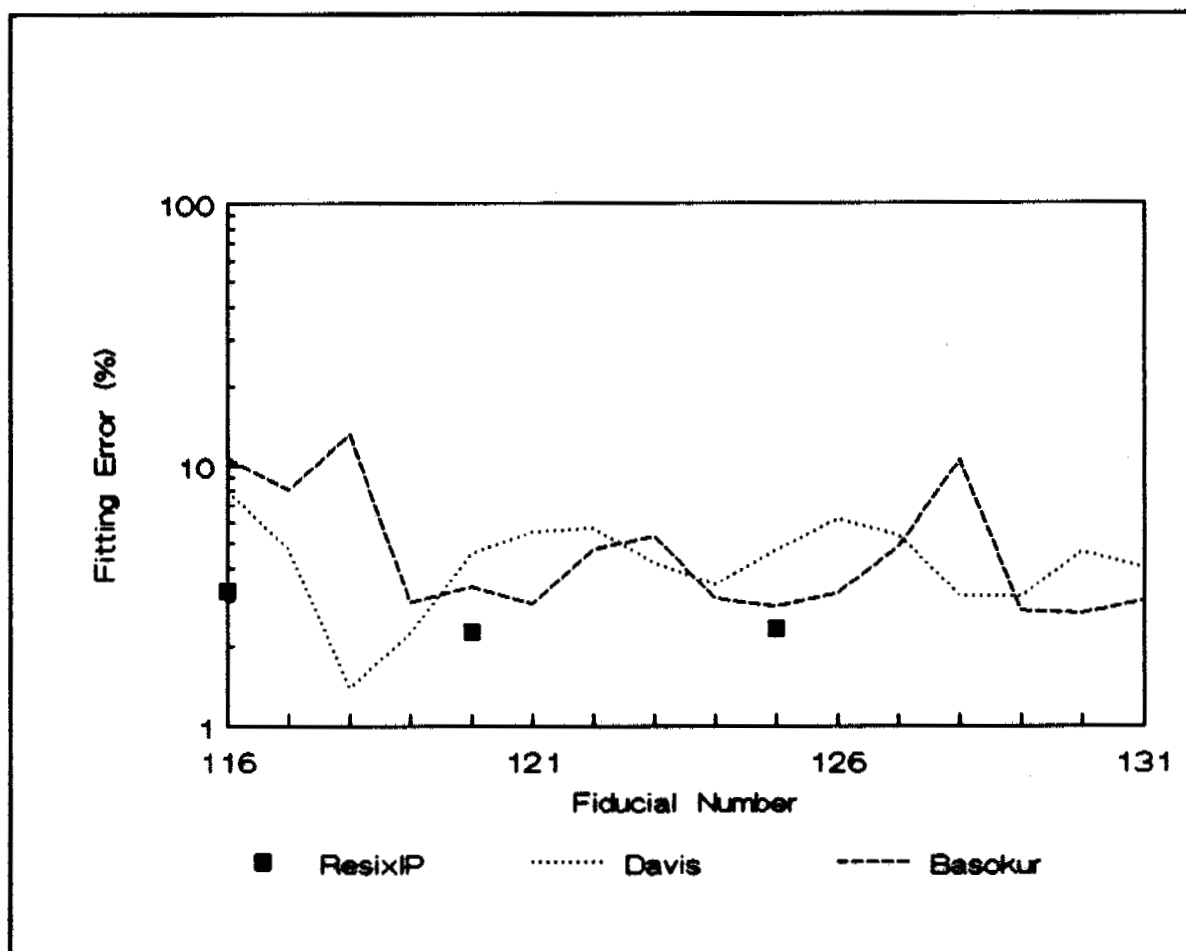


Figure 17: Fitting errors on Line J3S for three inversion techniques.

The ResixIP inversions appear to be well defined, and the interpreted thickness of overburden ranges from 16 to 21 metres, with resistivity values of 1.8 to 2.3 Ω -m and reasonable low fitting errors. The half-space resistivity values are appropriately in the thousands of ohm-metres. Once again, there is a conflict between the acoustic indication of outcrop and the ResixIP indication of a well-defined overburden layer.

Davis on this line does not always show an overburden layer. At Fids 116 to 118, 127 to 129, and 131, Davis sets the second layer infinitely thick. At Fid 123 the second layer thickness is set to 0. Between these sections, the interpreted overburden is from 15 to 30 metres thick with a resistivity ranging from 1.2 to 6.0 Ω -m. Where interpreted to be present within the range of the array, the half-space has quite high resistivity values.

On Line J3S Basokur fits almost all of the section with one layer (the seawater) on a half-space. At only 3 fids (120, 121 and 125) does Basokur show 7 to 25 m of overburden with 2 to 6 Ω -m. Even this interpretation is overly optimistic in showing such thick overburden. As on the other lines, bedrock resistivity values are less than ten ohm-metres, which is in accord with the apparent resistivity soundings, if not with the acoustic interpretation and

expected bedrock resistivity values.

On all three Fundy lines the use of a 10-metre array does not help the problem of resolving thin layers on bedrock. In areas of small vertical contrasts in resistivity, the array should provide information to depths of 30 to 40 metres. Because of the large resistivity contrast between seawater and bedrock, however, the resolving power of the array is very limited. Under such conditions even fixing the known depth and resistivity of the water does not improve the vertical resolution of the readings. It is unfortunate that efforts to improvise a logarithmic array for this survey were unsuccessful, because such an array should improve vertical resolution.

Running Inversions, Conception Bay Data

Figure 18 shows the survey area in Conception Bay, west of St. John's. At this site, several attempts were made to improvise a logarithmic array. On 23 December 1993, profiles were run on coincident lines with a 25 metre multi-dipole array (Line L1) and with a makeshift logarithmic streamer which gave the first 5 channels of the Hardy array specified in Table II (Line L5). The survey was run along the 10 metre bathymetric contour, over a bottom known from grab sampling to be dominantly sands and gravels lying on bedrock. Acoustic measurements by other C-CORE workers in the past year have indicated that the cover was thin, but penetration of acoustic signals to bedrock was rare.

Figure 19 (in pocket) shows the raw data collected with dipole and logarithmic arrays, together with the results of inversions with four routines. Although the south-west part of Line L5 was coincident with Line 1, Line 5 extended farther north than Line 1; only the coincident part is shown in Figure 19. A salinometer was used to obtain water resistivity, and the vessel's depth sounder was read at intervals as well.

Figure 20 shows the distribution of fitting errors along the lines for the various inversion schemes. Because Line L5, run with the logarithmic array, was longer than the others, a complete data set is included in Appendix A as Printout A-9. For multi-dipole inversions, the average fitting error for Davis was 3.39%, and for Basokur 3.99%. For the five fids at which ResixIP inversions were performed (Fids 2, 8, 13, 18 and 22), average fitting errors for ResixIP, Davis and Basokur were 3.45%, 3.33% and 4.18% respectively.

The Hardy inversion was complicated by having only five values of apparent resistivity, while the routine was written for six. A sixth value was estimated for each sounding by extrapolation. The Hardy routine fitted all soundings with an average error of 8.6 %, and the five equivalent to Fids 2, 8, 13, 18 and 22 with an average error of 7.77%. The Hardy routine moves its model parameters a limited amount in each inversion, and it appears to have taken the first four fids (-3 to 0) to settle into a stable fitting error. This error is a bit higher than was expected, but could probably be reduced with a logarithmic array built for the purpose. In the next phase of development of the MICRO-WIP, it is planned both to increase the number of channels and to build an appropriate logarithmic array.

Four of the five inversions with ResixIP showed a thin layer (2.5 to 3 m,

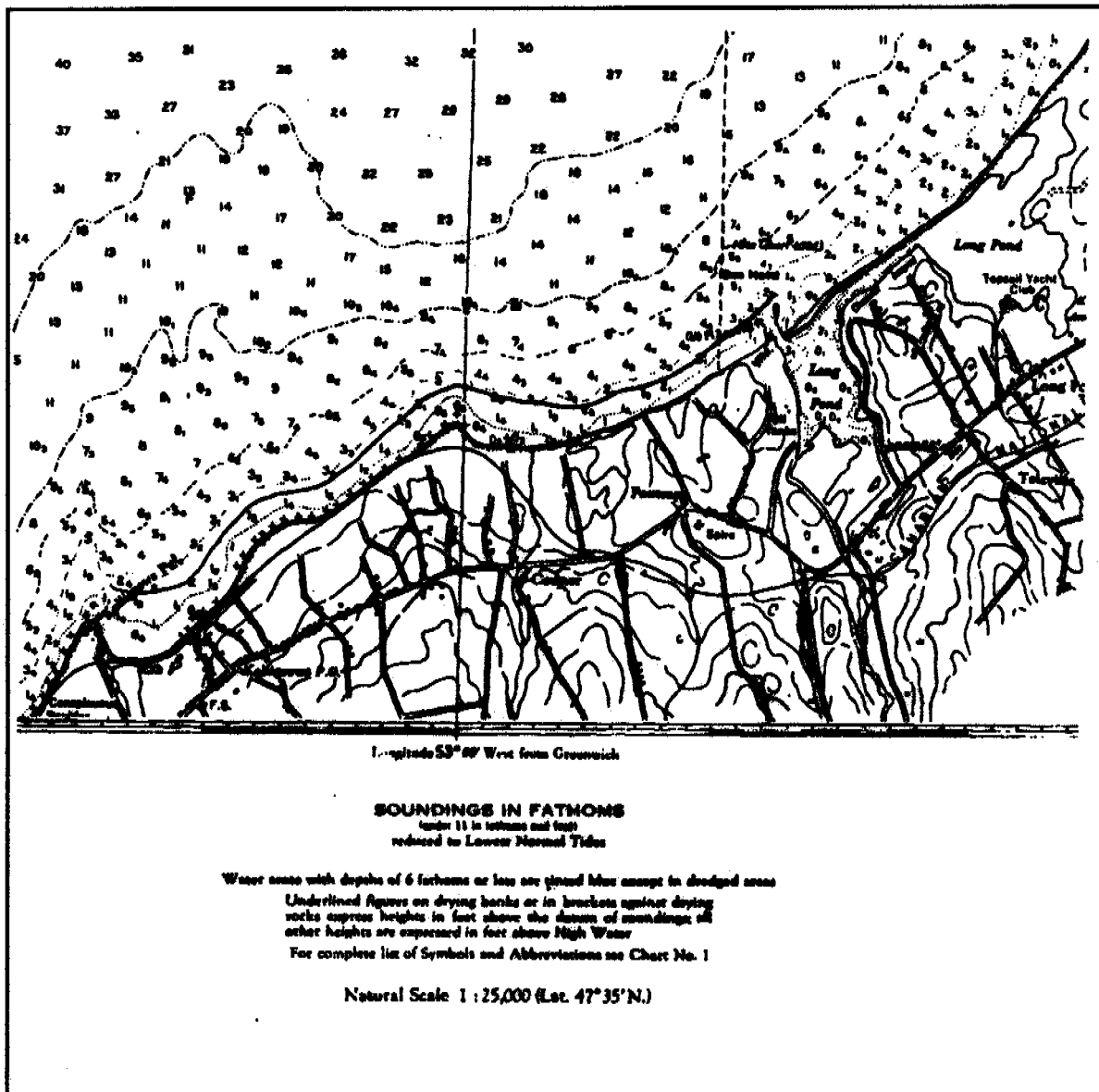


Figure 18: Location of survey line, Conception Bay.

0.16 to 0.18 $\Omega\text{-m}$) above a half-space of about 200 $\Omega\text{-m}$. The fifth set a 6 m layer of 0.37 $\Omega\text{-m}$ on a 20 $\Omega\text{-m}$ half-space. Without acoustic or other control, it is difficult to say how accurate the interpretation is. C-CORE will be running acoustic profiles with a new system in the area in the near future, and control will ultimately be available.

Inversions with the Davis routine show an intermittent thin layer on a half-space with resistivity values from 180 to 430 $\Omega\text{-m}$. The overburden layer is about a metre thick at the south end of the line, but thins to 0 for Fids -1 to 1, thickens to about 2.5 m for Fids 2 to 7, thins again for Fids 8 to 11, and then thickens to 2 to 3 metres, with one thicker area near Fid 21. Where there is some thickness to the layer, the resistivity is interpreted to be about .18

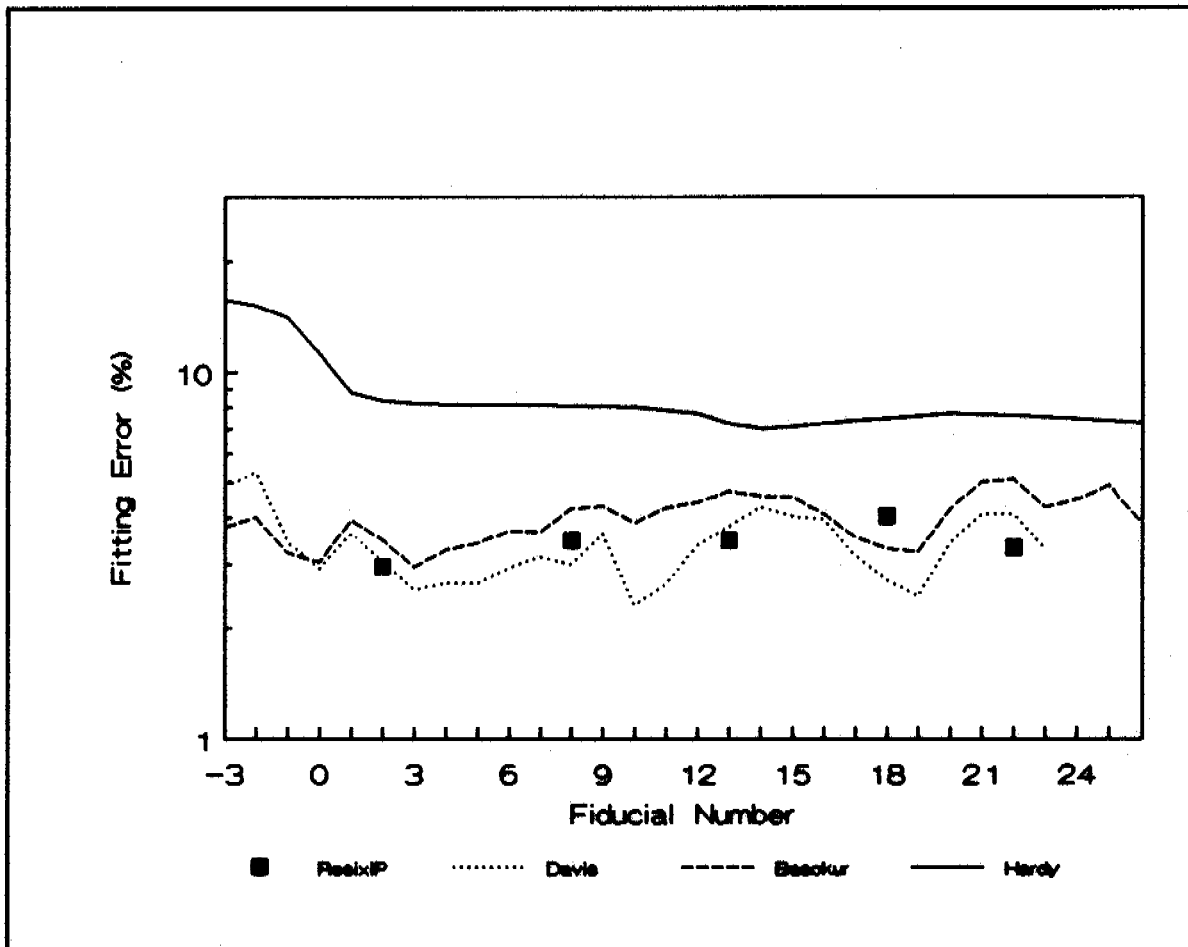


Figure 20: Distribution of fitting errors on Lines L1 and L5, Conception Bay.

Ω -m. This interpretation agrees well with that of ResixIP.

The Basokur routine gives a somewhat different picture. On the south-west part of the line, Basokur sets the thickness and resistivity of the second layer to 0, and fits a resistivity of 4.8 to 6.8 to the half-space. North-east, of Fid 13, there is a second layer which increases in thickness to a maximum of 37 metres, before decreasing to about 20 m at the end of the line. This layer has resistivity values of 5 to 8 Ω -m, and lies on a half-space of about 3.4 Ω -m.

The Hardy routine starts out with a high fitting error, and takes the first five fids to settle to an error of about 8 percent decreasing to about 7 percent along the line. Once stable, Hardy fits a second layer of 5 to 13 metres in thickness, with a resistivity of about .16 to .38 Ω -m. The half-space has a resistivity of 5 to 13 Ω -m. The Hardy routine thus gives half-space resistivities which fall between those from Davis and Basokur, and a second layer thicker than that of Davis, and thinner than that of Basokur, at the north-east end of the line. The Hardy routine agrees with Davis and ResixIP in assigning to the second layer resistivity values of less than one Ω -m.

Discussion of Running Inversions

The work done in inverting resistivity data from three different areas demonstrates that it is possible to set up a program to collect resistivity data, while at the same time inverting it in terms of a layered model. It is difficult to choose any inversion algorithm which is better than the others in all situations. In running inversions there is no time to optimise the model after the inversion, as there is when individual soundings are being handled by an interpreter. Generally, the fitting errors are larger than can be achieved by an operator making repeated adjustments one each model interactively.

Each inversion offers a different type of model after inversion. ResixIP provides a fit which is relatively close in configuration to the starting model. Davis tends to choose either very high or very low resistivity values for the half-space, and to incorporate most of the changes along the line into the parameters of the second layer. Basokur tends to provide the lowest half-space resistivity that will fit the sounding data, and also tends to reduce the second layer to minimum thickness at times.

All routines, particularly Davis, are sensitive to the starting model. Because each inverted model is used as the start for the next inversion, the routines do not track well when there are strong changes in apparent resistivity along the survey line. It is possible that such rapid lateral changes invalidate the idea of carrying out 1D inversions, and that recourse must be made to 2D modelling in such cases.

Of the routines investigated, only ResixIP offered a simple way to investigate the limits of equivalence. The work described above, however, indicates that, for a given sounding, there are equivalent resistivity-depth functions which give as low a fitting error as the original ResixIP case, yet do not fall within the equivalence envelope defined by ResixIP. It is clear that some constraints can be applied if something is known of the geology, but equally clear that these constraints are difficult to change in real time.

Influence of Starting Models

During the inversions reported upon above, it became clear that starting models have an influence on the results of the inversion.

To demonstrate this impact, which is particularly pronounced with the Davis routine, the data for Lines 22A and 45A from the Beaufort Sea were rerun with different starting models. Table VIII shows the starting models used for these tests.

The Line 22A test measures the impact of changing the resistivity of the half-space. The first attempt at a starting model used 27.4 Ω -m, twice the apparent resistivity for $n = 6$, as the half-space value. The Davis routine (A-10 in Appendix A) fitted a very low resistivity to the half-space, with an error in the first fit of 60%, and on the whole line of 77%. When the starting half-space resistivity was raised by an order of magnitude to 285 Ω -m, Davis then fitted a

very high value (53.7 k Ω -m) (A-11 in Appendix A). This second starting model reduced the error by an order of magnitude. With some fine tuning the error might be reduced still further, but this would not be possible in a running inversion. Unfortunately the fit deteriorates within a few fids to an overall average error of 59%, probably because the fitted half-space resistivity is too high to provide stability when put into subsequent inversions as a starting model.

Line	Line 22A				Line 45A			
Printout (Appendix A)	A-10		A-11		A-7		A-13 A-12 (no error, Fid 5253)	
Parameter	Start	First Fit	Start	First Fit	Start	First Fit	Start	First Fit
Water (fixed) Resistivity Depth	1.25 1.0	1.25 1.0	1.25 1.0	1.25 1.0	5.75 2.8	5.75 2.8	5.75 2.8	5.75 2.8
Second Layer Resistivity Depth	5.63 5.0	14.3 2.8	4.59 3.39	7.23 34.7	1.73 5.0	1.94 27.9	1.75 153	1.75 154
Half-Space Resistivity	27.4	7.2	285	53654	2.88	1.4	785	784
Error (%)		60.2		5.95		4.07		8.31
Mean Error (%) For Whole Line	76.7		58.7		55.1		56.7	

Table VIII: Starting models and first fits, Davis inversion routine.

The Line 45A pair includes a change in second layer thickness as well as half-space resistivity. The model for Printout A-7 (Appendix A) used 2.88 Ω -m, twice the apparent resistivity at $n = 6$, as a starting value for the half-space, and 1.73 Ω -m, the apparent resistivity for $n = 3$, as the starting value for the second layer. The result for the first fid was a thickening of the second layer with little change in resistivity, and a drop in the resistivity of the half-space. Some adjustment could reduce the fitting error from the observed 4 %, if a single data set was being inverted. The second starting model used a much

thicker second layer and a much more resistive half-space; the inversion results (A-13, Appendix A) show the second layer and the half-space unchanged, and a fitting error of 8 %. Note that both A-7 and A-13 show quite small fitting errors until Fid 5253, where a misread gain has resulted in an erroneous apparent resistivity value of 9.86 $\Omega\text{-m}$. In an attempt to match the jump in apparent resistivity for $n = 6$, the Davis routine raised the half-space resistivity from 214 $\Omega\text{-m}$ to 99999 $\Omega\text{-m}$. The result of this inversion was the starting model for the next data set on the line, and Davis never recovered from the sharp change in half-space resistivity. Basokur, on the other hand, (A-8, Appendix A) fitted that value with a high error (101 %), and was not deflected from tracking the following data sets. Such an abrupt change in one apparent resistivity throws the Davis routine into a strong misfit, from which it never really recovers. Both A-7 and A-13 result in fitting errors of 55 % averaged over the entire line.

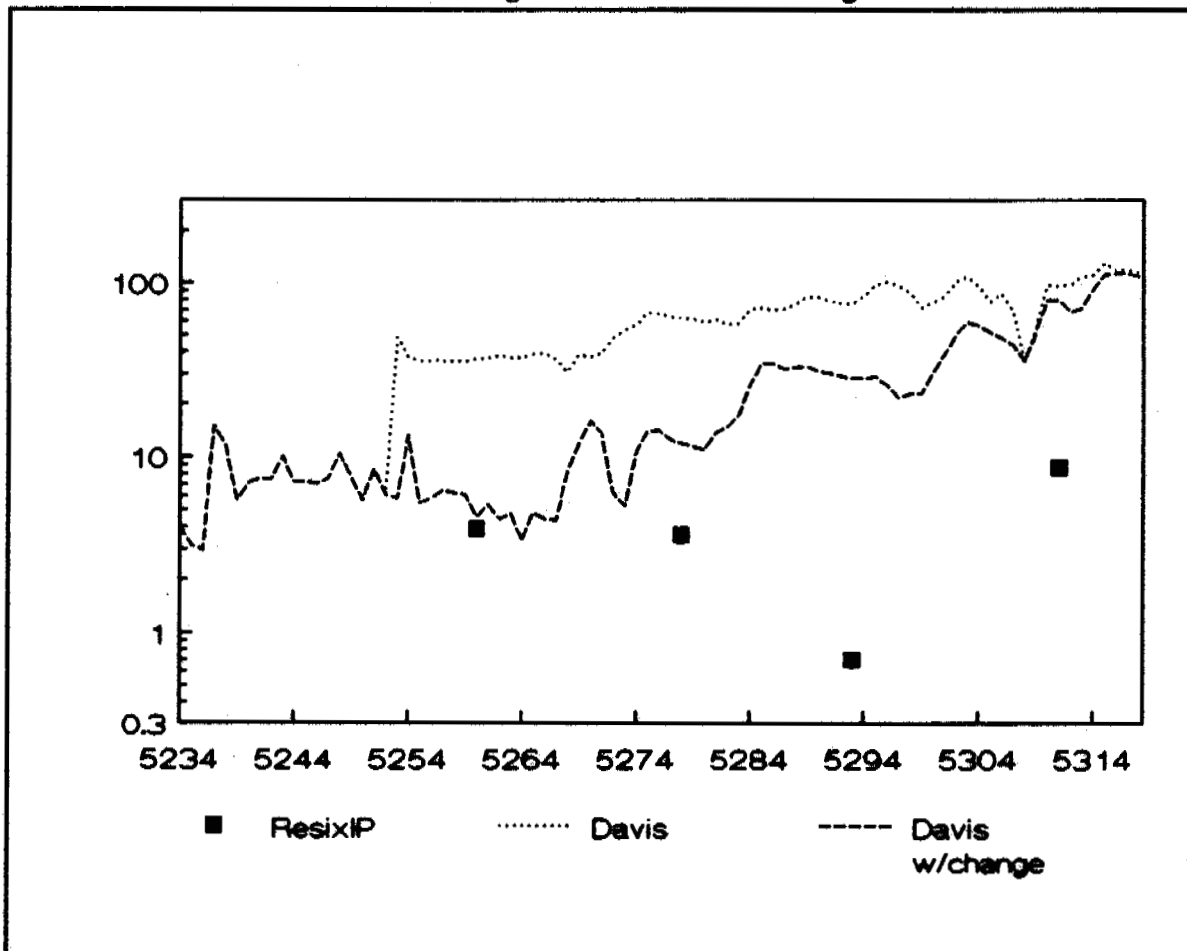


Figure 21: Comparison of fitting errors for Davis routine in Line 45A with and without correction of the high apparent resistivity value at Fid 5253.

To appraise the impact of the incorrect apparent resistivity value on Line 45A, the resistivity for $n = 6$ at Fid 5253, Line 45A, was changed from 9.86 $\Omega\text{-m}$ to 1.56 $\Omega\text{-m}$. The inversion results are shown in Printout A-12 in Appendix A. Figure 21 shows the resulting change in the distribution of fitting errors on the line. With the correction, the Davis routine held realistic half-space

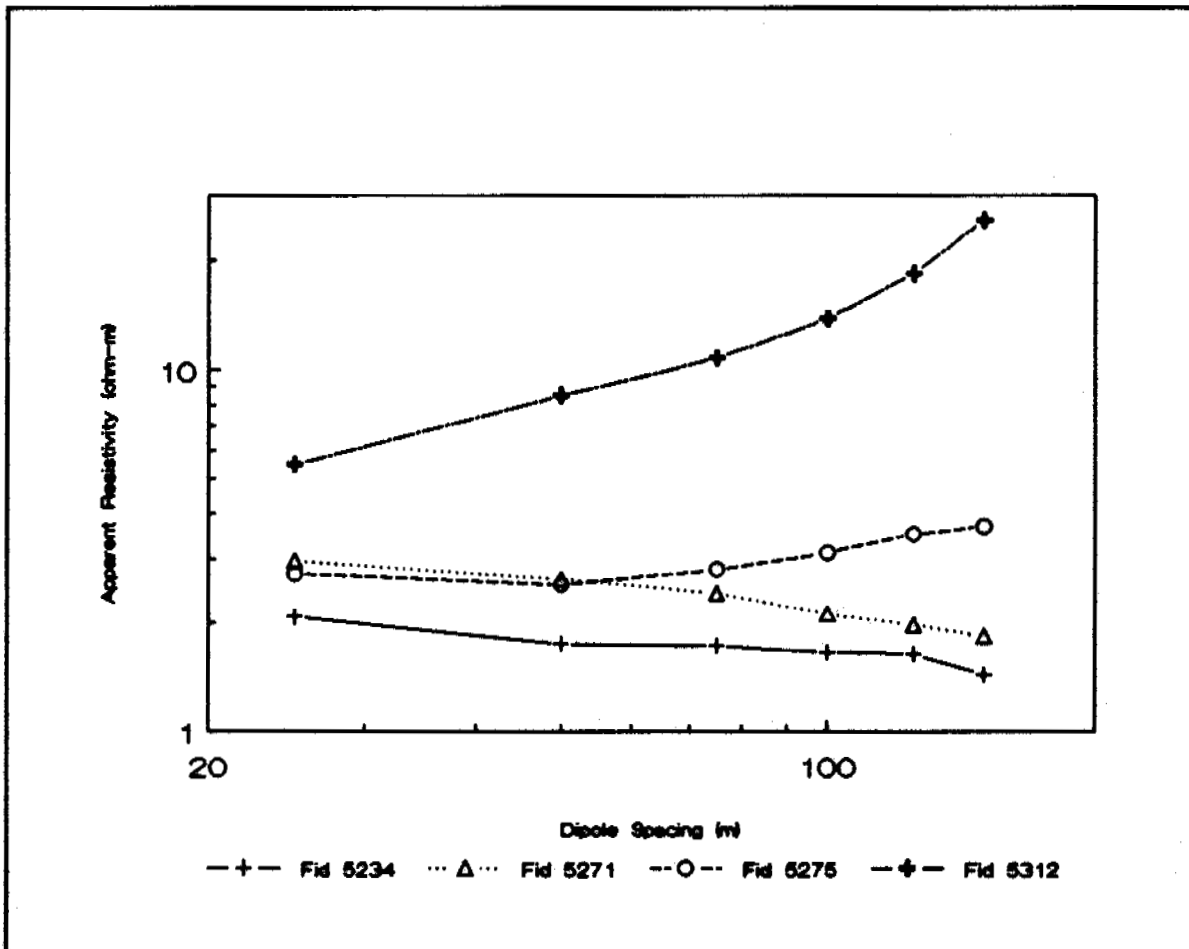


Figure 22: Sounding curves from Line 45A, Beaufort Sea, showing change in slope with position.

resistivity values from the start of the line to Fid 5273, at which the slope of the sounding curve changed from negative to positive. To illustrate this change, Figure 22 shows four sounding curves from Line 45A:

- at Fid 5234, the first fid of the line (fit shown in Table VIII),
- at Fids 5271 and 5275, just each side of the change, and
- at Fid 5312, the highest apparent resistivity for $n = 6$.

At the change in slope (Fid 5273), Davis set the half-space resistivity to zero $\Omega\text{-m}$ for the low-resistivity half-space starting model (Printout A-12), and to 100 $\text{k}\Omega\text{-m}$ for the high-resistivity half-space starting model (Printout A-13). For both cases, from then to the end of the line, the fit gradually worsened. If the Davis routine were to be used for running inversion, it would be necessary to provide for an automatic halt for correction of the starting model, or else an automated resetting of the starting model, when conditions changed in such ways.

The Basokur routine did not appear to be as sensitive to the abrupt change as Davis. To see if the Hardy routine was sensitive, the apparent resistivity

for $n = 6$ at Fid 111 was increased from 2 to 10 Ω -m, and the inversion was run again. The results are shown on Printout A-14, Appendix A. While the fitting error is higher at Fid 111, there is no real change in the inversion on the rest of the line. It appears that Davis is the most sensitive of the routines to changes in the starting model. For this reason, Davis is the least attractive routine for automated running inversions.

Inversions with Fixed Layer Thicknesses

Evaluation of the equivalent models determined by inversion shows that frequently the equivalence arises from the difficulty in separating the thickness of a layer from its resistivity value. To avoid this difficulty, the possibility was investigated of fixing layer thicknesses so that the inversion was called on to determine resistivity values only. With fixed thicknesses, it is possible to increase the number of layers above the half-space to six. The first layer, the water, has resistivity and thickness known from direct measurement, so that there are six unknown resistivity values in such a model. The resistivity values thus determined are used to construct a resistivity-depth curve.

In this approach six model resistivity values are calculated for six apparent resistivity values. Noise in any apparent resistivity value will be reflected in fluctuations in interpreted model resistivity values. If the model layers are sufficiently thin in the shallow part of the model, and if the field data are smooth enough, then this approach can yield useful information on the properties of the shallow sub-bottom.

To test this idea, a seven-layer model (i.e., six layers on a half-space) model was established. The first layer (water) thickness and resistivity were fixed as observed in the survey. The thicknesses of layers 2 through 6 were held fixed. The Davis inversion routine was used with the observed apparent resistivity values for Line 10D to determine the resistivity values of layers 2 through 6 and of the half-space. All fids on this line (967 to 1208) were included in the running inversion.

Several ways of fitting a seven-layer model were tested, as outlined in Table IX below. Each row in the table represents an increase in computation time over the preceding one.

Test 1:

In Test 1, each data set in the line was first inverted using the Davis routine and a 7-layer model with fixed thicknesses. For the starting model of each inversion, the layer thicknesses were held constant. The values used for first layer (water) thickness and resistivity were the ones recorded at the time of the survey. Table X shows the starting model for the first inversion. The second to sixth layer thicknesses used held constant at 1, 2, 4, 8, and 16 meters. The resistivities from the final model from each inversion was used as the starting model for the next.

The full set of results is listed in Appendix A, Printout A-16. The distribution of the fitting error along the line is shown in Figure 23. The mean fitting error for the whole line is 18.9 %, which compares favourably with 64 %

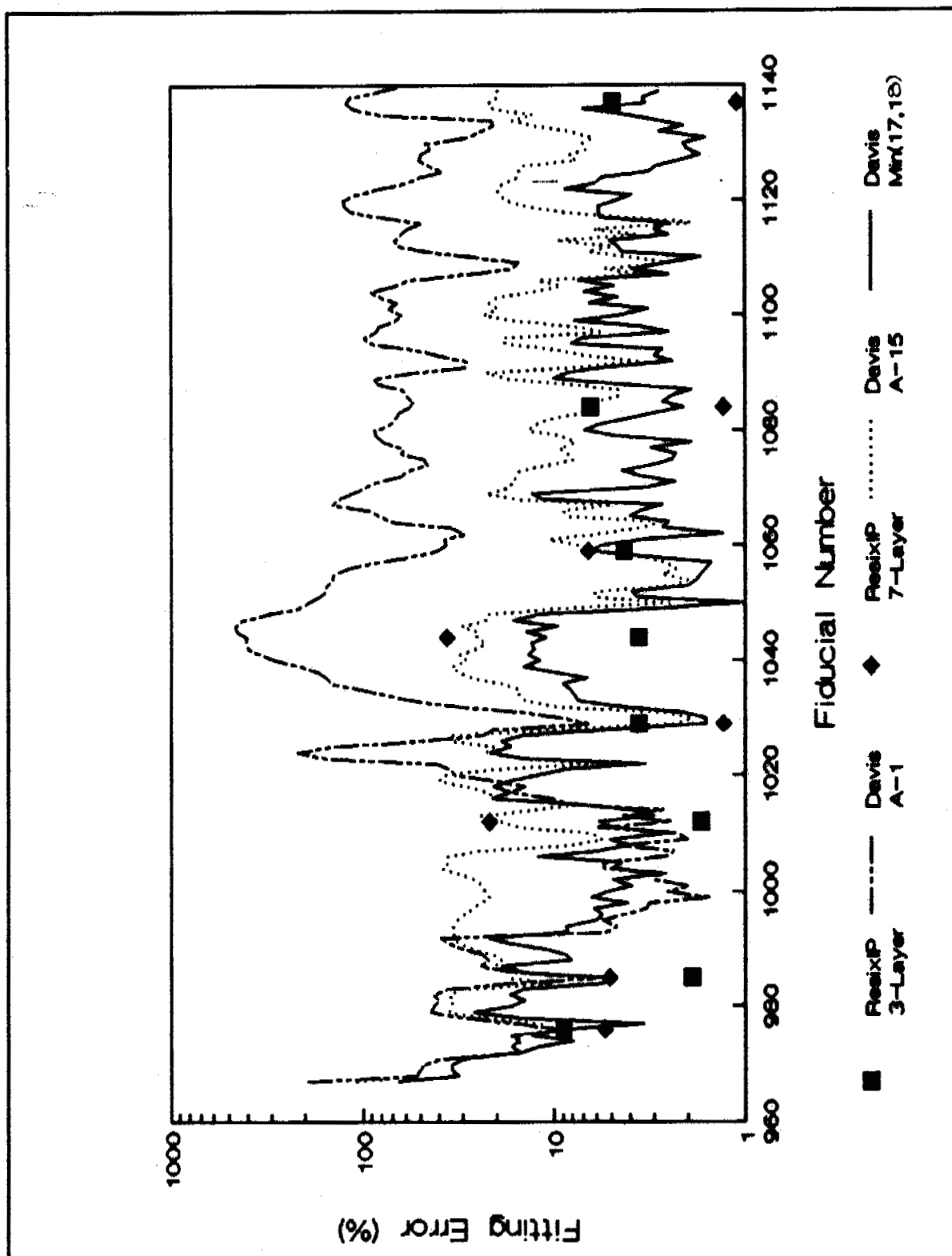


Figure 23: Distribution of fitting errors along Line 10D for various approaches to multi-set inversion with the Davis routine.

Test	Start Models for first fid (7 layers)	Subsequent Starting Models	Routine & Appendix A Printout	Mean Error (%), up to Fid 1208 Fid 1139
1	1 set, T fixed 1 set Rho	Same T set, but Rho set from last fid	Davis A-15	18.9 17.2
2	Best fit from Test 1	Best fit from Test 1	ResixIP	
3	5 sets T fixed 1 set Rho	Same T set, but Rho set from last fid	Davis A-16	
4a	3 High Rho x 5 T sets. 16th start: best fit of the 15 inversions.	Same 3x5 sets. 16th start: best fit of 15 inversions at last fid. Best outcome kept.	Davis A-17	- 11.8
4b	3 Low Rho x 5 T sets 16th start: best fit of the 15 inversions.	Same 3x5 sets. 16th start: best fit of 15 inversions at last fid. Best outcome kept.	Davis A-18	- 9.5

Table IX: Summary of tests with 7 fixed layers, Davis and ResixIP.

for the initial trial (see Table II above). It appears that the Davis routine does not get as easily removed from close fits as is the case with the three-layer model fitted above. The half-space resistivity rises steadily along the line, in a manner which is not consistent with the behaviour of the apparent resistivity values in the pseudosection of Appendix A, Printout A-1. The resistivity of the second layer (1 m thick) remains low ($>1 \Omega\text{-m}$) all along the line. Resistivity of the second, third and fourth layers rises consistently along the line, while the resistivity of the sixth layer is generally less than $1 \Omega\text{-m}$ except from Fid 1140 to Fid 1161, where it rises to levels of about $16 \Omega\text{-m}$. As the resistivity values of the third, fourth and fifth layers and the half-space rise, so does the fitting error.

Test 2:

In Test 2, the same starting model (Table X) was inverted with ResixIP at eleven selected fids. The same fids were selected that were used for the comparisons of Table III. The values shown in Table X were used as the starting model for each inversion using the ResixIP routine. Values for first layer thickness and resistivity used were the ones recorded at the time of the survey. Model thicknesses were held constant.

The results of the inversions are listed in Table B-1 in Appendix B. The errors of fit for the seven-layer models are shown in Figure 23. In some cases, (Fids 1029, 1084, 1137) the seven-layer error is lower than the three-layer error. These solutions show a smooth progression of resistivity with increasing

depth. Fids 976 and 1059 show oscillation in resistivity variation with depth which probably reflects small fluctuations in the sounding curve. Fids 1164 and 1192 show gross errors, and their resistivity distribution still resembles that of the starting model. It is possible that in these cases the starting model is too unrealistic to allow a reasonable progression to a fit.

Table X: Starting model for inversions of Test 1 and Test 2

Layer	Thickness m	Resistivity Ω -m
1	Water Depth	Water Rho
2	2	10
3	3	100
4	5	500
5	8	750
6	12	1000
7	Infinite	5000

Test 3:

In Test 3, each data set was inverted 5 times using the Davis routine. Five different layering combinations were used.

The layer resistivities of the final model were used as the starting model layer resistivities for inversion of the next set of apparent resistivity values. The best models from these inversions were then used as the starting models in ResixIP.

The five sets of thickness are as follows:

Set 1: Tlayl, 2, 3, 5, 8, 12
Set 2: Tlayl, 4, 4, 4, 8, 16
Set 3: Tlayl, 2, 4, 6, 8, 10
Set 4: Tlayl, 3, 4.8, 6, 6.9, 7.8
Set 5: Tlayl, 2.2, 3.1, 4, 5.2, 7

After a set of apparent resistivities was inverted, the model with the lowest error was selected for retention. Printout A-16, Appendix A, shows the full set of results from this test.

For the set of selected fids shown in Table III, the final models from the Davis inversions were then used as the starting models for a seven-layer inversion with ResixIP. The results of these inversions are compared with the Davis models in Table B-2, Appendix B.

Test 4a:

Test 4 was carried out in two parts. For each part, each data set was inverted 16 times with a different starting model each time. In each case, the 16th starting model was the best fit model of the inversion of the previous data set. The final model with the smallest error was recorded.

Each data set was inverted 16 times. The starting models were made up of combinations of thicknesses and resistivities as follows:

T-set 1:	Tlayl, 2, 3, 5, 8, 12
T-set 2:	Tlayl, 4, 4, 4, 8, 16
T-set 3:	Tlayl, 2, 4, 6, 8, 10
T-set 4:	Tlayl, 3, 4.8, 6, 6.9, 7.8
T-set 5:	Tlayl, 2.2, 3.1, 4, 5.2, 7
R-set 1:	Rlayl, 10, 50, 100, 500, 1000, 5000
R-set 2:	Rlayl, 10, 1000, 1000, 10k, 10k, 10k
R-set 3:	Rlayl, 10, 10k, 10k, 10k, 1000, 1000

As an example, Starting Model 1 was made up of T-set 1 and R-set 1, Starting Model 2 of T-set 1 and R-set 2, and so on. In each case, the 16th starting model was the best fit model of the previous inversion. The model from each set of inversions with the lowest error was retained. A full set of results is shown as Printout A-17 in Appendix A. Because of the great amount of computation time, only Fids 967 to 1139 were used for this test. Even so, computation time on a 486-33Mhz machine was twenty-two hours for this test. Over this interval, the mean fitting error was 11.8 %.

At the same set of selected fids shown in Table III, the final models from the Davis inversions were then used as the starting models for a seven-layer inversion with ResixIP. The results of these inversions are compared with the Davis models in Table B-3, Appendix B.

Test 4b:

Each data set was inverted 16 times as in the previous section but with the starting model values which used mainly lower resistivity values as follows:

T-set 1:	Tlayl, 2, 2, 3, 5, 10
T-set 2:	Tlayl, 2, 2, 2, 2, 2
T-set 3:	Tlayl, 4, 4, 4, 4, 4
T-set 4:	Tlayl, 2, 2, 2, 4, 8
T-set 5:	Tlayl, 3, 3, 3, 5, 15
R-set 1:	Rlayl, 5, 10, 20, 40, 80, 160
R-set 2:	Rlayl, 10, 10, 10, 10, 10, 10
R-set 3:	Rlayl, 50, 50, 50, 50, 50, 50

As before, the 16th starting model was the best fit model of the previous inversion. A full set of results is shown as Printout A-18 in Appendix A. Again because of the great amount of computation time, only Fids 967 to 1139 were used for this test. Over this interval, the mean fitting error was 9.5 %.

Because the two halves of this test really represent one full range of resistivity values and thicknesses, the two sets of results were combined by selecting for each fid the model with the lower error of fit. With this selection, the mean error of fit was reduced to 7.7 %.

At the same set of selected fids shown in Table III, the final models from the Davis inversions were then used as the starting models for a seven-layer inversion with ResixIP. The results of these inversions are compared with the Davis models in Table B-4, Appendix B.

Trials on Theoretical Models:

Included in Basokur, 1989 is a set of apparent resistivities recorded using a Schlumberger array. The area surveyed consisted of a soil layer, a layer of pebble-supported stream deposits (alluvium), and clay. The clay layer was known to start at 27m. The sounding and results of the Basokur inversion are shown in Tables XI and XII.

Electrode Spacing AB/2	Measured Apparent Resistivity
4	4.13
5	4.23
6	4.51
7	4.95
8	5.24
9	5.30
10	5.87
12	6.16
15	6.55
20	7.06
25	7.26
30	7.57
40	7.77
50	7.13
60	7.16
70	6.58
80	6.61
90	6.38
100	6.07

Table XI: Schlumberger sounding from Basokur.

To check the validity of the Basokur routine, the data in Table XI was inverted using ResixIP. Although the Basokur routine does not require a starting model, the routine as published requires considerable user input during the progression of the inversion. Fortunately, the test data set is so well defined that the inversion was performed using the default values calculated by the routine.

ResixIP requires a starting model. The data in Table XI were inverted by ResixIP with the model in Table XII as the starting model (first layer parameters were left free). The results shown in Table XII had a fitting error of 1.9 percent. It can be seen that the Basokur model is quite similar to the ResixIP model.

The Basokur test data was also inverted with ResixIP and different starting models. It was assumed that the first layer thickness and resistivity were known. Two inversions were performed using the starting model shown in Tables XIIIa and XIIIb. The results in Table XIIIa were calculated allowing first layer resistivity and thickness to be varied by ResixIP. The fitting error was 2.7 percent. In Table XIIIb, the first layer parameter were held fixed. The fitting error was also 2.7

percent. Knowing that the depth of the half space is at 27m, it is clear that for the starting model in Table XIII, a more accurate solution was achieved by fixing the first layer parameters.

	Basokur Inversion		ResixIP Inversion (1.9 %)					
Layer	T m	Rho Q-m	T min	T best	T max	Rho min	Rho best	Rho max
1	4	4	2.6	3.4	4.3	3.3	3.6	3.9
2	21	9.2	14.2	22.2	33.5	8.3	9.1	10.0
3		5.2				4.5	5.2	5.8

Table XII: Inversion with ResixIP of solution by Basokur of sounding of Table XI.

	Starting Model		ResixIP Inversion First layer free (2.7 %)					
Layer	T m	Rho Q-m	T min	T best	T max	Rho min	Rho best	Rho max
1	4	4	4.2	5.3	6.2	3.5	3.9	4.2
2	10	100	1.3	5.9	7.3	14.3	22.6	59.9
3		10				5.5	5.9	6.3

Table XIIIa: Inversion with ResixIP, all layers free.

	Starting Model		ResixIP Inversion First layer fixed (2.7 %)					
Layer	T m	Rho Q-m	T min	T best	T max	Rho min	Rho best	Rho max
1	4	4	-	4	-	-	4	-
2	10	100	14.1	23.1	33.5	8.6	9.1	9.7
3		10				4.6	5.1	5.9

Table XIIIb: Inversion with ResixIP, first layer fixed.

	Starting Model		ResixIP Inversion (1.9 %)					
Layer	T m	Rho Q-m	T min	T best	T max	Rho min	Rho best	Rho max
1	10	1	2.6	3.3	4.1	3.2	3.6	3.9
2	10	10	15.9	23.3	35.7	8.3	9.0	9.7
3		100				4.3	5.1	5.9

Table XIV: Inversion with ResixIP with all layers free.

Finally, the Basokur data was inverted by ResixIP using the starting model shown in Table XIV. As the starting models of the previous two inversions were based on some prior knowledge of the first layer parameters, this starting model was more general. First layer parameters were free. Table XIV also shows the results of the inversion. The fitting error was 1.9 percent. It can be seen that even for a general starting model, good results were achieved without prior knowledge of the first layer.

To compare the performance of the inversion routines, ResixIP was used to create a theoretical sounding for a dipole-dipole array. The sounding consisted of apparent resistivities for 19 dipole spacings. In the context of marine soundings, the idea of 19 dipole spacings is optimistic, but the data sets are theoretically valid. Table XV shows the sets of apparent resistivities produced for dipole-dipole arrays with 5 and 10 m dipoles.

Table XVI shows the models corresponding to the soundings. The apparent resistivities from Table XV were then inverted by the Davis and Basokur routines.

Dipole Multiple n	Apparent Resistivity 5 m dipoles Model A	Apparent Resistivity 5 m dipoles (Model B) and 10 m dipoles (Model C)
2	4.17	3.25
3	4.21	4.19
4	4.43	5.58
5	4.80	7.07
6	5.23	8.57
7	5.66	10.08
8	6.05	11.60
9	6.38	13.13
10	6.64	14.67
11	6.83	16.21
12	6.96	17.76
13	7.03	19.31
14	7.04	20.86
15	7.01	22.41
16	6.93	23.96
17	6.83	25.50
18	6.69	27.03
19	6.54	28.56
20	6.36	30.07

Table XV: Theoretical soundings for multi-dipole array.

Model	Layer	ResixIP Inversion First layer free						Error of fit (%)
		T min	T best	T max	Rho min	Rho best	Rho max	
A	1	10.7	10.8	11.0	4.2	4.2	4.2	.035
	2	21.7	23.4	24.8	10.2	10.5	10.9	
	3				1.8	2.0	2.3	
B	1	5.7	5.8	5.8	3.3	3.3	3.3	.03
	2	9.6	14.9	21.8	812	1113	1534	
	3				0.0	0.6	4.8	
C	1	11.5	11.7	11.8	3.2	3.3	3.3	.039
	2	9.6	14.9	21.8	729	1272	3055	
	3				0.0	0.6	5.4	

Table XVI: Models for soundings of Table XV.

To begin, the apparent resistivities for Model A (Table XV), with starting values from Table XVI, were inverted with the Davis inversion routine. In the first iteration, the routine returned with the model shown as Pass 1 in Table XVII, with a fitting error of 0.11 percent. As expected, the routine converged quickly and adjusted the starting model minimally.

The same sounding (Model A, Table XV) was inverted twice more with the Davis routine and two other starting models Pass 2 and Pass 3, shown in Table XVII. When the Pass 2 starting model was used, the Davis routine converged after 5 iterations with the model shown. Although the fitting error was 2.9 %, the resemblance between interpreted model and source model was not close. When the Pass 3 model was used as the starting model, the Davis routine was unable to converge.

The Basokur inversion routine does not require a starting model. Instead, the user is required to indicate the branches of the Resistivity Transform curve. For a sounding that has 19 apparent resistivities being inverted into 3 layer model, there are 17 possible branch combinations. To make the inversion routine automated, each set of 19 apparent resistivities was inverted 17 times, once with each of the possible branch combinations. The model with the smallest fitting error was chosen as the final model. When the Model A set of apparent resistivities (Table XV) was inverted with the Basokur routine, the model shown in Table XVIII was fitted with an error of 0.6 percent.

Layer	Starting Thickness m	Starting Resistivity $\Omega\text{-m}$	Fitted Thickness m	Fitted Resistivity $\Omega\text{-m}$	Fitting Error (%)
Pass 1					
1	10.8	4.2	10.9	4.2	.11
2	23.2	10.5	23.0	10.6	
3		2.0		2.0	
Pass 2					
1	10.9	4.2	10.9	4.2	2.9
2	10	100	0.9	83.2	
3		10		5.9	
Pass 3			No Convergence		
1	10.9	4.2			
2	25	80			
3		5			

Table XVII: Inversions of Theoretical Model A with Davis routine.

The apparent resistivities from Model B were inverted by the Basokur routine. The best fit had an error of 19.5 percent and produced the model shown in Pass 5. The apparent resistivities from Model C were inverted by the Basokur routine. The best fit had an error of 19.5 percent and produced the model shown in Pass 6.

The apparent resistivities from Model B, with values from Table XVI as the starting model, were inverted using the Davis inversion routine (Pass 7). Again in the first iteration, the routine returned with the model shown with a fitting error of 0.05 percent. As expected, the routine converged quickly and adjusted the starting model minimally. The same sounding (Model B) was also inverted by the Davis routine using the starting model shown in Pass 8. The routine converged after 4 iterations with the model shown. The fitting error was 2.4 percent, but the fit is not close to the original model.

Finally, the apparent resistivities for Model C (10 m dipoles) were inverted. Using the values in Table XVI as the starting model, they were inverted using the Davis inversion routine (Pass 10). Again in the first iteration, the routine returned with the model shown, with a fitting error of 0.38 percent. As expected, the routine converged quickly and adjusted the starting model minimally. The same sounding (Model C) was also inverted by the Davis routine using the starting model shown in Pass 10. The routine converged after 7 iterations with the model shown. The fitting error was 1.1 percent.

Layer	Starting Thickness m	Starting Rho Ω -m	Fitted Thickness m	Fitted Rho Ω -m	Fitting Error (%)
Pass 4, Model A 1 2 3	Not Required for Basokur		10.9 1.3	4.2 67.5 5.1	.6
Pass 5, Model B 1 2 3			5.8 0.0	3.3 30.7 90.7	19.5
Pass 6, Model C 1 2 3			11.7 0.0	3.3 14.4 88.7	19.5
Pass 7, Model B 1 2 3	5.8 14.9	3.3 1113 0.6	5.6 14.9	3.3 1113 0.6	.05
Pass 8, Model B 1 2 3	5.8 10	3.3 10 100	5.8 37.3	3.3 227 11.6	2.4
Pass 9, Model C 1 2 3	11.7 14.9	3.3 1272 0.6	11.7 17.4	3.3 1272 0.6	.38
Pass 10, Model C 1 2 3	11.7 10	3.3 100 10	11.7 49.7	3.3 426 0	1.1

Table XVIII: Inversions of Theoretical Models with Basokur and Davis routines.

In comparison with the ResixIP routine, the Basokur routine generally gave unreliable results when MICRO-WIP field data were inverted. For this routine to operate accurately, it appears that the data set must contain well-defined inflection points. It was hypothesized that since the MICRO-WIP data consists of only six data pairs with subtle inflection points, the Basokur routine would be unable to invert reliably. To test this hypothesis, an artificial sounding was created in which the inflection points were well defined. Using ResixIP, the theoretical sounding was developed for a dipole-dipole array with 19 spacings ranging from 5 - 150 m. The apparent resistivities were adjusted until the fitting error was minimized. The resulting apparent resistivities were then inverted using the Basokur routine. The results are outlined in the following tables.

Dipole Spacing n	Spacing m	Apparent Resistivity $\Omega\text{-m}$	ρ_{ho} ResixIP $\Omega\text{-m}$	ρ_{ho} Basokur $\Omega\text{-m}$
1	5	4.3	4.28	4.30
2	10	4.23	4.24	4.22
3	15	4.35	4.35	4.39
4	20	4.65	4.61	4.60
5	25	4.95	4.96	4.95
6	30	5.3	5.32	5.35
7	35	6.0	5.96	5.99
8	40	6.5	6.45	6.45
9	45	6.8	6.81	6.82
10	50	7.06	7.06	7.09
11	55	7.26	7.20	7.25
12	60	7.3	7.25	7.30
13	65	7.2	7.22	7.26
14	70	7.13	7.13	7.14
15	75	7.05	6.99	6.97
16	80	6.75	6.81	6.78
17	85	6.61	6.61	6.57
18	90	6.38	6.38	6.35
19	95	6.07	6.10	6.14

Table XIX: Comparison of synthetic sounding curve with inverted results from ResixIP and Basokur.

Parameter	Layer	ResixIP	Basokur
Resistivity $\Omega\text{-m}$	1	4.3	4.3
	2	8.2 - 8.6	7.0
	3	2.6 - 3.9	3.0
Thickness m	1	9.3	9.3
	2	37.6 - 49.8	46.9

Table XX: Inverted models from ResixIP and Basokur for synthetic sounding of Table XIX.

As can be seen from the preceding tables, the Basokur routine can reliably invert dipole soundings provided there are many points on the sounding curve. MICRO-WIP soundings, however, portray only a small section of this curve. This routine is therefore not dependable when inverting MICRO-WIP data, unless more dipole spacings can be measured.

SUMMARY AND DISCUSSION

This note has described the basis for five routines for inverting one-dimensional resistivity soundings obtained with the MICRO-WIP system. Such soundings have six apparent resistivity values for six spacings of the multi-dipole array. To prepare an interpretation, a data set is selected from the

resistivity pseudosection for processing. The set of six resistivity values (the field data set) is then inverted in terms of a one-dimensional (1-D) layered model, to provide estimates of the thickness and resistivity of successively deeper layers under the location of the field data set. In general, inverting such data sets in terms of two unknown layers on a half-space is pushing the limits of normal interpretation of electrical soundings. Interpretation of electrical soundings is much simpler when the data set contains many more apparent resistivity values than the desired model embodies parameters.

For inversion of each data set from a MICRO-WIP survey, the first layer is constrained to be equal to the observed water depth, and the first layer resistivity is set to that recorded in the field survey log. The model values gained from the inversion process are then used to calculate the resistivity values which would be observed over the model (the model data set).

Among the routines, Zohdy, a direct interpretation scheme, was assessed but not used for MICRO-WIP data because of the problems involved in changing the multi-dipole values to equivalent ones which would have been read with a Schlumberger array. Zohdy is set up for Schlumberger data alone, and significant effort would be needed to alter it to accept other arrays. Zohdy is also very dependent on the shape of the sounding curve, and would thus be more than usually dependent on having many apparent resistivity values.

Basokur, also a direct interpretation scheme, uses the shape of the curve to decide approximate limits of influence of each layer on the curve shape, and thus works best when the sounding is well overdetermined. It expects the operator to make such decisions. Consequently, automated use of this inversion routine would involve considerable programming to replace the interactive decision-making. This is not a trivial problem. Running Basokur with a pre-selected set of limits works reasonably well when the limits are correct, but if the limits chosen do not match the situation, then the sounding is poorly interpreted. Basokur executes quite quickly and could be used in real time with no limitations. It would be useful, however, only if more dipoles can be measured with the MICRO-WIP.

Davis is a matrix-inversion scheme similar to ResixIP. It uses much the same formulation, but its user interface is not well developed, and neither inversion nor cut-and-try modelling can be easily carried out. It is quite sensitive to the choice of starting model, and is probably a poor choice for running inversion. On the other hand, its minimal user interface makes it much easier to modify to run automatically. Davis runs quite slowly, and could not be run in real time on the data-acquisition computer. It would be feasible to pass apparent resistivity data sets to a second computer in real time, and to run Davis on the second computer. This could provide adequate computation time to keep up with the results.

Hardy is a Monte-Carlo system of iterative inversion. In many ways it is very attractive for small data sets, because it makes no initial assumptions about the curve shape. Convergence to a low error of fit, however, requires that the starting model be relatively close to the true situation, as it has limited ability to move far from the original solution. In running inversions this may not be a serious limitation, because the starting model would normally be the

best fit to the previous data set. As in the data shown here, the routine could take several sets of data to close in on an adequate model.

The developmental programming carried out in this study has resulted in the availability of several routines set up to run in continuous mode. If the real-time running inversion did not produce a satisfactory model, then it is now possible to re-run the data with a different routine or with a different starting model. It would also be possible to stop a continuous inversion if the fit deteriorated, to put in a new model. Other schemes could also be developed for setting up a starting model, either for each inversion or when fitting errors exceed some pre-set criterion.

The standard inversion routine used at C-CORE is ResixIP, provided by Interpex Ltd. ResixIP is a forward and inverse modelling program for interpreting IP and resistivity sounding data in terms of a layered earth (1-D) model. It is based on the ridge-regression inversion process, and seems to be reasonably reliable even if only six apparent resistivity values are used. Sounding curves are entered as a function of the dipole spacing n . Apparent resistivity data can be interpreted with or without IP data.

Forward modelling with ResixIP allows the user to calculate a synthetic resistivity sounding curve for a model with up to ten plane layers. Resistivity sounding curves are calculated using linear filters, following the approach described in Ghosh, (1971 a and b), Das and Ghosh (1974), and Davis et. al. (1979).

Inverse modelling with ResixIP allows the user to obtain a model which best fits the data in a least-squares sense. This is done by using ridge regression, a technique which is described by Inman (1975), to adjust the parameters of a starting model in an iterative manner. Selected parameters of the starting model can be constrained so that they will not be adjusted by the inversion scheme. Starting models can contain up to 10 layers for resistivity inversion, although most of the models used in this work had four layers.

ResixIP runs well when it receives much user input. It is a commercial package, however, and source code is not available. Any automation of ResixIP to run continuous inversion would require the action of the manufacturer, and fairly radical changes to the data filing system.

In future, it appears likely that the running inversions would be carried out by either Hardy or Davis, and ResixIP would be used to check solutions, or to do forward modelling. Modifications to the MICRO-WIP system are being considered. Increasing the number of channels would add points to the sounding curve, and thus ease the problem of too few data points to support the model being fitted. Furthermore, it now appears that there would be some advantage in developing an array which could be towed on the bottom in areas where the bottom is not rough. Use of more dipoles, and use of a bottom-towed streamer, will require engineering as well as programming development.

With the present equipment, the most useful approach is to use a logarithmic array, with six channels. Data could be inverted in real time with the Hardy routine. Some development will be needed to ensure that the starting

model is sufficiently close to enable convergence in the limited number of iterations used in the Hardy routine.

Wherever possible, the operator must take advantage of any available acoustic information with which to limit the uncertainties associated with inversion of MICRO-WIP data.

REFERENCES

- Basokur, A.T., 1984, A numerical direct interpretation method of resistivity soundings using the Pekeris model: *Geophysical Prospecting*, 32, 6, p. 1131-1146.
- Basokur, A.T., 1990, Microcomputer program for the direct interpretation of resistivity sounding data: *Computers and Geoscience*, 16, 4, 587-601.
- Das, U.C., and Ghosh, D.P., 1974, The determination of filter coefficients for the computation of standard curves for dipole resistivity sounding over layered earth by linear digital filtering: *Geoph. Prosp.*, 22, 4, p. 765-780.
- Davis, P. A., 1979, Interpretation of resistivity sounding data: computer programs for solutions to the forward and inverse problems: *Minnesota Geol. Surv., Information Circular 17*, 23 p.
- Dyck, A.V., Scott, W.J. and Lobach, J., 1983, Waterborne resistivity-induced polarization survey of Collins Bay, Wollaston Lake: in Cameron, E.M., ed., *Uranium Exploration in Athabasca Basin, Saskatchewan, Canada*, *Geol. Surv. Can. Paper 82-11*, p. 281-289.
- Ghosh, D.P., 1971a, The application of linear filter theory to the direct interpretation of geoelectric resistivity sounding measurements: *Geoph. Prosp.*, 19, 2, p. 192-217.
- Ghosh, D.P., 1971b, Inverse filter coefficients for the computation of apparent resistivity standard curves for a horizontally-stratified earth: *Geoph. Prosp.*, 19, 4, p. 769-775.
- Inman, 1975, Resistivity inversion with ridge regression: *Geophysics*, 40, 5, p. 798-817.
- Johansen, H.K., 1977, A man/computer interpretation system for resistivity soundings over a horizontally-stratified earth: *Geophysical Prospecting*, 25, p. 667-691.
- Jupp, D.L.B., and Vozoff, K., 1975, Stable iterative methods for the inversion of geophysical data: *Geophys. Jour. Roy. Astr. Soc.*, 28, 1, p. 97-109.
- Keller, G.V., and Frischknecht, F.C., 1966, *Electrical methods in geophysical prospecting*: Pergamon Press.
- Koefoed, O., 1969, An analysis of equivalence in resistivity sounding: *Geoph. Prosp.*, 17, 3, p. 327-335.
- Lasfargues, P., 1957, *Prospection électrique par courants continus*: Masson et Cie., Paris, 290 p.

Szaraniec, E., 1982, Uncertain resistivity sounding and equivalent models: Geoph. Prosp., 30, 1, p. 127-154.

Verma, R.K., and Mallik, K., 1979, Detectability of intermediate conductive and resistive layers by time-domain electromagnetic sounding: Geophysics, 44, 11, p. 1862-1878.

Zohdy, A.A.R., 1974, Use of Dar Zarrouk curves in the interpretation of vertical electric soundings: United States Geol. Surv., Bull. 1313-D, 41 p.

- Lines, L.R., and Treitel, S., 1984, Tutorial: a review of least squares inversion and its application to geophysical problems: *Geophysical Prospecting*, 32, 1, p. 159-186.
- Lobach, J.L. and Scott, W.J., 1980, A system for resistivity surveying in water: in Scott, W.J. and Brown, R.J.E., eds., *Nat. Res. Counc. Can., Tech. Mem.* 128, p. 35-45.
- Marquardt, 1970, Generalised inverses, ridge regression, biased linear estimation, and nonlinear estimation: *Technometrics*, 12, 3, p. 591-612.
- Meju, M.A., 1988, The deep electrical resistivity structure of the Great Glen Fault, Scotland: unpubl. Ph.D. Thesis, Univ. Edinburgh, 280 p.
- Meju, M.A., 1992, An effective ridge regression procedure for resistivity data inversion: *Computers & Geology*, 18, 2/3, p. 99-118.
- Narayan, S., 1990, Two-dimensional resistivity inversion: M.Sc. thesis, Univ. of Calif., Riverside.
- Rocroi, J.P., 1975, Contribution à l'étude de l'équivalence en prospection électrique (courant continu et magnétotellurique): *Geoph. Prosp.*, v.23, n.4, p. 765-778.
- Santini, R., and Zambrano, R., 1981, A numerical method of calculating the kernel function from Schlumberger apparent resistivity data: *Geophysical Prospecting*, 29, 1, p. 108-127.
- Scott, W.J., 1975, Preliminary experiments in marine resistivity near Tuktoyaktuk, District of Mackenzie: *Geol. Surv. Can., Paper* 75-1A, p. 141-135.
- Scott, W.J. and MacKay, J.R., 1977, Reliability of permafrost thickness determination by DC resistivity soundings: in Scott, W.J. and Brown, R.J.E., eds., *Tech. Mem.* 119, *Nat. Res. Counc. Can.*, p. 25-38.
- Scott, W.J., Laing, J.S., and Botha, W.J., 1983, Waterborne resistivity-induced polarization survey in Prudhoe Bay. *Proc. 1983 Offshore Technology Conference*, p. 227-230.
- Scott, W.J. and Maxwell, F.K., 1989, Marine resistivity survey for granular materials, Beaufort Sea: *Can. Jour. Expl. Geophysics*, 25, 2, p. 104-114.
- Scott, W.J., 1992, Real-time interpretation of marine resistivity: Presented at NOGAP Symposium on Granular Resources in the Beaufort Sea, Calgary, Feb 1992.
- Scott, W.J., English, G.M., and Smyth, S.J., 1993, A study of noise in marine resistivity systems; preliminary results: in *Proc. Fourth Can. Marine. Geotech. Conf.*, in press.

APPENDIX A

Figures

Figure A-1; RTT 1000 record for Line J1S, Bay of Fundy.

Figure A-2: RTT 1000 record for Line J2N, Bay of Fundy.

Figure A-3: RTT 1000 record for Line J3S, Bay of Fundy.

Beaufort Sea Running Inversion Printouts

A-1	Line 10D:	Davis
A-2	Line 10D:	Basokur
A-3	Line 22A:	Davis
A-4	Line 22A:	Basokur
A-5	Line 44A:	Davis
A-6	Line 44A:	Basokur
A-7	Line 45A:	Davis
A-8	Line 45A:	Basokur

Conception Bay Printouts

A-9	Line L5:	Hardy
-----	----------	-------

Tests of Starting Models

A-10	Line 22A:	Davis
A-11	Line 22A:	Davis
A-12	Line 45A:	Davis, error in n=6 apparent resistivity at Fid 5253 removed.
A-13	Line 45A:	Davis
A-14	Line L5:	Hardy, error in n=6 apparent resistivity inserted at Fid 111.
A-15	Line 10D:	Davis, 7-layer inversion, one starting model, one inversion per fid.
A-16	Line 10D:	Davis, inversion with 5 different sets of 7-layer models.
A-17	Line 10D:	Davis, 3 high-resistivity x 5 thickness sets of models at each fid, plus best fit from last fid.
A-18	Line 10D:	Davis, 3 low-resistivity x 5 thickness sets of models at each fid, plus best fit from last fid.

SOUTH

NORTH

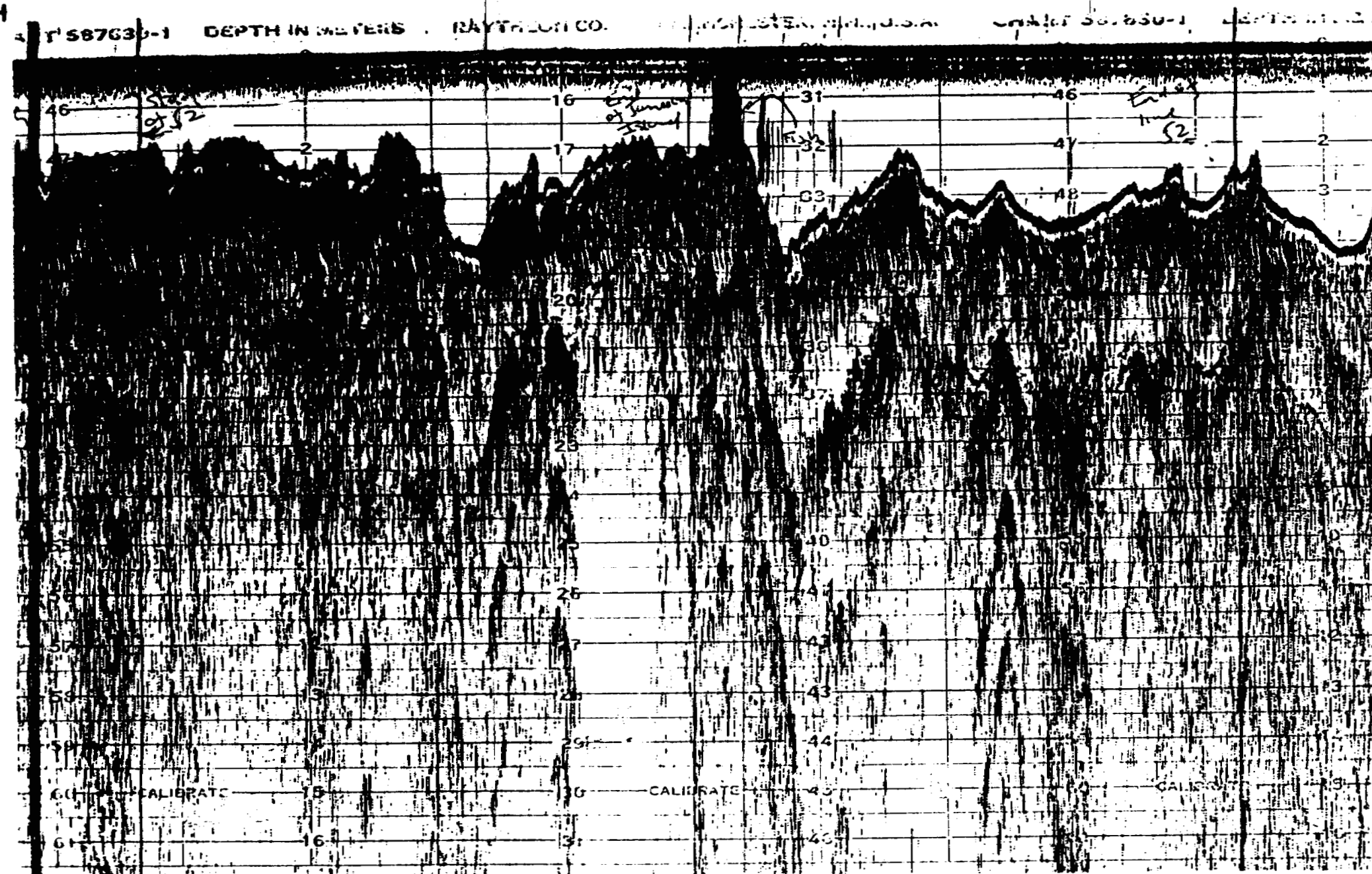


FIGURE A-2: RTT1000 record for line J2N

NORTH

7630-1 DEPTH IN METERS RAYTHEON CO. MANCHESTER, N.H. U.S.A.

SOUTH

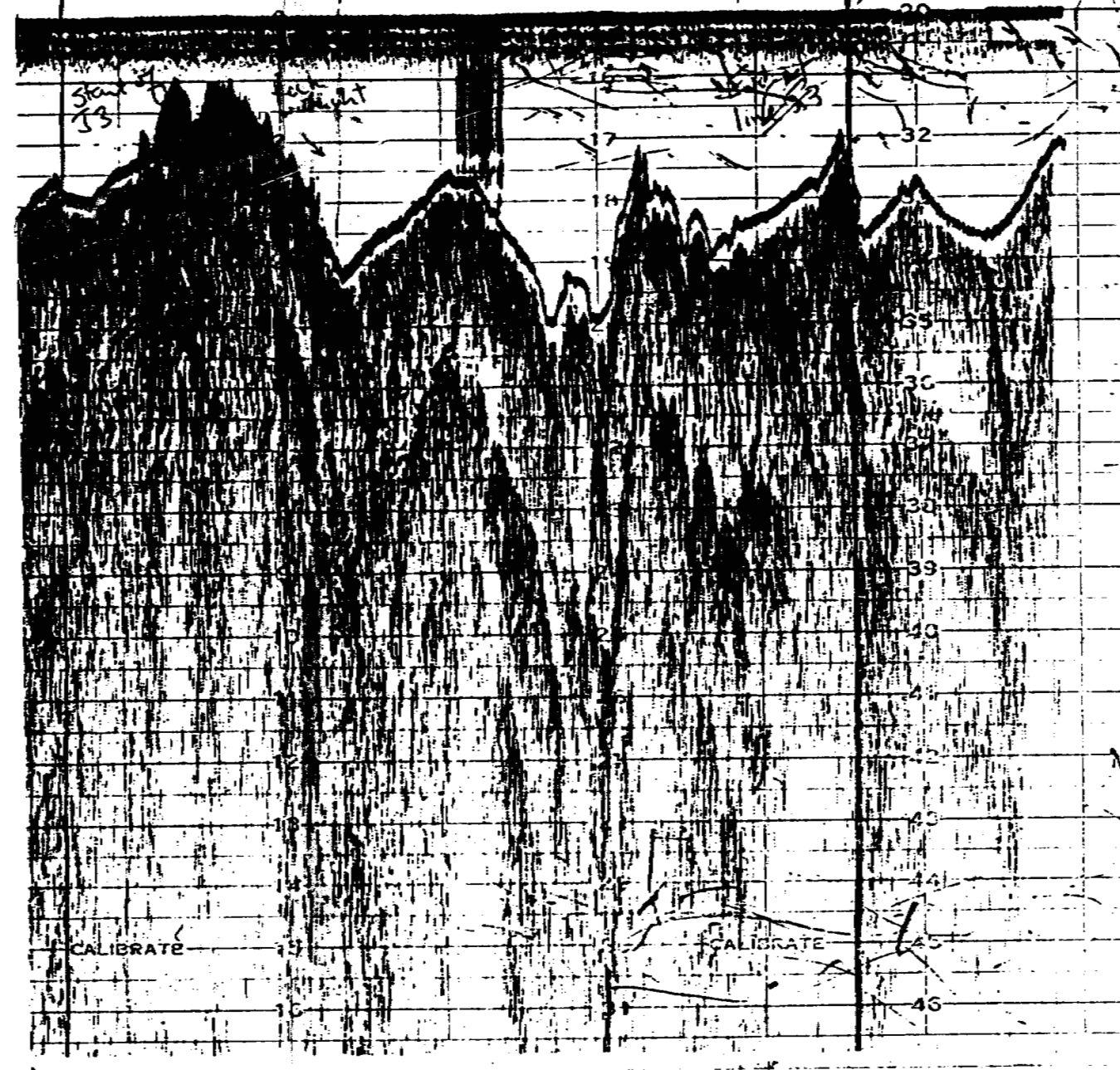


FIGURE A-3: RTT1000 record for line J3S

CLIENT: Atlantic Geoscience
PROJECT: 3-40213
LOCATION: Beaufort Sea
10 m DIPOLES

LINE L10ded.OWT

Processing date: 03-24-1994
CHARGEABILITY (mV/V)

RESISTIVITY (ohm-m)

Depth(m)

				1	2	3	4	5	6	7	8	9	10
2.64			2.98										
	2.22		2.16										
2.73	3.47		1.05	0.84									*
	7.16	2.20	0.92	0.60	967	100.03	1.11	1.43					
					19:08:45		24.77	6.30	193.84				
3.49	4.73	0.35	0.81	0.79	0.34								C
	5.96	3.85	0.75	0.66	0.27	968	101.94	0.00	1.43				
						19:09:17	0.02	6.60	52.39				
3.78	3.87	5.91	0.75	0.66	0.53								C
	4.47	4.56	0.69	0.56	0.41	969	101.94	0.00	1.43				
						19:09:49	0.01	5.80	50.14				
3.84	4.21	4.46	0.74	0.60	0.46								C
	2.62	4.93	0.67	0.52	0.35	970	101.94	0.00	1.43				
						19:10:21	0.01	5.50	47.51				
3.56	4.37	4.82	0.80	0.58	0.42								C
	2.41	5.20	0.73	0.49	0.33	971	101.94	0.00	1.43				
						19:10:53	0.01	5.00	39.36				
3.27	3.92	5.23	0.87	0.65	0.39								C
	2.10	4.51	0.84	0.57	0.31	972	101.94	0.00	1.43				
						19:11:25	0.01	4.20	14.77				
2.54	3.28	2.10	1.11	0.78	0.48								C
	1.64	3.63	1.07	0.70	0.39	973	101.94	0.00	1.43				
						19:11:57	0.01	4.30	16.93				
2.54	2.59	1.65	1.11	0.98	0.61								C
	1.60	2.90	1.09	0.88	0.47	974	101.94	0.00	1.43				
						19:12:29	0.00	4.40	15.43				
2.20	2.49	3.90	1.28	1.02	0.76								C
	4.76	2.82	1.15	0.90	0.59	975	101.94	0.00	1.43				
						19:13:01	0.00	4.60	16.36				
2.14	2.56	2.73	1.32	0.99	0.74								C
	3.61	3.05	1.24	0.83	0.55	976	101.94	0.00	1.43				
						19:13:33	0.00	4.20	8.86				
1.91	2.29	2.95	1.47	1.10	0.69								C
	3.20	2.64	1.39	0.96	0.52	977	101.94	0.00	1.43				
						19:14:05	0.01	3.40	15.44				
1.94	1.98	2.51	1.44	1.27	0.81								C
	3.06	2.16	1.44	1.17	0.63	978	101.94	0.00	1.43				
						19:14:37	0.00	2.70	28.27				

5.25	1.72	1.86
2.65	1.69	1.33
4.06	4.63	3.88
2.52	5.45	3.84
3.83	2.93	3.11
2.39	2.96	3.56
2.51	2.78	3.00
1.60	2.80	3.45
1.36	1.97	2.71
2.04	2.12	2.88
2.99	1.26	2.09
2.10	1.34	2.12
3.51	3.78	1.65
2.75	3.87	2.32
4.21	5.27	3.67
4.62	3.49	2.18
4.06	3.16	3.21
2.79	4.54	1.77
4.77	3.91	3.61
3.41	3.85	2.08
2.98	4.54	3.67
4.04	2.57	2.80
3.23	3.80	2.78
4.37	2.80	3.20
3.33	2.55	2.95
4.06	2.61	3.24
3.18	2.30	2.67
3.87	2.34	3.17
3.08	2.13	2.44
3.76	2.17	3.06
3.05	2.10	2.29
3.62	2.10	3.01
2.95	1.99	2.17

1.58	1.46	1.09
1.68	1.48	0.94
1.76	1.66	1.52
1.75	1.65	1.33
1.87	1.73	1.63
1.85	1.71	1.43
2.89	1.82	1.69
2.80	1.81	1.47
5.10	2.59	1.87
4.86	2.40	1.76
9.56	3.94	2.43
8.41	3.74	2.37
8.28	6.74	3.05
6.57	4.91	2.17
4.98	4.94	3.45
3.91	3.69	2.31
3.52	3.22	3.17
3.19	2.82	2.84
3.01	2.62	2.84
2.62	2.27	2.45
2.38	2.26	2.05
2.21	1.97	1.82
2.20	2.00	1.83
2.05	1.81	1.59
2.14	1.99	1.72
2.20	1.95	1.57
2.24	2.20	1.90
2.31	2.16	1.61
2.31	2.37	2.08
2.37	2.33	1.66
2.33	2.40	2.20
2.47	2.40	1.69
2.41	2.53	2.32

979	101.94	8:00	1:43	43.78
19:15:09				
980	101.94	8:00	1:43	42.59
19:15:41				
981	101.94	8:00	1:45	40.10
19:16:13				
982	101.94	8:00	1:45	43.02
19:16:45				
983	101.94	8:00	1:45	36.22
19:17:17				
984	101.94	8:00	1:45	17.57
19:17:49				
985	101.94	8:00	1:45	5.89
19:18:21				
986	101.94	8:00	1:45	15.97
19:18:54				
987	101.94	8:00	1:45	24.47
19:19:25				
988	101.94	8:00	1:45	22.06
19:19:57				
989	101.94	8:00	1:45	23.57
19:20:28				
990	101.94	8:00	1:43	29.78
19:21:01				
991	101.94	8:00	1:43	35.67
19:21:32				
992	101.94	8:00	1:43	38.97
19:22:05				
993	2.49	1:17	1:43	5.38
19:22:36				
994	2.53	0:01	1:43	4.69
19:23:08				

0*

C

C

C

C

C

C

C

C

C

C

C

C

C

0*

C

3.62	2.04	2.87	2.46	2.47	1.77	995 19:23:40	2.66	0:00	1:43	5.60
2.93	2.04	2.21	2.43	2.47	2.29	996 19:24:12	2.76	0:00	1:43	4.35
3.62	2.13	2.97	2.47	2.37	1.71	997 19:24:44	2.79	0:00	1:37	3.28
3.15	2.10	2.33	2.26	2.41	2.17	998 19:25:16	2.70	0:01	1:37	3.19
3.90	2.21	3.23	2.29	2.28	1.57	999 19:25:48	2.70	0:01	1:37	1.53
3.14	2.25	2.43	2.27	2.25	2.08	1000 19:26:20	2.70	0:01	1:37	2.55
4.04	2.44	3.37	2.21	2.08	1.51	1001 19:26:52	2.55	0:01	1:37	1.97
3.32	2.44	2.81	2.15	2.08	1.81	1002 19:27:24	2.54	0:01	1:37	2.98
4.26	2.70	3.90	2.10	1.88	1.31	1003 19:27:58	2.27	0:01	1:37	2.83
3.39	2.53	3.11	2.11	2.00	1.63	1004 19:28:28	2.07	0:00	1:37	5.50
4.32	2.79	4.19	2.07	1.82	1.22	1005 19:29:00	2.07	0:00	1:37	5.49
3.37	2.58	3.20	2.11	1.96	1.59	1006 19:29:32	2.04	0:00	1:41	2.62
4.28	2.84	4.28	2.09	1.79	1.19	1007 19:30:04	2.67	0:00	1:41	2.36
3.40	2.51	3.23	2.10	2.02	1.58	1008 19:30:36	9.92	0:01	1:41	4.58
4.23	2.69	4.25	2.11	1.89	1.20	1009 19:31:08	6775.1	1:35	1:41	2.00
3.85	2.44	2.99	1.86	2.08	1.71	1010 19:31:40	6775.1	2:22	1:41	2.30
4.58	2.51	3.96	1.96	2.02	1.29	1011 19:32:12	6775.0	3:50	1:43	5.91
3.92	2.53	2.65	1.82	2.01	1.91					
3.53	2.52	3.37	1.93	2.01	1.51					
3.54	2.52	2.60	2.02	2.01	1.95					
2.23	2.60	3.40	1.99	1.95	1.50					
2.97	2.64	2.81	2.42	1.92	1.80					
1.82	2.65	3.68	2.45	1.91	1.39					
1.64	2.16	2.52	4.29	2.37	2.01					
2.72	2.38	2.85	3.89	2.12	1.78					
2.94	1.51	2.68	5.81	3.31	1.89					
3.67	1.92	3.25	4.87	2.62	1.57					
2.22	4.79	2.61	6.35	3.88	1.95					
3.26	1.73	3.55	5.46	2.91	1.44					
2.17	2.27	2.40	6.49	4.44	2.12					
3.11	4.51	3.45	5.73	3.38	1.48					
2.27	2.10	1.96	6.23	4.81	2.57					
3.21	3.13	2.95	5.54	4.07	1.72					

2.35	2.13	1.50	6.03	4.74	3.33	1012	6775.2	5:19	1:43	2.46
3.35	3.18	2.14	5.33	4.00	2.36	19:32:44		19:50	2:20	
2.42	2.17	4.29	5.87	4.65	3.59	1013	554.78	7:98	1:43	4.37
3.43	3.08	1.87	5.27	4.12	2.69	19:33:16		31:13	3:90	
3.59	2.35	2.73	3.98	4.41	3.72	1014	554.94	3:70	1:43	2.67
4.07	3.78	1.76	3.25	3.45	2.86	19:33:48		12:78	3:20	
3.87	4.02	3.62	3.69	2.55	2.92	1015	554.98	0:02	1:35	8.28
3.78	4.67	2.44	2.48	1.86	2.17	19:34:20		0:17	2:80	
6.33	6.65	5.82	2.30	1.60	1.29	1016	38574.	2:06	1:35	10.18
5.54	4.76	6.33	1.62	1.08	0.83	19:34:52		11:40	1:30	
2.92	3.85	4.06	2.45	1.33	0.89	1017	38574.	2:29	1:35	16.93
1.98	4.42	3.34	2.23	1.16	0.76	19:35:24		15:33	1:20	
1.74	2.58	1.98	4.11	1.97	1.02	1018	38574.	3:05	1:35	14.06
1.32	3.05	3.00	3.30	1.67	0.85	19:35:56		17:85	1:10	
2.34	1.63	1.38	6.85	3.17	1.45	1019	38574.	4:61	1:35	20.21
2.55	1.69	1.77	7.16	3.12	1.49	19:36:28		19:30	1:00	
2.59	2.76	2.98	10.95	6.95	3.50	1020	38574.	8:89	1:35	32.92
1.45	2.84	2.47	12.00	7.58	2.73	19:37:02		19:68	1:80	
4.07	4.42	1.48	7.32	11.65	6.88	1021	38574.	8:89	1:41	35.00
9.91	3.52	2.99	6.64	9.66	4.27	19:37:32		19:68	1:20	
4.16	6.77	4.53	5.12	5.57	7.61	1022	38574.	8:89	1:41	41.30
4.13	6.29	2.86	4.33	4.37	4.45	19:38:04		19:68	1:10	
3.27	3.17	6.43	4.40	3.22	3.45	1023	38574.	8:89	1:43	156.44
5.85	4.18	6.54	3.17	2.07	2.18	19:38:36		19:68	1:00	
3.39	4.97	4.79	4.32	2.10	1.58	1024	38574.	8:89	1:43	218.04
2.71	3.38	3.73	3.41	1.51	1.37	19:39:08		19:68	1:00	
2.32	1.97	3.87	6.08	2.64	1.32	1025	38574.	8:89	1:43	148.24
1.86	2.44	3.74	4.73	2.12	1.36	19:39:40		19:68	1:00	
1.77	3.22	2.71	8.12	4.33	1.94	1026	38574.	8:89	1:43	52.87
2.67	1.32	2.89	8.87	3.78	1.83	19:40:12		19:68	1:00	
2.45	1.26	1.25	15.29	7.84	3.98	1027	38574.	8:89	1:43	23.48
3.10	2.80	1.39	16.10	9.15	3.58	19:40:44		19:68	1:00	
3.28	3.60	2.77	21.74	14.16	7.35					

4.85	2.30	4.57
3.45	3.35	2.44
5.08	2.11	2.58
3.68	3.50	2.22
5.33	2.18	2.37
4.45	3.73	2.32
4.91	2.40	2.47
4.03	4.68	2.52
4.14	2.80	2.54
2.66	4.02	2.68
4.70	3.17	2.60
3.12	3.08	2.97
2.17	3.60	2.85
3.79	3.59	3.33
2.69	4.24	3.13
4.21	4.53	3.91
2.95	3.93	3.68
4.72	1.88	4.59
3.29	2.56	4.02
2.77	1.98	2.08
3.79	2.53	3.61
3.12	2.25	2.05
4.62	2.81	3.59
3.37	3.03	2.26
2.59	4.15	3.93
3.72	3.54	3.16
2.81	4.64	3.34
3.60	3.87	3.44
2.73	3.78	2.02
3.63	3.92	4.40
2.81	2.31	2.50
4.28	3.96	2.42
3.16	2.25	2.60

18.45	11.01	4.24
20.66	15.19	8.33
17.64	11.94	4.91
19.37	14.53	9.09
16.82	11.56	5.34
16.14	13.69	8.71
13.42	10.54	5.12
12.17	10.95	8.03
10.80	9.05	4.98
10.68	9.42	7.58
9.53	8.03	4.87
9.16	8.26	6.83
8.16	7.08	4.45
7.53	7.11	6.12
6.60	6.04	4.06
6.79	5.65	5.24
6.02	4.84	3.47
6.09	5.33	4.46
5.42	4.94	3.17
5.14	5.07	4.86
4.73	5.01	3.53
4.56	4.50	4.92
3.88	4.53	3.55
4.23	3.37	4.49
3.42	3.09	3.26
3.83	2.88	3.22
3.16	2.76	2.69
3.96	2.64	2.96
3.25	2.34	2.48
3.93	2.60	2.32
3.16	2.19	2.02
3.34	2.58	2.09
2.82	2.24	1.94

1028	38574.	18.58	1:43	20.75
19:41:16		15:04	1:00	
1029	38574.	18.58	1:43	6.59
19:41:48		15:04	1:00	
1030	38574.	18.58	1:43	8.81
19:42:20		15:04	1:00	
1031	38574.	18.58	1:43	13.55
19:42:52		15:04	1:00	
1032	38574.	18.58	1:43	30.29
19:43:24		15:04	1:00	
1033	38574.	21.21	1:43	54.01
19:43:56		19:12	1:00	
1034	38574.	21.21	1:43	73.70
19:44:28		19:12	1:00	
1035	38574.	21.21	1:43	102.57
19:45:00		19:12	1:00	
1036	38574.	21.21	1:43	145.31
19:45:32		19:12	1:00	
1037	38574.	21.21	1:43	153.76
19:46:06		19:12	1:00	
1038	38574.	21.21	1:43	169.89
19:46:36		19:12	1:00	
1039	38574.	21.21	1:43	207.38
19:47:08		19:12	1:00	
1040	38574.	21.21	1:43	286.34
19:47:40		19:12	1:00	
1041	38574.	21.21	1:47	338.70
19:48:12		19:12	1:00	
1042	38574.	21.21	1:47	396.70
19:48:44		19:12	1:00	
1043	38574.	21.21	1:47	406.54
19:49:16		19:12	1:00	
1044	38574.	21.21	1:47	400.65
19:49:48		19:12	1:00	

4.54	4.19	2.22
3.24	2.35	2.40
1.81	4.44	2.53
2.79	2.42	2.80
1.59	3.84	2.32
2.20	2.17	2.43
2.62	2.77	2.29
1.38	1.48	2.59
3.28	1.85	1.69
4.18	4.38	2.34
3.14	1.60	1.51
2.32	2.62	2.45
3.15	1.61	1.41
2.19	2.50	2.35
2.88	1.45	3.75
2.07	2.25	2.00
2.72	5.49	2.31
1.96	2.26	1.96
2.48	3.46	2.35
1.81	2.17	2.01
2.28	3.21	2.29
1.64	2.01	1.98
1.92	2.90	2.12
1.36	1.81	1.78
1.46	2.44	1.90
4.25	1.55	1.60
4.58	2.00	1.66
2.32	3.26	4.21
3.26	1.76	1.43
2.61	2.39	3.13
3.90	1.92	4.53
2.88	2.43	2.73
3.72	1.92	2.47

3.15	2.44	2.27
2.74	2.15	2.11
3.87	2.31	2.00
3.18	2.09	1.81
4.40	2.67	2.18
4.04	2.33	2.08
6.30	3.74	2.21
6.30	3.39	1.95
8.69	5.44	2.96
7.60	4.41	2.16
9.05	6.24	3.30
7.62	4.84	2.06
9.02	6.20	3.52
8.05	5.07	2.16
9.87	6.87	4.12
8.52	5.60	2.51
10.42	7.02	4.37
8.97	5.59	2.57
11.41	7.36	4.30
9.70	5.81	2.50
12.39	7.92	4.41
10.65	6.25	2.53
14.70	8.77	4.76
12.80	6.95	2.81
19.18	10.37	5.28
16.18	8.06	3.12
23.62	12.62	6.03
19.03	9.50	3.57
21.93	14.22	6.96
17.00	10.57	4.06
18.31	13.06	7.95
15.44	10.42	4.65
19.17	13.06	8.20

1045 19:50:20	38574.	21.21 19.12	1.47 1.00	453.89
1046 19:50:52	38574.	21.21 19.12	1.47 1.00	464.10
1047 19:51:24	38574.	21.21 19.12	1.67 1.00	432.11
1048 19:51:56	38574.	21.21 19.12	1.67 1.00	315.68
1049 19:52:28	38574.	21.21 19.12	1.67 1.00	220.44
1050 19:53:00	38574.	21.21 19.12	1.79 1.00	193.20
1051 19:53:32	38574.	21.21 19.12	1.79 1.00	170.13
1052 19:54:04	38574.	21.21 19.12	1.79 1.00	156.54
1053 19:54:36	38574.	21.21 19.12	1.79 1.00	153.58
1054 19:55:09	38574.	21.21 19.12	1.79 1.00	145.45
1055 19:55:40	38574.	21.21 19.12	2.04 1.00	142.44
1056 19:56:12	38574.	21.21 19.12	2.04 1.00	119.44
1057 19:56:44	38574.	21.21 19.12	2.04 1.00	89.85
1058 19:57:16	38574.	21.21 19.12	1.92 1.00	57.86
1059 19:57:48	38574.	21.21 19.12	1.92 1.00	40.91
1060 19:58:20	38574.	21.21 19.12	1.92 1.00	36.59

2.56	2.32	2.46
3.68	1.68	2.29
2.66	2.13	2.48
4.50	1.81	2.25
3.24	2.25	2.34
3.66	2.29	2.31
4.09	3.08	2.52
2.54	2.86	3.26
4.29	3.57	3.19
2.94	2.74	3.42
5.33	3.37	3.36
3.27	3.73	3.48
2.33	4.74	3.85
3.47	3.93	4.81
2.13	2.23	4.73
2.98	3.14	2.02
1.87	1.73	1.54
2.76	2.95	1.68
1.75	1.69	4.21
2.40	2.75	1.65
1.51	1.57	3.46
2.30	2.37	1.54
5.76	3.53	3.22
1.99	2.34	4.22
3.28	2.71	2.92
1.90	2.09	2.69
3.23	2.54	2.90
2.11	2.13	2.59
3.63	2.64	2.80
2.10	2.34	2.67
3.70	2.85	2.84
2.29	2.42	2.94
3.94	2.92	3.16

17.34	10.91	5.13
19.45	14.86	8.80
16.72	11.83	5.09
15.92	13.89	8.96
13.85	11.19	5.39
13.26	11.16	8.75
10.95	8.41	5.04
11.13	8.86	6.31
10.43	7.13	3.99
9.69	9.25	5.96
8.44	7.60	3.79
8.74	6.86	5.88
7.59	5.42	3.32
8.24	6.50	4.26
8.36	5.70	2.70
9.55	8.13	5.03
9.40	7.23	3.23
10.28	8.61	5.94
10.01	7.43	3.61
11.80	9.24	6.07
11.56	7.94	3.68
12.31	10.67	6.49
11.71	9.05	3.95
14.20	10.81	7.26
13.59	9.36	4.35
14.80	12.08	7.55
13.84	9.98	4.38
13.36	11.86	7.83
12.29	9.65	4.52
13.42	10.79	7.59
12.08	8.93	4.47
12.35	10.46	6.92
11.38	8.70	4.03

1061	38574.	21:21	1:00	37.27
19:58:52		19:12	1:00	
1062	38574.	21:21	1:00	29.32
19:59:24		19:12	1:00	
1063	38574.	21:21	1:00	34.91
19:59:56		19:12	1:00	
1064	38574.	21:21	1:00	70.61
20:00:28		19:12	1:00	
1065	38574.	21:21	1:00	80.86
20:01:00		19:12	1:00	
1066	38574.	21:21	1:00	91.31
20:01:32		19:12	1:00	
1067	38574.	21:21	1:00	144.02
20:02:04		19:12	1:00	
1068	38574.	21:21	1:00	137.31
20:02:36		19:12	1:00	
1069	38574.	21:21	1:00	113.76
20:03:08		19:12	1:00	
1070	38574.	21:21	1:00	97.58
20:03:40		19:12	1:00	
1071	38574.	21:21	1:00	84.47
20:04:13		19:12	1:00	
1072	38574.	21:21	1:00	62.84
20:04:44		19:12	1:00	
1073	38574.	21:21	1:00	58.97
20:05:16		19:12	1:00	
1074	38574.	21:21	1:00	45.74
20:05:48		19:12	1:00	
1075	38574.	21:21	1:00	47.58
20:06:20		19:12	1:00	
1076	38574.	21:21	1:00	62.63
20:06:52		19:12	1:00	
1077	38574.	21:21	1:00	61.84
20:07:24		19:12	1:00	

2.37	2.54	2.90	11.98	9.98	7.02	1078	38574.	21:21	1:66	77.28	e	*
4.21	3.17	3.03	10.70	8.07	4.20	20:07:56						
2.53	2.87	3.24	11.19	8.88	6.32	1079	38574.	21:21	1:66	84.46	e	*
3.15	3.48	3.48	9.88	7.33	3.67	20:08:28						
2.38	2.90	3.40	11.92	8.77	6.00	1080	38574.	21:21	1:66	86.43	e	*
1.55	3.38	3.33	11.25	7.54	3.83	20:09:00						
2.27	2.57	3.19	12.45	9.85	6.38	1081	38574.	21:21	1:66	71.50	e	*
1.50	3.09	3.27	11.61	8.24	3.90	20:09:32						
2.05	2.47	2.97	13.77	10.27	6.84	1082	38574.	21:21	1:66	68.09	e	*
4.37	2.98	3.09	12.30	8.55	4.11	20:10:04						
1.96	2.41	3.00	14.40	10.49	6.78	1083	38574.	21:21	1:66	64.59	e	*
3.42	2.94	3.13	13.07	8.65	4.07	20:10:36						
1.88	2.25	2.96	14.95	11.25	6.88	1084	38574.	21:21	1:66	56.99	e	*
3.31	2.76	3.15	13.46	9.20	4.04	20:11:08						
1.90	2.21	2.83	14.78	11.45	7.18	1085	38574.	21:21	1:66	54.20	e	*
3.34	2.72	3.04	13.35	9.34	4.18	20:11:40						
1.90	2.24	2.77	14.83	11.28	7.32	1086	38574.	21:21	1:66	59.47	e	*
3.48	2.85	3.02	12.84	8.93	4.21	20:12:12						
2.28	2.35	2.93	12.47	10.77	6.94	1087	38574.	21:21	1:66	61.50	e	*
4.14	2.95	3.17	10.86	8.64	4.01	20:12:44						
2.73	2.79	2.99	10.42	9.12	6.81	1088	38574.	21:21	1:66	82.79	e	*
3.33	3.42	3.13	9.47	7.48	4.06	20:13:17						
2.44	3.07	3.34	11.64	8.29	6.12	1089	38574.	21:21	1:66	88.08	e	*
1.52	3.56	3.33	11.60	7.21	3.82	20:13:48						
1.65	2.29	3.23	17.21	11.15	6.35	1090	38574.	21:21	1:66	53.70	e	*
4.10	2.50	3.05	16.89	10.28	4.19	20:14:20						
4.87	1.69	2.37	18.61	14.83	8.54	1091	38574.	21:21	1:66	28.96	e	*
2.74	2.21	2.61	16.23	11.45	4.86	20:14:52						
4.53	1.87	2.38	15.81	13.44	8.51	1092	38574.	21:21	1:66	28.63	e	*
3.09	2.31	2.65	14.42	10.94	4.79	20:15:24						
2.07	2.06	2.41	13.73	12.26	8.41	1093	38574.	21:21	1:66	39.81	e	*
3.57	2.53	2.61	12.53	10.02	4.87	20:15:56						
2.83	2.28	2.57	10.10	11.09	7.90							

4.77	2.75	2.79
3.06	3.02	2.78
1.96	3.43	2.91
2.37	3.06	3.21
1.60	3.50	3.14
2.30	2.76	3.33
1.63	3.48	3.37
2.40	2.87	3.59
1.64	3.56	3.67
2.60	2.70	3.49
1.65	3.15	3.36
2.57	2.52	2.93
1.62	2.79	2.80
2.43	2.53	2.54
1.61	2.93	2.45
2.66	2.56	2.78
1.71	2.82	2.70
2.55	2.70	2.52
1.79	3.09	2.41
2.10	3.15	2.89
1.60	3.90	2.75
2.39	2.90	3.57
1.67	3.57	3.19
1.72	2.71	3.37
3.39	3.14	3.23
4.50	2.02	3.05
2.89	2.76	3.35
3.90	2.06	3.03
2.71	2.57	3.23
3.95	1.87	2.59
2.85	2.40	2.72
4.54	1.98	2.52
3.45	2.64	2.75

9.43	9.25	4.55
9.31	8.44	7.32
9.02	7.44	4.37
11.97	8.31	6.36
10.94	7.29	4.05
12.32	9.21	6.12
10.72	7.32	3.78
11.81	8.84	5.69
10.72	7.16	3.47
10.96	9.43	5.85
10.61	8.12	3.79
11.05	10.05	6.98
10.83	9.11	4.55
11.67	10.02	7.97
10.87	8.68	5.16
10.68	9.91	7.31
10.26	8.99	4.71
11.12	9.43	8.04
9.79	8.26	5.24
13.42	8.10	7.07
10.94	6.57	4.62
11.84	8.77	5.73
10.51	7.17	4.00
16.53	9.39	6.06
14.94	8.14	3.94
19.19	12.46	6.68
15.38	9.19	3.82
18.34	12.27	6.71
16.39	9.94	3.96
18.13	13.43	7.85
15.59	10.53	4.66
15.92	12.76	8.04
12.97	9.65	4.62

1094	38574.	21:21	1:67	52.49
20:16:28		19:12	1:00	
1095	38574.	21:21	1:67	89.19
20:17:00		19:12	1:00	
1096	38574.	21:21	1:67	98.83
20:17:32		19:12	1:00	
1097	38574.	21:21	1:67	85.57
20:18:04		19:12	1:00	
1098	38574.	21:21	1:67	82.04
20:18:36		19:12	1:00	
1099	38574.	21:21	1:67	67.78
20:19:08		19:12	1:00	
1100	38574.	21:21	1:67	62.76
20:19:40		19:12	1:00	
1101	38574.	21:21	1:82	73.14
20:20:12		19:12	1:00	
1102	38574.	21:21	1:82	65.84
20:20:44		19:12	1:00	
1103	38574.	21:21	1:82	80.27
20:21:16		19:12	1:00	
1104	38574.	21:21	1:82	91.21
20:21:48		19:12	1:10	
1105	38574.	21:21	1:82	67.72
20:22:21		19:12	1:20	
1106	38574.	21:42	1:82	58.48
20:22:52		19:55	1:30	
1107	38574.	21:42	1:82	29.88
20:23:24		19:55	1:40	
1108	38574.	21:42	1:82	16.76
20:23:56		19:55	1:40	
1109	38574.	21:42	1:82	15.18
20:24:28		19:55	1:40	
1110	38574.	21:42	1:82	26.02
20:25:00		19:55	1:40	

3.65	2.54	2.90
4.20	3.43	3.16
2.63	3.04	3.73
4.91	3.99	3.90
2.41	3.30	4.09
1.66	3.98	4.12
2.34	2.88	3.79
1.74	3.84	3.74
2.44	3.01	4.05
1.72	3.70	3.97
2.62	3.10	3.69
1.98	4.13	3.80
3.18	3.71	4.39
2.49	5.09	4.53
3.67	3.20	4.01
2.72	2.93	3.83
3.88	1.98	3.07
2.79	3.10	2.22
3.72	1.86	2.96
2.63	2.86	2.15
3.34	1.73	2.77
2.20	2.61	1.95
2.70	1.39	2.44
1.80	2.06	1.79
2.44	4.57	2.08
1.66	1.81	1.57
2.16	2.76	1.81
4.71	1.65	4.11
2.33	2.58	1.69
3.92	1.56	3.51
2.06	2.48	1.56
3.76	3.93	3.10
2.07	2.66	5.16

13.54	10.02	7.03
10.66	7.51	4.04
10.86	8.38	5.49
9.20	6.42	3.29
11.81	7.75	5.01
10.60	6.42	3.10
12.10	8.81	5.39
10.12	6.65	3.42
11.60	8.47	5.05
10.22	6.91	3.22
10.86	8.24	5.54
8.92	6.21	3.36
8.98	6.92	4.69
7.14	5.08	2.85
7.78	5.57	3.76
6.54	4.34	2.32
7.38	5.10	3.32
6.40	4.11	2.27
7.68	5.42	3.43
6.75	4.45	2.34
8.53	5.79	3.67
8.06	4.88	2.60
10.50	7.18	4.15
9.75	6.13	2.80
11.64	8.45	4.85
10.62	6.93	3.19
13.07	9.24	5.54
11.67	7.61	3.70
12.16	9.82	5.93
11.42	8.00	3.64
13.70	10.22	6.39
11.90	8.24	4.10
13.63	9.54	6.20

1111	38574.	21.42	1.82	46.22
20:25:32		19.55	1.86	
1112	38574.	21.42	1.82	63.99
20:26:04		19.55	1.86	
1113	38574.	22.64	1.82	67.79
20:26:36		23.83	1.86	
1114	38574.	22.64	1.82	63.28
20:27:08		23.83	1.86	
1115	38574.	22.64	1.82	58.76
20:27:40		23.83	1.86	
1116	38574.	22.64	1.45	48.52
20:28:12		23.83	1.50	
1117	38574.	22.64	1.45	77.81
20:28:44		23.83	1.50	
1118	38574.	22.64	1.45	114.64
20:29:16		23.83	1.40	
1119	38574.	22.64	1.45	123.89
20:29:48		23.83	1.40	
1120	38574.	22.64	1.45	126.06
20:30:20		23.83	1.30	
1121	38574.	22.64	1.45	110.07
20:30:52		23.83	1.30	
1122	38574.	22.64	1.47	84.23
20:31:25		23.83	1.25	
1123	38574.	22.64	1.47	60.74
20:31:56		23.83	1.20	
1124	38574.	22.64	1.47	50.52
20:32:28		23.83	1.20	
1125	38574.	22.64	1.47	37.85
20:33:00		23.83	1.20	
1126	38574.	22.64	1.47	44.39
20:33:32		23.83	1.20	

3.82	3.49	3.56	11.69	7.29	3.58	1127	38574.	22:64	1:45	50.08		
1.93	2.67	3.64	14.55	9.51	5.61	20:34:04		23:83	1:20			
3.57	3.47	3.84	12.51	7.34	3.32	1128	38574.	22:64	1:45	49.43		*
						20:34:36		23:83	1:20			
1.96	2.50	3.61	14.38	10.15	5.65	1129	38574.	22:64	1:45	43.79		*
3.71	3.28	3.79	12.06	7.75	3.36	20:35:08		23:83	1:20			
1.96	2.61	3.50	14.37	9.74	5.82	1130	38574.	22:64	1:45	46.72		*
3.62	3.32	3.71	12.32	7.68	3.44	20:35:40		23:83	1:20			
2.03	2.55	3.50	13.89	9.93	5.82	1131	38574.	22:64	1:37	28.73		*
3.84	3.37	3.84	11.68	7.57	3.33	20:36:12		23:83	1:40			
2.35	2.70	3.67	12.03	9.42	5.57	1132	38574.	22:64	1:37	24.27		*
4.32	3.52	4.02	10.36	7.25	3.18	20:36:44		23:83	1:50			
2.95	3.00	3.70	9.91	8.49	5.53	1133	38577.	20:25	1:37	20.51		*
5.27	3.82	4.03	8.73	6.68	3.17	20:37:16		30:20	1:60			
3.66	3.66	3.89	7.81	7.19	5.25	1134	38577.	16:17	1:37	21.04		*
2.74	4.60	4.11	6.49	5.73	3.11	20:37:48		28:01	1:65			
4.53	3.45	4.62	6.41	5.11	4.56	1135	38577.	16:17	1:37	81.50		*
3.49	5.01	4.65	5.16	3.79	2.82	20:38:20		28:01	1:60			
3.81	2.52	5.36	5.67	4.02	2.82	1136	38577.	16:17	1:37	111.72		*
3.60	3.99	4.87	4.96	3.21	1.84	20:38:52		28:01	1:55			
2.29	2.45	3.90	6.18	4.14	2.62	1137	38577.	16:17	1:37	121.32		*
3.37	3.90	2.84	5.29	3.27	1.79	20:39:24		28:01	1:50			
2.11	2.34	3.95	6.69	4.33	2.59	1138	38577.	16:17	1:37	115.75		*
3.11	3.73	2.95	5.74	3.43	1.72	20:39:56		28:01	1:45			
1.81	2.13	3.80	7.78	4.73	2.69	1139	38577.	16:17	1:22	81.76		*
2.62	3.34	2.86	6.78	3.82	1.78	20:40:29		28:01	1:45			
1.56	1.80	3.38	8.94	5.60	3.02	1140	38577.	16:17	1:22	60.57		*
2.30	2.87	2.68	7.69	4.43	1.90	20:41:00		28:01	1:40			
1.49	1.58	2.95	9.36	6.35	3.46	1141	38577.	16:17	1:22	39.56		*
2.14	2.45	2.31	8.26	5.17	2.19	20:41:32		28:01	1:40			
4.87	1.44	2.47	10.38	6.92	4.10	1142	38577.	16:17	1:22	35.87		*
1.97	2.30	2.00	8.96	5.49	2.51	20:42:04		28:01	1:40			
2.80	5.31	2.43	10.17	7.25	4.16	1143	38577.	16:17	1:22	38.56		*
2.07	2.27	2.05	8.55	5.56	2.46	20:42:36		28:01	1:35			

3.37	3.80	2.48	8.51	6.73	4.09	1144	38577	16:17	1:32	43.74	e	*
2.55	2.46	2.09	6.97	5.16	2.41	20:43:08		28:01	1:35			
3.82	4.46	2.59	7.51	5.75	3.92	1145	38577	16:17	1:32	62.43	e	*
2.81	2.82	2.13	6.33	4.52	2.37	20:43:40		28:01	1:35			
4.34	3.39	2.90	6.60	5.19	3.52	1146	38577	16:17	1:32	84.07	e	*
3.16	3.16	2.37	5.65	4.03	2.14	20:44:12		28:01	1:36			
3.72	2.28	3.32	5.68	4.47	3.07	1147	38577	16:17	1:32	96.73	e	*
3.77	3.67	2.51	4.75	3.48	2.02	20:44:44		28:01	1:36			
2.72	2.48	3.42	5.22	4.09	2.98	1148	38577	16:17	1:38	112.69	e	*
3.74	3.61	2.28	4.78	3.53	2.21	20:45:16		28:01	1:38			
2.56	2.33	3.24	5.54	4.35	3.14	1149	38577	16:17	1:38	108.80	e	*
3.29	3.33	2.19	5.43	3.83	2.31	20:45:48		28:01	1:38			
2.23	2.03	3.05	6.34	4.96	3.34	1150	38577	16:17	1:38	92.81	e	*
2.95	3.01	2.18	6.05	4.23	2.31	20:46:20		28:01	1:38			
1.96	1.88	2.86	7.19	5.35	3.55	1151	38577	16:17	1:38	78.54	e	*
2.63	2.75	2.18	6.76	4.61	2.32	20:46:52		28:01	1:38			
1.73	1.67	2.80	8.12	5.99	3.62	1152	38577	16:17	1:38	64.27	e	*
2.42	2.65	2.13	7.33	4.78	2.36	20:47:24		28:01	1:38			
1.60	1.61	2.77	8.74	6.21	3.67	1153	38577	16:17	1:47	67.00	e	*
2.26	2.54	2.15	7.84	4.99	2.35	20:47:56		28:01	1:46			
1.43	1.54	2.69	9.72	6.48	3.77	1154	38577	16:17	1:47	58.10	e	*
2.06	2.46	2.08	8.57	5.14	2.42	20:48:28		28:01	1:45			
4.77	1.43	2.61	10.53	6.98	3.88	1155	38577	16:17	1:47	41.01	e	*
1.85	2.23	2.07	9.53	5.67	2.44	20:49:00		28:01	1:50			
3.26	4.76	2.43	8.89	8.10	4.20	1156	38577	16:17	1:47	43.60	e	*
2.42	2.43	1.84	7.75	5.34	2.73	20:49:32		28:01	1:50			
3.99	4.45	2.92	7.28	5.75	3.50	1157	38577	16:17	1:47	44.28	e	*
2.80	2.78	1.64	6.41	4.76	3.06	20:50:04		28:01	1:55			
4.61	1.94	2.19	6.21	5.21	4.60	1158	38577	16:17	1:47	75.33	e	*
3.50	3.11	1.64	5.11	4.12	3.06	20:50:36		28:01	1:50			
0.34	2.52	2.99	12.09	4.02	3.42	1159	38577	16:17	1:47	105.72	e	*
-2.48	3.94	1.91	10.19	3.24	2.63	20:51:21		28:01	1:55			
-3.42	-0.02	3.45	4.25	767.2	2.96							

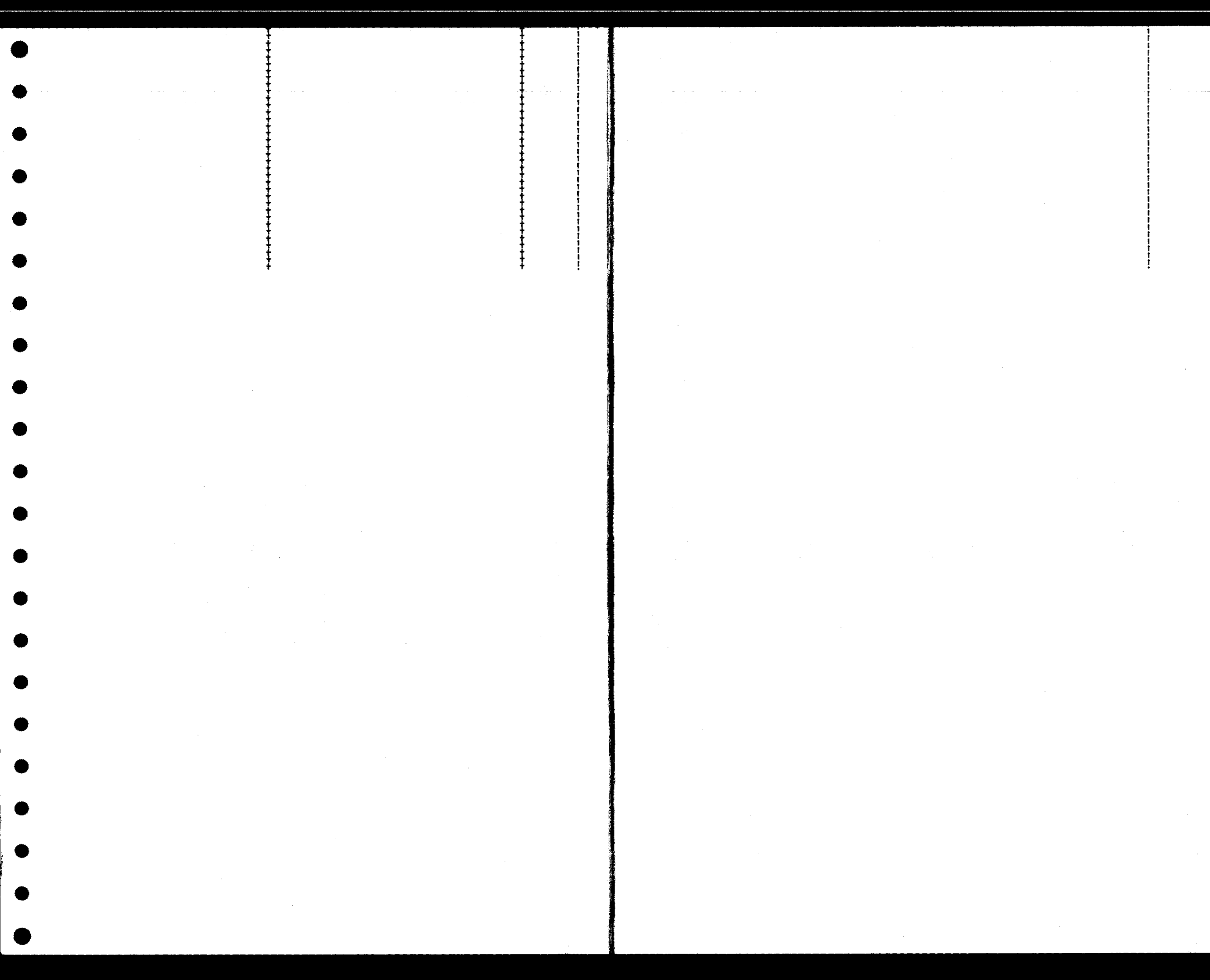
2.37	6.25	1.84
-0.12	-0.26	-3.27
0.08	-3.75	-2.42
4.16	89.79	2.23
-0.10	-0.04	0.35
3.82	12.41	3.13
-2.50	0.01	1.70
0.02	0.05	3.16
0.02	0.08	1.78
-3.57	-3.14	-0.13
0.03	-0.07	2.18
-0.07	-0.02	0.11
2.36	-0.07	2.22
3.05	-0.00	0.10
-0.01	-0.12	2.07
2.90	3.03	3.39
-0.02	4.41	2.05
0.09	-0.04	3.84
-0.06	0.06	2.40
-2.43	-2.49	3.90
-0.02	-3.86	2.52
2.47	-0.09	3.83
1.83	-0.11	2.70
0.03	0.13	4.03
0.01	-3.75	2.79
-2.43	0.04	3.53
-0.06	0.04	2.45
-2.83	-0.21	3.00
-0.12	-3.79	1.96
3.29	3.18	-0.30
2.43	0.13	2.20
0.05	3.31	4.37
0.04	1.98	2.60

3.83	1.50	2.72
3.61	1775	0.91
3.36	3.47	0.28
3.50	1291	3.66
3.34	3.02	1.91
3.80	3.25	3.34
3.62	3.15	3.05
3.96	3.35	3.29
3.65	3.06	2.91
4.07	3.30	2.95
3.68	2.97	2.38
4.22	3.33	2.83
3.86	3.05	2.34
4.76	3.49	3.08
4.08	3.14	2.51
5.00	3.42	3.06
4.27	2.94	2.53
5.51	3.62	2.70
4.88	3.05	2.16
5.97	4.16	2.66
5.16	3.36	2.06
5.88	4.19	2.71
4.97	3.21	1.93
6.22	4.19	2.58
5.56	3.46	1.86
5.98	4.78	2.94
5.25	4.02	2.12
5.16	4.32	3.46
4.10	3.44	2.65
4.41	3.27	2.99
3.73	2.61	2.38
4.65	3.14	2.38
4.01	2.62	1.99

1160	38577.	24.56	1.47	726.84
20:52:44		25.92	1:60	
1161	38577.	45.16	1.52	255.72
20:53:17		32.88	1:60	
1162	38577.	24.33	1.52	202.87
20:53:48		51.58	1:60	
1163	38577.	5.38	1.52	3.72
20:54:20		35.38	1:60	
1164	38577.	5.38	1.52	14.13
20:54:52		35.38	1:60	
1165	38577.	5.38	1.52	17.22
20:55:24		35.38	1:55	
1166	38577.	5.38	1.50	15.57
20:55:56		35.38	1:50	
1167	38577.	5.38	1.50	15.76
20:56:28		35.38	1:50	
1168	38577.	5.38	1.50	27.84
20:57:00		35.38	1:50	
1169	38577.	6.58	1.50	30.74
20:57:32		29.61	1:50	
1170	38577.	6.58	1.50	34.55
20:58:04		29.61	1:50	
1171	38577.	6.58	1.50	38.99
20:58:36		29.61	1:50	
1172	38577.	6.71	1.50	28.39
20:59:08		29.61	1:50	
1173	38577.	7.70	1.50	17.40
20:59:40		28.34	1:50	
1174	38577.	7.70	1.50	28.05
21:00:12		28.34	1:50	
1175	38577.	7.70	1.50	55.53
21:00:44		28.34	1:50	
1176	38577.	7.70	1.50	48.37
21:01:16		28.34	1:50	

-2.95	0.06	4.14	4.91	3.39	2.51	1177	38577	7.70	1.64	40.79	@	*
-2.15	1.83	2.29	4.22	2.83	2.29	21:01:48		28:34	1:60			
3.03	-2.91	3.87	4.78	3.57	2.68	1178	38577	7.70	1.64	34.09	@	*
0.02	-1.73	2.27	4.17	2.99	2.28	21:02:20		28:34	1:60			
0.02	-2.92	3.67	4.65	3.55	2.83	1179	38577	7.70	1.64	33.32	@	*
-2.20	-1.72	2.18	4.13	3.01	2.38	21:02:52		28:34	1:60			
-2.68	2.88	3.59	5.42	3.60	2.89	1180	38577	7.70	1.64	33.23	@	*
-1.91	-1.68	2.14	4.76	3.10	2.42	21:03:23		28:34	1:60			
-2.45	2.57	0.04	5.94	4.04	2.91	1181	38577	7.70	1.64	22.54	@	*
-1.79	1.54	2.18	5.08	3.36	2.38	21:03:56		28:34	1:60			
0.01	2.43	0.10	6.01	4.26	3.11	1182	38577	7.70	1.64	19.23	@	*
-1.79	5.50	2.05	5.07	3.54	2.54	21:04:27		28:34	1:60			
-2.55	-0.03	3.20	5.69	4.16	3.24	1183	38577	7.70	1.61	22.54	@	*
-1.88	-0.05	2.02	4.83	3.39	2.56	21:05:01		28:34	1:60			
2.55	2.56	3.41	5.69	4.05	3.04	1184	38577	7.70	1.58	19.92	@	*
-0.00	-3.85	2.09	4.96	3.37	2.48	21:05:31		28:34	1:70			
-0.01	-0.01	3.42	5.71	4.11	3.03	1185	38577	7.70	1.56	17.26	@	*
1.85	-0.01	2.11	4.91	3.42	2.45	21:06:03		28:34	1:70			
-2.63	0.02	-0.00	5.53	4.07	3.09	1186	38577	7.70	1.54	15.76	@	*
-1.95	0.05	2.06	4.65	3.34	2.51	21:06:35		28:34	1:60			
2.71	-0.02	3.43	5.36	3.80	3.02	1187	38577	7.70	1.52	18.88	@	*
-2.01	4.12	2.10	4.51	3.15	2.46	21:07:07		28:34	1:60			
3.80	-0.03	3.57	3.87	3.74	2.90	1188	38577	7.70	1.48	18.29	@	*
-2.69	4.12	-0.01	3.42	3.15	2.41	21:07:40		28:34	1:60			
-0.12	0.32	3.54	2.89	2.96	2.93	1189	38577	7.70	1.47	41.88	@	*
0.09	-4.97	2.16	2.71	2.62	2.40	21:08:11		28:34	1:60			
-2.50	-4.10	4.07	2.89	2.53	2.55	1190	4965	2.76	1.47	5.32	@	*
-3.27	2.20	2.43	2.77	2.36	2.13	21:08:43		28:06	1:60			
2.51	0.03	4.47	2.90	2.61	2.32	1191	4965	2.76	1.45	5.79	@	*
-3.28	2.14	2.71	2.77	2.42	1.92	21:09:15		27:82	1:60			
2.67	-3.94	0.03	2.71	2.63	2.33	1192	4965	2.77	1.43	6.04	@	*
3.45	-2.14	2.67	2.63	2.42	1.94	21:09:47		27:64	1:60			
2.76	0.07	0.04	2.63	2.51	2.36							

3.49	0.01	2.68	2.60	2.34	1.94	1193	4426.8	29.44	1.80	5.60		
-2.73	-0.06	-0.03	2.65	2.47	2.32	21:10:19						
-3.53	2.24	2.70	2.57	2.32	1.92	1194	4426.8	29.44	1.80	5.89		*
-2.30	0.03	-0.02	3.17	2.42	2.28	21:10:53						
-3.03	2.29	2.74	3.00	2.26	1.89	1195	4426.8	29.45	1.80	4.81		*
-0.10	-3.73	-0.04	4.00	2.79	2.22	21:11:23						
0.16	-0.13	2.76	3.88	2.57	1.88	1196	4426.8	26.31	1.80	5.78		*
-1.66	-0.24	-0.29	5.68	3.70	2.51	21:11:55						
1.74	-1.53	2.58	5.21	3.42	2.01	1197	4426.9	24.13	1.80	7.88		*
0.08	-2.33	3.18	5.95	4.46	3.26	21:12:27						
1.80	1.63	2.12	5.03	3.68	2.44	1198	12295.	19.99	1.70	5.74		*
0.00	0.08	-0.07	5.34	4.16	3.19	21:12:59						
-1.94	0.03	2.18	4.66	3.43	2.37	1199	12295.	20.08	1.70	5.79		*
0.01	0.01	0.02	5.15	3.99	3.08	21:13:31						
0.02	0.02	2.23	4.59	3.43	2.33	1200	12295.	20.89	1.70	5.09		*
0.39	-2.62	0.03	5.73	3.95	3.07	21:14:03						
1.79	-3.88	2.25	5.10	3.34	2.30	1201	12295.	21.13	1.70	5.74		*
0.04	2.38	-0.02	6.36	4.36	2.98	21:14:35						
1.77	3.61	2.31	5.12	3.59	2.24	1202	12267.	18.47	1.75	5.45		*
-0.18	-2.53	0.07	6.11	4.09	3.05	21:15:07						
0.20	-3.97	2.32	5.04	3.26	2.24	1203	10902.	15.26	1.75	3.07		*
0.52	2.44	3.69	7.27	4.38	2.81	21:15:39						
5.69	-0.50	2.40	5.02	3.69	2.16	1204	10902.	16.58	1.75	5.79		*
-3.36	-0.29	3.31	4.33	3.78	3.13	21:16:11						
2.06	-4.24	2.35	4.41	3.06	2.20	1205	10902.	14.58	1.80	8.98		*
2.33	-2.69	3.73	12.18	3.85	2.78	21:16:45						
1.69	-0.00	2.42	11.02	3.25	2.14	1206	10893.	22.17	1.80	8.21		*
2.24	2.04	-0.02	9.60	10.20	2.92	21:17:24						
2.63	2.40	2.34	12.98	9.23	2.22	1207	10895.	21.91	1.80	14.93		*
2.78	2.10		71.30	10.10		21:17:56						
2.32	1.94		16.95	5.27		1208	56.53	40.62	1.45	67.49		C
2.35			16.70			21:18:40						
2.15					9.09							



Processing date: 03-24-1994
CHARGEABILITY (mV/V)

RESISTIVITY (ohm-m)

Depth(m)

[illegible]

3.06	2.16	2.01	1.44	1.17	0.63	978 19:14:37	1.42	2.09 6:00	1.43 2:70	4.24
5.25	1.72	1.86	1.58	1.46	1.09	979 19:15:09	1.13	1.41 22:01	1.43 2:50	2.68
2.65	1.69	1.33	1.68	1.48	0.94	980 19:15:41	1.32	1.57 23:02	1.43 2:40	1.57
4.06	4.63	3.88	1.76	1.66	1.52	981 19:16:13	0.63	1.69 245:15	1.45 2:00	1.33
2.52	5.45	3.84	1.75	1.65	1.33	982 19:16:45	2.16	1.82 16:16	1.45 1:00	0.52
3.83	2.93	3.11	1.87	1.73	1.63	983 19:17:17	4.55	2.41 10:09	1.45 1:55	2.41
2.39	2.96	3.56	1.85	1.71	1.43	984 19:17:49	7.66	0.59 8:02	1.45 1:40	3.17
2.51	2.78	3.00	2.89	1.82	1.69	985 19:18:21	15.25	28.87 8:00	1.45 1:50	3.54
1.60	2.80	3.45	2.80	1.81	1.47	986 19:18:54	18.19	0.00 8:00	1.45 1:50	0.89
1.36	1.97	2.71	5.10	2.59	1.87	987 19:19:25	9.58	0.00 8:01	1.45 1:55	3.61
2.04	2.12	2.88	4.86	2.40	1.76	988 19:19:57	6.03	1.14 3:34	1.45 1:00	1.21
2.99	1.26	2.09	9.56	3.94	2.43	989 19:20:28	4.03	1.40 5:23	1.45 1:05	1.65
2.10	1.34	2.12	8.41	3.74	2.37	990 19:21:01	3.41	1.66 8:47	1.43 1:70	0.51
3.51	3.78	1.65	8.28	6.74	3.05	991 19:21:32	2.53	1.79 9:18	1.43 1:70	1.96
2.75	3.87	2.32	6.57	4.91	2.17	992 19:22:05	1.92	2.04 41:30	1.43 1:75	0.84
4.21	5.27	3.67	4.98	4.94	3.45	993 19:22:36	1.80	2.12 28:05	1.43 1:00	0.69
4.62	3.49	2.18	3.91	3.69	2.31	994 19:23:08	1.95	2.21 28:10	1.43 1:05	1.14
4.06	3.16	3.21	3.52	3.22	3.17					
2.79	4.54	1.77	3.19	2.82	2.84					
4.77	3.91	3.61	3.01	2.62	2.84					
3.41	3.85	2.08	2.62	2.27	2.45					
2.98	4.54	3.67	2.38	2.26	2.05					
4.04	2.57	2.80	2.21	1.97	1.82					
3.23	3.80	2.78	2.20	2.00	1.83					
4.37	2.80	3.20	2.05	1.81	1.59					
3.33	2.55	2.95	2.14	1.99	1.72					
4.06	2.61	3.24	2.20	1.95	1.57					
3.18	2.30	2.67	2.24	2.20	1.90					
3.87	2.34	3.17	2.31	2.16	1.61					
3.08	2.13	2.44	2.31	2.37	2.08					
3.76	2.17	3.06	2.37	2.33	1.66					
3.05	2.10	2.29	2.33	2.40	2.20					
3.62	2.10	3.01	2.47	2.40	1.69					

C

*

*

*

*

*

C*

C

C

C

C *

C *

C *

C *

C *

C *

C *

2.95	1.99	2.17	2.41	2.53	2.32	995	1.75	2.21	1.43	0.85	*
3.62	2.04	2.87	2.46	2.47	1.77	19:23:40		27:36	1:40		
2.93	2.04	2.21	2.43	2.47	2.29	996	2.00	2.22	1.43	0.90	*
3.62	2.13	2.97	2.47	2.37	1.71	19:24:12		39:49	1:45		
3.15	2.10	2.33	2.26	2.41	2.17	997	2.31	2.31	1.37	1.14	C
3.90	2.21	3.23	2.29	2.28	1.57	19:24:44		0:00	2:00		
3.14	2.25	2.43	2.27	2.25	2.08	998	1.86	2.08	1.37	0.79	*
4.04	2.44	3.37	2.21	2.08	1.51	19:25:16		144:22	2:00		
3.32	2.44	2.81	2.15	2.08	1.81	999	2.43	0:00	1:37	1.23	C
4.26	2.70	3.90	2.10	1.88	1.31	19:25:48		0:01	1:30		
3.39	2.53	3.11	2.11	2.00	1.63	1000	2.10	2.84	1:37	1.30	C
4.32	2.79	4.19	2.07	1.82	1.22	19:26:20		0:00	1:30		
3.37	2.58	3.20	2.11	1.96	1.59	1001	2.07	3.42	1:37	1.33	C
4.28	2.84	4.28	2.09	1.79	1.19	19:26:52		0:00	1:30		
3.40	2.51	3.23	2.10	2.02	1.58	1002	2.02	2.10	1:37	1.37	C
4.23	2.69	4.25	2.11	1.89	1.20	19:27:24		0:00	1:30		
3.85	2.44	2.99	1.86	2.08	1.71	1003	2.01	2.02	1:37	1.04	C
4.58	2.51	3.96	1.96	2.02	1.29	19:27:58		0:00	1:30		
3.92	2.53	2.65	1.82	2.01	1.91	1004	1.31	2.78	1:37	1.41	*
3.53	2.52	3.37	1.93	2.01	1.51	19:28:28		25:71	1:35		
3.54	2.52	2.60	2.02	2.01	1.95	1005	1.19	2.71	1:37	0.89	*
2.23	2.60	3.40	1.99	1.95	1.50	19:29:00		27:68	1:30		
2.97	2.64	2.81	2.42	1.92	1.80	1006	2.36	1.92	1:41	1.27	*
1.82	2.65	3.68	2.45	1.91	1.39	19:29:32		14:50	1:35		
1.64	2.16	2.52	4.29	2.37	2.01	1007	2.72	2.14	1:41	2.11	* *
2.72	2.38	2.85	3.89	2.12	1.78	19:30:04		2:30	1:35		
2.94	1.51	2.68	5.81	3.31	1.89	1008	6.80	0:00	1:41	2.06	C
3.67	1.92	3.25	4.87	2.62	1.57	19:30:36		0:01	1:30		
2.22	4.79	2.61	6.35	3.88	1.95	1009	10.68	0:00	1:41	0.56	C
3.26	1.73	3.55	5.46	2.91	1.44	19:31:08		0:01	1:30		
2.17	2.27	2.40	6.49	4.44	2.12	1010	11.31	0:00	1:41	0.21	C
3.11	4.51	3.45	5.73	3.38	1.48	19:31:40		0:01	1:30		
2.27	2.10	1.96	6.23	4.81	2.57						

3.21	3.13	2.95
2.35	2.13	1.50
3.35	3.18	2.14
2.42	2.17	4.29
3.43	3.08	1.87
3.59	2.35	2.73
4.07	3.78	1.76
3.87	4.02	3.62
3.78	4.67	2.44
6.33	6.65	5.82
5.54	4.76	6.33
2.92	3.85	4.06
1.98	4.42	3.34
1.74	2.58	1.98
1.32	3.05	3.00
2.34	1.63	1.38
2.55	1.69	1.77
2.59	2.76	2.98
1.45	2.84	2.47
4.07	4.42	1.48
9.91	3.52	2.99
4.16	6.77	4.53
4.13	6.29	2.86
3.27	3.17	6.43
5.85	4.18	6.54
3.39	4.97	4.79
2.71	3.38	3.73
2.32	1.97	3.87
1.86	2.44	3.74
1.77	3.22	2.71
2.67	1.32	2.89
2.45	1.26	1.25
3.10	2.80	1.39

5.54	4.07	1.72
6.03	4.74	3.33
5.33	4.00	2.36
5.87	4.65	3.59
5.27	4.12	2.69
3.98	4.41	3.72
3.25	3.45	2.86
3.69	2.55	2.92
2.48	1.86	2.17
2.30	1.60	1.29
1.62	1.08	0.83
2.45	1.33	0.89
2.23	1.16	0.76
4.11	1.97	1.02
3.30	1.67	0.85
6.85	3.17	1.45
7.16	3.12	1.49
10.95	6.95	3.50
12.00	7.58	2.73
7.32	11.65	6.88
6.64	9.66	4.27
5.12	5.57	7.61
4.33	4.37	4.45
4.40	3.22	3.45
3.17	2.07	2.18
4.32	2.10	1.58
3.41	1.51	1.37
6.08	2.64	1.32
4.73	2.12	1.36
8.12	4.33	1.94
8.87	3.78	1.83
15.29	7.84	3.98
16.10	9.15	3.58

1011	19:32:12	10.84	0:00	1:43	0.72
1012	19:32:44	10.67	0:00	1:43	0.45
1013	19:33:16	9.79	14:88	1:43	0.46
1014	19:33:48	9.79	10:37	1:43	1.60
1015	19:34:20	7.05	0:00	1:35	4.37
1016	19:34:52	8.28	0:00	1:35	15.98
1017	19:35:24	3.74	0:00	1:35	11.06
1018	19:35:56	3.98	1:34	1:35	2.74
1019	19:36:28	6.39	2:80	1:35	5.29
1020	19:37:02	5.97	10:59	1:35	2.22
1021	19:37:32	10.38	12:62	1:41	7.40
1022	19:38:04	12.21	0:00	1:41	1.47
1023	19:38:36	10.76	0:00	1:43	2.29
1024	19:39:08	10.19	0:00	1:43	7.20
1025	19:39:40	8.98	0:00	1:43	2.46
1026	19:40:12	11.52	0:00	1:43	3.11
1027	19:40:44	6.48	7:81	1:43	5.45

3.16	2.25	2.60
4.54	4.19	2.22
3.24	2.35	2.40
1.81	4.44	2.53
2.79	2.42	2.80
1.59	3.84	2.32
2.20	2.17	2.43
2.62	2.77	2.29
1.38	1.48	2.59
3.28	1.85	1.69
4.18	4.38	2.34
3.14	1.60	1.51
2.32	2.62	2.45
3.15	1.61	1.41
2.19	2.50	2.35
2.88	1.45	3.75
2.07	2.25	2.00
2.72	5.49	2.31
1.96	2.26	1.96
2.48	3.46	2.35
1.81	2.17	2.01
2.28	3.21	2.29
1.64	2.01	1.98
1.92	2.90	2.12
1.36	1.81	1.78
1.46	2.44	1.90
4.25	1.55	1.60
4.58	2.00	1.66
2.32	3.26	4.21
3.26	1.76	1.43
2.61	2.39	3.13
3.90	1.92	4.53
2.88	2.43	2.73

2.82	2.24	1.94
3.15	2.44	2.27
2.74	2.15	2.11
3.87	2.31	2.00
3.18	2.09	1.81
4.40	2.67	2.18
4.04	2.33	2.08
6.30	3.74	2.21
6.30	3.39	1.95
8.69	5.44	2.96
7.60	4.41	2.16
9.05	6.24	3.30
7.62	4.84	2.06
9.02	6.20	3.52
8.05	5.07	2.16
9.87	6.87	4.12
8.52	5.60	2.51
10.42	7.02	4.37
8.97	5.59	2.57
11.41	7.36	4.30
9.70	5.81	2.50
12.39	7.92	4.41
10.65	6.25	2.53
14.70	8.77	4.76
12.80	6.95	2.81
19.18	10.37	5.28
16.18	8.06	3.12
23.62	12.62	6.03
19.03	9.50	3.57
21.93	14.22	6.96
17.00	10.57	4.06
18.31	13.06	7.95
15.44	10.42	4.65

1044	19:49:48
1045	19:50:20
1046	19:50:52
1047	19:51:24
1048	19:51:56
1049	19:52:28
1050	19:53:00
1051	19:53:32
1052	19:54:04
1053	19:54:36
1054	19:55:09
1055	19:55:40
1056	19:56:12
1057	19:56:44
1058	19:57:16
1059	19:57:48
1060	19:58:20

7.66	1.56	1.47	2.83
5.61	1.46	1.47	1.67
5.64	1.79	1.47	1.34
6.75	1.37	1.67	2.94
5.78	1.85	1.67	0.69
8.89	0.80	1.67	3.95
14.83	0.80	1.79	0.50
15.65	0.80	1.79	3.06
14.29	0.80	1.79	0.38
16.73	0.80	1.79	1.28
17.89	0.80	1.79	1.15
19.87	0.80	2.04	1.46
21.39	0.80	2.04	0.68
26.20	0.80	2.04	0.56
30.95	61.24	1.92	0.48
42.37	52.84	1.92	2.70
37.78	55.00	1.92	4.10

3.72	1.92	2.47	19.17	13.06	8.20	1061	26.82	187.11	1:82	1.71
2.56	2.32	2.46	17.34	10.91	5.13	19:58:52				
3.68	1.68	2.29	19.45	14.86	8.80	1062	28.27	49.96	1:82	2.99
2.66	2.13	2.48	16.72	11.83	5.09	19:59:24				
4.50	1.81	2.25	15.92	13.89	8.96	1063	29.47	56.22	1:82	0.45
3.24	2.25	2.34	13.85	11.19	5.39	19:59:56				
3.66	2.29	2.31	13.26	11.16	8.75	1064	29.69	8:00	1:82	1.74
4.09	3.08	2.52	10.95	8.41	5.04	20:00:28				
2.54	2.86	3.26	11.13	8.86	6.31	1065	29.68	8:00	1:68	2.21
4.29	3.57	3.19	10.43	7.13	3.99	20:01:00				
2.94	2.74	3.42	9.69	9.25	5.96	1066	16.34	8:00	1:68	2.12
5.33	3.37	3.36	8.44	7.60	3.79	20:01:32				
3.27	3.73	3.48	8.74	6.86	5.88	1067	17.12	8:00	1:68	0.50
2.33	4.74	3.85	7.59	5.42	3.32	20:02:04				
3.47	3.93	4.81	8.24	6.50	4.26	1068	14.00	8:00	1:68	2.32
2.13	2.23	4.73	8.36	5.70	2.70	20:02:36				
2.98	3.14	2.02	9.55	8.13	5.03	1069	8.64	14.26	1:68	3.05
1.87	1.73	1.54	9.40	7.23	3.23	20:03:08				
2.76	2.95	1.68	10.28	8.61	5.94	1070	12.67	8:00	1:68	2.59
1.75	1.69	4.21	10.01	7.43	3.61	20:03:40				
2.40	2.75	1.65	11.80	9.24	6.07	1071	13.81	8:00	1:68	2.65
1.51	1.57	3.46	11.56	7.94	3.68	20:04:13				
2.30	2.37	1.54	12.31	10.67	6.49	1072	15.97	8:00	1:68	3.46
5.76	3.53	3.22	11.71	9.05	3.95	20:04:44				
1.99	2.34	4.22	14.20	10.81	7.26	1073	16.63	8:00	1:68	2.02
3.28	2.71	2.92	13.59	9.36	4.35	20:05:16				
1.90	2.09	2.69	14.80	12.08	7.55	1074	18.70	74.59	1:68	3.14
3.23	2.54	2.90	13.84	9.98	4.38	20:05:48				
2.11	2.13	2.59	13.36	11.86	7.83	1075	20.62	125.86	1:72	2.46
3.63	2.64	2.80	12.29	9.65	4.52	20:06:20				
2.10	2.34	2.67	13.42	10.79	7.59	1076	20.48	8:00	1:72	2.03
3.70	2.85	2.84	12.08	8.93	4.47	20:06:52				
2.29	2.42	2.94	12.35	10.46	6.92					

3.94	2.92	3.16
2.37	2.54	2.90
4.21	3.17	3.03
2.53	2.87	3.24
3.15	3.48	3.48
2.38	2.90	3.40
1.55	3.38	3.33
2.27	2.57	3.19
1.50	3.09	3.27
2.05	2.47	2.97
4.37	2.98	3.09
1.96	2.41	3.00
3.42	2.94	3.13
1.88	2.25	2.96
3.31	2.76	3.15
1.90	2.21	2.83
3.34	2.72	3.04
1.90	2.24	2.77
3.48	2.85	3.02
2.28	2.35	2.93
4.14	2.95	3.17
2.73	2.79	2.99
3.33	3.42	3.13
2.44	3.07	3.34
1.52	3.56	3.33
1.65	2.29	3.23
4.10	2.50	3.05
4.87	1.69	2.37
2.74	2.21	2.61
4.53	1.87	2.38
3.09	2.31	2.65
2.07	2.06	2.41
3.57	2.53	2.61

11.38	8.70	4.03
11.98	9.98	7.02
10.70	8.07	4.20
11.19	8.88	6.32
9.88	7.33	3.67
11.92	8.77	6.00
11.25	7.54	3.83
12.45	9.85	6.38
11.61	8.24	3.90
13.77	10.27	6.84
12.30	8.55	4.11
14.40	10.49	6.78
13.07	8.65	4.07
14.95	11.25	6.88
13.46	9.20	4.04
14.78	11.45	7.18
13.35	9.34	4.18
14.83	11.28	7.32
12.84	8.93	4.21
12.47	10.77	6.94
10.86	8.64	4.01
10.42	9.12	6.81
9.47	7.48	4.06
11.64	8.29	6.12
11.60	7.21	3.82
17.21	11.15	6.35
16.89	10.28	4.19
18.61	14.83	8.54
16.23	11.45	4.86
15.81	13.44	8.51
14.42	10.94	4.79
13.73	12.26	8.41
12.53	10.02	4.87

* 1077	21.48	8:00	1:72	0.77
20:07:24				
* 1078	19.15	8:00	1:72	2.00
20:07:56				
* 1079	20.46	8:00	1:72	0.62
20:08:28				
* 1080	17.22	8:00	1:72	0.87
20:09:00				
* 1081	18.06	8:00	1:72	1.68
20:09:32				
* 1082	18.82	8:00	1:72	2.22
20:10:04				
* 1083	22.46	8:00	1:75	0.46
20:10:36				
* 1084	23.10	8:00	1:75	1.51
20:11:08				
* 1085	24.44	8:00	1:75	0.95
20:11:40				
* 1086	24.75	8:00	1:75	1.56
20:12:12				
* 1087	25.67	8:00	1:75	0.25
20:12:44				
* 1088	21.35	8:00	1:75	0.33
20:13:17				
* 1089	16.48	8:00	1:67	0.37
20:13:48				
* 1090	12.62	14:76	1:67	1.73
20:14:20		8:00		
* 1091	24.35	31:46	1:67	5.99
20:14:52		8:00		
* 1092	28.84	39:80	1:67	0.84
20:15:24		8:00		
* 1093	22.68	53:36	1:67	1.43
20:15:56		8:00		

3.45	2.64	2.75	12.97	9.65	4.62	1110	31.07	32.73	1.82	1.49
3.65	2.54	2.90	13.54	10.02	7.03	20:25:00		0.00	1.40	
4.20	3.43	3.16	10.66	7.51	4.04	1111	28.24	32.12	1.82	1.63
2.63	3.04	3.73	10.86	8.38	5.49	20:25:32		0.00	1.50	
4.91	3.99	3.90	9.20	6.42	3.29	1112	22.65	34.16	1.82	3.53
2.41	3.30	4.09	11.81	7.75	5.01	20:26:04		0.00	1.50	
1.66	3.98	4.12	10.60	6.42	3.10	1113	18.61	0.00	1.82	1.82
2.34	2.88	3.79	12.10	8.81	5.39	20:26:36		0.00	1.50	
1.74	3.84	3.74	10.12	6.65	3.42	1114	18.00	36.80	1.82	2.64
2.44	3.01	4.05	11.60	8.47	5.05	20:27:08		0.00	1.50	
1.72	3.70	3.97	10.22	6.91	3.22	1115	18.15	42.67	1.82	1.86
2.62	3.10	3.69	10.86	8.24	5.54	20:27:40		0.00	1.50	
1.98	4.13	3.80	8.92	6.21	3.36	1116	19.14	23.19	1.45	1.57
3.18	3.71	4.39	8.98	6.92	4.69	20:28:12		0.00	1.50	
2.49	5.09	4.53	7.14	5.08	2.85	1117	18.34	26.19	1.45	1.14
3.67	3.20	4.01	7.78	5.57	3.76	20:28:44		0.00	1.50	
2.72	2.93	3.83	6.54	4.34	2.32	1118	17.59	0.00	1.45	2.60
3.88	1.98	3.07	7.38	5.10	3.32	20:29:16		0.00	1.40	
2.79	3.10	2.22	6.40	4.11	2.27	1119	14.64	0.00	1.45	2.43
3.72	1.86	2.96	7.68	5.42	3.43	20:29:48		0.01	1.40	
2.63	2.86	2.15	6.75	4.45	2.34	1120	12.71	0.00	1.45	0.49
3.34	1.73	2.77	8.53	5.79	3.67	20:30:20		0.01	1.30	
2.20	2.61	1.95	8.06	4.88	2.60	1121	12.66	0.00	1.45	0.40
2.70	1.39	2.44	10.50	7.18	4.15	20:30:52		0.01	1.30	
1.80	2.06	1.79	9.75	6.13	2.80	1122	12.64	0.00	1.47	2.96
2.44	4.57	2.08	11.64	8.45	4.85	20:31:25		0.00	1.25	
1.66	1.81	1.57	10.62	6.93	3.19	1123	17.12	0.00	1.47	3.03
2.16	2.76	1.81	13.07	9.24	5.54	20:31:56		0.00	1.20	
4.71	1.65	4.11	11.67	7.61	3.70	1124	16.47	39.07	1.47	2.31
2.33	2.58	1.69	12.16	9.82	5.93	20:32:28		0.00	1.20	
3.92	1.56	3.51	11.42	8.00	3.64	1125	20.10	30.73	1.47	1.66
2.06	2.48	1.56	13.70	10.22	6.39	20:33:00		0.00	1.20	
3.76	3.93	3.10	11.90	8.24	4.10	1126	16.64	24.55	1.47	3.89
						20:33:32		0.00	1.20	

2.07	2.66	5.16
3.82	3.49	3.56
1.93	2.67	3.64
3.57	3.47	3.84
1.96	2.50	3.61
3.71	3.28	3.79
1.96	2.61	3.50
3.62	3.32	3.71
2.03	2.55	3.50
3.84	3.37	3.84
2.35	2.70	3.67
4.32	3.52	4.02
2.95	3.00	3.70
5.27	3.82	4.03
3.66	3.66	3.89
2.74	4.60	4.11
4.53	3.45	4.62
3.49	5.01	4.65
3.81	2.52	5.36
3.60	3.99	4.87
2.29	2.45	3.90
3.37	3.90	2.84
2.11	2.34	3.95
3.11	3.73	2.95
1.81	2.13	3.80
2.62	3.34	2.86
1.56	1.80	3.38
2.30	2.87	2.68
1.49	1.58	2.95
2.14	2.45	2.31
4.87	1.44	2.47
1.97	2.30	2.00
2.80	5.31	2.43

13.63	9.54	6.20
11.69	7.29	3.58
14.55	9.51	5.61
12.51	7.34	3.32
14.38	10.15	5.65
12.06	7.75	3.36
14.37	9.74	5.82
12.32	7.68	3.44
13.89	9.93	5.82
11.68	7.57	3.33
12.03	9.42	5.57
10.36	7.25	3.18
9.91	8.49	5.53
8.73	6.68	3.17
7.81	7.19	5.25
6.49	5.73	3.11
6.41	5.11	4.56
5.16	3.79	2.82
5.67	4.02	2.82
4.96	3.21	1.84
6.18	4.14	2.62
5.29	3.27	1.79
6.69	4.33	2.59
5.74	3.43	1.72
7.78	4.73	2.69
6.78	3.82	1.78
8.94	5.60	3.02
7.69	4.43	1.90
9.36	6.35	3.46
8.26	5.17	2.19
10.38	6.92	4.10
8.96	5.49	2.51
10.17	7.25	4.16

1127 20:34:04	22.36	30.16 0.00	1:45 1:20	0.65
1128 20:34:36	21.98	30.19 0.00	1:45 1:20	0.30
1129 20:35:08	24.04	29.48 0.00	1:45 1:20	0.89
1130 20:35:40	23.42	29.77 0.00	1:45 1:20	1.09
1131 20:36:12	25.41	26.06 0.00	1:37 1:20	0.82
1132 20:36:44	25.00	25.33 0.00	1:37 1:20	0.67
1133 20:37:16	20.52	21.37 0.00	1:37 1:20	0.25
1134 20:37:48	15.81	19.20 0.00	1:37 1:20	0.53
1135 20:38:20	12.31	35.31 0.00	1:37 1:20	0.76
1136 20:38:52	12.13	8.89 0.00	1:37 1:20	3.84
1137 20:39:24	9.53	8.89 0.00	1:37 1:20	0.45
1138 20:39:56	10.79	8.89 0.00	1:37 1:20	0.98
1139 20:40:29	11.55	8.89 0.00	1:22 1:45	1.02
1140 20:41:00	11.58	52.15 0.00	1:22 1:40	0.45
1141 20:41:32	13.64	25.21 0.00	1:22 1:40	0.73
1142 20:42:04	14.18	20.77 0.00	1:22 1:40	1.21

2.07	2.27	2.05	8.55	5.56	2.46	1143	16.73	22.03	1:22	0.99
3.37	3.80	2.48	8.51	6.73	4.09	20:42:36		0:00	1:35	
2.55	2.46	2.09	6.97	5.16	2.41	1144	16.80	23.83	1:22	0.88
3.82	4.46	2.59	7.51	5.75	3.92	20:43:08		0:00	1:35	
2.81	2.82	2.13	6.33	4.52	2.37	1145	12.95	33.83	1:22	1.90
4.34	3.39	2.90	6.60	5.19	3.52	20:43:40		0:00	1:35	
3.16	3.16	2.37	5.65	4.03	2.14	1146	13.65	8:00	1:22	0.68
3.72	2.28	3.32	5.68	4.47	3.07	20:44:12		0:01	1:30	
3.77	3.67	2.51	4.75	3.48	2.02	1147	12.74	8:00	1:22	0.82
2.72	2.48	3.42	5.22	4.09	2.98	20:44:44		0:01	1:30	
3.74	3.61	2.28	4.78	3.53	2.21	1148	9.77	8:00	1:28	1.89
2.56	2.33	3.24	5.54	4.35	3.14	20:45:16		0:01	1:30	
3.29	3.33	2.19	5.43	3.83	2.31	1149	7.54	8:00	1:28	0.38
2.23	2.03	3.05	6.34	4.96	3.34	20:45:48		0:01	1:30	
2.95	3.01	2.18	6.05	4.23	2.31	1150	7.52	8:00	1:28	2.51
1.96	1.88	2.86	7.19	5.35	3.55	20:46:20		0:01	1:30	
2.63	2.75	2.18	6.76	4.61	2.32	1151	9.13	8:00	1:28	2.69
1.73	1.67	2.80	8.12	5.99	3.62	20:46:52		0:01	1:30	
2.42	2.65	2.13	7.33	4.78	2.36	1152	11.05	8:00	1:28	3.71
1.60	1.61	2.77	8.74	6.21	3.67	20:47:24		0:00	1:35	
2.26	2.54	2.15	7.84	4.99	2.35	1153	13.33	8:00	1:47	2.11
1.43	1.54	2.69	9.72	6.48	3.77	20:47:56		0:00	1:40	
2.06	2.46	2.08	8.57	5.14	2.42	1154	14.89	8:00	1:47	1.60
4.77	1.43	2.61	10.53	6.98	3.88	20:48:28		0:00	1:45	
1.85	2.23	2.07	9.53	5.67	2.44	1155	14.76	30:00	1:47	2.08
3.26	4.76	2.43	8.89	8.10	4.20	20:49:00		0:00	1:50	
2.42	2.43	1.84	7.75	5.34	2.73	1156	18.00	25.37	1:47	11.09
3.99	4.45	2.92	7.28	5.75	3.50	20:49:32		0:00	1:50	
2.80	2.78	1.64	6.41	4.76	3.06	1157	14.57	46.85	1:47	5.10
4.61	1.94	2.19	6.21	5.21	4.60	20:50:04		0:00	1:55	
3.50	3.11	1.64	5.11	4.12	3.06	1158	13.47	8:00	1:47	1.46
0.34	2.52	2.99	12.09	4.02	3.42	20:50:36		0:01	1:50	
-2.48	3.94	1.91	10.19	3.24	2.63	1159	12.76	8:00	1:47	0.70
						20:51:21		0:01	1:55	

-3.42	-0.02	3.45	4.25	767.2	2.96	1160	0.00	0:00	1:47	999.00	C
2.37	6.25	1.84	3.83	1.50	2.72	20:52:44					
-0.12	-0.26	-3.27	3.61	1775	0.91	1161	0.00	0:00	1:52	999.00	C
0.08	-3.75	-2.42	3.36	3.47	0.28	20:53:17					
4.16	89.79	2.23	3.50	1291	3.66	1162	0.00	0:00	1:52	999.00	C
-0.10	-0.04	0.35	3.34	3.02	1.91	20:53:48					
3.82	12.41	3.13	3.80	3.25	3.34	1163	4.97	3:22	1:52	0.99	*
-2.50	0.01	1.70	3.62	3.15	3.05	20:54:20		12:76	1:50		
0.02	0.05	3.16	3.96	3.35	3.29	1164	5.33	2:65	1:52	0.89	*
0.02	0.08	1.78	3.65	3.06	2.91	20:54:52		7:25	1:50		
-3.57	-3.14	-0.13	4.07	3.30	2.95	1165	6.00	2:41	1:52	0.51	*
0.03	-0.07	2.18	3.68	2.97	2.38	20:55:24		6:43	1:55		
-0.07	-0.02	0.11	4.22	3.33	2.83	1166	6.19	2:67	1:54	1.63	*
2.36	-0.07	2.22	3.86	3.05	2.34	20:55:56		7:55	1:50		
3.05	-0.00	0.10	4.76	3.49	3.08	1167	6.45	2:61	1:54	0.78	*
-0.01	-0.12	2.07	4.08	3.14	2.51	20:56:28		6:50	1:50		
2.90	3.03	3.39	5.00	3.42	3.06	1168	8.06	0:00	1:54	2.01	C
-0.02	4.41	2.05	4.27	2.94	2.53	20:57:00		0:01	1:50		
0.09	-0.04	3.84	5.51	3.62	2.70	1169	8.35	0:00	1:54	1.60	C
-0.06	0.06	2.40	4.88	3.05	2.16	20:57:32		0:01	1:50		
-2.43	-2.49	3.90	5.97	4.16	2.66	1170	8.88	0:00	1:54	0.26	C
-0.02	-3.86	2.52	5.16	3.36	2.06	20:58:04		0:01	1:50		
2.47	-0.09	3.83	5.88	4.19	2.71	1171	10.61	0:00	1:54	0.93	C
1.83	-0.11	2.70	4.97	3.21	1.93	20:58:36		0:01	1:50		
0.03	0.13	4.03	6.22	4.19	2.58	1172	9.93	0:00	1:54	1.92	C
0.01	-3.75	2.79	5.56	3.46	1.86	20:59:08		0:01	1:50		
-2.43	0.04	3.53	5.98	4.78	2.94	1173	10.39	0:00	1:54	0.71	C
-0.06	0.04	2.45	5.25	4.02	2.12	20:59:40		0:01	1:50		
-2.83	-0.21	3.00	5.16	4.32	3.46	1174	10.95	0:00	1:54	0.79	C
-0.12	-3.79	1.96	4.10	3.44	2.65	21:00:12		0:01	1:50		
3.29	3.18	-0.30	4.41	3.27	2.99	1175	9.89	0:00	1:54	3.32	C
2.43	0.13	2.20	3.73	2.61	2.38	21:00:44		0:01	1:50		
0.05	3.31	4.37	4.65	3.14	2.38						

0.04	1.98	2.60	4.01	2.62	1.99	1176 21:01:16	8.01	0:00 0:01	1:64 1:60	0.82	
-2.95	0.06	4.14	4.91	3.39	2.51	1177 21:01:48	8.14	0:00 0:01	1:64 1:60	1.09	C
-2.15	1.83	2.29	4.22	2.83	2.29	1178 21:02:20	8.63	0:00 0:01	1:64 1:60	1.12	C
3.03	-2.91	3.87	4.78	3.57	2.68	1179 21:02:52	8.37	2:00 4:41	1:64 1:60	1.19	@ *
0.02	-1.73	2.27	4.17	2.99	2.28	1180 21:03:23	7.62	1:78 3:78	1:64 1:60	0.82	@ *
0.02	-2.92	3.67	4.65	3.55	2.83	1181 21:03:56	9.52	1:39 2:44	1:64 1:60	0.75	@ *
-2.20	-1.72	2.18	4.13	3.01	2.38	1182 21:04:27	10.63	0:00 0:01	1:64 1:60	1.14	C
-2.68	2.88	3.59	5.42	3.60	2.89	1183 21:05:01	11.34	0:00 0:01	1:61 1:60	0.80	C
-1.91	-1.68	2.14	4.76	3.10	2.42	1184 21:05:31	10.30	0:00 0:01	1:58 1:50	0.78	C
-2.45	2.57	0.04	5.94	4.04	2.91	1185 21:06:03	10.32	0:00 0:01	1:56 1:50	0.32	C
-1.79	1.54	2.18	5.08	3.36	2.38	1186 21:06:35	10.51	0:00 0:01	1:54 1:50	0.46	C
0.01	2.43	0.10	6.01	4.26	3.11	1187 21:07:07	10.49	0:00 0:01	1:52 1:50	1.13	C
-1.79	5.50	2.05	5.07	3.54	2.54	1188 21:07:40	9.89	0:00 0:01	1:49 1:40	1.32	C
-2.55	-0.03	3.20	5.69	4.16	3.24	1189 21:08:11	6.38	1:34 5:05	1:47 1:40	1.37	@ *
-1.88	-0.05	2.02	4.83	3.39	2.56	1190 21:08:43	3.84	2:18 6:53	1:47 1:40	1.12	@ *
2.55	2.56	3.41	5.69	4.05	3.04	1191 21:09:15	3.78	2:20 6:21	1:45 1:40	0.64	@ *
-0.00	-3.85	2.09	4.96	3.37	2.48	1192 21:09:47	3.76	2:20 7:59	1:43 1:40	0.93	@ *
-0.01	-0.01	3.42	5.71	4.11	3.03						
1.85	-0.01	2.11	4.91	3.42	2.45						
-2.63	0.02	-0.00	5.53	4.07	3.09						
-1.95	0.05	2.06	4.65	3.34	2.51						
2.71	-0.02	3.43	5.36	3.80	3.02						
-2.01	4.12	2.10	4.51	3.15	2.46						
3.80	-0.03	3.57	3.87	3.74	2.90						
-2.69	4.12	-0.01	3.42	3.15	2.41						
-0.12	0.32	3.54	2.89	2.96	2.93						
0.09	-4.97	2.16	2.71	2.62	2.40						
-2.50	-4.10	4.07	2.89	2.53	2.55						
-3.27	2.20	2.43	2.77	2.36	2.13						
2.51	0.03	4.47	2.90	2.61	2.32						
-3.28	2.14	2.71	2.77	2.42	1.92						
2.67	-3.94	0.03	2.71	2.63	2.33						
3.45	-2.14	2.67	2.63	2.42	1.94						

[illegible]

2.15

9.09

CLIENT: Atlantic Geoscience
PROJECT: 3-40213
LOCATION: Beaufort Sea
25 m DIPOLES

Processing date: 03-24-1994
CHARGEABILITY (mV/V)

RESISTIVITY (ohm-m)

Depth (m)

[illegible]

0.05	-0.01	-0.01	29.28	17.41	7.08	20:24:19						
1.65	0.02	1.87	38.80	22.73	12.17	3302	41600.	30.67	1.12	34.21		*
3.22	0.02	3.96	31.01	16.27	7.19	20:24:51		48.47	1:20			
-0.01	0.00	0.02	37.28	24.26	11.60	3303	41600.	30.67	1.12	35.39		*
0.02	0.01	-0.07	30.64	17.79	6.66	20:25:23		48.47	1:20			
-0.02	-0.02	1.88	36.29	24.18	12.12	3304	41600.	30.67	1.12	35.64		*
-0.09	-0.06	-0.12	28.95	16.70	6.42	20:25:55		48.47	1:20			
-0.03	-0.15	-0.00	34.65	20.98	11.06	3305	41600.	30.67	1.12	42.34		*
3.84	0.01	0.02	26.03	14.86	6.64	20:26:27		48.47	1:20			
-0.01	0.01	-0.08	34.63	20.05	10.65	3306	41600.	30.67	1.12	58.23		*
3.76	2.07	-0.15	26.57	13.77	6.20	20:27:00		48.47	1:20			
-0.10	3.01	2.43	30.20	18.98	9.39	3307	41600.	30.67	1.12	68.85		*
-0.21	0.10	1.47	22.07	12.72	5.29	20:27:31		48.47	1:20			
-2.55	-3.62	0.10	25.07	15.77	8.47	3308	41600.	30.67	1.12	75.63		*
-0.10	-2.60	2.31	18.96	10.96	4.93	20:28:03		48.47	1:20			
-0.06	-0.08	-0.07	24.00	14.85	8.07	3309	41600.	30.67	1.12	79.18		*
-0.03	-0.01	2.25	19.84	11.21	5.07	20:28:35		48.47	1:20			
2.71	-3.82	0.05	23.72	14.94	8.09	3310	41600.	30.67	1.12	81.53		*
2.26	-2.62	2.28	17.72	10.88	5.01	20:29:07		48.47	1:20			
-0.15	0.14	-2.80	18.36	13.76	8.14	3311	41600.	30.67	1.12	82.47		*
-2.81	2.75	-2.35	14.28	10.39	4.85	20:29:39		48.47	1:30			
0.14	5.06	-2.97	15.86	11.31	7.70	3312	41600.	30.67	1.12	109.98		*
0.00	-3.20	-2.46	13.08	8.91	4.63	20:30:11		48.47	1:30			
-4.20	0.06	-3.33	15.24	10.92	6.85	3313	41600.	30.67	1.12	123.28		*
-3.08	0.01	-2.69	13.00	8.75	4.25	20:30:43		48.47	1:30			
-4.03	-5.29	0.07	15.89	10.81	6.60	3314	41600.	30.67	1.12	125.14		*
3.06	0.06	2.90	13.09	8.45	3.94	20:31:15		48.47	1:30			
0.03	-0.00	-3.50	14.86	11.02	6.53	3315	41600.	30.67	1.12	111.53		*
-0.05	-0.01	2.84	13.11	9.02	4.03	20:31:47		48.47	1:30			
4.09	0.09	0.02	15.67	11.43	7.07	3316	41600.	30.67	1.12	104.36		*
-2.87	-3.01	-2.53	13.96	9.50	4.52	20:32:19		48.47	1:30			
0.27	-2.95		12.49	7.75		3317	41600.	30.67	1.12	95.37		*
2.74	-2.34		10.42	4.88		20:32:51		48.47	1:30			

-0.03

2.39

7.98

4.79

Processing date: 03-24-1994

CHARGEABILITY (mV/V)

RESISTIVITY (ohm-m)

Depth(m)

Left Column				Right Column				Time				Speed			
0.04				13.70				0	0	0	0	0	0	0	0
-3.77				10.53											
-5.07	-2.86			12.56	7.94			3290	30.76	0.00	1.25		1.95		
0.22	-2.02			9.62	5.63			20:18:27							
-5.49	-3.19	-0.11		11.60	7.14	4.30		3291	28.27	0.00	1.25		2.37		
-0.02	-0.04	0.09		8.61	5.45	3.50		20:18:59							
-0.07	0.13	-2.39		11.86	6.87	4.76		3292	24.05	0.00	1.25		4.34		
-0.22	-0.07	-2.91		9.85	5.76	3.90		20:19:31							
0.12	0.19	-2.22		14.35	8.54	5.13		3293	20.95	0.00	1.25		2.16		
0.21	-1.60	-2.88		12.81	7.13	3.94		20:20:03							
-0.04	-0.10	-1.99		17.57	11.17	5.73		3294	23.25	0.00	1.25		2.14		
2.61	-4.67	-2.90		15.26	9.42	3.92		20:20:35							
-3.17	-4.96	0.06		19.56	13.51	7.36		3295	31.06	0.00	1.12		4.47		
2.37	-0.01	-2.55		16.81	10.79	4.47		20:21:07							
-0.11	0.01	1.47		21.38	13.98	8.36		3296	36.73	0.00	1.12		0.97		
0.15	0.11	-1.97		18.79	11.71	5.80		20:21:39							
0.15	3.37	0.09		26.04	16.97	10.16		3297	34.54	0.00	1.12		2.33		
0.09	1.97	-1.61		23.62	14.52	7.08		20:22:11							
0.07	-2.80	1.92		31.10	20.37	11.85		3298	38.56	106.79	1.12		4.68		
-5.66	-1.76	1.93		26.49	16.19	7.42		20:22:44							
-1.85	-0.02	-1.88		34.46	21.36	12.12		3299	52.01	74.99	1.12		1.58		
-3.60	-1.77	-0.08		27.69	16.13	7.45		20:23:15							
1.74	-2.57	0.00		36.56	22.16	12.39		3300	59.54	74.58	1.12		2.16		
3.29	-1.68	-0.08		30.31	17.00	7.38		20:23:47							

0.03	2.37	-1.88	36.33	24.08	12.15	3301	70.95	71.92	1:12	2.97
0.05	-0.01	-0.01	29.28	17.41	7.08	20:24:19	0:00	0:00	1:20	
1.65	0.02	1.87	38.80	22.73	12.17	3302	71.74	73.26	1:12	1.14
3.22	0.02	3.96	31.01	16.27	7.19	20:24:51	0:00	0:00	1:20	
-0.01	0.00	0.02	37.28	24.26	11.60	3303	76.88	77.02	1:12	1.71
0.02	0.01	-0.07	30.64	17.79	6.66	20:25:23	0:00	0:00	1:20	
-0.02	-0.02	1.88	36.29	24.18	12.12	3304	74.60	75.36	1:12	4.36
-0.09	-0.06	-0.12	28.95	16.70	6.42	20:25:55	0:00	0:00	1:20	
-0.03	-0.15	-0.00	34.65	20.98	11.06	3305	75.23	77.08	1:12	1.62
3.84	0.01	0.02	26.03	14.86	6.64	20:26:27	0:00	0:00	1:20	
-0.01	0.01	-0.08	34.63	20.05	10.65	3306	68.49	72.81	1:12	2.72
3.76	2.07	-0.15	26.57	13.77	6.20	20:27:00	0:00	0:00	1:20	
-0.10	3.01	2.43	30.20	18.98	9.39	3307	71.79	76.05	1:12	2.27
-0.21	0.10	1.47	22.07	12.72	5.29	20:27:31	0:00	0:00	1:20	
-2.55	-3.62	0.10	25.07	15.77	8.47	3308	59.60	71.85	1:12	5.08
-0.10	-2.60	2.31	18.96	10.96	4.93	20:28:03	0:00	0:00	1:20	
-0.06	-0.08	-0.07	24.00	14.85	8.07	3309	43.07	72.92	1:12	3.24
-0.03	-0.01	2.25	19.84	11.21	5.07	20:28:35	0:00	0:00	1:20	
2.71	-3.82	0.05	23.72	14.94	8.09	3310	41.32	73.38	1:12	0.48
2.26	-2.62	2.28	17.72	10.88	5.01	20:29:07	0:00	0:00	1:20	
-0.15	0.14	-2.80	18.36	13.76	8.14	3311	41.12	66.09	1:12	4.05
-2.81	2.75	-2.35	14.28	10.39	4.85	20:29:39	0:00	0:00	1:30	
0.14	5.06	-2.97	15.86	11.31	7.70	3312	36.80	8:00	1:12	2.97
0.00	-3.20	-2.46	13.08	8.91	4.63	20:30:11	0:01	0:01	1:30	
-4.20	0.06	-3.33	15.24	10.92	6.85	3313	28.99	8:00	1:12	1.71
-3.08	0.01	-2.69	13.00	8.75	4.25	20:30:43	0:01	0:01	1:30	
-4.03	-5.29	0.07	15.89	10.81	6.60	3314	28.07	8:00	1:12	1.51
3.06	0.06	2.90	13.09	8.45	3.94	20:31:15	0:01	0:01	1:30	
0.03	-0.00	-3.50	14.86	11.02	6.53	3315	29.08	8:00	1:12	1.89
-0.05	-0.01	2.84	13.11	9.02	4.03	20:31:47	0:01	0:01	1:30	
4.09	0.09	0.02	15.67	11.43	7.07	3316	25.05	8:00	1:12	1.70
-2.87	-3.01	-2.53	13.96	9.50	4.52	20:32:19	0:01	0:01	1:30	
0.27	-2.95		12.49	7.75		3317	24.93	8:00	1:12	3.12

2.74

-2.34

10.42

4.88

20:32:51

-0.03

7.98

2.39

4.79

LINE L44aed.0WT

CLIENT: Atlantic Geoscience
PROJECT: 3-40213
LOCATION: Beaufort Sea
25 m DIPOLES

Processing date: 03-24-1994
CHARGEABILITY (mV/V)

RESISTIVITY (ohm-in)

Depth (m)

Left Column				Right Column				Far Right Column			
-0.05				24.51							
-2.57				21.11							
-3.25	1.91			27.06	17.43			5100	14513.	8:30	1:39
	2.52	-0.12			23.00	13.46		20:18:21			1.87
-0.07	0.01	0.08		26.89	18.74	9.43		5101	14513.	8:33	1:39
	-2.55	-0.02	-2.89		22.76	14.29	5.76	20:18:53			2.38
3.13	-6.66	-3.33		25.58	18.58	9.97		5102	14513.	8:33	1:39
	-2.67	-2.93	-2.76		21.80	14.18	6.01	20:19:25			2.61
-4.51	0.01	-3.38		20.84	17.96	9.82		5103	14513.	8:32	1:39
	-0.45	0.07	-2.89		17.65	13.59	5.76	20:19:57			3.36
-5.75	-1.04	3.58		11.66	14.37	9.30		5104	14510.	14:59	1:39
	5.81	-0.28	0.10		10.06	11.39	5.98	20:20:29		34:97	10.64
-3.63	-0.19	-3.61		8.79	9.12	9.18		5105	14510.	18:00	1:39
	0.03	0.35	-2.68		8.66	8.34	6.20	20:21:01		70:08	65.79
-0.08	0.10	-5.16		8.97	7.99	6.49		5106	14510.	18:00	1:39
	-3.64	0.16	-3.71		7.95	6.36	4.48	20:21:33		70:08	105.59
-2.80	-5.16	-3.50		8.24	6.40	4.73		5107	14510.	18:00	1:39
	0.17	0.09	-4.21		6.73	5.05	3.93	20:22:05		70:08	128.05
3.32	-0.00	-3.78		6.92	5.77	4.36		5108	14510.	18:00	1:39
	-4.57	0.00	-0.06		6.30	5.04	3.86	20:22:38		70:08	139.97
-0.21	2.94	3.75		7.04	5.59	4.40		5109	14510.	18:00	1:39
	4.67	-3.39	-4.38		6.18	4.86	3.77	20:23:09		70:08	151.61
2.82	-2.98	-3.78		8.12	5.56	4.36		5110	14510.	18:00	1:43
	-3.76	0.23	-4.30		7.67	5.02	3.83	20:23:41		70:08	155.46
2.41	-0.06	-3.84		9.53	7.09	4.28		5111	14510.	18:00	1:43

0.20	0.18	0.12	9.12	6.43	3.69	20:24:13	70:08	2:10	100.93	
-0.25	-0.19	-0.28	12.42	9.41	5.88	5112	14510.	70:08	2:10	58.11
-0.32	-0.25	-3.37	14.44	10.06	4.93	20:24:45				
1.44	2.86	-1.81	19.95	15.69	9.09	5113	14510.	70:08	2:10	31.46
-4.04	3.56	-2.96	21.32	13.52	5.54	20:25:17				
0.24	-4.74	-1.76	24.60	17.35	9.35	5114	14510.	70:07	2:10	32.05
-2.82	-3.15	-2.97	20.32	13.05	5.54	20:25:49				
-3.34	-1.46	-1.83	24.39	16.52	9.00	5115	14510.	70:07	2:10	34.99
-2.78	-3.25	-3.02	20.63	12.61	5.43	20:26:21				
3.80	1.97	-1.89	23.21	16.59	8.65	5116	14510.	70:08	2:10	33.44
0.06	-3.20	-3.07	19.61	12.79	5.34	20:26:53				
0.43	2.01	-1.82	20.93	16.30	8.99	5117	14510.	70:08	2:10	33.81
0.03	0.05	-2.99	18.20	12.65	5.48	20:27:25				
-1.15	0.07	0.03	17.47	14.96	8.84	5118	14510.	70:08	2:10	41.40
3.65	-0.35	-3.02	15.07	11.68	5.42	20:27:57				
-0.08	-0.10	-2.01	17.48	12.58	8.14	5119	14510.	70:08	2:10	58.25
3.85	4.20	-3.32	14.76	9.64	4.93	20:28:29				
-2.59	-2.73	-2.40	17.11	11.95	6.80	5120	14510.	70:08	2:00	64.16
3.87	4.17	-3.71	14.67	9.54	4.40	20:29:01				
-2.18	-0.01	-0.00	18.05	12.38	6.72	5121	14510.	70:08	2:00	64.26
3.64	4.20	-3.82	15.45	9.60	4.27	20:29:33				
-0.18	-0.01	-0.00	18.75	12.93	6.78	5122	14510.	70:08	2:00	68.55
0.07	-0.00	-3.86	15.95	9.85	4.22	20:30:06				
-0.02	-0.03	-2.47	19.20	12.57	6.60	5123	14510.	70:08	2:00	78.61
3.69	-0.18	-4.09	15.32	9.03	3.98	20:30:37				
0.15	-2.76	-2.68	15.57	11.79	6.07	5124	14510.	70:08	2:00	83.22
-0.34	4.19	4.36	12.73	8.72	3.74	20:31:09				
0.12	-0.16	-0.05	13.28	9.96	5.78	5125	14510.	70:08	2:00	94.19
-1.38	1.11	-4.41	10.77	7.48	3.68	20:31:41				
3.01	3.60	-0.00	13.12	9.01	5.42	5126	14510.	70:08	2:00	97.28
0.09	2.06	-4.45	11.68	7.33	3.65	20:32:13				
2.38	-3.16	-2.92	15.57	10.26	5.56	5127	14510.	70:08	2:00	81.31
1.50	0.14	-4.37	14.43	8.65	3.71	20:32:45				

0.25	0.08	-2.60	17.41	12.84	6.23	5128	14510.	20:63	1:41	54.23	*
-1.81	1.63	-4.15		14.97	9.73	20:33:17		20:08	2:00		
0.03	0.00	-2.27	17.75	12.34	7.14	5129	14510.	20:63	1:41	43.04	*
-0.11	-0.00	-3.40		15.64	10.17	20:33:49		20:08	2:00		
2.18	2.29	0.02	20.58	14.12	8.00	5130	14510.	20:63	1:41	34.68	*
-1.49	3.85	-3.04		18.96	11.99	20:34:21		20:08	2:00		
-0.12	0.13	-1.78	25.25	17.01	9.05	5131	14510.	20:63	1:38	25.65	*
-4.37	0.36	-0.01		22.73	13.57	20:34:53		20:08	2:00		
-0.22	-0.00	-0.08	27.41	18.56	9.53	5132	14510.	27:64	1:38	25.27	*
2.11	2.38	-2.67		23.47	14.96	20:35:25		72:57	1:30		
0.07	-0.06	2.04	29.29	20.46	11.24	5133	14510.	28:75	1:38	16.91	*
-0.05	0.04	0.09		26.61	16.85	20:35:58		72:55	1:30		
2.35	1.79	-2.49	32.93	23.65	13.01	5134	14510.	34:89	1:38	19.31	*
0.04	2.03	-1.99		30.51	19.71	20:36:29		70:41	1:30		
2.20	0.10	0.04	41.00	26.48	14.41	5135	14510.	40:15	1:38	22.56	*
0.03	-1.91	0.04		35.58	20.35	20:37:01		70:50	1:30		
0.13	-0.03	-2.26	43.85	28.68	14.28	5136	14510.	60:63	1:38	28.59	*
1.92	0.05	-0.04		36.43	21.78	20:37:33		85:53	1:30		
-0.20	-0.03	0.02	44.41	29.77	15.50	5137	14510.	60:63	1:38	27.51	*
3.77	-0.04	-1.84		37.37	21.85	20:38:05		85:53	1:30		
0.02	-0.07	-0.05	49.11	28.50	15.16	5138	14510.	60:63	1:38	21.40	*
0.03	0.13	-1.61		38.45	21.66	20:38:37		85:53	1:30		
-0.11	0.13	1.89	44.27	32.66	17.08	5139	14477.	73:06	1:38	11.61	*
-3.52	-0.07	-4.44		40.02	27.45	20:39:09		72:59	1:30		
-1.97	-2.31	0.06	36.49	34.82	20.83	5140	14477.	78:21	1:38	3.96	*
-0.63	1.39	-3.29		31.71	28.52	20:39:41		60:95	1:30		
-3.74	-3.01	5.33	22.84	27.26	20.95	5141	14477.	78:21	1:38	22.00	*
1.92	0.37	-2.81		20.14	22.39	20:40:13		60:95	1:30		
3.70	-4.42	-3.40	20.84	18.18	19.06	5142	14477.	78:21	1:38	85.31	*
-2.83	-4.78	-3.04		19.88	16.80	20:40:45		60:95	1:30		
-3.24	0.03	-4.85	23.18	18.69	13.28	5143	14477.	78:21	1:38	117.70	*
-0.03	-2.57	-5.18		21.53	15.66	20:41:17		60:95	1:30		
0.09	0.00	-3.06	27.04	18.40	10.65	5144	14477.	78:21	1:39		*

-2.50	3.29	0.15	22.50	12.37	5.25	20:41:50	60.95	1:60	148.67	
3.18	5.53	4.18	27.88	14.62	7.68	5145	14477.	78.21	1:38	155.02
-0.15	-3.88	-0.03	17.82	10.38	5.17	20:42:21	60.95	1:38		
-3.71	-2.29	0.11	21.08	14.05	8.28	5146	14477.	78.21	1:38	157.14
-0.05	0.06	0.03	17.50	11.89	5.18	20:42:53	60.95	1:38		
0.28	2.09	3.60	21.88	15.33	8.90	5147	14477.	78.21	1:38	150.38
-0.00	-0.02	-2.84	19.37	12.26	5.66	20:43:25	60.95	1:38		
0.04	-1.99	0.08	25.29	16.12	9.41	5148	14477.	78.21	1:38	145.65
-0.13	-3.01	-2.56	21.68	13.34	6.28	20:43:57	60.95	1:40		
-0.29	1.73	-3.06	31.56	18.59	10.50	5149	14477.	78.21	1:38	125.44
0.13	0.08	-2.49	28.14	14.99	6.45	20:44:29	60.95	1:40		
-2.20	2.54	-2.99	34.52	23.21	10.75	5150	14477.	78.21	1:32	85.08
0.02	0.16	-2.40	29.41	18.00	6.70	20:45:01	60.95	1:32		
-2.61	-0.36	-0.16	33.74	24.82	13.40	5151	14477.	78.21	1:32	61.96
1.80	2.01	-1.97	29.47	19.94	8.21	20:45:33	60.95	1:32		
0.17	-0.14	-2.02	30.44	24.86	15.89	5152	14477.	78.21	1:32	51.60
2.10	-1.86	-0.06	26.71	21.56	10.30	20:46:05	60.95	1:32		
-0.31	3.20	-0.04	25.59	24.80	17.99	5153	14477.	78.21	1:32	39.60
-0.01	-0.02	-1.71	24.08	23.03	12.30	20:46:37	60.95	1:32		
3.30	0.09	0.01	25.85	23.93	19.73	5154	14477.	78.21	1:32	54.46
-2.13	-0.06	-0.07	26.32	21.49	13.34	20:47:09	60.95	1:32		
-2.62	-0.08	-0.00	29.81	23.86	17.77	5155	14477.	78.21	1:32	70.06
0.05	1.93	-3.23	26.65	20.79	12.40	20:47:41	60.95	1:32		
3.14	0.20	0.02	28.46	24.79	18.13	5156	14477.	78.21	1:32	69.15
0.08	-0.03	3.84	28.45	23.31	10.48	20:48:13	60.95	1:32		
-0.16	-0.04	-0.09	34.21	27.20	16.64	5157	14477.	78.21	1:32	73.97
-1.82	-1.90	0.09	30.82	21.11	9.00	20:48:45	60.95	1:32		
0.11	-3.13	-0.04	36.26	25.52	14.87	5158	14477.	78.21	1:32	68.29
-0.03	-1.97	4.61	32.05	20.30	8.69	20:49:17	60.95	1:32		
0.07	-0.37	2.14	40.06	27.40	14.95	5159	14477.	78.21	1:32	61.80
-0.04	1.84	0.05	35.62	21.74	8.94	20:49:49	60.95	1:32		
-0.01	0.01	-2.06	45.68	29.60	15.56	5160	14477.	78.21	1:32	55.44
-5.47	0.01	-4.42	38.50	22.14	9.06	20:50:21	60.95	1:32		

1.73	-0.05	-0.02	48.77	30.52	15.78	5161	14477.	78.21	1:32	49.75	e	*
-3.46	0.07	-4.27	40.42	23.08	9.37	20:50:53		60.95	1:30			
-1.60	-0.08	-0.03	48.96	32.28	16.49	5162	14477.	78.21	1:30	44.50	e	*
3.45	-1.33	4.17	40.55	24.32	9.59	20:51:25		60.95	1:30			
-0.16	-2.21	1.88	42.92	32.24	17.02	5163	14477.	78.21	1:30	45.32	e	*
3.96	-0.01	0.03	35.37	24.05	9.74	20:51:57		60.95	1:30			
2.49	-0.10	-1.88	32.97	28.77	16.96	5164	14477.	78.21	1:30	54.21	e	*
0.28	0.07	0.05	28.05	21.89	9.66	20:52:29		60.95	1:30			
-2.65	-0.17	0.04	29.02	23.06	15.71	5165	14477.	78.21	1:30	72.13	e	*
-1.69	-2.16	4.26	25.17	18.52	9.39	20:53:01		60.95	1:30			
2.84	-0.28	2.20	28.27	22.00	14.48	5166	14477.	78.21	1:30	72.68	e	*
-2.14	0.12	4.18	26.15	19.02	9.58	20:53:33		60.95	1:30			
0.12	-0.69	0.07	32.24	24.02	15.85	5167	14477.	78.21	1:30	63.24	e	*
1.84	-1.90	3.79	30.36	21.04	10.56	20:54:05		60.95	1:30			
0.18	-0.08	0.04	37.99	27.39	17.22	5168	14477.	78.21	1:30	48.50	e	*
-3.07	-0.05	3.49	34.58	23.51	11.47	20:54:37		60.95	1:30			
0.03	-0.00	0.02	42.37	29.97	18.46	5169	14477.	78.21	1:30	44.64	e	*
0.09	-1.71	-3.57	35.73	23.42	11.21	20:55:09		60.95	1:30			
0.25	0.03	1.84	39.10	29.19	17.31	5170	14477.	78.21	1:33	47.52	e	*
-4.20	-1.75	0.06	33.31	22.88	10.59	20:55:41		60.95	1:30			
-2.31	-0.04	1.87	36.47	27.79	16.99	5171	14477.	78.21	1:33	49.89	e	*
-4.49	0.02	-0.01	31.11	22.00	10.48	20:56:13		60.95	1:30			
2.20	-0.05	1.88	36.90	26.63	16.95	5172	14477.	78.21	1:33	49.77	e	*
4.17	0.06	0.06	33.54	22.53	10.84	20:56:45		60.95	1:30			
-0.02	-0.12	1.78	38.70	30.82	17.93	5173	14477.	78.21	1:33	39.00	e	*
-3.82	-0.05	-0.09	36.61	26.29	11.22	20:57:17		60.95	1:30			
-2.33	-2.45	-0.02	37.90	32.61	19.93	5174	14477.	78.21	1:33	41.12	e	*
4.17	4.54	0.03	33.54	25.97	11.43	20:57:49		60.95	1:30			
2.64	-0.17	5.97	33.90	27.42	18.35	5175	14477.	78.21	1:33	55.62	e	*
-4.93	-0.13	-3.73	28.35	21.40	10.72	20:58:21		60.95	1:30			
0.54	3.35	-0.05	6601	23.85	16.17	5176	14477.	78.21	1:33	67.70	e	*
100.3	4.00	-3.95	542.2	19.91	10.12	20:58:48		60.95	1:30			
-999	-999	-0.01	719.8	503.0	15.68	5177	14477.	78.21	1:33		e	*

-4.75	-95.4	0.04	29.41	217.4	9.87	20:59:53	60.95	1:30	80.71	
-5.08	4.80	53.19	34.27	24.88	86.03	5178	14477.	274.03	1:33	124.15
4.73	0.01	23.80	29.52	19.98	23.33	21:00:25	31.80	1:30		
0.10	0.03	4.35	33.45	25.08	14.62	5179	14473.	73.12	1:33	77.91
-0.02	4.03	0.05	29.12	19.70	8.44	21:00:57	138.64	1:30		
-2.18	3.35	0.13	40.98	23.86	13.98	5180	14473.	73.12	1:33	81.79
4.19	4.38	1.48	33.38	18.16	8.13	21:01:29	138.64	1:30		
-1.84	-0.19	-4.72	46.47	27.39	13.52	5181	14473.	73.12	1:33	54.39
-3.49	-0.26	1.92	40.09	22.08	8.30	21:02:01	138.64	1:30		
0.04	2.41	-0.20	46.88	33.16	16.32	5182	14473.	73.12	1:33	18.94
3.56	-0.14	0.11	39.25	26.18	9.81	21:02:33	138.64	1:40		
0.12	-0.07	0.21	47.66	33.15	20.15	5183	14473.	73.12	1:33	9.01
-0.35	0.17	4.50	44.64	29.43	13.85	21:03:05	138.64	1:40		
-2.91	-0.07	0.03	58.25	42.78	24.62	5184	14473.	103.14	1:33	15.13
-0.04	0.12	-2.61	55.74	36.47	15.29	21:03:37	137.60	1:40		
-0.23	2.86	-2.46	62.39	46.58	25.83	5185	14471.	147.98	1:33	23.16
-0.28	-0.25	-2.95	50.10	33.72	13.52	21:04:09	65.85	1:40		
5.26	0.40	-0.24	42.58	37.36	21.93	5186	14471.	147.98	1:33	31.98
0.22	0.08	-3.10	34.36	28.20	12.88	21:04:41	65.85	1:40		
-0.29	3.92	-0.07	38.31	30.37	21.39	5187	14471.	147.98	1:33	70.23
-4.19	-3.45	-3.39	33.38	23.36	11.85	21:05:13	65.85	1:40		
-0.18	-3.20	-0.22	34.33	24.90	15.60	5188	14471.	147.98	1:33	101.10
-5.26	0.09	4.47	26.50	18.76	8.99	21:05:45	65.85	1:40		
-2.67	0.29	1.06	33.79	19.69	12.87	5189	14471.	147.98	1:33	137.72
0.20	-4.20	-3.71	23.62	14.07	7.48	21:06:17	65.85	1:40		
3.87	-4.60	-0.03	23.11	17.42	10.66	5190	14471.	147.98	1:33	140.29
0.40	-2.77	-2.18	18.45	14.38	7.31	21:06:49	65.85	1:40		
-0.03	3.10	2.70	30.20	15.59	11.72	5191	14471.	36.18	1:33	71.57
2.22	0.34	-2.17	25.10	12.76	7.36	21:07:21	197.66	1:50		
0.34	0.11	0.47	30.67	22.26	10.57	5192	14471.	36.18	1:33	29.90
-0.15	-0.04	0.12	28.37	19.31	6.69	21:07:53	197.66	1:50		
0.13	1.64	-0.15	36.64	21.69	13.39	5193	14471.	39.30	1:33	14.29
-1.96	-0.35	-0.23	28.53	17.16	8.30	21:08:26	197.66	2:00		

0.02	0.23	0.26	32.72	28.15	14.88	5194	14418.	54.71	1.33	11.39	*
-3.43	-1.59	-1.71		33.40	25.05	21:08:57		444.07	2:00		
2.78	0.13	-0.04	30.51	30.54	18.22	5195	0.00	99999	1.33		*
-5.86	-4.90	-1.65		24.07	23.83	21:09:29		9999.0	4:50	30.26	
-3.03	-0.63	1.98	29.18	17.75	16.08	5196	85156.	99999	1.33		C
2.41	6.00	-4.43		23.23	13.35	21:10:01		0.00	2:50	39.54	
-0.19	-0.39	-2.95	35.22	19.29	10.87	5197	99999.	99999	1.33		C
0.05	0.20	0.96		27.91	14.47	21:10:33		0.00	2:50	31.74	
0.26	2.05	-0.21	36.16	20.45	9.28	5198	99999.	99999	1.33		C
0.07	0.23	-0.14		31.59	14.87	21:11:05		0.00	2:20	32.19	
2.45	-0.09	-2.99	35.92	26.17	10.82	5199	93478.	99999	1.33		C
-4.05	0.07	0.34		29.86	20.23	21:11:37		0.00	2:20	23.97	
2.72	0.34	2.16	28.68	23.00	14.72	5200	99999.	99999	1.33		C
-4.32	2.16	-1.74		21.73	16.80	21:12:09		0.00	2:20	32.86	
-0.06	-0.70	2.64	24.52	16.40	12.12	5201	99999.	99999	1.43		*
-0.05	2.98	-2.14		18.04	11.84	21:12:41		9999.0	2:20	8.76	
0.20	0.27	0.51	21.99	12.69	8.40	5202	99999.	58.87	1.43		*
3.66	-4.61	3.54		15.29	8.61	21:13:13		28.50	2:00	9.11	
-3.64	0.23	1.30	23.08	10.20	5.35	5203	99999.	58.04	1.43		*
-3.43	-6.26	-4.29		16.31	6.44	21:13:45		28.87	2:00	15.67	
-0.52	-2.99	-4.12	23.63	10.68	3.87	5204	99999.	58.45	1.43		*
-0.05	0.05	-0.07		16.32	7.30	21:14:17		43.51	1:30	63.60	
0.03	-0.38	0.51	24.60	11.58	5.92	5205	99999.	58.50	1.43		*
-3.06	-0.09	0.23		18.21	9.50	21:14:49		43.58	1:30	40.19	
-0.13	0.34	-0.02	29.89	14.78	7.45	5206	99999.	58.50	1.43		*
2.23	3.84	-4.26		24.97	11.94	21:15:21		43.58	1:30	23.05	
2.84	1.53	-1.67	31.34	20.02	9.62	5207	99999.	58.50	1.43		*
-2.13	-2.20	-0.16		26.13	17.52	21:15:54		43.58	1:30	28.99	
-0.13	1.67	4.20	30.94	23.58	15.12	5208	0.00	7396.8	1.43		*
-0.09	-1.82	0.12		27.53	21.82	21:16:25		6221.7	2:00	72.58	
0.32	-0.19	0.12	30.59	28.06	19.77	5209	4311.3	184.66	1.43		*
-5.45	0.01	4.39		32.01	27.01	21:16:57		4212.4	2:00	44.35	
0.15	2.32	2.63	25.32	33.01	24.32	5210	4311.5	55.69	1.43		*

-0.08	-3.04	0.07	26.97	31.08	15.11	21:17:29	4212.4	2.00	13.47	
3.05	-2.94	2.68	29.10	25.57	24.34	5211	4311.5	35.70	1.43	*
0.03	0.38	-3.21	27.39	19.81	12.75	21:18:01	4212.4	2.30	28.91	
0.06	0.21	0.32	30.81	21.53	13.13	5212	4311.5	34.40	1.43	*
0.30	1.21	-6.11	25.11	15.07	6.67	21:18:33	4212.4	2.30	78.78	
0.12	-4.33	0.55	29.38	18.33	8.90	5213	4311.5	26.86	1.43	*
-2.56	-3.72	-3.99	21.78	10.91	3.99	21:19:05	4212.4	2.30	94.53	
-3.95	-1.28	-3.95	22.75	12.46	5.94	5214	4311.5	23.60	1.43	*
-4.35	-5.02	-0.04	12.91	7.92	3.80	21:19:37	4212.4	2.30	95.61	
-4.78	-0.05	-0.04	13.87	10.01	5.97	5215	4311.5	16.46	1.43	*
4.53	0.01	-4.16	12.29	8.32	3.81	21:20:09	4212.4	2.30	68.67	
-0.26	0.03	-2.59	13.19	10.84	6.14	5216	9678.1	15.43	1.43	*
0.12	1.81	-0.03	11.91	8.77	3.86	21:20:41	9999.0	2.30	61.49	
3.20	-0.09	-2.51	12.99	10.29	6.32	5217	29437.	12.47	1.43	*
-4.93	-2.00	-4.15	11.29	7.97	3.82	21:21:13	9999.0	2.50	52.71	
-0.32	-0.13	-2.88	11.50	9.02	5.52	5218	29437.	12.47	1.43	*
0.31	-2.32	-4.36	9.65	6.85	3.64	21:21:46	9999.0	2.50	69.24	
-4.48	0.17	-0.09	9.92	7.78	4.83	5219	29437.	12.47	1.43	*
0.22	-0.17	-4.92	8.41	5.92	3.23	21:22:17	9999.0	2.60	86.17	
-0.05	0.26	-3.96	8.79	6.49	4.02	5220	29437.	12.47	1.43	*
-8.04	-0.07	-5.33	6.93	4.87	2.98	21:22:49	9999.0	2.60	101.38	
-3.73	-5.57	-0.02	6.01	5.70	3.66	5221	29437.	12.47	1.43	*
-0.28	-3.31	-0.00	4.54	4.78	2.98	21:23:21	9999.0	2.60	106.03	
-4.49	-3.29	-4.29	4.95	4.66	3.70	5222	29437.	12.47	1.43	*
-0.06	-4.04	2.61	79.16	3.85	3.04	21:23:53	9999.0	2.70	146.01	
0.18	-0.11	-0.27	4.28	3.66	3.16	5223	29437.	12.47	1.43	*
0.00	2.92	-2.69	23.89	3.21	2.95	21:24:25	9999.0	2.70	173.11	
0.05	0.04	0.02	4.26	3.57	2.84	5224	29437.	12.47	1.43	*
0.00	-0.00	-2.81	23.69	3.20	2.82	21:24:57	9999.0	2.70	177.36	
-4.99	0.04	-5.59	4.42	3.66	2.84	5225	29437.	12.47	1.43	*
-3.66	0.02	2.80	10.02	3.23	2.83	21:25:29	9999.0	2.70	174.21	
-1.77	0.14	0.02	4.49	3.65	2.87	5226	29437.	12.47	1.43	*
-0.04	-0.11	-2.75	3.82	3.27	2.88	21:26:01	9999.0	2.70	169.70	

-0.57	0.16	0.04	3.36	3.48	2.90
-0.27	-0.13	-2.72	3.10	3.08	2.92
1.99	5.64	5.63	2.65	2.82	2.82
-1.21	3.03	-2.65	2.36	2.61	2.99
0.30	0.21	-1.74	1.84	2.28	2.65
-2.58	0.10	-0.00	1.86	2.36	2.99
0.46	-0.09	-0.05	1.58	1.90	2.58
-0.25	-3.76	-2.67	1.80	2.11	2.98
-0.05	0.19	-2.74	1.80	1.96	2.32
2.75	-3.83	-3.23	1.93	2.07	2.47
7.21	-3.52	3.33	1.82	1.90	1.91
0.43	-0.11	-0.01	1.77	1.77	2.07
4.70	0.00		1.68	1.74	
-4.63	-3.84		1.71	2.06	
0.01			1.74		
-3.83			2.07		

5227	29437.	12.47	1.43	193.39
21:26:33		9999.0	2:70	
5228	29437.	12.47	1.43	246.49
21:27:05		9999.0	2:70	
5229	29437.	12.47	1.43	309.77
21:27:38		9999.0	2:70	
5230	29437.	12.47	1.43	408.61
21:28:09		9999.0	2:70	
5231	29437.	12.47	1.43	448.47
21:28:41		9999.0	2:70	
5232	29437.	12.47	1.43	445.38
21:29:13		9999.0	2:70	
5233	29437.	12.47	1.43	465.25
21:29:45		9999.0	2:80	

*
*
*
*
*
*
*

CLIENT: Atlantic Geoscience
PROJECT: 3-40213
LOCATION: Beaufort Sea
25 m DIPOLES

Processing date: 03-24-1994
CHARGEABILITY (mV/V)

RESISTIVITY (ohm-m)

Depth(n)

[illegible]

2.41	-0.06	-3.84	9.53	7.09	4.28	5111	13.11	4.14	1.43	3.70	*
0.20	0.18	0.12	9.12	6.43	3.69	20:24:13		11.90	2.10		
-0.25	-0.19	-0.28	12.42	9.41	5.88	5112	8.36	9.05	1.43	2.48	*
-0.32	-0.25	-3.37	14.44	10.06	4.93	20:24:45		175.65	2.10		
1.44	2.86	-1.81	19.95	15.69	9.09	5113	8.61	12.61	1.43	12.35	*
-4.04	3.56	-2.96	21.32	13.52	5.54	20:25:17		65.43	2.10		
0.24	-4.74	-1.76	24.60	17.35	9.35	5114	31.33	34.03	1.43	10.74	C
-2.82	-3.15	-2.97	20.32	13.05	5.54	20:25:49		0.00	2.10		
-3.34	-1.46	-1.83	24.39	16.52	9.00	5115	44.41	46.50	1.43	3.60	C
-2.78	-3.25	-3.02	20.63	12.61	5.43	20:26:21		0.00	2.10		
3.80	1.97	-1.89	23.21	16.59	8.65	5116	43.78	45.80	1.43	3.10	C
0.06	-3.20	-3.07	19.61	12.79	5.34	20:26:53		0.00	2.10		
0.43	2.01	-1.82	20.93	16.30	8.99	5117	39.83	42.98	1.43	3.83	C
0.03	0.05	-2.99	18.20	12.65	5.48	20:27:25		0.00	2.10		
-1.15	0.07	0.03	17.47	14.96	8.84	5118	34.43	40.77	1.43	3.99	C
3.65	-0.35	-3.02	15.07	11.68	5.42	20:27:57		0.00	2.10		
-0.08	-0.10	-2.01	17.48	12.58	8.14	5119	27.58	47.27	1.43	4.40	C
3.85	4.20	-3.32	14.76	9.64	4.93	20:28:29		0.00	2.10		
-2.59	-2.73	-2.40	17.11	11.95	6.80	5120	27.58	56.81	1.41	3.21	C
3.87	4.17	-3.71	14.67	9.54	4.40	20:29:01		0.00	2.00		
-2.18	-0.01	-0.00	18.05	12.38	6.72	5121	26.14	57.28	1.41	3.92	C
3.64	4.20	-3.82	15.45	9.60	4.27	20:29:33		0.00	2.00		
-0.18	-0.01	-0.00	18.75	12.93	6.78	5122	28.01	47.61	1.41	4.85	C
0.07	-0.00	-3.86	15.95	9.85	4.22	20:30:06		0.00	2.00		
-0.02	-0.03	-2.47	19.20	12.57	6.60	5123	31.39	48.61	1.41	3.87	C
3.69	-0.18	-4.09	15.32	9.03	3.98	20:30:37		0.00	2.00		
0.15	-2.76	-2.68	15.57	11.79	6.07	5124	33.01	50.88	1.41	2.79	C
-0.34	4.19	4.36	12.73	8.72	3.74	20:31:09		0.00	2.00		
0.12	-0.16	-0.05	13.28	9.96	5.78	5125	25.26	92.94	1.41	1.88	C
-1.38	1.11	-4.41	10.77	7.48	3.68	20:31:41		0.00	2.00		
3.01	3.60	-0.00	13.12	9.01	5.42	5126	24.46	0.00	1.41	2.38	C
0.09	2.06	-4.45	11.68	7.33	3.65	20:32:13		0.01	2.00		
2.38	-3.16	-2.92	15.57	10.26	5.56	5127	20.68	0.00	1.41		C

1.50	0.14	-4.37	14.43	8.65	3.71	20:32:45	0.01	2.00	4.19	
0.25	0.08	-2.60	17.41	12.84	6.23	5128	22.70	311.60	1.41	C
-1.81	1.63	-4.15	14.97	9.73	3.91	20:33:17	0.00	2.00	6.88	
0.03	0.00	-2.27	17.75	12.34	7.14	5129	27.32	63.45	1.41	C
-0.11	-0.00	-3.40	15.64	10.17	4.79	20:33:49	0.00	2.00	1.86	
2.18	2.29	0.02	20.58	14.12	8.00	5130	24.77	42.75	1.41	C
-1.49	3.85	-3.04	18.96	11.99	5.31	20:34:21	0.00	2.00	3.20	
-0.12	0.13	-1.78	25.25	17.01	9.05	5131	30.87	35.38	1.39	C
-4.37	0.36	-0.01	22.73	13.57	5.40	20:34:53	0.00	2.00	7.08	
-0.22	-0.00	-0.08	27.41	18.56	9.53	5132	43.66	45.53	1.39	C
2.11	2.38	-2.67	23.47	14.96	6.05	20:35:25	0.00	1.90	3.73	
0.07	-0.06	2.04	29.29	20.46	11.24	5133	46.59	46.90	1.39	C
-0.05	0.04	0.09	26.61	16.85	7.18	20:35:58	0.00	1.90	2.81	
2.35	1.79	-2.49	32.93	23.65	13.01	5134	42.54	46.79	1.39	*
0.04	2.03	-1.99	30.51	19.71	8.11	20:36:29	334.44	1.80	4.72	
2.20	0.10	0.04	41.00	26.48	14.41	5135	47.98	60.29	1.39	*
0.03	-1.91	0.04	35.58	20.35	8.46	20:37:01	180.30	1.80	7.11	
0.13	-0.03	-2.26	43.85	28.68	14.28	5136	69.01	118.77	1.39	*
1.92	0.05	-0.04	36.43	21.78	8.60	20:37:33	53.51	1.80	3.25	
-0.20	-0.03	0.02	44.41	29.77	15.50	5137	76.98	132.67	1.39	*
3.77	-0.04	-1.84	37.37	21.85	8.77	20:38:05	80.80	1.70	5.03	
0.02	-0.07	-0.05	49.11	28.50	15.16	5138	80.37	157.57	1.39	*
0.03	0.13	-1.61	38.45	21.66	10.02	20:38:37	48.35	1.70	0.86	
-0.11	0.13	1.89	44.27	32.66	17.08	5139	113.91	0.00	1.70	C
-3.52	-0.07	-4.44	40.02	27.45	10.83	20:39:09	0.00	1.70	3.44	
-1.97	-2.31	0.06	36.49	34.82	20.83	5140	93.30	0.00	1.70	C
-0.63	1.39	-3.29	31.71	28.52	12.27	20:39:41	0.00	1.70	6.32	
-3.74	-3.01	5.33	22.84	27.26	20.95	5141	64.59	80.43	1.70	*
1.92	0.37	-2.81	20.14	22.39	14.38	20:40:13	58.43	1.70	2.47	
3.70	-4.42	-3.40	20.84	18.18	19.06	5142	31.56	40.64	1.70	C
-2.83	-4.78	-3.04	19.88	16.80	13.37	20:40:45	0.00	1.70	2.48	
-3.24	0.03	-4.85	23.18	18.69	13.28	5143	25.72	28.87	1.70	C
-0.03	-2.57	-5.18	21.53	15.66	7.85	20:41:17	0.00	1.70	6.72	

0.09	0.00	-3.06	27.04	18.40	10.65	5144	37.65	52.22	1:39	12.44	C
-2.50	3.29	0.15	22.50	12.37	5.25	20:41:50		0:00	1:60		
3.18	5.53	4.18	27.88	14.62	7.68	5145	54.29	65.16	1:39	4.80	C
-0.15	-3.88	-0.03	17.82	10.38	5.17	20:42:21		0:00	1:60		
-3.71	-2.29	0.11	21.08	14.05	8.28	5146	49.43	71.14	1:39	10.86	C
-0.05	0.06	0.03	17.50	11.89	5.18	20:42:53		0:00	1:50		
0.28	2.09	3.60	21.88	15.33	8.90	5147	31.88	126.45	1:39	3.40	C
-0.00	-0.02	-2.84	19.37	12.26	5.66	20:43:25		0:00	1:50		
0.04	-1.99	0.08	25.29	16.12	9.41	5148	32.52	206.76	1:39	1.78	C
-0.13	-3.01	-2.56	21.68	13.34	6.28	20:43:57		0:00	1:40		
-0.29	1.73	-3.06	31.56	18.59	10.50	5149	38.54	69.03	1:39	4.23	C
0.13	0.08	-2.49	28.14	14.99	6.45	20:44:29		0:00	1:40		
-2.20	2.54	-2.99	34.52	23.21	10.75	5150	52.91	60.93	1:32	3.89	C
0.02	0.16	-2.40	29.41	18.00	6.70	20:45:01		0:00	1:30		
-2.61	-0.36	-0.16	33.74	24.82	13.40	5151	60.01	64.18	1:32	2.23	C
1.80	2.01	-1.97	29.47	19.94	8.21	20:45:33		0:00	1:30		
0.17	-0.14	-2.02	30.44	24.86	15.89	5152	57.40	61.48	1:32	2.13	C
2.10	-1.86	-0.06	26.71	21.56	10.30	20:46:05		0:00	1:30		
-0.31	3.20	-0.04	25.59	24.80	17.99	5153	46.91	47.00	1:32	2.59	C
-0.01	-0.02	-1.71	24.08	23.03	12.30	20:46:37		0:00	1:50		
3.30	0.09	0.01	25.85	23.93	19.73	5154	34.90	36.49	1:32	5.21	C
-2.13	-0.06	-0.07	26.32	21.49	13.34	20:47:09		0:00	1:50		
-2.62	-0.08	-0.00	29.81	23.86	17.77	5155	34.34	40.27	1:32	3.33	C
0.05	1.93	-3.23	26.65	20.79	12.40	20:47:41		0:00	1:30		
3.14	0.20	0.02	28.46	24.79	18.13	5156	38.32	40.81	1:32	4.56	C
0.08	-0.03	3.84	28.45	23.31	10.48	20:48:13		0:00	1:30		
-0.16	-0.04	-0.09	34.21	27.20	16.64	5157	38.40	40.56	1:32	9.97	C
-1.82	-1.90	0.09	30.82	21.11	9.00	20:48:45		0:00	1:30		
0.11	-3.13	-0.04	36.26	25.52	14.87	5158	57.62	61.10	1:32	4.04	C
-0.03	-1.97	4.61	32.05	20.30	8.69	20:49:17		0:00	1:30		
0.07	-0.37	2.14	40.06	27.40	14.95	5159	60.64	62.20	1:32	4.55	C
-0.04	1.84	0.05	35.62	21.74	8.94	20:49:49		0:00	1:30		
-0.01	0.01	-2.06	45.68	29.60	15.56	5160	73.46	73.67	1:32		C

-5.47	0.01	-4.42	38.50	22.14	9.06	20:50:21	0.00	1:30	5.19	
1.73	-0.05	-0.02	48.77	30.52	15.78	5161	49.77	95.09	1:32	*
-3.46	0.07	-4.27	40.42	23.08	9.37	20:50:53	308.17	1:30	2.50	
-1.60	-0.08	-0.03	48.96	32.28	16.49	5162	73.91	109.78	1:30	*
3.45	-1.33	4.17	40.55	24.32	9.59	20:51:25	167.80	1:30	2.65	
-0.16	-2.21	1.88	42.92	32.24	17.02	5163	74.50	111.56	1:30	*
3.96	-0.01	0.03	35.37	24.05	9.74	20:51:57	166.32	1:30	2.33	
2.49	-0.10	-1.88	32.97	28.77	16.96	5164	66.13	85.00	1:30	*
0.28	0.07	0.05	28.05	21.89	9.66	20:52:29	342.18	1:30	2.72	
-2.65	-0.17	0.04	29.02	23.06	15.71	5165	57.84	64.02	1:30	C
-1.69	-2.16	4.26	25.17	18.52	9.39	20:53:01	0.00	1:30	2.43	
2.84	-0.28	2.20	28.27	22.00	14.48	5166	45.69	59.54	1:30	C
-2.14	0.12	4.18	26.15	19.02	9.58	20:53:33	0.00	1:30	2.11	
0.12	-0.69	0.07	32.24	24.02	15.85	5167	41.19	50.71	1:30	C
1.84	-1.90	3.79	30.36	21.04	10.56	20:54:05	0.00	1:30	3.88	
0.18	-0.08	0.04	37.99	27.39	17.22	5168	47.76	49.04	1:30	C
-3.07	-0.05	3.49	34.58	23.51	11.47	20:54:37	0.00	1:30	4.11	
0.03	-0.00	0.02	42.37	29.97	18.46	5169	65.35	65.36	1:30	C
0.09	-1.71	-3.57	35.73	23.42	11.21	20:55:09	0.00	1:30	5.46	
0.25	0.03	1.84	39.10	29.19	17.31	5170	0.00	81.22	1:33	*
-4.20	-1.75	0.06	33.31	22.88	10.59	20:55:41	1065.9	1:30	2.68	
-2.31	-0.04	1.87	36.47	27.79	16.99	5171	71.57	72.22	1:33	C
-4.49	0.02	-0.01	31.11	22.00	10.48	20:56:13	0.00	1:30	2.74	
2.20	-0.05	1.88	36.90	26.63	16.95	5172	61.67	63.66	1:33	C
4.17	0.06	0.06	33.54	22.53	10.84	20:56:45	0.00	1:30	2.06	
-0.02	-0.12	1.78	38.70	30.82	17.93	5173	55.18	55.29	1:33	*
-3.82	-0.05	-0.09	36.61	26.29	11.22	20:57:17	295.21	1:30	4.03	
-2.33	-2.45	-0.02	37.90	32.61	19.93	5174	53.46	62.12	1:33	*
4.17	4.54	0.03	33.54	25.97	11.43	20:57:49	348.13	1:30	7.27	
2.64	-0.17	5.97	33.90	27.42	18.35	5175	68.65	69.75	1:33	C
-4.93	-0.13	-3.73	28.35	21.40	10.72	20:58:21	0.00	1:30	3.52	
0.54	3.35	-0.05	6601	23.85	16.17	5176	57.16	63.40	1:33	C
100.3	4.00	-3.95	542.2	19.91	10.12	20:58:48	0.00	1:30	2.00	

-999	-999	-0.01	719.8	503.0	15.68	5177	0.00	6.82	1.33	999.00	C
-4.75	-95.4	0.04	29.41	217.4	9.87	20:59:53		0.00	1:30		C
-5.08	4.80	53.19	34.27	24.88	86.03	5178	0.00	24.41	1.33	634.08	C
4.73	0.01	23.80	29.52	19.98	23.33	21:00:25		0.00	1:30		C
0.10	0.03	4.35	33.45	25.08	14.62	5179	56.74	61.74	1.33	4.09	C
-0.02	4.03	0.05	29.12	19.70	8.44	21:00:57		0.00	1:30		C
-2.18	3.35	0.13	40.98	23.86	13.98	5180	57.99	64.62	1.33	3.36	C
4.19	4.38	1.48	33.38	18.16	8.13	21:01:29		0.00	1:30		C
-1.84	-0.19	-4.72	46.47	27.39	13.52	5181	76.22	76.58	1.33	2.43	C
-3.49	-0.26	1.92	40.09	22.08	8.30	21:02:01		0.00	1:30		C
0.04	2.41	-0.20	46.88	33.16	16.32	5182	84.33	121.52	1.33	3.89	*
3.56	-0.14	0.11	39.25	26.18	9.81	21:02:33		49.26	1:40		*
0.12	-0.07	0.21	47.66	33.15	20.15	5183	79.44	124.30	1.33	2.02	*
-0.35	0.17	4.50	44.64	29.43	13.85	21:03:05		33.57	1:40		*
-2.91	-0.07	0.03	58.25	42.78	24.62	5184	61.11	471.32	1.33	6.33	*
-0.04	0.12	-2.61	55.74	36.47	15.29	21:03:37		4.34	1:40		*
-0.23	2.86	-2.46	62.39	46.58	25.83	5185	138.77	0.00	1.33	10.48	C
-0.28	-0.25	-2.95	50.10	33.72	13.52	21:04:09		0.00	1:40		C
5.26	0.40	-0.24	42.58	37.36	21.93	5186	185.65	0.00	1.33	2.54	C
0.22	0.08	-3.10	34.36	28.20	12.88	21:04:41		0.00	1:40		C
-0.29	3.92	-0.07	38.31	30.37	21.39	5187	39.55	79.97	1.33	5.55	*
-4.19	-3.45	-3.39	33.38	23.36	11.85	21:05:13		343.77	1:40		*
-0.18	-3.20	-0.22	34.33	24.90	15.60	5188	76.25	76.49	1.33	3.39	C
-5.26	0.09	4.47	26.50	18.76	8.99	21:05:45		0.00	1:40		C
-2.67	0.29	1.06	33.79	19.69	12.87	5189	70.09	74.73	1.33	1.71	C
0.20	-4.20	-3.71	23.62	14.07	7.48	21:06:17		0.00	1:40		C
3.87	-4.60	-0.03	23.11	17.42	10.66	5190	66.11	73.26	1.33	8.48	C
0.40	-2.77	-2.18	18.45	14.38	7.31	21:06:49		0.00	1:40		C
-0.03	3.10	2.70	30.20	15.59	11.72	5191	36.88	73.15	1.33	2.27	C
2.22	0.34	-2.17	25.10	12.76	7.36	21:07:21		0.00	1:50		C
0.34	0.11	0.47	30.67	22.26	10.57	5192	48.51	49.70	1.33	5.39	C
-0.15	-0.04	0.12	28.37	19.31	6.69	21:07:53		0.00	1:50		C
0.13	1.64	-0.15	36.64	21.69	13.39	5193	56.58	74.43	1.33		*

-1.96	-0.35	-0.23	28.53	17.16	8.30	21:08:26	60.38	2.00	2.74	
0.02	0.23	0.26	32.72	28.15	14.88	5194	62.51	0.00	1.33	C
-3.43	-1.59	-1.71	33.40	25.05	9.34	21:08:57		0.00	2.00	5.65
2.78	0.13	-0.04	30.51	30.54	18.22	5195	190.54	0.00	1.33	C
-5.86	-4.90	-1.65	24.07	23.83	9.65	21:09:29		0.00	4.50	12.07
-3.03	-0.63	1.98	29.18	17.75	16.08	5196	55.34	250.37	1.33	*
2.41	6.00	-4.43	23.23	13.35	10.86	21:10:01		22.54	2.60	2.03
-0.19	-0.39	-2.95	35.22	19.29	10.87	5197	48.56	92.22	1.33	*
0.05	0.20	0.96	27.91	14.47	7.47	21:10:33		50.42	2.60	3.76
0.26	2.05	-0.21	36.16	20.45	9.28	5198	64.70	157.83	1.33	*
0.07	0.23	-0.14	31.59	14.87	4.85	21:11:05		46.21	2.20	1.65
2.45	-0.09	-2.99	35.92	26.17	10.82	5199	86.68	0.00	1.33	C
-4.05	0.07	0.34	29.86	20.23	6.91	21:11:37		0.00	2.20	4.21
2.72	0.34	2.16	28.68	23.00	14.72	5200	66.11	332.25	1.33	*
-4.32	2.16	-1.74	21.73	16.80	9.13	21:12:09		15.16	2.20	2.10
-0.06	-0.70	2.64	24.52	16.40	12.12	5201	0.00	61.43	1.43	*
-0.05	2.98	-2.14	18.04	11.84	7.54	21:12:41		1038.9	2.20	3.93
0.20	0.27	0.51	21.99	12.69	8.40	5202	48.24	54.90	1.43	C
3.66	-4.61	3.54	15.29	8.61	4.67	21:13:13		0.00	2.00	6.55
-3.64	0.23	1.30	23.08	10.20	5.35	5203	44.37	57.12	1.43	C
-3.43	-6.26	-4.29	16.31	6.44	2.76	21:13:45		0.00	2.00	7.41
-0.52	-2.99	-4.12	23.63	10.68	3.87	5204	41.70	268.09	1.43	C
-0.05	0.05	-0.07	16.32	7.30	2.67	21:14:17		0.00	1.30	9.81
0.03	-0.38	0.51	24.60	11.58	5.92	5205	53.95	0.00	1.43	C
-3.06	-0.09	0.23	18.21	9.50	3.88	21:14:49		0.00	1.30	8.23
-0.13	0.34	-0.02	29.89	14.78	7.45	5206	41.15	282.52	1.43	C
2.23	3.84	-4.26	24.97	11.94	5.39	21:15:21		0.00	1.30	4.02
2.84	1.53	-1.67	31.34	20.02	9.62	5207	50.07	81.42	1.43	C
-2.13	-2.20	-0.16	26.13	17.52	7.41	21:15:54		0.00	1.30	1.90
-0.13	1.67	4.20	30.94	23.58	15.12	5208	52.43	71.63	1.43	*
-0.09	-1.82	0.12	27.53	21.82	10.50	21:16:25		26.82	2.00	2.27
0.32	-0.19	0.12	30.59	28.06	19.77	5209	43.98	7.64	1.43	C
-5.45	0.01	4.39	32.01	27.01	13.86	21:16:57		0.00	2.00	2.53

0.15	2.32	2.63	25.32	33.01	24.32	5210	33.46	0.00	1.43	4.68	C
-0.08	-3.04	0.07	26.97	31.08	15.11	21:17:29		0.00	2.00		
3.05	-2.94	2.68	29.10	25.57	24.34	5211	31.30	42.67	1.43		*
0.03	0.38	-3.21	27.39	19.81	12.75	21:18:01		23.02	2.30	12.37	
0.06	0.21	0.32	30.81	21.53	13.13	5212	40.86	52.88	1.43		*
0.30	1.21	-6.11	25.11	15.07	6.67	21:18:33		188.02	2.30	10.09	
0.12	-4.33	0.55	29.38	18.33	8.90	5213	26.59	80.19	1.43		*
-2.56	-3.72	-3.99	21.78	10.91	3.99	21:19:05		289.19	2.30	7.49	
-3.95	-1.28	-3.95	22.75	12.46	5.94	5214	0.00	82.00	1.43		*
-4.35	-5.02	-0.04	12.91	7.92	3.80	21:19:37		554.57	2.30	12.15	
-4.78	-0.05	-0.04	13.87	10.01	5.97	5215	44.47	50.21	1.43		C
4.53	0.01	-4.16	12.29	8.32	3.81	21:20:09		0.00	2.30	16.76	
-0.26	0.03	-2.59	13.19	10.84	6.14	5216	19.42	56.98	1.43		C
0.12	1.81	-0.03	11.91	8.77	3.86	21:20:41		0.00	2.30	4.05	
3.20	-0.09	-2.51	12.99	10.29	6.32	5217	19.41	51.93	1.43		C
-4.93	-2.00	-4.15	11.29	7.97	3.82	21:21:13		0.00	2.50	6.24	
-0.32	-0.13	-2.88	11.50	9.02	5.52	5218	20.46	124.79	1.43		C
0.31	-2.32	-4.36	9.65	6.85	3.64	21:21:46		0.00	2.50	3.61	
-4.48	0.17	-0.09	9.92	7.78	4.83	5219	22.30	0.00	1.43		C
0.22	-0.17	-4.92	8.41	5.92	3.23	21:22:17		0.01	2.60	4.79	
-0.05	0.26	-3.96	8.79	6.49	4.02	5220	20.42	0.00	1.43		C
-8.04	-0.07	-5.33	6.93	4.87	2.98	21:22:49		0.01	2.60	3.12	
-3.73	-5.57	-0.02	6.01	5.70	3.66	5221	16.97	0.00	1.43		C
-0.28	-3.31	-0.00	4.54	4.78	2.98	21:23:21		0.01	2.60	3.66	
-4.49	-3.29	-4.29	4.95	4.66	3.70	5222	10.17	0.00	1.43		C
-0.06	-4.04	2.61	79.16	3.85	3.04	21:23:53		0.02	2.70	7.42	
0.18	-0.11	-0.27	4.28	3.66	3.16	5223	50.96	148.91	1.43		*
0.00	2.92	-2.69	23.89	3.21	2.95	21:24:25		68.34	2.70	325.39	
0.05	0.04	0.02	4.26	3.57	2.84	5224	19.28	54.41	1.43		C
0.00	-0.00	-2.81	23.69	3.20	2.82	21:24:57		0.00	2.70	98.00	
-4.99	0.04	-5.59	4.42	3.66	2.84	5225	19.05	57.76	1.43		C
-3.66	0.02	2.80	10.02	3.23	2.83	21:25:29		0.00	2.70	96.49	
-1.77	0.14	0.02	4.49	3.65	2.87	5226	12.56	0.00	1.43		C

-0.04	-0.11	-2.75	3.82	3.27	2.88	21:26:01	0.02	2.70	32.82
-0.57	0.16	0.04	3.36	3.48	2.90	5227	8.40	2.06	1.43
-0.27	-0.13	-2.72	3.10	3.08	2.92	21:26:33	13.24	2.70	4.70
1.99	5.64	5.63	2.65	2.82	2.82	5228	6.39	2.51	1.43
-1.21	3.03	-2.65	2.36	2.61	2.99	21:27:05	24.59	2.70	4.64
0.30	0.21	-1.74	1.84	2.28	2.65	5229	4.91	2.48	1.43
-2.58	0.10	-0.00	1.86	2.36	2.99	21:27:38	37.25	2.70	3.59
0.46	-0.09	-0.05	1.58	1.90	2.58	5230	2.45	2.03	1.43
-0.25	-3.76	-2.67	1.80	2.11	2.98	21:28:09	71.28	2.70	2.16
-0.05	0.19	-2.74	1.80	1.96	2.32	5231	1.32	1.81	1.43
2.75	-3.83	-3.23	1.93	2.07	2.47	21:28:41	43.58	2.70	6.03
7.21	-3.52	3.33	1.82	1.90	1.91	5232	2.65	1.83	1.43
0.43	-0.11	-0.01	1.77	1.77	2.07	21:29:13	42.01	2.70	6.77
4.70	0.00		1.68	1.74		5233	2.85	1.75	1.43
-4.63	-3.84		1.71	2.06		21:29:45	38.18	2.80	4.02
0.01			1.74						
-3.83			2.07						

*
*
*
*
*
*
*
*
*
*

CLIENT: Atlantic Geoscience
PROJECT: 3-40213
LOCATION: Beaufort Sea
25 m DIPOLES

LINE L45aed.W02 A-7

Processing date: 03-28-1994
CHARGEABILITY (mV/V)

RESISTIVITY (ohm-m)

								Depth(m)									
								0	8	8	6	8	5	8	8	8	0
-3.01				1.44													
0.07				1.64													
0.07	0.11			1.51	1.66												
3.03	-0.01			1.64	1.73			5234	1.40	1.94	5.75	4.07					*
2.93	4.69	3.60		1.50	1.69	1.75		21:33:21		27.86	2.80						
-2.99	0.04	0.01		1.60	1.74	2.08		5235	1.44	1.94	5.75	3.14					*
1.40	0.05	-3.56		3.03	1.68	1.78		21:33:53		27.86	2.80						
0.03	0.01	-3.81		1.69	1.76	2.07		5236	1.43	1.95	5.75	2.95					*
7.76	4.69	-3.57		1.31	1.68	1.77		21:34:25		27.85	2.80						
-0.25	-4.47	3.83		1.67	1.77	2.06		5237	291.02	68.88	5.75	14.96					*
-0.19	0.12	0.01		1.57	1.69	1.78		21:34:57		68.88	2.80						
0.10	0.24	0.02		1.64	1.74	2.07		5238	280.41	158.29	5.75	11.70					*
0.29	-4.74	-3.58		1.97	1.66	1.77		21:35:29		158.29	2.70						
-0.31	0.00	0.02		1.62	1.74	2.06		5239	279.48	143.68	5.75	5.72					*
2.62	4.73	-0.01		1.65	1.67	1.75		21:36:01		143.68	2.70						
3.22	4.52	0.02		1.71	1.75	2.06		5240	279.30	104.58	5.75	7.11					*
-2.34	-4.42	0.06		1.72	1.79	1.83		21:36:33		104.58	2.70						
-3.37	0.01	-3.69		1.62	1.85	2.14		5241	279.25	137.16	5.46	7.56					*
-0.22	4.55	0.03		1.46	1.74	1.92		21:37:05		137.16	2.70						
-0.25	-3.88	3.46		1.63	1.82	2.28		5242	279.25	137.16	5.46	7.45					*
-2.79	4.43	0.01		1.57	1.72	1.93		21:37:37		137.16	2.70						
-0.07	-4.09	-3.52		1.71	1.88	2.24		5243	279.25	137.16	5.46	10.09					*
2.30	-4.37	-3.31		1.61	1.81	1.91		21:38:09		137.16	2.70						
-3.19	4.19	0.02		1.64	1.89	2.15		5244	279.11	151.31	5.46	7.20					*
0.11	3.78	-0.01		1.61	1.81	1.90		21:38:41		151.31	2.70						
-3.21	0.03	0.00		1.72	1.92	2.15		5245	279.11	151.31	5.46	7.19					*
								21:39:13			2.60						

-0.37	-0.22	0.02	1.61	1.84	1.92	5246	278.99	152.67	5.46	7.02	*
-3.04	-0.01	0.01	1.71	1.92	2.13	21:39:45					
-2.01	-4.41	-3.27	2.37	1.76	1.93	5247	278.99	152.67	5.46	7.56	*
-3.36	0.05	0.03	1.65	1.84	2.18	21:40:17					
-0.16	-0.01	0.01	1.55	1.69	1.93	5248	289.63	86.78	5.46	10.42	*
0.14	-4.41	-3.54	1.52	1.79	2.24	21:40:49					
-2.24	0.00	-3.38	1.85	1.65	1.87	5249	284.90	142.99	5.46	7.74	*
2.80	-4.49	0.04	1.60	1.76	2.18	21:41:21					
-2.73	0.09	-3.51	1.42	1.65	1.80	5250	273.19	106.81	5.46	5.67	*
-3.33	-0.00	3.78	1.65	1.73	2.09	21:41:54					
0.10	4.80	-0.01	1.54	1.64	1.76	5251	273.13	145.51	5.15	8.51	*
0.08	-4.58	-3.87	1.56	1.73	2.04	21:42:25					
-2.02	-4.75	-3.59	9.86	1.67	1.76	5252	273.13	145.51	5.15	6.11	*
-3.16	4.64	-3.87	1.58	1.70	2.04	21:42:57					
-3.57	0.01	-0.03	2.63	1.64	1.73	5253	99999.	10.17	5.15	49.13	*
3.51	0.01	-3.90	1.57	1.69	2.02	21:43:29					
-0.37	-0.02	0.03	1.55	1.70	1.73	5254	99999.	34.32	5.15	37.26	*
2.88	-4.57	-3.90	1.67	1.73	2.03	21:44:01					
-0.13	4.73	-3.67	1.57	1.67	1.72	5255	99999.	35.38	5.15	35.39	*
0.48	0.01	3.90	1.55	1.70	2.03	21:44:33					
-2.87	-4.86	-3.65	1.53	1.63	1.73	5256	99999.	35.38	5.15	35.67	*
-0.32	0.01	-0.00	1.54	1.70	2.02	21:45:05					
0.05	-1.48	0.00	1.53	1.65	1.72	5257	99999.	35.38	5.15	35.59	*
3.08	0.02	-0.01	1.58	1.69	2.02	21:45:37					
2.53	0.19	-0.00	1.53	1.65	1.72	5258	99999.	35.38	5.15	35.31	*
-3.45	0.02	0.01	1.60	1.70	2.02	21:46:09					
-2.16	0.06	-3.66	1.85	1.68	1.73	5259	99999.	35.38	5.15	35.38	*
3.31	4.59	-3.88	1.67	1.72	2.03	21:46:41					
-0.22	-1.76	-0.00	1.57	1.66	1.75	5260	99999.	34.58	5.15	36.55	*
2.94	-4.50	0.01	1.65	1.76	2.04	21:47:13					
-2.61	0.05	3.58	1.62	1.71	1.77	5261	99999.	34.57	5.15	36.88	*
-0.25	4.43	0.00	1.71	1.78	2.04	21:47:45					
0.04	-1.69	0.01	1.62	1.76	1.79	5262	99999.	34.63	5.15	38.47	*

-0.58	-4.32	-3.89
-0.27	-1.30	-3.49
2.88	0.03	3.88
-2.49	1.61	3.42
-3.03	-0.01	-0.03
0.20	0.04	0.00
2.82	-0.03	-0.00
0.07	-0.04	3.46
3.18	-0.07	-3.84
0.04	-0.03	-0.04
-0.10	-0.03	0.06
-2.24	-0.04	-3.62
2.98	-4.36	0.08
2.60	1.66	3.32
0.12	0.18	0.07
-0.14	4.86	-2.79
2.30	-0.04	-0.12
-1.85	-3.73	0.07
-0.18	-3.27	2.66
0.07	-0.34	-2.39
-1.77	-0.04	-2.66
2.27	-2.56	-2.39
5.80	-0.02	-0.02
0.07	-0.00	2.37
-3.64	2.77	-0.01
-2.21	-0.00	0.02
-0.35	0.01	0.02
0.15	-0.00	-0.03
3.30	-2.89	-2.90
2.30	2.61	0.01
-3.76	0.04	-2.84
0.09	0.02	-2.45
3.62	0.01	-2.79

1.78	1.83	2.03
1.73	1.78	1.81
1.74	1.86	2.04
1.62	1.81	1.85
1.75	1.89	2.06
1.59	1.80	1.89
1.69	1.87	2.07
1.69	1.72	1.83
1.73	1.76	2.06
1.68	1.74	1.75
1.73	1.77	2.00
1.75	1.76	1.74
1.77	1.81	2.07
1.69	1.83	1.91
1.76	2.03	2.37
1.84	1.94	2.27
1.98	2.19	2.67
2.23	2.12	2.49
2.48	2.42	2.96
2.93	2.70	2.64
3.11	2.69	2.97
3.37	3.02	2.65
3.41	2.87	2.91
3.69	3.19	2.67
3.51	2.86	2.84
3.71	3.12	2.59
3.41	2.81	2.81
3.63	3.07	2.55
3.43	2.73	2.73
3.59	3.03	2.48
3.33	2.74	2.78
3.64	3.06	2.58
3.34	2.75	2.83

21:48:17			
5263	99999.	35:03	5:15 37.00
21:48:49			
5264	99999.	35:03	5:15 37.07
21:49:21			
5265	99999.	34:57	5:15 38.66
21:49:53			
5266	99999.	34:57	5:15 39.52
21:50:25			
5267	99999.	34:57	5:15 36.31
21:50:57			
5268	99999.	34:57	5:15 30.73
21:51:29			
5269	99999.	10:05	5:15 38.83
21:52:02			
5270	99999.	11:24	6:45 37.41
21:52:33			
5271	99999.	11:52	6:45 39.84
21:53:05			
5272	99999.	12:30	6:45 48.01
21:53:37			
5273	99999.	13:53	6:45 54.12
21:54:09			
5274	99999.	14:00	6:45 57.54
21:54:41			
5275	99999.	15:19	6:45 67.78
21:55:13			
5276	99999.	15:19	6:45 66.49
21:55:45			
5277	99999.	15:19	6:45 63.77
21:56:17			
5278	99999.	15:19	6:45 62.63
21:56:49			

0.02	2.61	0.02	3.61	3.02	2.56	5279	9999.	15:10	6:45	62.06	*
-4.14	0.01	-2.75	3.31	2.77	2.88	21:57:21					
-2.22	-2.56	-2.42	3.98	3.08	2.61	5280	9999.	15:10	5:88	59.15	*
3.46	-0.01	-2.75	3.65	2.82	2.88	21:57:54					
0.04	0.08	2.40	4.48	3.34	2.63	5281	9999.	15:20	5:88	61.79	*
-0.03	-0.06	-2.73	4.18	2.98	2.89	21:58:25					
0.07	-0.06	0.05	4.97	3.78	2.71	5282	9999.	16:25	5:88	57.81	*
0.09	-0.09	-2.69	4.73	3.43	2.93	21:58:57					
-2.79	-1.78	-2.07	5.85	4.45	3.06	5283	9999.	17:40	5:88	58.75	*
-1.99	-0.07	-2.50	5.71	4.01	3.16	21:59:29					
-0.15	-3.64	0.04	7.26	5.29	3.41	5284	9999.	19:46	5:88	71.06	*
0.06	-0.00	-2.45	6.85	4.43	3.23	22:00:01					
2.73	-2.78	-1.86	8.09	5.68	3.39	5285	9999.	19:46	5:88	72.16	*
1.77	0.01	-2.44	6.66	4.33	3.23	22:00:33					
2.35	0.00	-0.00	7.63	5.33	3.34	5286	9999.	19:46	5:88	70.40	*
-1.97	0.01	0.03	6.40	4.17	3.26	22:01:05					
0.08	2.99	0.03	7.17	5.28	3.35	5287	9999.	19:46	5:88	70.76	*
0.02	-1.82	-2.38	6.21	4.33	3.32	22:01:37					
3.24	-2.92	-1.82	6.78	5.40	3.47	5288	9999.	19:46	5:88	75.79	*
0.01	-0.02	-0.00	5.98	4.28	3.26	22:02:09					
2.73	-0.08	-1.87	6.18	5.01	3.38	5289	9999.	19:46	5:88	83.06	*
-1.77	-1.94	-2.55	5.42	4.08	3.10	22:02:41					
-0.02	-0.01	-1.97	6.24	4.60	3.20	5290	9999.	19:46	5:15	82.67	*
-2.43	2.10	-0.04	5.36	3.75	2.91	22:03:13					
0.02	3.18	2.10	6.13	4.59	3.01	5291	9999.	19:46	5:15	79.25	*
-2.35	0.00	-2.84	5.47	3.77	2.78	22:03:45					
-0.09	0.63	-0.00	6.04	4.63	3.01	5292	9999.	19:46	5:15	76.94	*
0.03	2.05	2.75	5.37	3.85	2.87	22:04:17					
4.03	0.02	-1.99	5.47	4.77	3.17	5293	9999.	19:46	5:15	75.94	*
0.03	-1.92	-2.73	5.14	4.11	2.89	22:04:49					
3.88	-0.03	-0.00	5.19	4.57	3.33	5294	9999.	19:46	5:15	84.04	*
2.86	-0.05	-2.73	4.81	3.86	2.89	22:05:21					
0.10	3.62	-2.08	4.88	4.21	3.04	5295	9999.	19:52	5:15	97.72	*

[illegible]

0.28	0.04	3.99
-3.68	0.06	-3.30
3.63	-2.32	3.69
4.20	3.38	-2.87
-2.89	-0.03	3.77
-0.61	0.00	0.06
-0.06	-0.04	3.86
0.35	3.70	-3.82
0.15	-0.11	4.80
0.22	-4.35	0.02
2.51	0.23	0.01
0.04	1.35	-4.25
2.64	2.59	
-0.03	-4.25	
-0.02		
-4.14		

17.37	13.85	7.87
14.06	10.80	4.79
14.74	11.77	8.50
13.16	10.03	5.48
15.30	11.90	8.33
14.57	10.75	5.26
18.08	13.53	8.18
16.21	10.17	4.15
17.84	12.01	6.54
13.67	8.67	3.72
16.25	10.78	6.07
13.48	8.43	3.71
11.14	6.10	
8.76	3.71	
6.32		
3.81		

5312	9999.	48.69	4.76	98.54
22:14:56		58.14	1.90	
5313	9999.	48.69	4.76	107.80
22:15:28		58.14	1.90	
5314	9999.	48.75	4.76	111.42
22:16:01		58.24	2.40	
5315	9999.	48.75	4.76	132.07
22:16:33		58.24	2.40	
5316	9999.	48.77	4.76	118.75
22:17:05		58.31	2.70	
5317	9999.	48.77	4.76	119.94
22:17:37		58.31	2.70	
5318	9999.	48.77	4.76	114.57
22:18:10		58.31	2.70	

*
*
*
*
*
*
*
*

Processing date: 03-24-1994

CHARGEABILITY (mV/V)

RESISTIVITY (ohm-in)

Depth (m)

-3.01			1.44																																																																																																																																																																																																																																																																																																																																																																																																																																																																																																																																																																																																																																																																																																																																																																																																																																																																																																																																																																																																																																																																																																																																																																																																																																																																																																																																																																																																																																										
-------	--	--	------	--	--	--	--	--	--	--	--	--	--	--	--	--	--	--	--	--	--	--	--	--	--	--	--	--	--	--	--	--	--	--	--	--	--	--	--	--	--	--	--	--	--	--	--	--	--	--	--	--	--	--	--	--	--	--	--	--	--	--	--	--	--	--	--	--	--	--	--	--	--	--	--	--	--	--	--	--	--	--	--	--	--	--	--	--	--	--	--	--	--	--	--	--	--	--	--	--	--	--	--	--	--	--	--	--	--	--	--	--	--	--	--	--	--	--	--	--	--	--	--	--	--	--	--	--	--	--	--	--	--	--	--	--	--	--	--	--	--	--	--	--	--	--	--	--	--	--	--	--	--	--	--	--	--	--	--	--	--	--	--	--	--	--	--	--	--	--	--	--	--	--	--	--	--	--	--	--	--	--	--	--	--	--	--	--	--	--	--	--	--	--	--	--	--	--	--	--	--	--	--	--	--	--	--	--	--	--	--	--	--	--	--	--	--	--	--	--	--	--	--	--	--	--	--	--	--	--	--	--	--	--	--	--	--	--	--	--	--	--	--	--	--	--	--	--	--	--	--	--	--	--	--	--	--	--	--	--	--	--	--	--	--	--	--	--	--	--	--	--	--	--	--	--	--	--	--	--	--	--	--	--	--	--	--	--	--	--	--	--	--	--	--	--	--	--	--	--	--	--	--	--	--	--	--	--	--	--	--	--	--	--	--	--	--	--	--	--	--	--	--	--	--	--	--	--	--	--	--	--	--	--	--	--	--	--	--	--	--	--	--	--	--	--	--	--	--	--	--	--	--	--	--	--	--	--	--	--	--	--	--	--	--	--	--	--	--	--	--	--	--	--	--	--	--	--	--	--	--	--	--	--	--	--	--	--	--	--	--	--	--	--	--	--	--	--	--	--	--	--	--	--	--	--	--	--	--	--	--	--	--	--	--	--	--	--	--	--	--	--	--	--	--	--	--	--	--	--	--	--	--	--	--	--	--	--	--	--	--	--	--	--	--	--	--	--	--	--	--	--	--	--	--	--	--	--	--	--	--	--	--	--	--	--	--	--	--	--	--	--	--	--	--	--	--	--	--	--	--	--	--	--	--	--	--	--	--	--	--	--	--	--	--	--	--	--	--	--	--	--	--	--	--	--	--	--	--	--	--	--	--	--	--	--	--	--	--	--	--	--	--	--	--	--	--	--	--	--	--	--	--	--	--	--	--	--	--	--	--	--	--	--	--	--	--	--	--	--	--	--	--	--	--	--	--	--	--	--	--	--	--	--	--	--	--	--	--	--	--	--	--	--	--	--	--	--	--	--	--	--	--	--	--	--	--	--	--	--	--	--	--	--	--	--	--	--	--	--	--	--	--	--	--	--	--	--	--	--	--	--	--	--	--	--	--	--	--	--	--	--	--	--	--	--	--	--	--	--	--	--	--	--	--	--	--	--	--	--	--	--	--	--	--	--	--	--	--	--	--	--	--	--	--	--	--	--	--	--	--	--	--	--	--	--	--	--	--	--	--	--	--	--	--	--	--	--	--	--	--	--	--	--	--	--	--	--	--	--	--	--	--	--	--	--	--	--	--	--	--	--	--	--	--	--	--	--	--	--	--	--	--	--	--	--	--	--	--	--	--	--	--	--	--	--	--	--	--	--	--	--	--	--	--	--	--	--	--	--	--	--	--	--	--	--	--	--	--	--	--	--	--	--	--	--	--	--	--	--	--	--	--	--	--	--	--	--	--	--	--	--	--	--	--	--	--	--	--	--	--	--	--	--	--	--	--	--	--	--	--	--	--	--	--	--	--	--	--	--	--	--	--	--	--	--	--	--	--	--	--	--	--	--	--	--	--	--	--	--	--	--	--	--	--	--	--	--	--	--	--	--	--	--	--	--	--	--	--	--	--	--	--	--	--	--	--	--	--	--	--	--	--	--	--	--	--	--	--	--	--	--	--	--	--	--	--	--	--	--	--	--	--	--	--	--	--	--	--	--	--	--	--	--	--	--	--	--	--	--	--	--	--	--	--	--	--	--	--	--	--	--	--	--	--	--	--	--	--	--	--	--	--	--	--	--	--	--	--	--	--	--	--	--	--	--	--	--	--	--	--	--	--	--	--	--	--	--	--	--	--	--	--	--	--	--	--	--	--	--	--	--	--	--	--	--	--	--	--	--	--	--	--	--	--	--	--	--	--	--	--	--	--	--	--	--	--	--	--	--	--	--	--	--	--	--	--	--	--	--	--	--	--	--	--	--	--	--	--	--	--	--	--	--	--	--	--	--	--	--	--	--	--	--	--	--	--	--	--	--	--	--	--	--	--	--	--	--	--	--	--	--	--	--	--	--	--	--	--	--	--	--	--	--	--	--	--	--	--	--	--	--	--	--	--	--	--	--	--	--	--	--	--	--	--	--	--	--	--	--	--	--	--	--	--	--	--	--	--	--	--	--	--	--	--	--	--	--	--	--	--	--	--	--	--	--	--	--	--	--	--	--	--	--	--	--	--	--	--	--	--	--	--	--	--	--	--	--	--	--	--	--	--	--	--	--	--	--	--	--	--	--	--	--	--	--	--	--	--	--	--	--	--	--	--	--	--	--	--	--	--	--	--	--	--	--	--	--	--	--	--	--	--	--	--	--	--	--	--	--	--	--	--	--	--	--	--	--	--	--	--	--	--	--	--	--	--	--	--	--	--	--	--	--	--	--	--	--	--	--	--	--	--	--	--	--	--	--	--	--	--	--	--	--	--	--	--	--	--	--	--	--	--	--	--	--	--	--	--	--	--	--	--	--	--	--	--	--	--	--	--	--	--	--	--	--	--	--	--	--	--	--	--	--	--	--	--	--	--	--	--	--	--	--	--	--	--	--	--	--	--	--	--	--	--	--	--	--	--	--	--	--	--	--	--	--	--	--	--	--	--	--	--	--	--	--	--	--	--	--	--	--	--	--	--	--	--	--	--	--	--	--	--	--	--	--	--	--	--	--	--	--	--	--	--	--	--	--	--	--	--	--	--	--	--	--	--	--	--	--	--	--	--	--	--	--	--	--	--	--	--	--	--	--	--	--	--	--	--	--	--	--	--	--	--	--	--	--	--	--	--	--	--	--	--	--	--	--	--	--	--	--	--	--	--	--	--	--	--

0.11	3.78	-0.01	1.61	1.81	1.90	5245	0.00	217:97	5:46	12.04	*
-3.21	0.03	0.00	1.72	1.92	2.15	21:39:13					
-0.37	-0.22	0.02	1.61	1.84	1.92	5246	0.00	183:04	5:46	10.87	*
-3.04	-0.01	0.01	1.71	1.92	2.13	21:39:45					
-2.01	-4.41	-3.27	2.37	1.76	1.93	5247	0.00	144:72	5:46	11.16	*
-3.36	0.05	0.03	1.65	1.84	2.18	21:40:17					
-0.16	-0.01	0.01	1.55	1.69	1.93	5248	0.93	62:52	5:46	18.35	*
0.14	-4.41	-3.54	1.52	1.79	2.24	21:40:49					
-2.24	0.00	-3.38	1.85	1.65	1.87	5249	0.00	183:43	5:46	13.43	*
2.80	-4.49	0.04	1.60	1.76	2.18	21:41:21					
-2.73	0.09	-3.51	1.42	1.65	1.80	5250	0.00	104:78	5:46	15.17	*
-3.33	-0.00	3.78	1.65	1.73	2.09	21:41:54					
0.10	4.80	-0.01	1.54	1.64	1.76	5251	0.00	187:03	5:15	10.87	*
0.08	-4.58	-3.87	1.56	1.73	2.04	21:42:25					
-2.02	-4.75	-3.59	9.86	1.67	1.76	5252	0.00	147:90	5:15	11.59	*
-3.16	4.64	-3.87	1.58	1.70	2.04	21:42:57					
-3.57	0.01	-0.03	2.63	1.64	1.73	5253	22.15	0:00	5:15	101.27	C
3.51	0.01	-3.90	1.57	1.69	2.02	21:43:29					
-0.37	-0.02	0.03	1.55	1.70	1.73	5254	1.70	50:83	5:15	21.23	*
2.88	-4.57	-3.90	1.67	1.73	2.03	21:44:01					
-0.13	4.73	-3.67	1.57	1.67	1.72	5255	0.00	138:01	5:15	11.10	*
0.48	0.01	3.90	1.55	1.70	2.03	21:44:33					
-2.87	-4.86	-3.65	1.53	1.63	1.73	5256	0.00	137:36	5:15	12.19	*
-0.32	0.01	-0.00	1.54	1.70	2.02	21:45:05					
0.05	-1.48	0.00	1.53	1.65	1.72	5257	0.00	151:23	5:15	11.57	*
3.08	0.02	-0.01	1.58	1.69	2.02	21:45:37					
2.53	0.19	-0.00	1.53	1.65	1.72	5258	0.00	148:69	5:15	11.32	*
-3.45	0.02	0.01	1.60	1.70	2.02	21:46:09					
-2.16	0.06	-3.66	1.85	1.68	1.73	5259	0.00	150:67	5:15	11.17	*
3.31	4.59	-3.88	1.67	1.72	2.03	21:46:41					
-0.22	-1.76	-0.00	1.57	1.66	1.75	5260	0.00	95:48	5:15	13.30	*
2.94	-4.50	0.01	1.65	1.76	2.04	21:47:13					
-2.61	0.05	3.58	1.62	1.71	1.77						*

-0.25	4.43	0.00	1.71	1.78	2.04	5261	0.00	153.65	5:15	11.12	
0.04	-1.69	0.01	1.62	1.76	1.79	21:47:45					*
-0.58	-4.32	-3.89	1.78	1.83	2.03	5262	0.00	146.29	5:15	10.96	
-0.27	-1.30	-3.49	1.73	1.78	1.81	21:48:17					*
2.88	0.03	3.88	1.74	1.86	2.04	5263	0.00	145.92	5:15	10.56	
-2.49	1.61	3.42	1.62	1.81	1.85	21:48:49					*
-3.03	-0.01	-0.03	1.75	1.89	2.06	5264	0.00	128.18	5:15	11.36	
0.20	0.04	0.00	1.59	1.80	1.89	21:49:21					*
2.82	-0.03	-0.00	1.69	1.87	2.07	5265	0.00	150.43	5:15	10.13	
0.07	-0.04	3.46	1.69	1.72	1.83	21:49:53					*
3.18	-0.07	-3.84	1.73	1.76	2.06	5266	0.00	143.84	5:15	10.91	
0.04	-0.03	-0.04	1.68	1.74	1.75	21:50:25					*
-0.10	-0.03	0.06	1.73	1.77	2.00	5267	0.00	113.43	5:15	10.45	
-2.24	-0.04	-3.62	1.75	1.76	1.74	21:50:57					*
2.98	-4.36	0.08	1.77	1.81	2.07	5268	0.00	97.29	5:15	8.64	
2.60	1.66	3.32	1.69	1.83	1.91	21:51:29					*
0.12	0.18	0.07	1.76	2.03	2.37	5269	0.00	93.23	5:15	9.08	
-0.14	4.86	-2.79	1.84	1.94	2.27	21:52:02					*
2.30	-0.04	-0.12	1.98	2.19	2.67	5270	0.00	176.37	6:45	11.51	
-1.85	-3.73	0.07	2.23	2.12	2.49	21:52:33					*
-0.18	-3.27	2.66	2.48	2.42	2.96	5271	0.00	180.27	6:45	10.92	
0.07	-0.34	-2.39	2.93	2.70	2.64	21:53:05					*
-1.77	-0.04	-2.66	3.11	2.69	2.97	5272	0.00	134.72	6:45	6.96	
2.27	-2.56	-2.39	3.37	3.02	2.65	21:53:37					*
5.80	-0.02	-0.02	3.41	2.87	2.91	5273	0.40	82.71	6:45	6.88	
0.07	-0.00	2.37	3.69	3.19	2.67	21:54:09					*
-3.64	2.77	-0.01	3.51	2.86	2.84	5274	1.55	70.99	6:45	6.59	
-2.21	-0.00	0.02	3.71	3.12	2.59	21:54:41					*
-0.35	0.01	0.02	3.41	2.81	2.81	5275	2.42	69.38	6:45	8.25	
0.15	-0.00	-0.03	3.63	3.07	2.55	21:55:13					*
3.30	-2.89	-2.90	3.43	2.73	2.73	5276	2.70	68.73	6:45	8.02	
2.30	2.61	0.01	3.59	3.03	2.48	21:55:45					*
-3.76	0.04	-2.84	3.33	2.74	2.78	5277	2.58	68.06	6:45	8.35	
						21:56:17					

0.09	0.02	-2.45	3.64	3.06	2.58	5278	2.43	3.49	6.45	7.60	*
3.62	0.01	-2.79	3.34	2.75	2.83	21:56:49		64:38	2:30		
0.02	2.61	0.02	3.61	3.02	2.56	5279	2.53	3.51	6.45	8.41	*
-4.14	0.01	-2.75	3.31	2.77	2.88	21:57:21		64:49	2:30		
-2.22	-2.56	-2.42	3.98	3.08	2.61	5280	2.77	3.46	5.88	6.38	*
3.46	-0.01	-2.75	3.65	2.82	2.88	21:57:54		65:46	2:30		
0.04	0.08	2.40	4.48	3.34	2.63	5281	3.46	3.70	5.88	5.71	*
-0.03	-0.06	-2.73	4.18	2.98	2.89	21:58:25		110:70	3:00		
0.07	-0.06	0.05	4.97	3.78	2.71	5282	4.22	4.23	5.88	4.65	C
0.09	-0.09	-2.69	4.73	3.43	2.93	21:58:57		0:00	3:00		
-2.79	-1.78	-2.07	5.85	4.45	3.06	5283	3.62	270:46	5:88	3.43	*
-1.99	-0.07	-2.50	5.71	4.01	3.16	21:59:29		270:81	3:00		
-0.15	-3.64	0.04	7.26	5.29	3.41	5284	5.59	6:30	5:88	0.68	C
0.06	-0.00	-2.45	6.85	4.43	3.23	22:00:01		0:00	3:00		
2.73	-2.78	-1.86	8.09	5.68	3.39	5285	10.21	13:36	5:88	2.27	*
1.77	0.01	-2.44	6.66	4.33	3.23	22:00:33		13:26	3:00		
2.35	0.00	-0.00	7.63	5.33	3.34	5286	13.00	2:34	5:88	4.72	*
-1.97	0.01	0.03	6.40	4.17	3.26	22:01:05		11:07	3:00		
0.08	2.99	0.03	7.17	5.28	3.35	5287	11.14	3.47	5:88	4.90	*
0.02	-1.82	-2.38	6.21	4.33	3.32	22:01:37		14:08	3:00		
3.24	-2.92	-1.82	6.78	5.40	3.47	5288	9.53	3.48	5:88	3.76	*
0.01	-0.02	-0.00	5.98	4.28	3.26	22:02:09		14:44	3:00		
2.73	-0.08	-1.87	6.18	5.01	3.38	5289	8.05	3.40	5:88	4.76	*
-1.77	-1.94	-2.55	5.42	4.08	3.10	22:02:41		14:71	3:00		
-0.02	-0.01	-1.97	6.24	4.60	3.20	5290	8.27	3.18	5.15	3.99	*
-2.43	2.10	-0.04	5.36	3.75	2.91	22:03:13		15:55	3:00		
0.02	3.18	2.10	6.13	4.59	3.01	5291	8.52	3.26	5.15	3.73	*
-2.35	0.00	-2.84	5.47	3.77	2.78	22:03:45		16:37	3:00		
-0.09	0.63	-0.00	6.04	4.63	3.01	5292	8.07	3.35	5.15	4.05	*
0.03	2.05	2.75	5.37	3.85	2.87	22:04:17		16:34	3:00		
4.03	0.02	-1.99	5.47	4.77	3.17	5293	7.06	3.23	5.15	3.97	*
0.03	-1.92	-2.73	5.14	4.11	2.89	22:04:49		13:41	3:00		
3.88	-0.03	-0.00	5.19	4.57	3.33						*

2.86	-0.05	-2.73	4.81	3.86	2.89	5294	5.92	2.06	5.15	2.70		
0.10	3.62	-2.08	4.88	4.21	3.04	22:05:21		5.89	3.00			*
0.06	-0.05	2.90	4.29	3.46	2.72	5295	5.79	2.71	5.15	4.09		
-1.62	-0.26	-2.28	4.59	3.78	2.77	22:05:53		10.71	2.90			
3.04	2.48	3.13	4.11	3.18	2.52	5296	5.48	3.08	5.15	5.70		*
1.81	-4.01	-2.40	4.85	3.64	2.63	22:06:26		18.19	2.90			
-3.05	0.09	3.17	4.48	3.18	2.49	5297	4.81	3.01	5.15	5.82		*
0.14	0.06	0.08	5.23	4.14	2.73	22:06:57		12.97	2.90			
2.74	1.82	-0.05	5.05	3.84	2.58	5298	3.28	4.17	5.15	6.68		*
1.58	3.10	-0.05	6.79	4.98	3.32	22:07:29		292.08	2.90			
1.96	-1.77	-3.00	6.75	4.46	2.63	5299	3.84	4.51	5.15	2.69		*
-2.76	0.10	-0.06	7.99	6.29	3.68	22:08:01		117.61	2.90			
0.22	-2.11	-2.65	7.71	5.58	2.98	5300	6.20	6.39	4.88	2.45		C
0.19	-2.14	-5.19	9.28	7.32	4.61	22:08:33		8.00	2.90			
-3.73	0.00	-2.44	9.04	6.37	3.23	5301	7.39	8.48	4.88	0.64		C
0.16	1.86	-3.27	12.42	7.99	4.82	22:09:05		8.00	2.90			
2.38	-0.02	-2.44	10.89	6.47	3.23	5302	11.05	8.01	4.88	1.36		C
-1.55	-1.71	-0.06	14.28	9.04	4.63	22:09:37		8.01	2.90			
0.10	-0.02	-2.63	11.63	6.76	3.00	5303	19.58	8.01	4.88	0.75		C
4.43	1.76	0.10	15.11	8.90	4.67	22:10:08		8.01	2.90			
1.97	-2.32	0.09	12.15	6.80	3.14	5304	25.98	8.01	4.88	4.11		C
-0.03	-1.60	-0.10	16.28	9.78	4.97	22:10:41		8.01	2.90			
-0.01	-0.09	0.15	13.73	8.03	3.59	5305	25.39	8.01	4.88	6.01		C
2.12	-2.43	-2.50	19.93	12.33	6.34	22:11:13		8.01	2.90			
-0.08	2.94	0.12	17.96	10.23	4.05	5306	23.92	8.01	4.88	2.17		C
2.16	0.15	-2.05	20.46	15.28	7.69	22:11:45		8.01	2.90			
2.05	-3.15	-1.61	17.82	12.57	4.91	5307	31.42	8.01	4.88	0.74		C
0.15	0.03	-1.63	17.59	15.47	9.75	22:12:18		8.01	2.90			
3.01	-2.92	-4.51	16.11	13.49	6.42	5308	31.23	8.01	4.88	1.72		C
2.14	0.07	4.24	19.45	14.71	11.10	22:12:48		8.01	2.90			
0.38	-2.98	-2.20	18.92	13.25	7.16	5309	21.64	8.01	4.88	1.41		C
-0.01	0.09	3.15	25.43	17.53	10.01	22:13:21		8.01	2.90			
-0.15	-2.83	-2.80	22.13	13.11	5.67	5310	25.93	8.01	4.76	8.34		C
						22:13:52						

25.64	15.75	6.31
18.38	11.00	4.64
17.37	13.85	7.87
14.06	10.80	4.79
14.74	11.77	8.50
13.16	10.03	5.48
15.30	11.90	8.33
14.57	10.75	5.26
18.08	13.53	8.18
16.21	10.17	4.15
17.84	12.01	6.54
13.67	8.67	3.72
16.25	10.78	6.07
13.48	8.43	3.71
11.14	6.10	
8.76	3.71	
6.32		
		3.81

A - 9

Depth(m)

Time	Lat	Long	Alt	Dist	Time	Lat	Long	Alt	Dist
-47.2	6.36				2.05	1.45			
-14.2	15.89				2.08	1.04			
-3.00	-1.24				1.48	0.69			
-8.70	17.51	0.59			2.08	1.04	0.46		
-0.55	-2.45	-0.42			1.48	0.70	0.33		
-20.2	18.78	0.49			2.09	1.05	0.46		
8.76	0.24	-1.20			1.49	0.70	0.33		
-16.1	16.48	-1.08			2.11	1.06	0.46		
11.60	0.83	-1.05			1.51	0.70	0.33		
-30.2	16.05	-1.75			2.09	1.06	0.46		
3.65	2.17	-0.73			1.49	0.70	0.33		
-29.5	13.75	0.14			2.08	1.06	0.46		
14.24	1.10	-0.63			1.48	0.70	0.33		
-15.3	15.40	0.21			2.11	1.06	0.46		
9.33	-0.18	-0.54			1.51	0.70	0.33		
-36.0	15.77	-0.39			2.11	1.06	0.47		
-0.27	0.74	-1.38			1.51	0.70	0.33		
-38.5	15.06	0.12			2.09	1.06	0.47		
8.05	-0.38	-1.50			1.49	0.71	0.33		
-14.1	14.92	0.59			2.10	1.06	0.47		
10.52	-0.02	-1.32			1.50	0.71	0.33		
-37.3	16.45	1.63			2.11	1.08	0.47		
4.49	-0.66	-0.90			1.51	0.71	0.33		
-59.6	20.34	1.93			2.10	1.07	0.47		
1.20	-1.02	-0.59			1.50	0.71	0.34		
-14.3	14.75	0.67			2.08	1.06	0.47		

-29.9	7.17	1.44	1.81	0.98	0.44	127	5.62	8:33	10:36	7.30	0	*
-8.75	1.76	-1.11	1.21	0.65	0.32	11:30:30						
-26.0	10.64	3.00	1.82	0.98	0.44	128	5.62	8:33	10:36	7.33	0	*
6.36	1.68	-1.12	1.22	0.66	0.32	11:30:46						
-41.0	18.05	0.55	1.83	0.99	0.44	129	5.62	8:33	10:36	7.40	0	*
17.76	-1.20	-1.37	1.23	0.66	0.32	11:31:02						
-46.7	12.93	0.27	1.81	0.99	0.44	130	6.42	8:33	10:36	7.46	0	*
23.42	-1.76	-0.51	1.21	0.66	0.32	11:31:18						
-32.0	13.41	1.25	1.78	0.97	0.44	131	5.26	8:33	10:36	7.22	0	*
28.74	3.23	-0.04	1.18	0.64	0.32	11:31:34						
-17.5	16.73	0.55	1.78	0.94	0.44	132	6.00	8:29	10:36	6.92	0	*
9.33	1.82	-1.32	1.18	0.63	0.32	11:31:50						
-11.5	11.26	0.58	1.79	0.93	0.44	133	6.75	8:29	10:36	6.80	0	*
-9.40	-0.18	-1.58	1.19	0.62	0.33	11:32:06						
-27.7	16.95	1.20	1.83	0.93	0.44	134	7.09	8:29	10:36	6.82	0	*
-22.7	1.34	-1.10	1.23	0.63	0.33	11:32:22						
-44.3	19.59	-0.27	1.81	0.94	0.44	135	9.10	8:29	10:36	6.99	0	*
-9.09	-0.97	-1.13	1.21	0.64	0.33	11:32:38						
-54.7	8.06	1.37	1.80	0.96	0.44	136	9.10	8:29	10:36	7.18	0	*
-2.77	0.93	-1.39	1.20	0.65	0.33	11:32:54						
-52.5	15.95	1.63	1.81	0.96	0.44	137	7.97	8:29	10:36	7.22	0	*
8.31	-1.17	-0.77	1.21	0.65	0.33	11:33:10						
-33.9	25.11	-0.97	1.83	0.96	0.45	138	9.57	9:25	10:36	7.20	0	*
9.21	-5.37	-1.02	1.23	0.67	0.33	11:33:26						
-5.06	15.13	-0.60	1.86	0.97	0.45	139	8.38	9:21	10:36	6.97	0	*
2.34	-3.01	-1.45	1.26	0.68	0.33	11:33:42						
30.41	11.34	1.06	1.89	1.00	0.46	140	7.46	9:21	10:36	7.04	0	*
7.26	-2.36	-0.70	1.29	0.68	0.33	11:33:58						
-7.43	18.31	1.57	1.92	1.03	0.46	141	8.95	9:21	10:36	7.33	0	*
-1.24	-0.57	-0.66	1.32	0.70	0.33	11:34:14						
-32.6	18.93	-1.42	1.94	1.08	0.46	142	10.06	9:21	10:36	7.64	0	*
9.70	0.76	-0.42	1.34	0.72	0.33	11:34:30						
-0.00	10.05	-0.96	1.96	1.12	0.47							

10.54	-3.41	0.14
-31.6	5.51	1.61
-12.4	-2.06	0.03
-51.9	7.49	-0.33
-17.6	-0.01	-0.65
-34.4	9.66	-0.85
2.47	0.29	-0.41
-34.1	12.16	0.30
18.14	-0.45	-0.79
-28.3	15.14	0.85
10.97	-1.73	-1.18
-42.3	13.47	1.56
6.64	-0.95	-0.70
-44.9	13.26	0.91
2.92	0.43	-0.46
-33.1	16.92	0.44
0.08	2.63	0.00
-38.5	17.10	0.85
3.09	0.28	0.39
-39.3	17.70	1.36
3.10	-1.48	-0.32
-38.6	17.72	1.45
3.89	0.60	-0.79
-35.1	20.66	1.20
1.29	2.24	-0.64
-29.7	29.10	1.70
-5.25	-0.92	-0.24
26.19	0.54	
-3.00	-0.05	
0.58		
-0.91		

1.36	0.73	0.34
1.99	1.12	0.48
1.39	0.73	0.34
2.03	1.10	0.49
1.43	0.73	0.34
2.01	1.08	0.48
1.41	0.71	0.33
1.99	1.06	0.47
1.39	0.70	0.33
2.02	1.03	0.46
1.42	0.68	0.33
2.01	1.00	0.45
1.41	0.66	0.33
1.97	0.97	0.45
1.37	0.65	0.32
1.92	0.95	0.44
1.32	0.64	0.32
1.87	0.92	0.43
1.27	0.62	0.32
1.82	0.90	0.42
1.22	0.61	0.32
1.77	0.87	0.41
1.17	0.59	0.32
1.74	0.83	0.40
1.14	0.57	0.31
1.70	0.80	0.39
1.10	0.55	0.31
0.78	0.38	
0.54	0.31	
0.38		
0.31		

143	11:34:46
144	11:35:02
145	11:35:18
146	11:35:34
147	11:35:50
148	11:36:06
149	11:36:22
150	11:36:38
151	11:36:54
152	11:37:10
153	11:37:26
154	11:37:42
155	11:37:58
156	11:38:14
157	11:38:30
158	11:38:46
159	11:39:02

7.84	8:21	10:36	7.80
7.84	8:21	10:36	7.90
8.24	8:21	10:36	7.91
9.89	8:21	10:36	7.85
8.80	8:21	10:36	7.68
7.83	8:21	10:36	7.56
8.94	8:18	10:36	7.60
11.46	8:18	10:36	7.39
8.94	8:18	10:36	7.24
6.97	8:18	10:36	7.17
6.20	8:18	10:36	6.92
6.97	8:18	10:36	6.61
6.20	8:16	10:36	6.34
7.95	8:16	10:36	6.03
6.20	8:16	10:36	6.06

160
11:39:18

161
11:39:34

CLIENT: Atlantic Geoscience
 PROJECT: 3-40213
 LOCATION: Beaufort Sea
 25 m DIPOLES

LINE L22aed.W02 A-10

Processing date: 03-28-1994

CHARGEABILITY (mV/V)

RESISTIVITY (ohm-m)

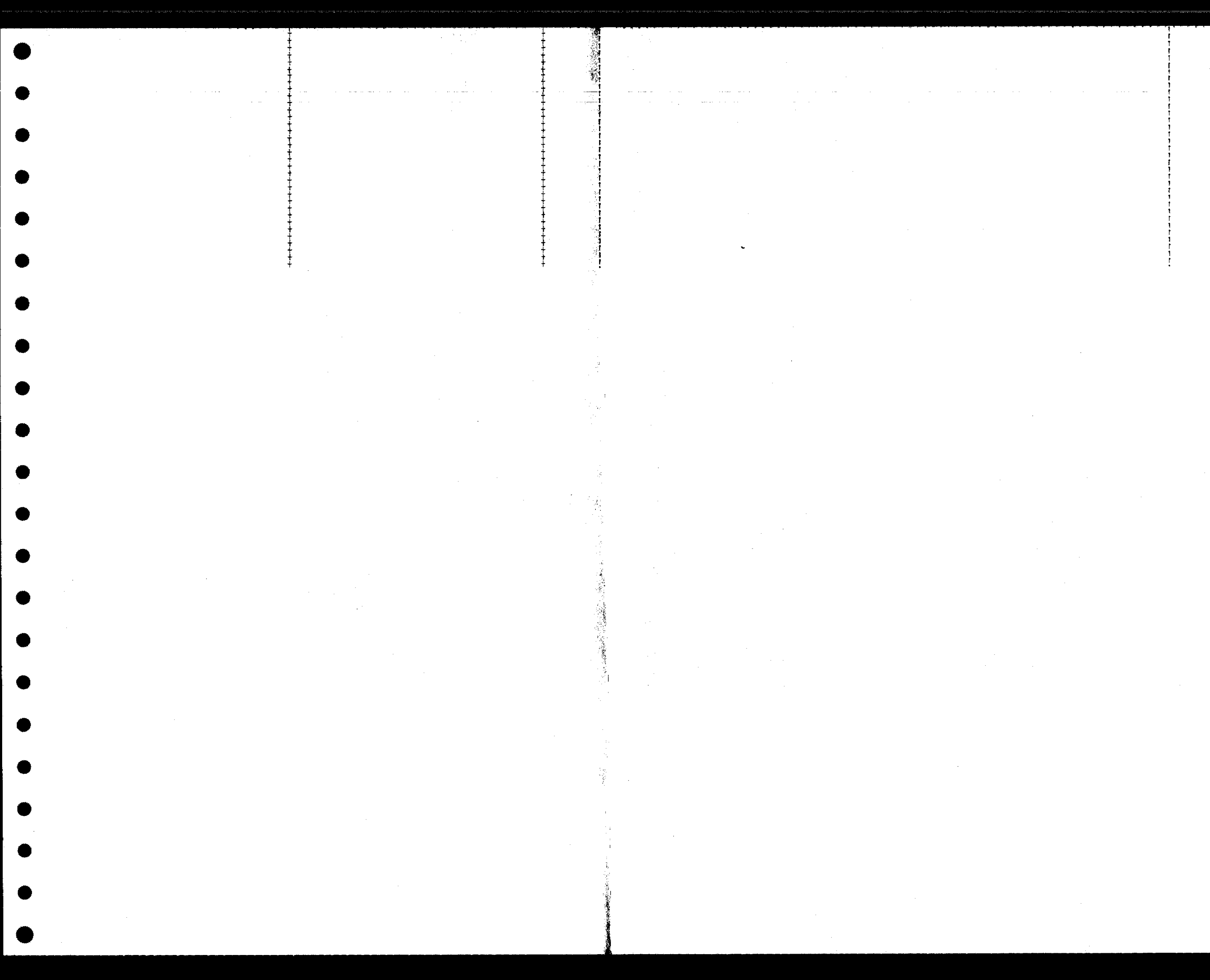
Depth(m)

								8	8	7	6	5	4	3	2	1
0.04				13.70												
-3.77				10.53												
-5.07	-2.86			12.56	7.94											
0.22	-2.02			9.62	5.63			3290	7.18	14.27	1.25	60.22				
-5.49	-3.19	-0.11		11.60	7.14	4.30		20:18:27		2.81	1.00					
-0.02	-0.04	0.09		8.61	5.45	3.50		3291	7.18	14.27	1.25	49.47				
-0.07	0.13	-2.39		11.86	6.87	4.76		20:18:59		2.81	1.00					
-0.22	-0.07	-2.91		9.85	5.76	3.90		3292	7.18	14.27	1.25	44.82				
0.12	0.19	-2.22		14.35	8.54	5.13		20:19:31		2.81	1.00					
0.21	-1.60	-2.88		12.81	7.13	3.94		3293	7.68	14.35	1.25	46.91				
-0.04	-0.10	-1.99		17.57	11.17	5.73		20:20:03		3.05	1.00					
2.61	-4.67	-2.90		15.26	9.42	3.92		3294	12.05	15.37	1.25	62.74				
-3.17	-4.96	0.06		19.56	13.51	7.36		20:20:35		5.75	1.00					
2.37	-0.01	-2.55		16.81	10.79	4.47		3295	12.31	15.54	1.12	39.87				
-0.11	0.01	1.47		21.38	13.98	8.36		20:21:07		5.84	1.00					
0.15	0.11	-1.97		18.79	11.71	5.80		3296	14.36	16.93	1.12	31.04				
0.15	3.37	0.09		26.04	16.97	10.16		20:21:39		8.58	1.00					
0.09	1.97	-1.61		23.62	14.52	7.08		3297	17.09	19.44	1.12	31.92				
0.07	-2.80	1.92		31.10	20.37	11.85		20:22:11		7.44	1.00					
-5.66	-1.76	1.93		26.49	16.19	7.42		3298	21.20	24.57	1.12	43.05				
-1.85	-0.02	-1.88		34.46	21.36	12.12		20:22:44		8.68	1.00					
-3.60	-1.77	-0.08		27.69	16.13	7.45		3299	21.20	24.57	1.12	45.45				
1.74	-2.57	0.00		36.56	22.16	12.39		20:23:15		8.68	1.00					
3.29	-1.68	-0.08		30.31	17.00	7.38		3300	21.85	25.68	1.12	51.14				
0.03	2.37	-1.88		36.33	24.08	12.15		20:23:47		8.98	1.00					
0.05	-0.01	-0.01		29.28	17.41	7.08		3301	23.15	31.68	1.12	49.66				
1.65	0.02	1.87		38.80	22.73	12.17		20:24:19		10.78	1.26					

3.22	0.02	3.96
-0.01	0.00	0.02
0.02	0.01	-0.07
-0.02	-0.02	1.88
-0.09	-0.06	-0.12
-0.03	-0.15	-0.00
3.84	0.01	0.02
-0.01	0.01	-0.08
3.76	2.07	-0.15
-0.10	3.01	2.43
-0.21	0.10	1.47
-2.55	-3.62	0.10
-0.10	-2.60	2.31
-0.06	-0.08	-0.07
-0.03	-0.01	2.25
2.71	-3.82	0.05
2.26	-2.62	2.28
-0.15	0.14	-2.80
-2.81	2.75	-2.35
0.14	5.06	-2.97
0.00	-3.20	-2.46
-4.20	0.06	-3.33
-3.08	0.01	-2.69
-4.03	-5.29	0.07
3.06	0.06	2.90
0.03	-0.00	-3.50
-0.05	-0.01	2.84
4.09	0.09	0.02
-2.87	-3.01	-2.53
0.27	-2.95	
2.74	-2.34	
-0.03		
2.39		

31.01	16.27	7.19
37.28	24.26	11.60
30.64	17.79	6.66
36.29	24.18	12.12
28.95	16.70	6.42
34.65	20.98	11.06
26.03	14.86	6.64
34.63	20.05	10.65
26.57	13.77	6.20
30.20	18.98	9.39
22.07	12.72	5.29
25.07	15.77	8.47
18.96	10.96	4.93
24.00	14.85	8.07
19.84	11.21	5.07
23.72	14.94	8.09
17.72	10.88	5.01
18.36	13.76	8.14
14.28	10.39	4.85
15.86	11.31	7.70
13.08	8.91	4.63
15.24	10.92	6.85
13.00	8.75	4.25
15.89	10.81	6.60
13.09	8.45	3.94
14.86	11.02	6.53
13.11	9.02	4.03
15.67	11.43	7.07
13.96	9.50	4.52
12.49	7.75	
10.42	4.88	
7.98		
4.79		

3302	25.15	31.66	1:12	56.50
20:24:51				
3303	25.15	31.66	1:12	58.33
20:25:23				
3304	25.15	31.66	1:12	58.40
20:25:55				
3305	25.15	31.66	1:12	65.48
20:26:27				
3306	25.15	31.66	1:12	83.85
20:27:00				
3307	25.15	31.66	1:12	96.10
20:27:31				
3308	25.15	31.66	1:12	99.87
20:28:03				
3309	25.15	31.66	1:12	100.73
20:28:35				
3310	25.15	31.66	1:12	103.84
20:29:07				
3311	25.15	31.66	1:12	105.78
20:29:39				
3312	25.15	31.66	1:12	130.20
20:30:11				
3313	25.15	31.66	1:12	142.72
20:30:43				
3314	25.15	31.66	1:12	143.14
20:31:15				
3315	25.15	31.66	1:12	125.44
20:31:47				
3316	25.15	31.66	1:12	113.27
20:32:19				
3317	25.15	31.66	1:12	106.99
20:32:51				



LINE L22aed.W03 A-11

RESISTIVITY (ohm-m)

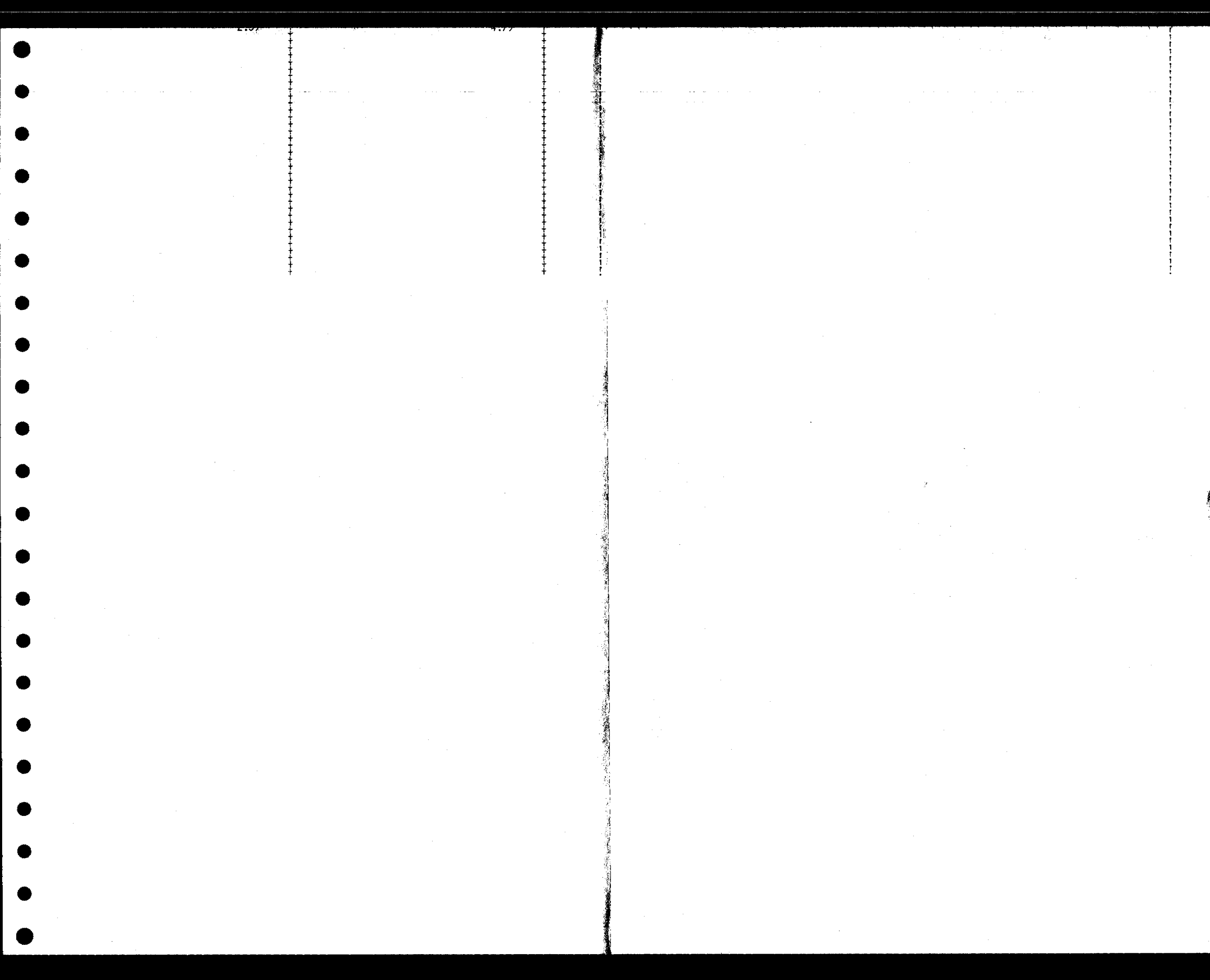
Depth(m)

3290	33654.	7:23 34:65	1:25 1:00	5.95
20:18:27				
3291	33654.	6:96 34:78	1:25 1:00	7.09
20:18:59				
3292	33654.	6:96 34:78	1:25 1:00	11.69
20:19:31				
3293	33654.	7:69 34:83	1:25 1:00	11.40
20:20:03				
3294	33654.	8:59 30:66	1:25 1:00	13.13
20:20:35				
3295	33654.	8:59 30:66	1:12 1:00	21.11
20:21:07				
3296	33654.	8:59 30:66	1:12 1:00	29.68
20:21:39				
3297	33654.	8:59 30:66	1:12 1:00	38.14
20:22:11				
3298	33653.	26:46 26:13	1:12 1:00	54.00
20:22:44				
3299	33653.	26:46 26:13	1:12 1:00	44.68
20:23:15				
3300	33653.	26:46 26:13	1:12 1:00	41.63
20:23:47				
3301	33653.	26:46 26:13	1:12 1:26	22.78
20:24:19				

1.05	0.02	1.07
3.22	0.02	3.96
-0.01	0.00	0.02
0.02	0.01	-0.07
-0.02	-0.02	1.88
-0.09	-0.06	-0.12
-0.03	-0.15	-0.00
3.84	0.01	0.02
-0.01	0.01	-0.08
3.76	2.07	-0.15
-0.10	3.01	2.43
-0.21	0.10	1.47
-2.55	-3.62	0.10
-0.10	-2.60	2.31
-0.06	-0.08	-0.07
-0.03	-0.01	2.25
2.71	-3.82	0.05
2.26	-2.62	2.28
-0.15	0.14	-2.80
-2.81	2.75	-2.35
0.14	5.06	-2.97
0.00	-3.20	-2.46
-4.20	0.06	-3.33
-3.08	0.01	-2.69
-4.03	-5.29	0.07
3.06	0.06	2.90
0.03	-0.00	-3.50
-0.05	-0.01	2.84
4.09	0.09	0.02
-2.87	-3.01	-2.53
0.27	-2.95	
2.74	-2.34	
-0.03		

38.80	22.75	12.17
31.01	16.27	7.19
37.28	24.26	11.60
30.64	17.79	6.66
36.29	24.18	12.12
28.95	16.70	6.42
34.65	20.98	11.06
26.03	14.86	6.64
34.63	20.05	10.65
26.57	13.77	6.20
30.20	18.98	9.39
22.07	12.72	5.29
25.07	15.77	8.47
18.96	10.96	4.93
24.00	14.85	8.07
19.84	11.21	5.07
23.72	14.94	8.09
17.72	10.88	5.01
18.36	13.76	8.14
14.28	10.39	4.85
15.86	11.31	7.70
13.08	8.91	4.63
15.24	10.92	6.85
13.00	8.75	4.25
15.89	10.81	6.60
13.09	8.45	3.94
14.86	11.02	6.53
13.11	9.02	4.03
15.67	11.43	7.07
13.96	9.50	4.52
12.49	7.75	
10.42	4.88	
7.98		

3302	53653.	26.46	1:12	29.59
20:24:51		28.13		
3303	53653.	26.46	1:12	26.88
20:25:23		28.13		
3304	53653.	26.46	1:12	29.13
20:25:55		28.13		
3305	53653.	26.46	1:12	38.47
20:26:27		28.13		
3306	53653.	26.46	1:12	53.71
20:27:00		28.13		
3307	53653.	26.46	1:12	63.91
20:27:31		28.13		
3308	53653.	26.46	1:12	77.54
20:28:03		28.13		
3309	53653.	26.46	1:12	85.06
20:28:35		28.13		
3310	53653.	26.46	1:12	86.77
20:29:07		28.13		
3311	53653.	26.46	1:12	87.85
20:29:39		28.13		
3312	53653.	26.47	1:12	121.81
20:30:11		28.14		
3313	53653.	26.47	1:12	136.95
20:30:43		28.14		
3314	53653.	26.47	1:12	140.28
20:31:15		28.14		
3315	53653.	26.47	1:12	128.67
20:31:47		28.14		
3316	53653.	26.47	1:12	124.29
20:32:19		28.14		
3317	53653.	26.47	1:12	112.14
20:32:51		28.14		



CLIENT: Atlantic Geoscience
 PROJECT: 3-40213
 LOCATION: Beaufort Sea
 25 m DIPOLES

LINE L45aed2.W04 A-12

Processing date: 03-28-1994
 CHARGEABILITY (mV/V)

RESISTIVITY (ohm-m)

								Depth(m)									
								8	8	8	7	6	5	4	3	2	1
-3.01				1.44													
0.07				1.64													
0.07	0.11			1.51	1.66												
3.03	-0.01			1.64	1.73												
2.93	4.69	3.60		1.50	1.69	1.75											
-2.99	0.04	0.01		1.60	1.74	2.08											
1.40	0.05	-3.56		3.03	1.68	1.78											
0.03	0.01	-3.81		1.69	1.76	2.07											
7.76	4.69	-3.57		1.31	1.68	1.77											
-0.25	-4.47	3.83		1.67	1.77	2.06											
-0.19	0.12	0.01		1.57	1.69	1.78											
0.10	0.24	0.02		1.64	1.74	2.07											
0.29	-4.74	-3.58		1.97	1.66	1.77											
-0.31	0.00	0.02		1.62	1.74	2.06											
2.62	4.73	-0.01		1.65	1.67	1.75											
3.22	4.52	0.02		1.71	1.75	2.06											
-2.34	-4.42	0.06		1.72	1.79	1.83											
-3.37	0.01	-3.69		1.62	1.85	2.14											
-0.22	4.55	0.03		1.46	1.74	1.92											
-0.25	-3.88	3.46		1.63	1.82	2.28											
-2.79	4.43	0.01		1.57	1.72	1.93											
-0.07	-4.09	-3.52		1.71	1.88	2.24											
2.30	-4.37	-3.31		1.61	1.81	1.91											
-3.19	4.19	0.02		1.64	1.89	2.15											
0.11	3.78	-0.01		1.61	1.81	1.90											
-3.21	0.03	0.00		1.72	1.92	2.15											
								5234	1.40	1.94	5.75	4.07					*
								21:33:21	27:86	27:86	2:80						
								5235	1.44	1.94	5.75	3.14					*
								21:33:53	27:86	27:86	2:80						
								5236	1.43	1.95	5.75	2.95					*
								21:34:25	27:85	27:85	2:80						
								5237	271.02	1.86	5.75	14.96					*
								21:34:57	68:88	68:88	2:80						
								5238	280.41	1.71	5.75	11.70					*
								21:35:29	158:29	158:29	2:70						
								5239	279.48	1.77	5.75	5.72					*
								21:36:01	143:68	143:68	2:70						
								5240	279.30	1.87	5.75	7.11					*
								21:36:33	104:58	104:58	2:70						
								5241	279.25	1.92	5.46	7.56					*
								21:37:05	137:16	137:16	2:70						
								5242	279.25	1.88	5.46	7.45					*
								21:37:37	137:16	137:16	2:70						
								5243	279.25	1.82	5.46	10.09					*
								21:38:09	137:16	137:16	2:70						
								5244	279.11	1.87	5.46	7.20					*
								21:38:41	151:31	151:31	2:70						
								5245	279.11	1.87	5.46	7.19					*
								21:39:13	151:31	151:31	2:60						

-0.37	-0.22	0.02	1.61	1.84	1.92	* 5246	278.99	152:29	5:48	7.02	*
-3.04	-0.01	0.01	1.71	1.92	2.13	* 21:39:45					
-2.01	-4.41	-3.27	2.37	1.76	1.93	* 5247	278.99	152:89	5:46	7.56	*
-3.36	0.05	0.03	1.65	1.84	2.18	* 21:40:17					
-0.16	-0.01	0.01	1.55	1.69	1.93	* 5248	289.63	86:92	5:46	10.42	*
0.14	-4.41	-3.54	1.52	1.79	2.24	* 21:40:49					
-2.24	0.00	-3.38	1.85	1.65	1.87	* 5249	284.90	142:95	5:46	7.74	*
2.80	-4.49	0.04	1.60	1.76	2.18	* 21:41:21					
-2.73	0.09	-3.51	1.42	1.65	1.80	* 5250	273.19	106:81	5:46	5.67	*
-3.33	-0.00	3.78	1.65	1.73	2.09	* 21:41:54					
0.10	4.80	-0.01	1.54	1.64	1.76	* 5251	273.13	145:51	5:15	8.51	*
0.08	-4.58	-3.87	1.56	1.73	2.04	* 21:42:25					
-2.02	-4.75	-3.59	1.56	1.67	1.76	* 5252	273.13	145:51	5:15	6.11	*
-3.16	4.64	-3.87	1.58	1.70	2.04	* 21:42:57					
-3.57	0.01	-0.03	2.63	1.64	1.73	* 5253	273.13	145:51	5:15	5.89	*
3.51	0.01	-3.90	1.57	1.69	2.02	* 21:43:29					
-0.37	-0.02	0.03	1.55	1.70	1.73	* 5254	280.55	75:84	5:15	13.17	*
2.88	-4.57	-3.90	1.67	1.73	2.03	* 21:44:01					
-0.13	4.73	-3.67	1.57	1.67	1.72	* 5255	269.30	145:09	5:15	5.48	*
0.48	0.01	3.90	1.55	1.70	2.03	* 21:44:33					
-2.87	-4.86	-3.65	1.53	1.63	1.73	* 5256	269.30	145:09	5:15	5.85	*
-0.32	0.01	-0.00	1.54	1.70	2.02	* 21:45:05					
0.05	-1.48	0.00	1.53	1.65	1.72	* 5257	269.30	145:09	5:15	6.47	*
3.08	0.02	-0.01	1.58	1.69	2.02	* 21:45:37					
2.53	0.19	-0.00	1.53	1.65	1.72	* 5258	269.26	145:37	5:15	6.27	*
-3.45	0.02	0.01	1.60	1.70	2.02	* 21:46:09					
-2.16	0.06	-3.66	1.85	1.68	1.73	* 5259	269.13	146:95	5:15	6.10	*
3.31	4.59	-3.88	1.67	1.72	2.03	* 21:46:41					
-0.22	-1.76	-0.00	1.57	1.66	1.75	* 5260	268.86	109:46	5:15	4.58	*
2.94	-4.50	0.01	1.65	1.76	2.04	* 21:47:13					
-2.61	0.05	3.58	1.62	1.71	1.77	* 5261	267.76	148:49	5:15	5.37	*
-0.25	4.43	0.00	1.71	1.78	2.04	* 21:47:45					
0.04	-1.69	0.01	1.62	1.76	1.79	* 5262	267.70	146:83	5:15	4.45	*

[illegible]

0.02	2.61	0.02	3.61	3.02	2.56	5279	0.00	3.01	6.45	11.49	*
-4.14	0.01	-2.75	3.31	2.77	2.88	21:57:21	1448.6	2.90			
-2.22	-2.56	-2.42	3.98	3.08	2.61	5280	0.00	3.03	5.88	10.87	*
3.46	-0.01	-2.75	3.65	2.82	2.88	21:57:54	1448.6	2.90			
0.04	0.08	2.40	4.48	3.34	2.63	5281	0.00	3.22	5.88	13.67	*
-0.03	-0.06	-2.73	4.18	2.98	2.89	21:58:25	1448.6	3.00			
0.07	-0.06	0.05	4.97	3.78	2.71	5282	0.00	3.65	5.88	14.60	*
0.09	-0.09	-2.69	4.73	3.43	2.93	21:58:57	1448.6	3.00			
-2.79	-1.78	-2.07	5.85	4.45	3.06	5283	0.00	4.07	5.88	17.33	*
-1.99	-0.07	-2.50	5.71	4.01	3.16	21:59:29	1444.4	3.00			
-0.15	-3.64	0.04	7.26	5.29	3.41	5284	0.00	4.51	5.88	25.99	*
0.06	-0.00	-2.45	6.85	4.43	3.23	22:00:01	1443.1	3.00			
2.73	-2.78	-1.86	8.09	5.68	3.39	5285	0.00	4.88	5.88	34.27	*
1.77	0.01	-2.44	6.66	4.33	3.23	22:00:33	1443.1	3.00			
2.35	0.00	-0.00	7.63	5.33	3.34	5286	0.00	4.88	5.88	34.48	*
-1.97	0.01	0.03	6.40	4.17	3.26	22:01:05	1443.1	3.00			
0.08	2.99	0.03	7.17	5.28	3.35	5287	0.00	4.82	5.88	32.11	*
0.02	-1.82	-2.38	6.21	4.33	3.32	22:01:37	1437.4	3.00			
3.24	-2.92	-1.82	6.78	5.40	3.47	5288	0.00	4.71	5.88	32.85	*
0.01	-0.02	-0.00	5.98	4.28	3.26	22:02:09	1430.4	3.00			
2.73	-0.08	-1.87	6.18	5.01	3.38	5289	0.00	4.44	5.88	33.15	*
-1.77	-1.94	-2.55	5.42	4.08	3.10	22:02:41	1425.1	3.00			
-0.02	-0.01	-1.97	6.24	4.60	3.20	5290	0.00	4.11	5.15	31.09	*
-2.43	2.10	-0.04	5.36	3.75	2.91	22:03:13	1422.0	3.00			
0.02	3.18	2.10	6.13	4.59	3.01	5291	0.00	4.15	5.15	30.15	*
-2.35	0.00	-2.84	5.47	3.77	2.78	22:03:45	1422.0	3.00			
-0.09	0.63	-0.00	6.04	4.63	3.01	5292	0.00	4.23	5.15	29.08	*
0.03	2.05	2.75	5.37	3.85	2.87	22:04:17	1422.0	3.00			
4.03	0.02	-1.99	5.47	4.77	3.17	5293	0.00	4.30	5.15	28.16	*
0.03	-1.92	-2.73	5.14	4.11	2.89	22:04:49	1422.0	3.00			
3.88	-0.03	-0.00	5.19	4.57	3.33	5294	0.00	4.00	5.15	28.28	*
2.86	-0.05	-2.73	4.81	3.86	2.89	22:05:21	1421.1	3.00			
0.10	3.62	-2.08	4.88	4.21	3.04	5295	0.00	3.69	5.15	29.03	*

0.06	-0.05	2.90	4.29	3.46	2.72	22:05:58	0.00	1415.6	5.15	25.76	*
-1.62	-0.26	-2.28	4.59	3.78	2.77	5296	0.00	1415.6	5.15	25.76	*
3.04	2.48	3.13	4.11	3.18	2.52	22:06:26					
1.81	-4.01	-2.40	4.85	3.64	2.63	5297	0.00	1414.8	5.15	21.64	*
-3.05	0.09	3.17	4.48	3.18	2.49	22:06:57					
0.14	0.06	0.08	5.23	4.14	2.73	5298	0.00	1413.8	5.15	22.88	*
2.74	1.82	-0.05	5.05	3.84	2.58	22:07:29					
1.58	3.10	-0.05	6.79	4.98	3.32	5299	0.00	1413.5	5.15	22.90	*
1.96	-1.77	-3.00	6.75	4.46	2.63	22:08:01					
-2.76	0.10	-0.06	7.99	6.29	3.68	5300	0.00	1413.1	4.88	30.79	*
0.22	-2.11	-2.65	7.71	5.58	2.98	22:08:33					
0.19	-2.14	-5.19	9.28	7.32	4.61	5301	0.00	1413.1	4.88	39.03	*
-3.73	0.00	-2.44	9.04	6.37	3.23	22:09:05					
0.16	1.86	-3.27	12.42	7.99	4.82	5302	0.00	1413.1	4.88	50.55	*
2.38	-0.02	-2.44	10.89	6.47	3.23	22:09:37					
-1.55	-1.71	-0.06	14.28	9.04	4.63	5303	0.00	1413.1	4.88	59.58	*
0.10	-0.02	-2.63	11.63	6.76	3.00	22:10:08					
4.43	1.76	0.10	15.11	8.90	4.67	5304	0.00	1413.1	4.88	56.74	*
1.97	-2.32	0.09	12.15	6.80	3.14	22:10:41					
-0.03	-1.60	-0.10	16.28	9.78	4.97	5305	0.00	1413.1	4.88	52.35	*
-0.01	-0.09	0.15	13.73	8.03	3.59	22:11:13					
2.12	-2.43	-2.50	19.93	12.33	6.34	5306	0.00	1413.1	4.88	48.33	*
-0.08	2.94	0.12	17.96	10.23	4.05	22:11:45					
2.16	0.15	-2.05	20.46	15.28	7.69	5307	0.00	1413.1	4.88	44.07	*
2.05	-3.15	-1.61	17.82	12.57	4.91	22:12:18					
0.15	0.03	-1.63	17.59	15.47	9.75	5308	0.00	1413.1	4.88	35.49	*
3.01	-2.92	-4.51	16.11	13.49	6.42	22:12:48					
2.14	0.07	4.24	19.45	14.71	11.10	5309	0.00	1413.1	4.88	52.60	*
0.38	-2.98	-2.20	18.92	13.25	7.16	22:13:21					
-0.01	0.09	3.15	25.43	17.53	10.01	5310	0.00	1413.1	4.76	79.98	*
-0.15	-2.83	-2.80	22.13	13.11	5.67	22:13:52					
-5.32	0.05	3.79	25.64	15.75	8.31	5311	0.00	1413.1	4.76	80.62	*
0.22	0.07	-0.01	18.38	11.00	4.64	22:14:25					

-0.28	0.04	3.99	17.37	13.85	7.87
-3.68	0.06	-3.30	14.06	10.80	4.79
3.63	-2.32	3.69	14.74	11.77	8.50
4.20	3.38	-2.87	13.16	10.03	5.48
-2.89	-0.03	3.77	15.30	11.90	8.33
-0.61	0.00	0.06	14.57	10.75	5.26
-0.06	-0.04	3.86	18.08	13.53	8.18
0.35	3.70	-3.82	16.21	10.17	4.15
0.15	-0.11	4.80	17.84	12.01	6.54
0.22	-4.35	0.02	13.67	8.67	3.72
2.51	0.23	0.01	16.25	10.78	6.07
0.04	1.35	-4.25	13.48	8.43	3.71
2.64	2.59		11.14	6.10	
-0.03	-4.25		8.76	3.71	
-0.02			6.32		
-4.14			3.81		

5312	0.00	14.55	4.76	68.83
22:14:56		1413.1	1:90	
5313	0.00	14.55	4.76	71.91
22:15:28		1413.1	1:90	
5314	0.00	14.55	4.76	91.81
22:16:01		1413.1	2:40	
5315	0.00	14.55	4.76	111.53
22:16:33		1413.1	2:40	
5316	0.00	14.55	4.76	113.59
22:17:05		1413.1	2:70	
5317	0.00	14.55	4.76	114.42
22:17:37		1413.1	2:70	
5318	0.00	14.55	4.76	108.87
22:18:10		1413.1	2:70	

*
*
*
*
*
*
*
*
*
*
*

CLIENT: Atlantic Geoscience
 PROJECT: 3-40213
 LOCATION: Beaufort Sea
 25 m DIPOLES

LINE L45aed.W03

A-13

Processing date: 03-28-1994
 CHARGEABILITY (mV/V)

RESISTIVITY (ohm-m)

Depth(m)

				0	0	0	0	0	0	0	0	0	0	0	0	0
-3.01				1.44												
0.07				1.64												
0.07	0.11			1.51	1.66											
3.03	-0.01			1.64	1.73											
2.93	4.69	3.60		1.50	1.69	1.75										
-2.99	0.04	0.01		1.60	1.74	2.08										
1.40	0.05	-3.56		3.03	1.68	1.78										
0.03	0.01	-3.81		1.69	1.76	2.07										
7.76	4.69	-3.57		1.31	1.68	1.77										
-0.25	-4.47	3.83		1.67	1.77	2.06										
-0.19	0.12	0.01		1.57	1.69	1.78										
0.10	0.24	0.02		1.64	1.74	2.07										
0.29	-4.74	-3.58		1.97	1.66	1.77										
-0.31	0.00	0.02		1.62	1.74	2.06										
2.62	4.73	-0.01		1.65	1.67	1.75										
3.22	4.52	0.02		1.71	1.75	2.06										
-2.34	-4.42	0.06		1.72	1.79	1.83										
-3.37	0.01	-3.69		1.62	1.85	2.14										
-0.22	4.55	0.03		1.46	1.74	1.92										
-0.25	-3.88	3.46		1.63	1.82	2.28										
-2.79	4.43	0.01		1.57	1.72	1.93										
-0.07	-4.09	-3.52		1.71	1.88	2.24										
2.30	-4.37	-3.31		1.61	1.81	1.91										
-3.19	4.19	0.02		1.64	1.89	2.15										
0.11	3.78	-0.01		1.61	1.81	1.90										
-3.21	0.03	0.00		1.72	1.92	2.15										
								5234	784.30	154.75	5.75	8.31				*
								21:33:21								
								5235	769.33	150.78	5.75	7.05				*
								21:33:53								
								5236	769.33	150.78	5.75	7.21				*
								21:34:25								
								5237	767.98	70.89	5.75	14.85				*
								21:34:57								
								5238	756.93	159.74	5.75	11.86				*
								21:35:29								
								5239	755.69	144.78	5.75	5.89				*
								21:36:01								
								5240	755.58	106.89	5.75	7.21				*
								21:36:33								
								5241	755.39	138.80	5.46	7.69				*
								21:37:05								
								5242	755.39	138.80	5.46	7.62				*
								21:37:37								
								5243	755.39	138.80	5.46	10.22				*
								21:38:09								
								5244	755.18	148.97	5.46	7.36				*
								21:38:41								
								5245	755.18	148.97	5.46	7.36				*
								21:39:13								

-0.37	-0.22	0.02	1.61	1.84	1.92	5246	754.80	151.92	5.46	7.18	*
-3.04	-0.01	0.01	1.71	1.92	2.13	21:39:45		151.94	2.60		
-2.01	-4.41	-3.27	2.37	1.76	1.93	5247	754.80	151.91	5.46	7.73	*
-3.36	0.05	0.03	1.65	1.84	2.18	21:40:17		151.94	2.60		
-0.16	-0.01	0.01	1.55	1.69	1.93	5248	742.47	151.95	5.46	10.54	*
0.14	-4.41	-3.54	1.52	1.79	2.24	21:40:49		87.01	2.60		
-2.24	0.00	-3.38	1.85	1.65	1.87	5249	737.69	140.35	5.46	7.92	*
2.80	-4.49	0.04	1.60	1.76	2.18	21:41:21		140.35	2.60		
-2.73	0.09	-3.51	1.42	1.65	1.80	5250	213.97	105.67	5.46	5.69	*
-3.33	-0.00	3.78	1.65	1.73	2.09	21:41:54		105.67	2.60		
0.10	4.80	-0.01	1.54	1.64	1.76	5251	213.93	154.40	5.15	8.29	*
0.08	-4.58	-3.87	1.56	1.73	2.04	21:42:25		154.40	2.60		
-2.02	-4.75	-3.59	9.86	1.67	1.76	5252	213.93	154.40	5.15	6.13	*
-3.16	4.64	-3.87	1.58	1.70	2.04	21:42:57		154.40	2.60		
-3.57	0.01	-0.03	2.63	1.64	1.73	5253	99999.	28.67	5.15	56.02	*
3.51	0.01	-3.90	1.57	1.69	2.02	21:43:29		28.67	2.60		
-0.37	-0.02	0.03	1.55	1.70	1.73	5254	99999.	37.20	5.15	36.60	*
2.88	-4.57	-3.90	1.67	1.73	2.03	21:44:01		37.20	2.60		
-0.13	4.73	-3.67	1.57	1.67	1.72	5255	99999.	37.20	5.15	36.39	*
0.48	0.01	3.90	1.55	1.70	2.03	21:44:33		37.20	2.70		
-2.87	-4.86	-3.65	1.53	1.63	1.73	5256	99999.	37.20	5.15	36.33	*
-0.32	0.01	-0.00	1.54	1.70	2.02	21:45:05		37.20	2.70		
0.05	-1.48	0.00	1.53	1.65	1.72	5257	99999.	37.20	5.15	36.49	*
3.08	0.02	-0.01	1.58	1.69	2.02	21:45:37		37.20	2.70		
2.53	0.19	-0.00	1.53	1.65	1.72	5258	99999.	37.20	5.15	36.25	*
-3.45	0.02	0.01	1.60	1.70	2.02	21:46:09		37.20	2.70		
-2.16	0.06	-3.66	1.85	1.68	1.73	5259	99999.	37.20	5.15	36.29	*
3.31	4.59	-3.88	1.67	1.72	2.03	21:46:41		37.20	2.70		
-0.22	-1.76	-0.00	1.57	1.66	1.75	5260	99999.	37.18	5.15	36.15	*
2.94	-4.50	0.01	1.65	1.76	2.04	21:47:13		37.18	2.70		
-2.61	0.05	3.58	1.62	1.71	1.77	5261	99999.	37.18	5.15	37.67	*
-0.25	4.43	0.00	1.71	1.78	2.04	21:47:45		37.18	2.70		
0.04	-1.69	0.01	1.62	1.76	1.79	5262	99999.	37.18	5.15		*

-0.58	-4.32	-3.89	1.78	1.83	2.03	21:48:17	37.18	2.78	37.73
-0.27	-1.30	-3.49	1.73	1.78	1.81	5263	99999.	8.84	5.15
2.88	0.03	3.88	1.74	1.86	2.04	21:48:49	37.18	2.78	37.64
-2.49	1.61	3.42	1.62	1.81	1.85	5264	99999.	8.85	5.15
-3.03	-0.01	-0.03	1.75	1.89	2.06	21:49:21	37.18	2.78	37.00
0.20	0.04	0.00	1.59	1.80	1.89	5265	99999.	8.85	5.15
2.82	-0.03	-0.00	1.69	1.87	2.07	21:49:53	37.18	2.80	36.67
0.07	-0.04	3.46	1.69	1.72	1.83	5266	99999.	8.85	5.15
3.18	-0.07	-3.84	1.73	1.76	2.06	21:50:25	37.18	2.80	37.19
0.04	-0.03	-0.04	1.68	1.74	1.75	5267	99999.	8.85	5.15
-0.10	-0.03	0.06	1.73	1.77	2.00	21:50:57	37.18	2.80	35.50
-2.24	-0.04	-3.62	1.75	1.76	1.74	5268	99999.	9.05	5.15
2.98	-4.36	0.08	1.77	1.81	2.07	21:51:29	37.89	2.80	30.41
2.60	1.66	3.32	1.69	1.83	1.91	5269	99999.	10.12	5.15
0.12	0.18	0.07	1.76	2.03	2.37	21:52:02	45.54	2.80	36.82
-0.14	4.86	-2.79	1.84	1.94	2.27	5270	99999.	10.26	6.45
2.30	-0.04	-0.12	1.98	2.19	2.67	21:52:33	45.82	2.80	33.35
-1.85	-3.73	0.07	2.23	2.12	2.49	5271	99999.	10.72	6.45
-0.18	-3.27	2.66	2.48	2.42	2.96	21:53:05	47.62	2.80	38.67
0.07	-0.34	-2.39	2.93	2.70	2.64	5272	99999.	11.87	6.45
-1.77	-0.04	-2.66	3.11	2.69	2.97	21:53:37	47.82	2.80	46.00
2.27	-2.56	-2.39	3.37	3.02	2.65	5273	99999.	12.05	6.45
5.80	-0.02	-0.02	3.41	2.87	2.91	21:54:09	45.77	2.80	53.00
0.07	-0.00	2.37	3.69	3.19	2.67	5274	99999.	12.50	6.45
-3.64	2.77	-0.01	3.51	2.86	2.84	21:54:41	45.67	2.80	56.77
-2.21	-0.00	0.02	3.71	3.12	2.59	5275	99999.	12.82	6.45
-0.35	0.01	0.02	3.41	2.81	2.81	21:55:13	45.86	2.90	62.34
0.15	-0.00	-0.03	3.63	3.07	2.55	5276	99999.	12.82	6.45
3.30	-2.89	-2.90	3.43	2.73	2.73	21:55:45	45.86	2.90	61.05
2.30	2.61	0.01	3.59	3.03	2.48	5277	99999.	12.82	6.45
-3.76	0.04	-2.84	3.33	2.74	2.78	21:56:17	45.86	2.90	58.50
0.09	0.02	-2.45	3.64	3.06	2.58	5278	99999.	12.82	6.45
3.62	0.01	-2.79	3.34	2.75	2.83	21:56:49	45.86	2.90	57.42

e

*

e

*

e

*

e

*

e

*

e

*

e

*

e

*

e

*

e

*

e

*

e

*

e

*

e

*

e

*

e

*

0.02	2.61	0.02	3.61	3.02	2.56	5279	9999.	13.92	6.45	56.87	@	*
-4.14	0.01	-2.75	3.31	2.77	2.88	21:57:21		45:80	2:30			
-2.22	-2.56	-2.42	3.98	3.08	2.61	5280	9999.	13.92	5.88	54.32	@	*
3.46	-0.01	-2.75	3.65	2.82	2.88	21:57:54		45:80	2:30			
0.04	0.08	2.40	4.48	3.34	2.63	5281	9999.	14.54	5.88	55.29	@	*
-0.03	-0.06	-2.73	4.18	2.98	2.89	21:58:25		45:73	3:00			
0.07	-0.06	0.05	4.97	3.78	2.71	5282	9999.	14.54	5.88	48.63	@	*
0.09	-0.09	-2.69	4.73	3.43	2.93	21:58:57		45:73	3:00			
-2.79	-1.78	-2.07	5.85	4.45	3.06	5283	9999.	15.94	5.88	54.18	@	*
-1.99	-0.07	-2.50	5.71	4.01	3.16	21:59:29		46:81	3:00			
-0.15	-3.64	0.04	7.26	5.29	3.41	5284	9999.	17.86	5.88	65.73	@	*
0.06	-0.00	-2.45	6.85	4.43	3.23	22:00:01		48:09	3:00			
2.73	-2.78	-1.86	8.09	5.68	3.39	5285	9999.	19.09	5.88	72.06	@	*
1.77	0.01	-2.44	6.66	4.33	3.23	22:00:33		48:42	3:00			
2.35	0.00	-0.00	7.63	5.33	3.34	5286	9999.	19.09	5.88	70.34	@	*
-1.97	0.01	0.03	6.40	4.17	3.26	22:01:05		48:42	3:00			
0.08	2.99	0.03	7.17	5.28	3.35	5287	9999.	19.09	5.88	70.68	@	*
0.02	-1.82	-2.38	6.21	4.33	3.32	22:01:37		48:42	3:00			
3.24	-2.92	-1.82	6.78	5.40	3.47	5288	9999.	19.09	5.88	75.96	@	*
0.01	-0.02	-0.00	5.98	4.28	3.26	22:02:09		48:42	3:00			
2.73	-0.08	-1.87	6.18	5.01	3.38	5289	9999.	19.09	5.88	83.77	@	*
-1.77	-1.94	-2.55	5.42	4.08	3.10	22:02:41		48:42	3:00			
-0.02	-0.01	-1.97	6.24	4.60	3.20	5290	9999.	19.09	5.15	83.91	@	*
-2.43	2.10	-0.04	5.36	3.75	2.91	22:03:13		48:42	3:00			
0.02	3.18	2.10	6.13	4.59	3.01	5291	9999.	19.09	5.15	80.48	@	*
-2.35	0.00	-2.84	5.47	3.77	2.78	22:03:45		48:42	3:00			
-0.09	0.63	-0.00	6.04	4.63	3.01	5292	9999.	19.09	5.15	77.94	@	*
0.03	2.05	2.75	5.37	3.85	2.87	22:04:17		48:42	3:00			
4.03	0.02	-1.99	5.47	4.77	3.17	5293	9999.	19.09	5.15	76.71	@	*
0.03	-1.92	-2.73	5.14	4.11	2.89	22:04:49		48:42	3:00			
3.88	-0.03	-0.00	5.19	4.57	3.33	5294	9999.	19.10	5.15	85.53	@	*
2.86	-0.05	-2.73	4.81	3.86	2.89	22:05:21		48:47	3:00			
0.10	3.62	-2.08	4.88	4.21	3.04	5295	9999.	19.10	5.15		@	*

17.37	13.85	7.87
14.06	10.80	4.79
14.74	11.77	8.50
13.16	10.03	5.48
15.30	11.90	8.33
14.57	10.75	5.26
18.08	13.53	8.18
16.21	10.17	4.15
17.84	12.01	6.54
13.67	8.67	3.72
16.25	10.78	6.07
13.48	8.43	3.71
11.14	6.10	
	8.76	3.71
	6.32	
		3.81

CLIENT: Atlantic Geoscience
PROJECT: 3-40213
LOCATION: Beaufort Sea
25 m DIPOLES

LINE L5.H05

A-14

Processing date: 03-28-1994
CHARGEABILITY (mV/V)

RESISTIVITY (ohm-m)

								Depth(m)									
								0	1	2	3	4	5	6	7	8	9
-47.2				2.05													
	6.36				1.45												
-14.2	15.89			2.08	1.04												
	-3.00	-1.24			1.48	0.69		98	1.85	2.61	10:36	15.74					*
-8.70	17.51	0.59		2.08	1.04	0.46											
	-0.55	-2.45	-0.42		1.48	0.70	0.33	99	1.85	1.43	10:36	15.19					*
-20.2	18.78	0.49		2.09	1.05	0.46											
	8.76	0.24	-1.20		1.49	0.70	0.33	100	2.11	2.85	10:36	14.10					*
-16.1	16.48	-1.08		2.11	1.06	0.46											
	11.60	0.83	-1.05		1.51	0.70	0.33	101	2.89	2.42	10:36	11.23					*
-30.2	16.05	-1.75		2.09	1.06	0.46											
	3.65	2.17	-0.73		1.49	0.70	0.33	102	5.09	8:38	10:36	8.77					*
-29.5	13.75	0.14		2.08	1.06	0.46											
	14.24	1.10	-0.63		1.48	0.70	0.33	103	8.94	8:38	10:36	8.37					*
-15.3	15.40	0.21		2.11	1.06	0.46											
	9.33	-0.18	-0.54		1.51	0.70	0.33	104	11.46	8:38	10:36	8.25					*
-36.0	15.77	-0.39		2.11	1.06	0.47											
	-0.27	0.74	-1.38		1.51	0.70	0.33	105	11.46	8:38	10:36	8.16					*
-38.5	15.06	0.12		2.09	1.06	0.47											
	8.05	-0.38	-1.50		1.49	0.71	0.33	106	13.09	8:38	10:36	8.16					*
-14.1	14.92	0.59		2.10	1.06	0.47											
	10.52	-0.02	-1.32		1.50	0.71	0.33	107	10.90	8:38	10:36	8.18					*
-37.3	16.45	1.63		2.11	1.08	0.47											
	4.49	-0.66	-0.90		1.51	0.71	0.33	108	11.66	8:38	10:36	8.13					*
-59.6	20.34	1.93		2.10	1.07	0.47											
	1.20	-1.02	-0.59		1.50	0.71	0.34	109	13.31	8:38	10:36	8.10					*

-14.3	14.75	0.67	10.00	1.06	0.47	110	11.66	8:38	10:36	8.09	0	*
6.77	-0.40	-1.16	1.48	0.71	0.34	11:25:46						
-6.64	9.66	-0.23	2.05	1.06	0.47	111	20.48	8:48	10:36	27.12	0	*
3.02	-1.21	-1.46	1.45	0.70	0.34	11:26:02						
-24.2	11.64	0.33	2.01	1.03	0.47	112	16.79	9:31	10:36	7.75	0	*
-5.84	1.41	-0.70	1.41	0.68	0.33	11:26:18						
-18.1	11.48	0.24	1.95	1.01	0.46	113	9.55	9:31	10:36	7.48	0	*
-4.97	2.01	-0.29	1.35	0.66	0.33	11:26:34						
-41.8	15.38	0.35	1.93	0.98	0.45	114	7.45	9:31	10:36	7.19	0	*
2.48	2.20	-0.45	1.33	0.65	0.33	11:26:50						
-43.2	23.00	-0.10	1.95	0.95	0.45	115	6.63	9:31	10:36	7.05	0	*
0.21	2.85	-0.72	1.35	0.65	0.33	11:27:06						
-23.8	22.98	-0.90	1.95	0.96	0.46	116	6.63	9:31	10:36	7.13	0	*
5.53	-1.73	-0.58	1.35	0.66	0.33	11:27:22						
-23.3	18.92	0.44	1.93	0.99	0.45	117	7.56	9:31	10:36	7.22	0	*
8.30	-3.20	-0.79	1.33	0.67	0.33	11:27:38						
-17.5	12.99	0.91	1.92	1.00	0.46	118	7.19	9:31	10:36	7.33	0	*
7.64	-3.23	-1.21	1.32	0.68	0.33	11:27:54						
-11.0	13.27	-0.33	1.94	1.01	0.46	119	7.19	9:31	10:36	7.39	0	*
3.83	-1.99	-0.67	1.34	0.69	0.33	11:28:10						
-29.8	11.69	-0.33	1.95	1.02	0.46	120	7.19	9:31	10:36	7.52	0	*
-0.97	1.95	-0.71	1.35	0.68	0.33	11:28:26						
-27.0	9.84	1.17	1.94	1.03	0.46	121	7.19	9:31	10:36	7.64	0	*
3.63	-0.05	-0.40	1.34	0.68	0.33	11:28:42						
-44.2	12.02	2.38	1.89	1.02	0.45	122	7.19	9:31	10:36	7.63	0	*
9.02	-0.90	0.10	1.29	0.67	0.33	11:28:58						
-35.7	7.20	0.83	1.88	1.02	0.45	123	6.40	9:31	10:36	7.63	0	*
8.03	0.82	-0.62	1.28	0.66	0.33	11:29:14						
-3.67	6.44	1.93	1.88	1.00	0.44	124	5.33	9:31	10:36	7.57	0	*
1.52	1.79	-1.44	1.28	0.66	0.32	11:29:42						
0.00	6.99	4.33	1.87	0.99	0.44	125	5.33	9:31	10:36	7.52	0	*
-2.08	2.03	-1.43	1.27	0.65	0.32	11:29:58						
-14.3	8.05	1.21	1.83	0.98	0.44	126	6.09	9:27	10:36	7.27	0	*
						11:30:14						

[illegible]

-0.00	10.05	-0.96	1.96	1.12	0.47	143	7.08	0:27	10:36	7.84	0	*
10.54	-3.41	0.14	1.36	0.73	0.34	11:34:46						
-31.6	5.51	1.61	1.99	1.12	0.48	144	6.74	0:27	10:36	7.90	0	*
-12.4	-2.06	0.03	1.39	0.73	0.34	11:35:02						
-51.9	7.49	-0.33	2.03	1.10	0.49	145	6.74	0:27	10:36	7.95	0	*
-17.6	-0.01	-0.65	1.43	0.73	0.34	11:35:18						
-34.4	9.66	-0.85	2.01	1.08	0.48	146	6.74	0:27	10:36	7.97	0	*
2.47	0.29	-0.41	1.41	0.71	0.33	11:35:34						
-34.1	12.16	0.30	1.99	1.06	0.47	147	7.69	0:24	10:36	7.78	0	*
18.14	-0.45	-0.79	1.39	0.70	0.33	11:35:50						
-28.3	15.14	0.85	2.02	1.03	0.46	148	8.22	0:24	10:36	7.57	0	*
10.97	-1.73	-1.18	1.42	0.68	0.33	11:36:06						
-42.3	13.47	1.56	2.01	1.00	0.45	149	8.64	0:24	10:36	7.65	0	*
6.64	-0.95	-0.70	1.41	0.66	0.33	11:36:22						
-44.9	13.26	0.91	1.97	0.97	0.45	150	9.87	0:21	10:36	7.53	0	*
2.92	0.43	-0.46	1.37	0.65	0.32	11:36:38						
-33.1	16.92	0.44	1.92	0.95	0.44	151	11.09	0:21	10:36	7.25	0	*
0.08	2.63	0.00	1.32	0.64	0.32	11:36:54						
-38.5	17.10	0.85	1.87	0.92	0.43	152	8.64	0:21	10:36	7.12	0	*
3.09	0.28	0.39	1.27	0.62	0.32	11:37:10						
-39.3	17.70	1.36	1.82	0.90	0.42	153	6.74	0:21	10:36	6.98	0	*
3.10	-1.48	-0.32	1.22	0.61	0.32	11:37:26						
-38.6	17.72	1.45	1.77	0.87	0.41	154	5.99	0:21	10:36	6.75	0	*
3.89	0.60	-0.79	1.17	0.59	0.32	11:37:42						
-35.1	20.66	1.20	1.74	0.83	0.40	155	6.30	0:21	10:36	6.45	0	*
1.29	2.24	-0.64	1.14	0.57	0.31	11:37:58						
-29.7	29.10	1.70	1.70	0.80	0.39	156	5.61	0:18	10:36	6.28	0	*
-5.25	-0.92	-0.24	1.10	0.55	0.31	11:38:14						
26.19	0.54		0.78	0.38		157	8.21	0:18	10:36	6.01	0	*
-3.00	-0.05		0.54	0.31		11:38:30						
0.58				0.38		158						
-0.91				0.31		11:38:46						
						159						
						11:39:02						

160
11:39:18

161
11:39:34

FID	Play1/	Tlay1	Play2/	Tlay2	Play3/	Tlay3	Play4/	Tlay4	Play5/	Tlay5	Play6/	Tlay6	Play7/Half	Spc	Error
967	1.4/	6.3	0.0/	1.0	1.3/	2.0	12.2/	4.0	21.8/	8.0	25.7/	16.0	97.8/Infinity		108.5
968	1.4/	6.6	0.0/	1.0	0.4/	2.0	12.1/	4.0	21.5/	8.0	25.8/	16.0	97.7/Infinity		52.9
969	1.4/	5.8	0.0/	1.0	0.2/	2.0	12.1/	4.0	21.5/	8.0	25.8/	16.0	97.7/Infinity		51.0
970	1.4/	5.5	0.0/	1.0	0.2/	2.0	12.1/	4.0	21.5/	8.0	25.8/	16.0	97.7/Infinity		48.4
971	1.4/	5.0	0.0/	1.0	0.1/	2.0	12.1/	4.0	21.5/	8.0	25.8/	16.0	97.7/Infinity		40.6
972	1.4/	4.2	0.1/	1.0	0.1/	2.0	12.1/	4.0	21.5/	8.0	25.8/	16.0	97.7/Infinity		15.2
973	1.4/	4.3	0.1/	1.0	0.1/	2.0	12.1/	4.0	21.5/	8.0	25.8/	16.0	97.7/Infinity		16.9
974	1.4/	4.4	0.3/	1.0	0.1/	2.0	12.1/	4.0	21.5/	8.0	25.8/	16.0	97.7/Infinity		14.7
975	1.4/	4.6	0.2/	1.0	0.1/	2.0	12.1/	4.0	21.5/	8.0	25.8/	16.0	97.7/Infinity		17.0
976	1.4/	4.2	0.2/	1.0	0.1/	2.0	12.1/	4.0	21.5/	8.0	25.8/	16.0	97.7/Infinity		9.8
977	1.4/	3.4	1.7/	1.0	0.1/	2.0	13.7/	4.0	26.8/	8.0	22.1/	16.0	100.7/Infinity		11.7
978	1.4/	2.7	1.1/	1.0	0.1/	2.0	13.7/	4.0	26.8/	8.0	22.1/	16.0	100.7/Infinity		23.2
979	1.4/	2.5	0.7/	1.0	0.1/	2.0	13.7/	4.0	26.8/	8.0	22.1/	16.0	100.7/Infinity		35.6
980	1.4/	2.4	0.6/	1.0	0.2/	2.0	13.7/	4.0	26.8/	8.0	22.1/	16.0	100.7/Infinity		35.0
981	1.4/	2.0	0.7/	1.0	0.2/	2.0	13.7/	4.0	26.8/	8.0	22.1/	16.0	100.7/Infinity		33.6
982	1.4/	1.8	1.0/	1.0	0.2/	2.0	13.7/	4.0	26.8/	8.0	22.1/	16.0	100.7/Infinity		35.5
983	1.4/	1.5	3.1/	1.0	0.2/	2.0	13.7/	4.0	26.8/	8.0	22.1/	16.0	100.7/Infinity		30.8
984	1.4/	1.4	5.6/	1.0	1.2/	2.0	1.5/	4.0	18.9/	8.0	25.2/	16.0	103.3/Infinity		10.6
985	1.4/	1.5	0.7/	1.0	2.6/	2.0	25.3/	4.0	24.8/	8.0	4.4/	16.0	325.8/Infinity		17.0
986	1.4/	1.5	0.4/	1.0	2.5/	2.0	25.3/	4.0	24.9/	8.0	3.3/	16.0	325.8/Infinity		17.5
987	1.4/	1.5	0.2/	1.0	2.5/	2.0	25.4/	4.0	24.9/	8.0	1.4/	16.0	325.8/Infinity		20.4
988	1.4/	1.6	0.2/	1.0	2.5/	2.0	25.4/	4.0	24.9/	8.0	1.5/	16.0	325.8/Infinity		18.9
989	1.4/	1.6	0.1/	1.0	2.5/	2.0	25.4/	4.0	25.0/	8.0	1.6/	16.0	325.8/Infinity		20.8
990	1.4/	1.7	0.1/	1.0	2.5/	2.0	25.4/	4.0	25.0/	8.0	1.6/	16.0	325.8/Infinity		26.5
991	1.4/	1.7	0.1/	1.0	2.5/	2.0	25.4/	4.0	25.0/	8.0	1.6/	16.0	325.8/Infinity		31.6
992	1.4/	1.8	0.1/	1.0	2.5/	2.0	25.4/	4.0	24.9/	8.0	2.2/	16.0	325.8/Infinity		33.5
993	1.4/	1.8	0.2/	1.0	2.5/	2.0	25.4/	4.0	24.9/	8.0	2.8/	16.0	325.8/Infinity		33.3
994	1.4/	1.9	0.2/	1.0	2.5/	2.0	25.3/	4.0	24.9/	8.0	3.2/	16.0	325.8/Infinity		33.9
995	1.4/	1.9	0.2/	1.0	2.5/	2.0	25.3/	4.0	24.9/	8.0	3.4/	16.0	325.8/Infinity		32.5
996	1.4/	2.0	0.2/	1.0	2.5/	2.0	25.3/	4.0	24.9/	8.0	3.4/	16.0	325.8/Infinity		29.5
997	1.4/	2.0	0.2/	1.0	2.5/	2.0	25.3/	4.0	24.9/	8.0	3.4/	16.0	325.8/Infinity		26.9
998	1.4/	2.0	0.1/	1.0	2.5/	2.0	25.3/	4.0	24.9/	8.0	3.5/	16.0	325.8/Infinity		24.7
999	1.4/	1.9	0.1/	1.0	2.5/	2.0	25.3/	4.0	24.9/	8.0	3.5/	16.0	325.8/Infinity		21.7
1000	1.4/	1.8	0.1/	1.0	2.5/	2.0	25.3/	4.0	24.9/	8.0	3.5/	16.0	325.8/Infinity		23.0
1001	1.4/	1.7	0.1/	1.0	2.5/	2.0	25.3/	4.0	24.9/	8.0	3.5/	16.0	325.8/Infinity		23.7
1002	1.4/	1.8	0.1/	1.0	2.5/	2.0	25.3/	4.0	24.9/	8.0	3.6/	16.0	325.8/Infinity		25.9
1003	1.4/	1.7	0.1/	1.0	2.5/	2.0	25.3/	4.0	24.8/	8.0	3.8/	16.0	325.8/Infinity		31.3
1004	1.4/	1.8	0.1/	1.0	2.5/	2.0	25.3/	4.0	24.8/	8.0	3.8/	16.0	325.8/Infinity		38.6
1005	1.4/	1.8	0.1/	1.0	2.5/	2.0	25.3/	4.0	24.8/	8.0	3.8/	16.0	325.8/Infinity		35.8
1006	1.4/	1.9	0.1/	1.0	2.5/	2.0	25.3/	4.0	24.8/	8.0	3.9/	16.0	325.8/Infinity		36.4
1007	1.4/	1.8	0.1/	1.0	2.5/	2.0	25.3/	4.0	24.8/	8.0	4.2/	16.0	325.8/Infinity		25.0
1008	1.4/	1.7	0.2/	1.0	23.2/	2.0	34.3/	4.0	14.3/	8.0	1.1/	16.0	326.1/Infinity		8.2
1009	1.4/	1.6	0.2/	1.0	748.6/	2.0	13.0/	4.0	2.3/	8.0	0.1/	16.0	3782.7/Infinity		5.6
1010	1.4/	1.5	0.2/	1.0	748.5/	2.0	13.0/	4.0	2.2/	8.0	0.5/	16.0	3782.7/Infinity		6.4
1011	1.4/	1.4	0.3/	1.0	748.6/	2.0	13.0/	4.0	2.4/	8.0	1.5/	16.0	3782.7/Infinity		15.2
1012	1.4/	2.2	0.3/	1.0	1671.0/	2.0	0.0/	4.0	0.0/	8.0	5.4/	16.0	4301.1/Infinity		18.8
1013	1.4/	3.9	0.6/	1.0	1669.2/	2.0	0.8/	4.0	0.4/	8.0	5.4/	16.0	4301.1/Infinity		24.4
1014	1.4/	3.2	0.3/	1.0	1669.2/	2.0	0.7/	4.0	0.0/	8.0	5.4/	16.0	4301.1/Infinity		13.1
1015	1.4/	2.8	0.1/	1.0	1662.3/	2.0	0.0/	4.0	0.0/	8.0	5.4/	16.0	4301.1/Infinity		7.4
1016	1.4/	1.3	0.1/	1.0	1662.3/	2.0	0.3/	4.0	0.2/	8.0	5.4/	16.0	4301.1/Infinity		20.8
1017	1.4/	1.2	0.1/	1.0	1662.3/	2.0	0.3/	4.0	0.2/	8.0	5.4/	16.0	4301.1/Infinity		22.1
1018	1.4/	1.1	0.1/	1.0	1662.4/	2.0	0.5/	4.0	0.6/	8.0	5.4/	16.0	4301.1/Infinity		28.9
1019	1.4/	1.0	0.2/	1.0	1664.4/	2.0	10.3/	4.0	2.9/	8.0	6.0/	16.0	4301.1/Infinity		39.9
1020	1.4/	1.8	0.6/	1.0	21704.0/	2.0	7184.7/	4.0	427.3/	8.0	0.0/	16.0	12502.5/Infinity		38.7
1021	1.4/	1.2	0.7/	1.0	21704.7/	2.0	7185.3/	4.0	427.8/	8.0	0.0/	16.0	12502.5/Infinity		21.0
1022	1.4/	1.1	0.3/	1.0	21704.8/	2.0	7185.1/	4.0	427.2/	8.0	0.2/	16.0	12502.5/Infinity		6.5
1023	1.4/	1.0	0.2/	1.0	21704.8/	2.0	7185.1/	4.0	427.2/	8.0	0.2/	16.0	12502.5/Infinity		14.8
1024	1.4/	1.0	0.1/	1.0	21704.8/	2.0	7185.1/	4.0	427.2/	8.0	0.2/	16.0	12502.5/Infinity		22.8

1025	1.4/	1.0	0.2/	1.0	21704.8/	2.0	7185.1/	4.0	427.2/	8.0	0.5/	16.0	12502.5/Infinity	20.7
1026	1.4/	1.0	0.3/	1.0	21704.7/	2.0	7185.3/	4.0	427.7/	8.0	2.0/	16.0	12502.5/Infinity	33.7
1027	1.4/	1.0	0.5/	1.0	21674.5/	2.0	7142.8/	4.0	379.0/	8.0	0.0/	16.0	12502.8/Infinity	34.2
1028	1.4/	1.0	0.9/	1.0	21674.9/	2.0	7143.1/	4.0	379.2/	8.0	0.0/	16.0	12502.8/Infinity	11.2
1029	1.4/	1.0	1.2/	1.0	21674.4/	2.0	7141.8/	4.0	377.2/	8.0	0.6/	16.0	12502.8/Infinity	2.3
1030	1.4/	1.0	1.0/	1.0	21674.7/	2.0	7141.7/	4.0	376.7/	8.0	0.0/	16.0	12502.8/Infinity	1.9
1031	1.4/	1.0	0.9/	1.0	21674.7/	2.0	7141.7/	4.0	376.7/	8.0	0.0/	16.0	12502.8/Infinity	2.6
1032	1.4/	1.0	0.8/	1.0	21674.6/	2.0	7141.6/	4.0	376.7/	8.0	0.4/	16.0	12502.8/Infinity	9.4
1033	1.4/	1.0	0.6/	1.0	21674.8/	2.0	7141.6/	4.0	376.4/	8.0	0.0/	16.0	12502.8/Infinity	14.2
1034	1.4/	1.0	0.5/	1.0	21675.0/	2.0	7141.7/	4.0	376.4/	8.0	0.1/	16.0	12502.8/Infinity	15.4
1035	1.4/	1.0	0.4/	1.0	21675.1/	2.0	7141.8/	4.0	376.3/	8.0	0.0/	16.0	12502.8/Infinity	15.2
1036	1.4/	1.0	0.3/	1.0	21675.2/	2.0	7141.8/	4.0	376.3/	8.0	0.1/	16.0	12502.8/Infinity	18.5
1037	1.4/	1.0	0.3/	1.0	21675.2/	2.0	7141.8/	4.0	376.3/	8.0	0.1/	16.0	12502.8/Infinity	26.4
1038	1.4/	1.0	0.3/	1.0	21675.2/	2.0	7141.8/	4.0	376.3/	8.0	0.1/	16.0	12502.8/Infinity	31.6
1039	1.4/	1.0	0.3/	1.0	21675.2/	2.0	7141.8/	4.0	376.3/	8.0	0.0/	16.0	12502.8/Infinity	34.3
1040	1.4/	1.0	0.2/	1.0	21675.2/	2.0	7141.8/	4.0	376.3/	8.0	0.0/	16.0	12502.8/Infinity	28.7
1041	1.5/	1.0	0.2/	1.0	21675.2/	2.0	7141.8/	4.0	376.3/	8.0	0.0/	16.0	12502.8/Infinity	31.4
1042	1.5/	1.0	0.1/	1.0	21675.2/	2.0	7141.8/	4.0	376.3/	8.0	0.0/	16.0	12502.8/Infinity	25.8
1043	1.5/	1.0	0.1/	1.0	21675.2/	2.0	7141.8/	4.0	376.3/	8.0	0.0/	16.0	12502.8/Infinity	22.8
1044	1.5/	1.0	0.1/	1.0	21675.2/	2.0	7141.8/	4.0	376.3/	8.0	0.0/	16.0	12502.8/Infinity	25.5
1045	1.5/	1.0	0.1/	1.0	21675.2/	2.0	7141.8/	4.0	376.3/	8.0	0.0/	16.0	12502.8/Infinity	24.9
1046	1.5/	1.0	0.1/	1.0	21675.2/	2.0	7141.8/	4.0	376.3/	8.0	0.0/	16.0	12502.8/Infinity	30.6
1047	1.7/	1.0	0.1/	1.0	21675.2/	2.0	7141.8/	4.0	376.3/	8.0	0.0/	16.0	12502.8/Infinity	22.9
1048	1.7/	1.0	0.2/	1.0	21675.4/	2.0	7141.9/	4.0	376.1/	8.0	0.0/	16.0	12502.8/Infinity	22.6
1049	1.7/	1.0	0.2/	1.0	21676.4/	2.0	7142.3/	4.0	375.8/	8.0	0.0/	16.0	12502.8/Infinity	9.9
1050	1.8/	1.0	0.3/	1.0	21676.3/	2.0	7142.3/	4.0	375.8/	8.0	0.0/	16.0	12502.8/Infinity	2.5
1051	1.8/	1.0	0.3/	1.0	21675.3/	2.0	7141.6/	4.0	375.6/	8.0	0.2/	16.0	12502.8/Infinity	6.1
1052	1.8/	1.0	0.3/	1.0	21675.8/	2.0	7141.9/	4.0	375.7/	8.0	0.0/	16.0	12502.8/Infinity	6.1
1053	1.8/	1.0	0.3/	1.0	21675.8/	2.0	7141.9/	4.0	375.7/	8.0	0.0/	16.0	12502.8/Infinity	2.4
1054	1.8/	1.0	0.4/	1.0	21675.8/	2.0	7141.9/	4.0	375.7/	8.0	0.0/	16.0	12502.8/Infinity	2.0
1055	2.0/	1.0	0.4/	1.0	21675.8/	2.0	7141.9/	4.0	375.7/	8.0	0.0/	16.0	12502.8/Infinity	2.7
1056	2.0/	1.0	0.4/	1.0	21675.8/	2.0	7141.9/	4.0	375.6/	8.0	0.0/	16.0	12502.8/Infinity	2.3
1057	2.0/	1.0	0.5/	1.0	21675.8/	2.0	7141.8/	4.0	375.6/	8.0	0.2/	16.0	12502.8/Infinity	2.6
1058	1.9/	1.0	0.8/	1.0	15321.6/	2.0	221.3/	4.0	213.7/	8.0	1.2/	16.0	12934.3/Infinity	3.4
1059	1.9/	1.0	0.9/	1.0	15319.0/	2.0	195.8/	4.0	203.6/	8.0	4.1/	16.0	12931.9/Infinity	5.6
1060	1.9/	1.0	0.9/	1.0	15319.0/	2.0	195.8/	4.0	203.6/	8.0	4.2/	16.0	12931.9/Infinity	7.5
1061	1.9/	1.0	0.8/	1.0	15319.0/	2.0	195.8/	4.0	203.6/	8.0	4.2/	16.0	12931.9/Infinity	10.6
1062	1.9/	1.0	1.0/	1.0	68980.1/	2.0	8879.3/	4.0	586.4/	8.0	0.6/	16.0	29433.7/Infinity	5.9
1063	1.9/	1.0	0.8/	1.0	68980.2/	2.0	8879.2/	4.0	586.0/	8.0	0.0/	16.0	29433.7/Infinity	3.5
1064	1.9/	1.0	0.7/	1.0	68980.5/	2.0	8879.4/	4.0	586.1/	8.0	0.7/	16.0	29433.7/Infinity	2.7
1065	1.7/	1.0	0.6/	1.0	68980.5/	2.0	8879.5/	4.0	586.2/	8.0	1.1/	16.0	29433.7/Infinity	8.5
1066	1.7/	1.0	0.5/	1.0	68981.0/	2.0	8879.5/	4.0	585.5/	8.0	0.0/	16.0	29433.7/Infinity	9.0
1067	1.7/	1.0	0.4/	1.0	68981.2/	2.0	8879.6/	4.0	585.5/	8.0	0.6/	16.0	29433.7/Infinity	5.0
1068	1.7/	1.0	0.4/	1.0	68981.2/	2.0	8879.6/	4.0	585.5/	8.0	0.3/	16.0	29433.7/Infinity	15.3
1069	1.7/	1.0	0.4/	1.0	68981.6/	2.0	8879.9/	4.0	585.5/	8.0	0.1/	16.0	29433.7/Infinity	22.6
1070	1.7/	1.0	0.5/	1.0	68982.1/	2.0	8880.3/	4.0	585.7/	8.0	0.1/	16.0	29433.7/Infinity	16.9
1071	1.7/	1.0	0.5/	1.0	68982.6/	2.0	8880.7/	4.0	585.9/	8.0	0.1/	16.0	29433.7/Infinity	16.7
1072	1.7/	1.0	0.6/	1.0	68983.6/	2.0	8881.5/	4.0	586.3/	8.0	0.1/	16.0	29433.7/Infinity	15.5
1073	1.7/	1.0	0.6/	1.0	68984.3/	2.0	8882.1/	4.0	586.6/	8.0	0.0/	16.0	29433.7/Infinity	15.1
1074	1.7/	1.0	0.7/	1.0	68984.9/	2.0	8882.6/	4.0	586.9/	8.0	0.0/	16.0	29433.7/Infinity	10.5
1075	1.7/	1.0	0.7/	1.0	68985.2/	2.0	8882.8/	4.0	587.0/	8.0	0.0/	16.0	29433.7/Infinity	7.9
1076	1.7/	1.0	0.6/	1.0	68986.0/	2.0	8883.5/	4.0	587.4/	8.0	0.0/	16.0	29433.7/Infinity	8.5
1077	1.7/	1.0	0.6/	1.0	68986.1/	2.0	8883.5/	4.0	587.5/	8.0	0.1/	16.0	29433.7/Infinity	9.3
1078	1.7/	1.0	0.5/	1.0	68986.5/	2.0	8883.8/	4.0	587.6/	8.0	0.0/	16.0	29433.7/Infinity	7.7
1079	1.7/	1.0	0.5/	1.0	68986.5/	2.0	8883.9/	4.0	587.6/	8.0	0.2/	16.0	29433.7/Infinity	9.1
1080	1.7/	1.0	0.5/	1.0	68986.6/	2.0	8883.9/	4.0	587.6/	8.0	0.1/	16.0	29433.7/Infinity	13.6
1081	1.7/	1.0	0.5/	1.0	68987.3/	2.0	8884.5/	4.0	587.9/	8.0	0.1/	16.0	29433.7/Infinity	12.5
1082	1.7/	1.0	0.6/	1.0	68987.9/	2.0	8885.0/	4.0	588.1/	8.0	0.1/	16.0	29433.7/Infinity	10.7
1083	1.8/	1.0	0.6/	1.0	68988.0/	2.0	8885.1/	4.0	588.2/	8.0	0.0/	16.0	29433.7/Infinity	7.2
1084	1.8/	1.0	0.6/	1.0	68988.2/	2.0	8885.3/	4.0	588.3/	8.0	0.0/	16.0	29433.7/Infinity	6.9
1085	1.8/	1.0	0.6/	1.0	68988.2/	2.0	8885.3/	4.0	588.3/	8.0	0.0/	16.0	29433.7/Infinity	6.1
1086	1.8/	1.0	0.6/	1.0	68989.9/	2.0	8886.6/	4.0	589.1/	8.0	0.0/	16.0	29433.7/Infinity	4.5
1087	1.8/	1.0	0.6/	1.0	68993.7/	2.0	8889.8/	4.0	591.0/	8.0	0.0/	16.0	29433.7/Infinity	4.6
1088	1.8/	1.0	0.5/	1.0	68993.9/	2.0	8890.0/	4.0	591.0/	8.0	0.3/	16.0	29433.7/Infinity	8.3
1089	1.7/	1.0	0.5/	1.0	68993.9/	2.0	8890.0/	4.0	591.0/	8.0	0.3/	16.0	29433.7/Infinity	17.6
1090	1.7/	1.0	0.7/	1.0	68995.1/	2.0	8890.6/	4.0	590.8/	8.0	0.1/	16.0	29433.7/Infinity	22.4

1091	1.7/	1.0	0.9/	1.0	69012.6/	2.0	8905.3/	4.0	601.3/	8.0	0.0/	16.0	29433.7/Infinity	7.3
1092	1.7/	1.0	0.8/	1.0	69012.9/	2.0	8905.5/	4.0	601.4/	8.0	0.0/	16.0	29433.7/Infinity	3.5
1093	1.7/	1.0	0.7/	1.0	69015.3/	2.0	8907.5/	4.0	602.7/	8.0	0.1/	16.0	29433.7/Infinity	6.8
1094	1.7/	1.0	0.6/	1.0	69015.5/	2.0	8907.7/	4.0	602.8/	8.0	0.0/	16.0	29433.7/Infinity	9.9
1095	1.7/	1.0	0.5/	1.0	69016.1/	2.0	8908.1/	4.0	602.9/	8.0	0.1/	16.0	29433.7/Infinity	17.7
1096	1.7/	1.0	0.5/	1.0	69016.2/	2.0	8908.2/	4.0	603.0/	8.0	0.1/	16.0	29433.7/Infinity	18.6
1097	1.7/	1.0	0.5/	1.0	69018.1/	2.0	8909.8/	4.0	603.6/	8.0	0.1/	16.0	29433.7/Infinity	5.5
1098	1.7/	1.0	0.5/	1.0	69018.1/	2.0	8909.8/	4.0	603.6/	8.0	0.1/	16.0	29433.7/Infinity	7.9
1099	1.7/	1.0	0.6/	1.0	69018.2/	2.0	8909.9/	4.0	603.6/	8.0	0.2/	16.0	29433.7/Infinity	15.7
1100	1.7/	1.0	0.6/	1.0	69018.9/	2.0	8910.4/	4.0	603.8/	8.0	0.1/	16.0	29433.7/Infinity	23.2
1101	1.8/	1.0	0.6/	1.0	69018.9/	2.0	8910.4/	4.0	603.8/	8.0	0.1/	16.0	29433.7/Infinity	19.6
1102	1.8/	1.0	0.6/	1.0	69018.9/	2.0	8910.4/	4.0	603.8/	8.0	0.1/	16.0	29433.7/Infinity	21.8
1103	1.8/	1.0	0.5/	1.0	69019.0/	2.0	8910.5/	4.0	603.8/	8.0	0.1/	16.0	29433.7/Infinity	19.8
1104	1.8/	1.1	0.5/	1.0	69019.0/	2.0	8910.5/	4.0	603.8/	8.0	0.1/	16.0	29433.7/Infinity	12.8
1105	1.8/	1.2	0.6/	1.0	69018.7/	2.0	8910.3/	4.0	603.7/	8.0	0.6/	16.0	29433.7/Infinity	9.1
1106	1.8/	1.3	0.6/	1.0	69018.9/	2.0	8910.3/	4.0	603.5/	8.0	0.1/	16.0	29433.7/Infinity	12.0
1107	1.8/	1.4	0.8/	1.0	69666.8/	2.0	9671.4/	4.0	2172.2/	8.0	0.3/	16.0	29433.7/Infinity	3.4
1108	1.8/	1.4	1.1/	1.0	69666.1/	2.0	9671.1/	4.0	2172.6/	8.0	2.0/	16.0	29433.7/Infinity	5.4
1109	1.8/	1.4	0.9/	1.0	69670.8/	2.0	9667.0/	4.0	2159.9/	8.0	0.0/	16.0	29433.7/Infinity	2.5
1110	1.8/	1.4	0.8/	1.0	69671.5/	2.0	9667.6/	4.0	2160.5/	8.0	0.0/	16.0	29433.7/Infinity	4.0
1111	1.8/	1.5	0.6/	1.0	69671.4/	2.0	9667.5/	4.0	2160.4/	8.0	0.0/	16.0	29433.7/Infinity	6.6
1112	1.8/	1.5	0.5/	1.0	69671.2/	2.0	9667.3/	4.0	2160.2/	8.0	0.0/	16.0	29433.7/Infinity	4.9
1113	1.8/	1.5	0.5/	1.0	69671.2/	2.0	9667.3/	4.0	2160.2/	8.0	0.0/	16.0	29433.7/Infinity	9.6
1114	1.8/	1.5	0.6/	1.0	69671.1/	2.0	9667.3/	4.0	2160.2/	8.0	0.6/	16.0	29433.7/Infinity	3.7
1115	1.8/	1.5	0.6/	1.0	69671.1/	2.0	9667.3/	4.0	2160.2/	8.0	0.6/	16.0	29433.7/Infinity	6.2
1116	1.4/	1.5	0.6/	1.0	69671.1/	2.0	9667.3/	4.0	2160.2/	8.0	0.6/	16.0	29433.7/Infinity	1.9
1117	1.4/	1.5	0.6/	1.0	69614.3/	2.0	9897.1/	4.0	2720.4/	8.0	2.5/	16.0	29441.7/Infinity	4.2
1118	1.4/	1.4	0.4/	1.0	69614.3/	2.0	9897.1/	4.0	2720.4/	8.0	2.6/	16.0	29441.7/Infinity	9.1
1119	1.4/	1.4	0.4/	1.0	69614.3/	2.0	9897.1/	4.0	2720.4/	8.0	2.6/	16.0	29441.7/Infinity	14.0
1120	1.4/	1.3	0.4/	1.0	69614.3/	2.0	9897.1/	4.0	2720.4/	8.0	2.6/	16.0	29441.7/Infinity	17.6
1121	1.4/	1.3	0.4/	1.0	69614.3/	2.0	9897.0/	4.0	2720.4/	8.0	2.6/	16.0	29441.7/Infinity	19.2
1122	1.5/	1.3	0.5/	1.0	69614.3/	2.0	9896.8/	4.0	2719.9/	8.0	2.9/	16.0	29441.7/Infinity	19.8
1123	1.5/	1.2	0.6/	1.0	69614.3/	2.0	9896.8/	4.0	2720.0/	8.0	4.2/	16.0	29441.7/Infinity	18.3
1124	1.5/	1.2	0.7/	1.0	69614.2/	2.0	9896.6/	4.0	2719.7/	8.0	4.6/	16.0	29441.7/Infinity	15.5
1125	1.5/	1.2	0.8/	1.0	69614.2/	2.0	9896.6/	4.0	2719.7/	8.0	5.2/	16.0	29441.7/Infinity	15.2
1126	1.5/	1.2	0.8/	1.0	69614.2/	2.0	9896.6/	4.0	2719.7/	8.0	5.2/	16.0	29441.7/Infinity	14.8
1127	1.4/	1.2	0.8/	1.0	69614.2/	2.0	9896.6/	4.0	2719.7/	8.0	5.2/	16.0	29441.7/Infinity	7.6
1128	1.4/	1.2	0.8/	1.0	69614.2/	2.0	9896.6/	4.0	2719.7/	8.0	5.2/	16.0	29441.7/Infinity	8.3
1129	1.4/	1.2	0.8/	1.0	69614.2/	2.0	9896.6/	4.0	2719.7/	8.0	5.6/	16.0	29441.7/Infinity	6.7
1130	1.4/	1.2	0.8/	1.0	69614.2/	2.0	9896.6/	4.0	2719.7/	8.0	5.6/	16.0	29441.7/Infinity	7.0
1131	1.4/	1.4	0.9/	1.0	69614.5/	2.0	9897.1/	4.0	2720.4/	8.0	8.2/	16.0	29441.7/Infinity	6.2
1132	1.4/	1.5	0.9/	1.0	69614.5/	2.0	9897.1/	4.0	2720.4/	8.0	8.2/	16.0	29441.7/Infinity	8.1
1133	1.4/	1.6	0.9/	1.0	69614.5/	2.0	9897.1/	4.0	2720.4/	8.0	8.1/	16.0	29441.7/Infinity	12.5
1134	1.4/	1.6	0.7/	1.0	69614.5/	2.0	9897.1/	4.0	2720.4/	8.0	8.1/	16.0	29441.7/Infinity	16.5
1135	1.4/	1.6	0.4/	1.0	69614.5/	2.0	9897.1/	4.0	2720.3/	8.0	8.0/	16.0	29441.7/Infinity	12.8
1136	1.4/	1.5	0.4/	1.0	69614.5/	2.0	9897.1/	4.0	2720.3/	8.0	8.0/	16.0	29441.7/Infinity	20.6
1137	1.4/	1.5	0.3/	1.0	69614.5/	2.0	9897.1/	4.0	2720.3/	8.0	8.0/	16.0	29441.7/Infinity	21.9
1138	1.4/	1.5	0.4/	1.0	69614.5/	2.0	9897.1/	4.0	2720.3/	8.0	8.0/	16.0	29441.7/Infinity	19.6
1139	1.2/	1.5	0.4/	1.0	69614.5/	2.0	9897.1/	4.0	2720.4/	8.0	9.3/	16.0	29441.7/Infinity	19.7
1140	1.2/	1.4	0.5/	1.0	69614.5/	2.0	9897.2/	4.0	2720.5/	8.0	11.2/	16.0	29441.7/Infinity	18.6
1141	1.2/	1.4	0.6/	1.0	69614.7/	2.0	9897.4/	4.0	2720.7/	8.0	14.3/	16.0	29441.7/Infinity	18.8
1142	1.2/	1.4	0.6/	1.0	69614.7/	2.0	9897.3/	4.0	2720.6/	8.0	15.5/	16.0	29441.7/Infinity	16.4
1143	1.2/	1.4	0.6/	1.0	69614.7/	2.0	9897.3/	4.0	2720.6/	8.0	15.5/	16.0	29441.7/Infinity	12.1
1144	1.2/	1.4	0.6/	1.0	69614.7/	2.0	9897.3/	4.0	2720.6/	8.0	15.5/	16.0	29441.7/Infinity	13.2
1145	1.2/	1.4	0.5/	1.0	69614.7/	2.0	9897.3/	4.0	2720.6/	8.0	15.5/	16.0	29441.7/Infinity	17.5
1146	1.2/	1.3	0.5/	1.0	69614.7/	2.0	9897.3/	4.0	2720.6/	8.0	15.5/	16.0	29441.7/Infinity	19.3
1147	1.2/	1.3	0.4/	1.0	69614.7/	2.0	9897.3/	4.0	2720.6/	8.0	15.5/	16.0	29441.7/Infinity	25.7
1148	1.3/	1.3	0.4/	1.0	69614.7/	2.0	9897.3/	4.0	2720.6/	8.0	15.5/	16.0	29441.7/Infinity	36.5
1149	1.3/	1.3	0.4/	1.0	69614.7/	2.0	9897.3/	4.0	2720.6/	8.0	15.5/	16.0	29441.7/Infinity	39.0
1150	1.3/	1.3	0.4/	1.0	69614.7/	2.0	9897.3/	4.0	2720.6/	8.0	15.5/	16.0	29441.7/Infinity	35.0
1151	1.3/	1.3	0.4/	1.0	69614.7/	2.0	9897.3/	4.0	2720.6/	8.0	15.5/	16.0	29441.7/Infinity	29.5
1152	1.3/	1.4	0.5/	1.0	69614.7/	2.0	9897.3/	4.0	2720.6/	8.0	15.5/	16.0	29441.7/Infinity	24.1
1153	1.5/	1.4	0.5/	1.0	69614.7/	2.0	9897.3/	4.0	2720.6/	8.0	15.5/	16.0	29441.7/Infinity	20.3
1154	1.5/	1.5	0.5/	1.0	69614.7/	2.0	9897.3/	4.0	2720.6/	8.0	15.5/	16.0	29441.7/Infinity	18.0
1155	1.5/	1.5	0.6/	1.0	69614.7/	2.0	9897.3/	4.0	2720.6/	8.0	16.8/	16.0	29441.7/Infinity	18.2
1156	1.5/	1.5	0.6/	1.0	69614.7/	2.0	9897.3/	4.0	2720.6/	8.0	16.8/	16.0	29441.7/Infinity	18.5

1157	1.5/	1.5	0.6/	1.0	69614.7/	2.0	9897.3/	4.0	2720.6/	8.0	16.8/	16.0	29441.7/Infinity	26.0
1158	1.5/	1.5	0.5/	1.0	69614.7/	2.0	9897.3/	4.0	2720.6/	8.0	16.8/	16.0	29441.7/Infinity	26.5
1159	1.5/	1.5	0.4/	1.0	69614.7/	2.0	9897.3/	4.0	2720.6/	8.0	16.8/	16.0	29441.7/Infinity	32.6
1160	1.5/	1.6	0.6/	1.0	69614.5/	2.0	9897.1/	4.0	2720.4/	8.0	15.9/	16.0	29441.7/Infinity	282.7
1161	1.5/	1.6	1.4/	1.0	69612.9/	2.0	9895.2/	4.0	2718.3/	8.0	6.6/	16.0	29441.7/Infinity	203.6
1162	1.5/	1.6	0.9/	1.0	69610.9/	2.0	9891.9/	4.0	2714.3/	8.0	0.0/	16.0	29441.7/Infinity	210.5
1163	1.5/	1.6	0.2/	1.0	69611.0/	2.0	9891.9/	4.0	2714.2/	8.0	0.4/	16.0	29441.7/Infinity	37.0
1164	1.5/	1.6	0.2/	1.0	69611.0/	2.0	9891.9/	4.0	2714.2/	8.0	0.3/	16.0	29441.7/Infinity	29.5
1165	1.5/	1.5	0.2/	1.0	69611.0/	2.0	9891.9/	4.0	2714.2/	8.0	0.3/	16.0	29441.7/Infinity	27.7
1166	1.6/	1.5	0.2/	1.0	69611.0/	2.0	9891.9/	4.0	2714.2/	8.0	0.3/	16.0	29441.7/Infinity	29.4
1167	1.6/	1.5	0.2/	1.0	69611.0/	2.0	9891.9/	4.0	2714.2/	8.0	0.3/	16.0	29441.7/Infinity	27.8
1168	1.6/	1.5	0.2/	1.0	69611.0/	2.0	9891.9/	4.0	2714.2/	8.0	0.3/	16.0	29441.7/Infinity	20.3
1169	1.6/	1.5	0.2/	1.0	69611.0/	2.0	9891.9/	4.0	2714.2/	8.0	0.3/	16.0	29441.7/Infinity	16.7
1170	1.6/	1.5	0.2/	1.0	69611.0/	2.0	9891.9/	4.0	2714.2/	8.0	0.4/	16.0	29441.7/Infinity	11.4
1171	1.6/	1.5	0.2/	1.0	69611.0/	2.0	9891.9/	4.0	2714.2/	8.0	0.4/	16.0	29441.7/Infinity	8.7
1172	1.6/	1.5	0.3/	1.0	69611.0/	2.0	9891.9/	4.0	2714.2/	8.0	0.4/	16.0	29441.7/Infinity	13.4
1173	1.6/	1.5	0.3/	1.0	69610.9/	2.0	9891.9/	4.0	2714.2/	8.0	0.6/	16.0	29441.7/Infinity	17.6
1174	1.6/	1.5	0.3/	1.0	69610.9/	2.0	9891.9/	4.0	2714.2/	8.0	0.6/	16.0	29441.7/Infinity	15.7
1175	1.6/	1.5	0.2/	1.0	69610.9/	2.0	9891.9/	4.0	2714.2/	8.0	0.6/	16.0	29441.7/Infinity	17.8
1176	1.6/	1.6	0.2/	1.0	69610.9/	2.0	9891.9/	4.0	2714.2/	8.0	0.6/	16.0	29441.7/Infinity	24.5
1177	1.6/	1.6	0.2/	1.0	69610.9/	2.0	9891.9/	4.0	2714.2/	8.0	0.6/	16.0	29441.7/Infinity	21.9
1178	1.6/	1.6	0.2/	1.0	69610.9/	2.0	9891.9/	4.0	2714.2/	8.0	0.6/	16.0	29441.7/Infinity	21.6
1179	1.6/	1.6	0.2/	1.0	69610.9/	2.0	9891.9/	4.0	2714.2/	8.0	0.6/	16.0	29441.7/Infinity	22.8
1180	1.6/	1.6	0.2/	1.0	69610.9/	2.0	9891.9/	4.0	2714.2/	8.0	0.6/	16.0	29441.7/Infinity	23.2
1181	1.6/	1.6	0.3/	1.0	69610.9/	2.0	9891.9/	4.0	2714.2/	8.0	0.6/	16.0	29441.7/Infinity	20.5
1182	1.6/	1.6	0.3/	1.0	69610.9/	2.0	9891.9/	4.0	2714.2/	8.0	0.7/	16.0	29441.7/Infinity	18.9
1183	1.6/	1.6	0.3/	1.0	69610.9/	2.0	9891.9/	4.0	2714.2/	8.0	0.7/	16.0	29441.7/Infinity	17.8
1184	1.6/	1.7	0.3/	1.0	69610.9/	2.0	9891.9/	4.0	2714.2/	8.0	0.7/	16.0	29441.7/Infinity	19.0
1185	1.6/	1.7	0.3/	1.0	69610.9/	2.0	9891.9/	4.0	2714.2/	8.0	0.7/	16.0	29441.7/Infinity	19.0
1186	1.5/	1.8	0.3/	1.0	69610.9/	2.0	9891.9/	4.0	2714.2/	8.0	0.7/	16.0	29441.7/Infinity	18.5
1187	1.5/	1.8	0.3/	1.0	69610.9/	2.0	9891.9/	4.0	2714.2/	8.0	0.7/	16.0	29441.7/Infinity	20.1
1188	1.5/	1.8	0.3/	1.0	69610.9/	2.0	9891.9/	4.0	2714.2/	8.0	0.7/	16.0	29441.7/Infinity	21.2
1189	1.5/	1.8	0.2/	1.0	69610.9/	2.0	9891.9/	4.0	2714.2/	8.0	0.7/	16.0	29441.7/Infinity	27.7
1190	1.5/	1.8	0.2/	1.0	69610.9/	2.0	9891.9/	4.0	2714.2/	8.0	0.6/	16.0	29441.7/Infinity	34.9
1191	1.4/	1.8	0.2/	1.0	69610.9/	2.0	9891.9/	4.0	2714.2/	8.0	0.6/	16.0	29441.7/Infinity	34.0
1192	1.4/	1.8	0.2/	1.0	69610.9/	2.0	9891.9/	4.0	2714.2/	8.0	0.6/	16.0	29441.7/Infinity	33.8
1193	1.4/	1.8	0.2/	1.0	69610.9/	2.0	9891.9/	4.0	2714.2/	8.0	0.6/	16.0	29441.7/Infinity	36.6
1194	1.4/	1.8	0.2/	1.0	69610.9/	2.0	9891.9/	4.0	2714.2/	8.0	0.6/	16.0	29441.7/Infinity	37.6
1195	1.4/	1.8	0.2/	1.0	69610.9/	2.0	9891.9/	4.0	2714.2/	8.0	0.6/	16.0	29441.7/Infinity	36.4
1196	1.4/	1.8	0.2/	1.0	69611.0/	2.0	9891.9/	4.0	2714.1/	8.0	0.3/	16.0	29441.7/Infinity	29.8
1197	1.4/	1.8	0.2/	1.0	69611.0/	2.0	9891.9/	4.0	2713.9/	8.0	0.4/	16.0	29441.7/Infinity	29.2
1198	1.4/	1.7	0.3/	1.0	69610.9/	2.0	9891.9/	4.0	2714.0/	8.0	1.3/	16.0	29441.7/Infinity	19.4
1199	1.4/	1.7	0.3/	1.0	69610.9/	2.0	9891.9/	4.0	2714.0/	8.0	1.3/	16.0	29441.7/Infinity	19.1
1200	1.4/	1.7	0.3/	1.0	69610.9/	2.0	9891.9/	4.0	2714.0/	8.0	1.3/	16.0	29441.7/Infinity	21.4
1201	1.3/	1.7	0.3/	1.0	69610.9/	2.0	9891.9/	4.0	2714.0/	8.0	1.3/	16.0	29441.7/Infinity	21.8
1202	1.3/	1.8	0.3/	1.0	69610.9/	2.0	9891.8/	4.0	2714.0/	8.0	1.3/	16.0	29441.7/Infinity	17.3
1203	1.4/	1.8	0.3/	1.0	69610.9/	2.0	9891.8/	4.0	2714.0/	8.0	1.3/	16.0	29441.7/Infinity	15.1
1204	1.4/	1.8	0.3/	1.0	69610.9/	2.0	9891.8/	4.0	2714.0/	8.0	1.3/	16.0	29441.7/Infinity	16.4
1205	1.4/	1.8	0.3/	1.0	69610.9/	2.0	9891.8/	4.0	2714.0/	8.0	1.3/	16.0	29441.7/Infinity	17.5
1206	1.4/	1.8	0.3/	1.0	69610.9/	2.0	9891.8/	4.0	2714.0/	8.0	1.2/	16.0	29441.7/Infinity	25.9
1207	1.4/	1.8	9.1/	1.0	99999.0/	2.0	99999.0/	4.0	99999.0/	8.0	7.4/	16.0	99999.0/Infinity	26.8
1208	1.4/	1.8	9.1/	1.0	99999.0/	2.0	99999.0/	4.0	99999.0/	8.0	7.4/	16.0	99999.0/Infinity	59.7

FID	Rlay1/ Tlay1		Rlay2/ Tlay2		Rlay3/ Tlay3		Rlay4/ Tlay4		Rlay5/ Tlay5		Rlay6/ Tlay6		Rlay7/Half Spc Error	
967	1.4/	6.3	0.2/	2.0	0.7/	3.0	2.0/	5.0	3.9/	8.0	10.2/	12.0	100.0/Infinity	119.1
968	1.4/	6.6	0.1/	2.2	0.4/	3.1	2.0/	4.0	3.9/	5.2	10.2/	7.0	100.0/Infinity	55.4
969	1.4/	5.8	0.1/	2.2	0.3/	3.1	1.9/	4.0	3.9/	5.2	10.2/	7.0	100.0/Infinity	53.7
970	1.4/	5.5	0.1/	2.2	0.2/	3.1	1.9/	4.0	3.9/	5.2	10.2/	7.0	100.0/Infinity	51.3
971	1.4/	5.0	0.1/	2.2	0.2/	3.1	1.9/	4.0	3.9/	5.2	10.2/	7.0	100.0/Infinity	44.1
972	1.4/	4.2	0.2/	2.0	0.2/	3.0	1.9/	5.0	3.9/	8.0	10.2/	12.0	100.0/Infinity	19.2
973	1.4/	4.3	0.4/	2.0	0.2/	3.0	1.9/	5.0	3.9/	8.0	10.2/	12.0	100.0/Infinity	20.7
974	1.4/	4.4	0.9/	2.0	0.2/	3.0	1.9/	5.0	3.9/	8.0	10.2/	12.0	100.0/Infinity	21.2
975	1.4/	4.6	0.9/	2.0	0.2/	3.0	1.9/	5.0	3.9/	8.0	10.2/	12.0	100.0/Infinity	27.3
976	1.4/	4.2	0.9/	2.0	0.2/	3.0	1.9/	5.0	3.9/	8.0	10.2/	12.0	100.0/Infinity	24.2
977	1.4/	3.4	1.2/	2.0	0.2/	3.0	1.9/	5.0	3.9/	8.0	10.2/	12.0	100.0/Infinity	13.8
978	1.4/	2.7	2.7/	2.0	0.3/	4.0	2.0/	6.0	3.7/	8.0	10.2/	10.0	100.0/Infinity	14.8
979	1.4/	2.5	3.4/	4.0	0.4/	4.0	2.0/	4.0	3.7/	8.0	10.2/	16.0	100.0/Infinity	21.1
980	1.4/	2.4	5.8/	2.2	0.4/	3.1	1.0/	4.0	3.5/	5.2	10.2/	7.0	100.0/Infinity	21.9
981	1.4/	2.0	1.0/	3.0	3.2/	4.8	3.1/	6.0	0.6/	6.9	0.6/	7.8	99.2/Infinity	10.5
982	1.4/	1.8	0.8/	2.2	2.6/	3.1	3.6/	4.0	3.4/	5.2	0.3/	7.0	99.0/Infinity	7.2
983	1.4/	1.5	0.9/	2.0	2.6/	4.0	5.4/	6.0	3.8/	8.0	0.3/	10.0	99.1/Infinity	14.8
984	1.4/	1.4	0.6/	2.2	58.7/	3.1	0.5/	4.0	0.1/	5.2	0.0/	7.0	291.9/Infinity	8.2
985	1.4/	1.5	0.7/	2.2	128.6/	3.1	1.5/	4.0	0.0/	5.2	0.0/	7.0	10000.0/Infinity	14.5
986	1.4/	1.5	0.5/	2.0	128.7/	4.0	1.6/	6.0	0.0/	8.0	0.0/	10.0	10000.0/Infinity	17.4
987	1.4/	1.5	0.4/	2.2	128.7/	3.1	1.7/	4.0	0.0/	5.2	0.0/	7.0	10000.0/Infinity	22.5
988	1.4/	1.6	0.3/	2.0	128.7/	3.0	1.7/	5.0	0.0/	8.0	0.2/	12.0	10000.0/Infinity	20.6
989	1.4/	1.6	0.2/	2.0	128.6/	3.0	1.7/	5.0	0.0/	8.0	0.2/	12.0	10000.0/Infinity	22.5
990	1.4/	1.7	0.2/	2.0	128.6/	3.0	1.7/	5.0	0.0/	8.0	0.2/	12.0	10000.0/Infinity	28.3
991	1.4/	1.7	0.2/	2.0	128.6/	3.0	1.7/	5.0	0.2/	8.0	0.2/	12.0	10000.0/Infinity	33.9
992	1.4/	1.8	0.5/	3.0	20.6/	4.8	1.3/	6.0	0.0/	6.9	13.4/	7.8	9999.6/Infinity	22.9
993	1.4/	1.8	0.4/	2.0	20.7/	3.0	1.4/	5.0	0.0/	8.0	13.4/	12.0	9999.6/Infinity	7.3
994	1.4/	1.9	0.5/	2.0	20.6/	3.0	1.5/	5.0	0.0/	8.0	13.4/	12.0	9999.6/Infinity	8.4
995	1.4/	1.9	0.5/	2.0	20.6/	3.0	1.5/	5.0	0.0/	8.0	13.4/	12.0	9999.6/Infinity	7.5
996	1.4/	2.0	0.4/	2.0	13.3/	3.0	7.6/	5.0	0.0/	8.0	13.4/	12.0	9999.6/Infinity	7.0
997	1.4/	2.0	0.4/	2.0	13.2/	3.0	7.6/	5.0	0.0/	8.0	13.4/	12.0	9999.6/Infinity	6.4
998	1.4/	2.0	0.4/	2.2	13.2/	3.1	7.6/	4.0	0.0/	5.2	13.4/	7.0	9999.6/Infinity	5.5
999	1.4/	1.9	0.3/	2.2	13.2/	3.1	7.6/	4.0	0.0/	5.2	13.4/	7.0	9999.6/Infinity	8.1
1000	1.4/	1.8	0.3/	2.2	13.2/	3.1	7.6/	4.0	0.0/	5.2	13.4/	7.0	9999.6/Infinity	7.0
1001	1.4/	1.7	0.3/	2.2	13.2/	3.1	7.6/	4.0	0.0/	5.2	13.4/	7.0	9999.6/Infinity	7.7
1002	1.4/	1.8	0.3/	2.2	13.2/	3.1	7.6/	4.0	0.0/	5.2	13.4/	7.0	9999.6/Infinity	8.2
1003	1.4/	1.7	0.4/	2.2	13.3/	3.1	7.6/	4.0	0.0/	5.2	13.4/	7.0	9999.6/Infinity	9.7
1004	1.4/	1.8	2.2/	4.0	1.0/	4.0	14.8/	4.0	0.4/	8.0	17.0/	16.0	8987.9/Infinity	7.2
1005	1.4/	1.8	2.8/	2.0	0.6/	3.0	11.1/	5.0	0.4/	8.0	63.3/	12.0	5187.1/Infinity	4.1
1006	1.4/	1.9	4.9/	2.2	0.6/	3.1	10.8/	4.0	0.4/	5.2	62.9/	7.0	5187.3/Infinity	6.7
1007	1.4/	1.8	2.8/	4.0	0.9/	4.0	29.8/	4.0	0.3/	8.0	10000.0/	16.0	10000.0/Infinity	6.6
1008	1.4/	1.7	2.8/	2.0	1.0/	4.0	29.8/	6.0	0.3/	8.0	10000.0/	10.0	10000.0/Infinity	11.3
1009	1.4/	1.6	0.8/	4.0	3.9/	4.0	40.7/	4.0	0.0/	8.0	10000.0/	16.0	10000.0/Infinity	20.2
1010	1.4/	1.5	0.9/	3.0	4.1/	4.8	40.4/	6.0	0.0/	6.9	10000.0/	7.8	10000.0/Infinity	11.0
1011	1.4/	1.4	0.8/	2.0	4.1/	4.0	40.4/	6.0	0.0/	8.0	10000.0/	10.0	10000.0/Infinity	7.9
1012	1.4/	2.2	1.0/	2.0	3.8/	4.0	40.3/	6.0	0.0/	8.0	10000.0/	10.0	10000.0/Infinity	12.1
1013	1.4/	3.9	1.1/	2.0	4.1/	4.0	39.2/	6.0	0.0/	8.0	10000.0/	10.0	10000.0/Infinity	21.2
1014	1.4/	3.2	1.1/	2.0	4.1/	4.0	39.2/	6.0	0.0/	8.0	10000.0/	10.0	10000.0/Infinity	8.7
1015	1.4/	2.8	0.3/	2.0	142.6/	4.0	71.3/	6.0	0.5/	8.0	9869.8/	10.0	10000.0/Infinity	4.5
1016	1.4/	1.3	0.2/	2.2	142.6/	3.1	71.3/	4.0	0.2/	5.2	9869.8/	7.0	10000.0/Infinity	21.3
1017	1.4/	1.2	0.2/	4.0	142.6/	4.0	71.3/	4.0	0.0/	8.0	9869.8/	16.0	10000.0/Infinity	19.3
1018	1.4/	1.1	0.2/	2.2	142.6/	3.1	71.3/	4.0	0.0/	5.2	9869.8/	7.0	10000.0/Infinity	24.8
1019	1.4/	1.0	0.4/	2.0	142.6/	3.0	71.3/	5.0	0.5/	8.0	9869.8/	12.0	10000.0/Infinity	35.9
1020	1.4/	1.8	5.2/	4.0	52.9/	4.0	0.2/	4.0	0.0/	8.0	9746.5/	16.0	9296.7/Infinity	5.8
1021	1.4/	1.2	3.7/	3.0	78.7/	4.8	0.0/	6.0	0.0/	6.9	0.0/	7.8	10000.0/Infinity	11.5
1022	1.4/	1.1	0.9/	3.0	140.0/	4.8	2.8/	6.0	3.6/	6.9	0.1/	7.8	9999.3/Infinity	4.4
1023	1.4/	1.0	0.5/	4.0	140.0/	4.0	2.8/	4.0	3.7/	8.0	0.0/	16.0	9999.3/Infinity	15.7
1024	1.4/	1.0	0.5/	4.0	140.2/	4.0	2.8/	4.0	3.9/	8.0	0.4/	16.0	9999.3/Infinity	22.9

1025	1.4/	1.0	0.6/	4.0	148.4/	4.0	25.3/	4.0	0.7/	8.0	0.7/	16.0	9999.2/Infinity	21.2
1026	1.4/	1.0	0.6/	2.2	148.2/	3.1	25.0/	4.0	2.6/	5.2	0.5/	7.0	9999.2/Infinity	26.9
1027	1.4/	1.0	2.3/	3.0	51.0/	4.8	7.9/	6.0	0.0/	6.9	251.0/	7.8	9947.0/Infinity	7.5
1028	1.4/	1.0	2.4/	2.0	137.6/	4.0	0.0/	6.0	0.0/	8.0	0.0/	10.0	10000.0/Infinity	12.7
1029	1.4/	1.0	4.0/	3.0	165.1/	4.8	0.0/	6.0	0.0/	6.9	0.0/	7.8	10000.0/Infinity	13.4
1030	1.4/	1.0	3.2/	3.0	264.6/	4.8	3.4/	6.0	7.1/	6.9	0.0/	7.8	10000.0/Infinity	5.8
1031	1.4/	1.0	3.4/	4.0	612.1/	4.0	22.3/	4.0	0.8/	8.0	0.0/	16.0	4304.5/Infinity	2.5
1032	1.4/	1.0	1.6/	2.2	554.8/	3.1	45.8/	4.0	18.1/	5.2	0.1/	7.0	4304.4/Infinity	8.9
1033	1.4/	1.0	1.2/	2.2	554.8/	3.1	45.7/	4.0	19.8/	5.2	0.1/	7.0	4304.4/Infinity	13.9
1034	1.4/	1.0	0.9/	2.0	554.9/	3.0	45.4/	5.0	20.1/	8.0	0.0/	12.0	4304.4/Infinity	15.0
1035	1.4/	1.0	0.8/	2.2	555.0/	3.1	45.3/	4.0	20.1/	5.2	0.0/	7.0	4304.4/Infinity	15.2
1036	1.4/	1.0	0.7/	2.2	555.0/	3.1	45.3/	4.0	20.0/	5.2	0.0/	7.0	4304.4/Infinity	18.8
1037	1.4/	1.0	0.6/	2.0	555.0/	3.0	45.3/	5.0	20.0/	8.0	0.0/	12.0	4304.4/Infinity	26.0
1038	1.4/	1.0	1.1/	4.0	555.1/	4.0	45.4/	4.0	19.9/	8.0	0.1/	16.0	4304.4/Infinity	29.7
1039	1.4/	1.0	0.4/	2.0	10000.0/	4.0	10000.0/	6.0	9864.8/	8.0	1.9/	10.0	0.0/Infinity	30.7
1040	1.4/	1.0	0.4/	2.0	10000.0/	4.0	10000.0/	6.0	9864.8/	8.0	1.9/	10.0	0.0/Infinity	27.5
1041	1.5/	1.0	0.6/	4.0	10000.0/	4.0	10000.0/	4.0	9864.8/	8.0	1.9/	16.0	0.0/Infinity	28.7
1042	1.5/	1.0	0.4/	3.0	10000.0/	4.8	10000.0/	6.0	9864.8/	6.9	1.9/	7.8	0.0/Infinity	24.0
1043	1.5/	1.0	0.5/	4.0	10000.0/	4.0	10000.0/	4.0	9864.8/	8.0	1.9/	16.0	0.0/Infinity	21.8
1044	1.5/	1.0	0.3/	2.2	10000.0/	3.1	10000.0/	4.0	9864.8/	5.2	1.9/	7.0	0.0/Infinity	24.7
1045	1.5/	1.0	0.5/	4.0	10000.0/	4.0	10000.0/	4.0	9864.8/	8.0	1.9/	16.0	0.0/Infinity	23.5
1046	1.5/	1.0	0.3/	2.2	10000.0/	3.1	10000.0/	4.0	9864.8/	5.2	1.9/	7.0	0.0/Infinity	28.3
1047	1.7/	1.0	0.3/	2.0	10000.0/	4.0	10000.0/	6.0	9864.8/	8.0	1.9/	10.0	0.0/Infinity	22.5
1048	1.7/	1.0	0.5/	3.0	10000.0/	4.8	10000.0/	6.0	9864.8/	6.9	1.9/	7.8	0.0/Infinity	22.1
1049	1.7/	1.0	1.0/	4.0	10000.0/	4.0	10000.0/	4.0	9864.8/	8.0	1.9/	16.0	0.0/Infinity	9.6
1050	1.8/	1.0	1.2/	4.0	10000.0/	4.0	10000.0/	4.0	9864.8/	8.0	1.9/	16.0	0.0/Infinity	1.6
1051	1.8/	1.0	1.3/	4.0	10000.0/	4.0	10000.0/	4.0	9864.8/	8.0	1.9/	16.0	0.0/Infinity	5.7
1052	1.8/	1.0	0.6/	2.0	10000.0/	3.0	10000.0/	5.0	10000.0/	8.0	0.0/	12.0	0.0/Infinity	3.4
1053	1.8/	1.0	0.7/	2.0	10000.0/	4.0	10000.0/	6.0	10000.0/	8.0	0.0/	10.0	0.0/Infinity	2.4
1054	1.8/	1.0	0.7/	2.0	10000.0/	3.0	10000.0/	5.0	10000.0/	8.0	0.0/	12.0	0.0/Infinity	2.1
1055	2.0/	1.0	1.6/	4.0	10000.0/	4.0	10000.0/	4.0	10000.0/	8.0	0.0/	16.0	0.0/Infinity	2.0
1056	2.0/	1.0	1.0/	2.2	10000.0/	3.1	10000.0/	4.0	10000.0/	5.2	0.0/	7.0	0.0/Infinity	1.8
1057	2.0/	1.0	1.0/	2.0	10000.0/	3.0	10000.0/	5.0	10000.0/	8.0	0.0/	12.0	0.0/Infinity	1.6
1058	1.9/	1.0	1.5/	2.2	9999.5/	3.1	9998.4/	4.0	10000.0/	5.2	54.2/	7.0	6.8/Infinity	5.5
1059	1.9/	1.0	1.9/	2.2	9999.4/	3.1	9998.3/	4.0	10000.0/	5.2	56.7/	7.0	12.6/Infinity	8.0
1060	1.9/	1.0	3.2/	4.0	9999.4/	4.0	9998.3/	4.0	10000.0/	8.0	56.7/	16.0	12.9/Infinity	5.7
1061	1.9/	1.0	1.7/	2.2	10000.0/	3.1	10000.0/	4.0	10000.0/	5.2	10000.0/	7.0	0.0/Infinity	6.0
1062	1.9/	1.0	1.9/	2.2	10000.0/	3.1	10000.0/	4.0	10000.0/	5.2	0.0/	7.0	10000.0/Infinity	3.5
1063	1.9/	1.0	1.6/	2.0	10000.0/	4.0	10000.0/	6.0	10000.0/	8.0	0.0/	10.0	10000.0/Infinity	3.5
1064	1.9/	1.0	1.2/	2.0	10000.0/	3.0	10000.0/	5.0	10000.0/	8.0	0.3/	12.0	10000.0/Infinity	2.4
1065	1.7/	1.0	1.1/	2.0	10000.0/	3.0	10000.0/	5.0	10000.0/	8.0	0.3/	12.0	10000.0/Infinity	8.0
1066	1.7/	1.0	0.9/	2.0	10000.0/	4.0	9999.9/	6.0	10000.0/	8.0	0.0/	10.0	10000.0/Infinity	8.8
1067	1.7/	1.0	1.1/	3.0	10000.0/	4.8	9999.9/	6.0	10000.0/	6.9	0.1/	7.8	10000.0/Infinity	4.6
1068	1.7/	1.0	0.7/	2.0	10000.0/	4.0	9999.9/	6.0	10000.0/	8.0	0.1/	10.0	10000.0/Infinity	15.2
1069	1.7/	1.0	1.2/	3.0	9998.7/	4.8	9997.5/	6.0	9997.1/	6.9	0.0/	7.8	10000.0/Infinity	22.0
1070	1.7/	1.0	1.7/	4.0	9999.1/	4.0	9995.1/	4.0	9992.5/	8.0	0.0/	16.0	10000.0/Infinity	16.3
1071	1.7/	1.0	1.5/	3.0	9999.5/	4.8	9994.5/	6.0	9991.8/	6.9	0.0/	7.8	10000.0/Infinity	16.6
1072	1.7/	1.0	1.8/	3.0	9999.9/	4.8	9994.5/	6.0	9991.6/	6.9	0.0/	7.8	10000.0/Infinity	15.4
1073	1.7/	1.0	2.3/	4.0	9999.3/	4.0	9990.1/	4.0	9984.7/	8.0	0.0/	16.0	10000.0/Infinity	14.7
1074	1.7/	1.0	2.0/	3.0	10000.0/	4.8	9989.9/	6.0	9988.6/	6.9	0.0/	7.8	10000.0/Infinity	10.5
1075	1.7/	1.0	2.7/	4.0	10000.0/	4.0	9987.0/	4.0	9983.8/	8.0	0.0/	16.0	10000.0/Infinity	7.8
1076	1.7/	1.0	1.2/	2.0	10000.0/	4.0	9987.4/	6.0	9985.1/	8.0	0.0/	10.0	10000.0/Infinity	8.4
1077	1.7/	1.0	1.2/	2.0	10000.0/	4.0	9987.5/	6.0	9985.2/	8.0	0.0/	10.0	10000.0/Infinity	9.3
1078	1.7/	1.0	1.6/	3.0	10000.0/	4.8	9987.1/	6.0	9984.8/	6.9	0.0/	7.8	10000.0/Infinity	7.7
1079	1.7/	1.0	1.4/	3.0	10000.0/	4.8	9986.9/	6.0	9984.1/	6.9	0.0/	7.8	10000.0/Infinity	9.2
1080	1.7/	1.0	1.9/	4.0	10000.0/	4.0	9985.4/	4.0	9981.3/	8.0	0.1/	16.0	10000.0/Infinity	13.3
1081	1.7/	1.0	2.1/	4.0	10000.0/	4.0	9984.2/	4.0	9978.8/	8.0	0.0/	16.0	10000.0/Infinity	12.4
1082	1.7/	1.0	2.3/	4.0	10000.0/	4.0	9984.2/	4.0	9978.5/	8.0	0.1/	16.0	10000.0/Infinity	10.6
1083	1.8/	1.0	2.3/	4.0	10000.0/	4.0	9984.4/	4.0	9978.2/	8.0	0.0/	16.0	10000.0/Infinity	7.1
1084	1.8/	1.0	2.5/	4.0	10000.0/	4.0	9984.5/	4.0	9978.0/	8.0	0.1/	16.0	10000.0/Infinity	6.8
1085	1.8/	1.0	2.6/	4.0	10000.0/	4.0	9984.6/	4.0	9977.9/	8.0	0.0/	16.0	10000.0/Infinity	6.0
1086	1.8/	1.0	2.5/	4.0	10000.0/	4.0	9984.9/	4.0	9978.1/	8.0	0.0/	16.0	10000.0/Infinity	4.5
1087	1.8/	1.0	2.4/	4.0	10000.0/	4.0	9985.2/	4.0	9978.1/	8.0	0.1/	16.0	10000.0/Infinity	4.5
1088	1.8/	1.0	1.5/	3.0	10000.0/	4.8	9985.3/	6.0	9978.2/	6.9	0.1/	7.8	10000.0/Infinity	8.3
1089	1.7/	1.0	1.4/	3.0	10000.0/	4.8	9985.4/	6.0	9978.2/	6.9	0.1/	7.8	10000.0/Infinity	17.2
1090	1.7/	1.0	1.9/	3.0	9996.3/	4.8	9979.9/	6.0	9971.9/	6.9	0.0/	7.8	10000.0/Infinity	21.5

1091	1.7/	1.0	1.7/	2.0	9996.6/	4.0	9980.1/	6.0	9972.3/	8.0	0.0/	10.0	10000.0/Infinity	7.3
1092	1.7/	1.0	1.7/	2.0	9996.7/	4.0	9980.1/	6.0	9972.3/	8.0	0.0/	10.0	10000.0/Infinity	3.5
1093	1.7/	1.0	2.2/	3.0	9997.1/	4.8	9980.2/	6.0	9972.7/	6.9	0.0/	7.8	10000.0/Infinity	6.7
1094	1.7/	1.0	1.8/	3.0	9998.6/	4.8	9979.9/	6.0	9975.5/	6.9	0.0/	7.8	10000.0/Infinity	9.8
1095	1.7/	1.0	1.3/	3.0	9997.1/	4.8	9975.7/	6.0	9969.6/	6.9	0.0/	7.8	10000.0/Infinity	17.2
1096	1.7/	1.0	1.7/	4.0	9997.7/	4.0	9973.1/	4.0	9964.6/	8.0	0.0/	16.0	10000.0/Infinity	17.9
1097	1.7/	1.0	1.9/	4.0	9997.9/	4.0	9973.0/	4.0	9964.3/	8.0	0.0/	16.0	10000.0/Infinity	5.4
1098	1.7/	1.0	2.0/	4.0	9997.9/	4.0	9973.0/	4.0	9964.4/	8.0	0.1/	16.0	10000.0/Infinity	7.8
1099	1.7/	1.0	1.2/	2.2	9998.1/	3.1	9973.1/	4.0	9964.2/	5.2	0.0/	7.0	10000.0/Infinity	15.6
1100	1.7/	1.0	1.2/	2.2	9998.3/	3.1	9972.6/	4.0	9962.8/	5.2	0.0/	7.0	10000.0/Infinity	22.8
1101	1.8/	1.0	1.6/	3.0	9999.2/	4.8	9970.8/	6.0	9959.4/	6.9	0.1/	7.8	10000.0/Infinity	19.1
1102	1.8/	1.0	1.3/	2.2	9999.3/	3.1	9970.6/	4.0	9958.6/	5.2	0.1/	7.0	10000.0/Infinity	21.5
1103	1.8/	1.0	1.5/	3.0	9997.7/	4.8	9967.5/	6.0	9954.5/	6.9	0.0/	7.8	10000.0/Infinity	19.2
1104	1.8/	1.1	1.4/	3.0	9997.8/	4.8	9967.5/	6.0	9954.6/	6.9	0.1/	7.8	10000.0/Infinity	12.7
1105	1.8/	1.2	1.1/	2.0	9997.8/	4.0	9967.5/	6.0	9954.6/	8.0	0.3/	10.0	10000.0/Infinity	9.5
1106	1.8/	1.3	1.1/	2.0	9997.9/	3.0	9967.5/	5.0	9954.4/	8.0	0.0/	12.0	10000.0/Infinity	12.0
1107	1.8/	1.4	2.5/	3.0	9982.1/	4.8	9957.4/	6.0	9949.3/	6.9	1.4/	7.8	10000.0/Infinity	3.0
1108	1.8/	1.4	2.0/	2.0	9982.0/	4.0	9957.1/	6.0	9948.8/	8.0	0.2/	10.0	10000.0/Infinity	5.4
1109	1.8/	1.4	2.0/	2.0	9982.0/	4.0	9957.1/	6.0	9948.8/	8.0	0.2/	10.0	10000.0/Infinity	2.6
1110	1.8/	1.4	2.7/	3.0	9981.8/	4.8	9957.3/	6.0	9949.3/	6.9	0.9/	7.8	10000.0/Infinity	1.8
1111	1.8/	1.5	2.8/	4.0	9995.0/	4.0	9977.2/	4.0	9970.3/	8.0	3.8/	16.0	9999.9/Infinity	4.4
1112	1.8/	1.5	1.1/	2.0	9994.9/	3.0	9977.1/	5.0	9970.3/	8.0	0.9/	12.0	9999.9/Infinity	5.1
1113	1.8/	1.5	1.0/	2.0	9994.9/	3.0	9977.1/	5.0	9970.3/	8.0	0.9/	12.0	9999.9/Infinity	12.4
1114	1.8/	1.5	1.1/	2.0	9994.9/	3.0	9977.1/	5.0	9970.3/	8.0	1.1/	12.0	9999.9/Infinity	6.2
1115	1.8/	1.5	1.1/	2.0	9994.9/	3.0	9977.1/	5.0	9970.3/	8.0	1.3/	12.0	9999.9/Infinity	9.0
1116	1.4/	1.5	1.1/	2.0	9994.9/	3.0	9977.1/	5.0	9970.3/	8.0	1.3/	12.0	9999.9/Infinity	3.8
1117	1.4/	1.5	0.9/	2.0	9995.0/	3.0	9977.4/	5.0	9970.7/	8.0	1.5/	12.0	9999.9/Infinity	4.5
1118	1.4/	1.4	0.7/	2.0	9995.0/	3.0	9977.4/	5.0	9970.7/	8.0	1.5/	12.0	9999.9/Infinity	8.9
1119	1.4/	1.4	0.7/	2.0	9995.0/	3.0	9977.4/	5.0	9970.7/	8.0	1.5/	12.0	9999.9/Infinity	13.2
1120	1.4/	1.3	0.7/	2.0	9995.0/	3.0	9977.4/	5.0	9970.7/	8.0	1.5/	12.0	9999.9/Infinity	16.4
1121	1.4/	1.3	0.7/	2.0	9995.0/	3.0	9977.5/	5.0	9970.7/	8.0	1.8/	12.0	9999.9/Infinity	18.3
1122	1.5/	1.3	1.2/	3.0	9990.6/	4.8	9976.0/	6.0	9971.4/	6.9	0.0/	7.8	10000.0/Infinity	13.8
1123	1.5/	1.2	1.0/	2.0	9990.7/	4.0	9976.0/	6.0	9971.2/	8.0	0.0/	10.0	10000.0/Infinity	11.3
1124	1.5/	1.2	2.2/	4.0	9983.2/	4.0	9970.5/	4.0	9968.1/	8.0	0.0/	16.0	10000.0/Infinity	8.3
1125	1.5/	1.2	1.9/	3.0	9983.5/	4.8	9969.5/	6.0	9966.1/	6.9	0.0/	7.8	10000.0/Infinity	8.2
1126	1.5/	1.2	1.2/	2.0	9984.1/	3.0	9970.1/	5.0	9966.6/	8.0	0.0/	12.0	10000.0/Infinity	8.0
1127	1.4/	1.2	1.2/	2.2	9984.1/	3.1	9970.0/	4.0	9966.6/	5.2	0.0/	7.0	10000.0/Infinity	2.6
1128	1.4/	1.2	1.2/	2.2	9984.1/	3.1	9970.0/	4.0	9966.6/	5.2	0.0/	7.0	10000.0/Infinity	2.3
1129	1.4/	1.2	2.0/	3.0	9984.0/	4.8	9970.2/	6.0	9966.2/	6.9	0.2/	7.8	10000.0/Infinity	1.8
1130	1.4/	1.2	1.8/	3.0	9984.0/	4.8	9970.2/	6.0	9966.1/	6.9	0.0/	7.8	10000.0/Infinity	2.4
1131	1.4/	1.4	1.5/	2.2	9984.2/	3.1	9970.3/	4.0	9966.1/	5.2	0.0/	7.0	10000.0/Infinity	3.9
1132	1.4/	1.5	1.5/	2.2	9984.2/	3.1	9970.3/	4.0	9966.1/	5.2	0.0/	7.0	10000.0/Infinity	2.8
1133	1.4/	1.6	1.2/	2.0	9984.1/	3.0	9970.1/	5.0	9965.8/	8.0	0.0/	12.0	10000.0/Infinity	2.9
1134	1.4/	1.6	1.8/	4.0	9983.3/	4.0	9969.5/	4.0	9965.6/	8.0	0.0/	16.0	10000.0/Infinity	5.1
1135	1.4/	1.6	0.9/	3.0	9783.3/	4.8	10000.0/	6.0	9194.6/	6.9	0.1/	7.8	10000.0/Infinity	5.1
1136	1.4/	1.5	0.5/	2.2	9783.4/	3.1	10000.0/	4.0	9194.5/	5.2	0.0/	7.0	10000.0/Infinity	7.9
1137	1.4/	1.5	0.5/	2.2	9783.4/	3.1	10000.0/	4.0	9194.5/	5.2	0.0/	7.0	10000.0/Infinity	6.7
1138	1.4/	1.5	0.5/	2.0	9783.4/	4.0	10000.0/	6.0	9194.5/	8.0	0.0/	10.0	10000.0/Infinity	5.5
1139	1.2/	1.5	0.6/	2.0	9783.3/	3.0	9999.9/	5.0	9194.4/	8.0	0.3/	12.0	10000.0/Infinity	6.8
1140	1.2/	1.4	0.7/	2.0	9783.3/	3.0	10000.0/	5.0	9194.7/	8.0	0.9/	12.0	10000.0/Infinity	8.4
1141	1.2/	1.4	0.9/	2.0	9783.9/	3.0	10000.0/	5.0	9196.3/	8.0	3.4/	12.0	10000.0/Infinity	11.1
1142	1.2/	1.4	1.8/	4.0	9798.8/	4.0	10000.0/	4.0	9275.7/	8.0	32.4/	16.0	10000.0/Infinity	8.6
1143	1.2/	1.4	1.5/	3.0	9798.8/	4.8	10000.0/	6.0	9275.8/	6.9	31.1/	7.8	10000.0/Infinity	4.3
1144	1.2/	1.4	1.4/	3.0	9798.8/	4.8	10000.0/	6.0	9275.8/	6.9	31.1/	7.8	10000.0/Infinity	6.0
1145	1.2/	1.4	1.1/	3.0	9798.8/	4.8	10000.0/	6.0	9275.8/	6.9	31.0/	7.8	10000.0/Infinity	9.3
1146	1.2/	1.3	0.7/	2.2	9798.8/	3.1	10000.0/	4.0	9275.8/	5.2	30.4/	7.0	10000.0/Infinity	11.2
1147	1.2/	1.3	0.6/	2.2	9798.8/	3.1	10000.0/	4.0	9275.8/	5.2	30.4/	7.0	10000.0/Infinity	18.7
1148	1.3/	1.3	0.8/	3.0	9798.8/	4.8	10000.0/	6.0	9275.8/	6.9	30.4/	7.8	10000.0/Infinity	24.8
1149	1.3/	1.3	1.0/	4.0	9798.8/	4.0	10000.0/	4.0	9275.8/	8.0	30.4/	16.0	10000.0/Infinity	26.8
1150	1.3/	1.3	0.6/	2.0	9797.7/	4.0	9999.6/	6.0	9276.6/	8.0	0.0/	10.0	10000.0/Infinity	22.5
1151	1.3/	1.3	1.1/	4.0	9796.4/	4.0	9993.1/	4.0	9266.8/	8.0	0.0/	16.0	10000.0/Infinity	13.7
1152	1.3/	1.4	1.3/	4.0	9796.6/	4.0	9993.3/	4.0	9266.8/	8.0	0.1/	16.0	10000.0/Infinity	9.1
1153	1.5/	1.4	1.3/	4.0	9797.1/	4.0	9993.1/	4.0	9265.9/	8.0	0.0/	16.0	10000.0/Infinity	6.0
1154	1.5/	1.5	1.5/	4.0	9797.2/	4.0	9993.1/	4.0	9266.0/	8.0	0.1/	16.0	10000.0/Infinity	3.6
1155	1.5/	1.5	1.3/	3.0	9797.2/	4.8	9993.1/	6.0	9265.9/	6.9	0.0/	7.8	10000.0/Infinity	4.0
1156	1.5/	1.5	1.3/	3.0	9797.2/	4.8	9993.1/	6.0	9265.9/	6.9	0.0/	7.8	10000.0/Infinity	12.0

1157	1.5/	1.5	1.5/	4.0	9797.3/	4.0	9993.2/	4.0	9265.9/	8.0	0.1/	16.0	10000.0/Infinity	14.2
1158	1.5/	1.5	1.2/	4.0	9797.4/	4.0	9993.2/	4.0	9266.0/	8.0	0.2/	16.0	10000.0/Infinity	12.4
1159	1.5/	1.5	1.0/	4.0	9797.4/	4.0	9993.2/	4.0	9266.0/	8.0	0.2/	16.0	10000.0/Infinity	19.1
1160	1.5/	1.6	1.0/	2.2	9797.4/	3.1	9993.2/	4.0	9266.0/	5.2	0.2/	7.0	10000.0/Infinity	353.8
1161	1.5/	1.6	1.4/	3.0	9803.2/	4.8	9992.1/	6.0	9280.6/	6.9	0.0/	7.8	10000.0/Infinity	101.5
1162	1.5/	1.6	1.4/	2.2	9803.2/	3.1	9992.1/	4.0	9280.6/	5.2	0.0/	7.0	10000.0/Infinity	164.7
1163	1.5/	1.6	0.8/	4.0	9803.3/	4.0	9992.1/	4.0	9280.6/	8.0	0.1/	16.0	10000.0/Infinity	37.8
1164	1.5/	1.6	0.4/	2.0	9803.4/	3.0	9992.0/	5.0	9280.3/	8.0	0.2/	12.0	10000.0/Infinity	28.9
1165	1.5/	1.5	0.4/	2.2	9803.4/	3.1	9992.0/	4.0	9280.2/	5.2	0.1/	7.0	10000.0/Infinity	26.8
1166	1.6/	1.5	0.8/	4.0	9803.5/	4.0	9991.9/	4.0	9280.0/	8.0	0.3/	16.0	10000.0/Infinity	28.7
1167	1.6/	1.5	0.4/	2.0	9803.6/	4.0	9991.8/	6.0	9279.8/	8.0	0.1/	10.0	10000.0/Infinity	27.3
1168	1.6/	1.5	0.4/	2.0	9803.6/	4.0	9991.8/	6.0	9279.8/	8.0	0.1/	10.0	10000.0/Infinity	19.9
1169	1.6/	1.5	0.4/	2.0	9803.6/	3.0	9991.8/	5.0	9279.8/	8.0	0.1/	12.0	10000.0/Infinity	16.5
1170	1.6/	1.5	0.8/	4.0	9802.7/	4.0	9989.2/	4.0	9276.3/	8.0	0.0/	16.0	10000.0/Infinity	10.6
1171	1.6/	1.5	0.8/	4.0	9802.7/	4.0	9989.2/	4.0	9276.3/	8.0	0.0/	16.0	10000.0/Infinity	7.9
1172	1.6/	1.5	0.9/	4.0	9802.8/	4.0	9989.3/	4.0	9276.4/	8.0	0.1/	16.0	10000.0/Infinity	12.8
1173	1.6/	1.5	1.1/	4.0	9802.9/	4.0	9989.3/	4.0	9276.3/	8.0	0.3/	16.0	10000.0/Infinity	17.2
1174	1.6/	1.5	0.7/	3.0	9802.9/	4.8	9989.2/	6.0	9276.1/	6.9	0.1/	7.8	10000.0/Infinity	15.2
1175	1.6/	1.5	0.7/	4.0	9802.9/	4.0	9989.2/	4.0	9276.1/	8.0	0.1/	16.0	10000.0/Infinity	16.9
1176	1.6/	1.6	0.4/	2.2	9802.9/	3.1	9989.2/	4.0	9276.0/	5.2	0.0/	7.0	10000.0/Infinity	22.5
1177	1.6/	1.6	0.4/	2.0	9802.9/	4.0	9989.2/	6.0	9276.0/	8.0	0.0/	10.0	10000.0/Infinity	21.5
1178	1.6/	1.6	0.4/	2.0	9802.9/	3.0	9989.2/	5.0	9276.0/	8.0	0.1/	12.0	10000.0/Infinity	20.9
1179	1.6/	1.6	0.4/	2.0	9802.9/	3.0	9989.2/	5.0	9276.0/	8.0	0.1/	12.0	10000.0/Infinity	22.2
1180	1.6/	1.6	0.4/	2.0	9802.9/	3.0	9989.2/	5.0	9276.0/	8.0	0.1/	12.0	10000.0/Infinity	22.5
1181	1.6/	1.6	0.5/	2.0	9802.9/	4.0	9989.2/	6.0	9276.0/	8.0	0.3/	10.0	10000.0/Infinity	20.8
1182	1.6/	1.6	0.5/	2.0	9802.9/	3.0	9989.2/	5.0	9276.0/	8.0	0.4/	12.0	10000.0/Infinity	19.6
1183	1.6/	1.6	0.5/	2.0	9802.9/	3.0	9989.2/	5.0	9276.0/	8.0	0.4/	12.0	10000.0/Infinity	18.5
1184	1.6/	1.7	0.5/	2.0	9802.9/	3.0	9989.2/	5.0	9276.0/	8.0	0.4/	12.0	10000.0/Infinity	19.8
1185	1.6/	1.7	0.5/	2.0	9802.9/	3.0	9989.2/	5.0	9276.0/	8.0	0.4/	12.0	10000.0/Infinity	19.7
1186	1.5/	1.8	0.5/	2.0	9802.9/	3.0	9989.2/	5.0	9276.0/	8.0	0.4/	12.0	10000.0/Infinity	19.2
1187	1.5/	1.8	0.5/	2.0	9802.9/	3.0	9989.2/	5.0	9276.0/	8.0	0.4/	12.0	10000.0/Infinity	20.9
1188	1.5/	1.8	0.5/	2.0	9802.9/	3.0	9989.2/	5.0	9276.0/	8.0	0.4/	12.0	10000.0/Infinity	22.0
1189	1.5/	1.8	0.8/	4.0	9802.9/	4.0	9989.2/	4.0	9276.0/	8.0	0.9/	16.0	10000.0/Infinity	27.6
1190	1.5/	1.8	0.3/	2.2	9802.8/	3.1	9989.0/	4.0	9275.7/	5.2	0.0/	7.0	10000.0/Infinity	30.6
1191	1.4/	1.8	0.6/	4.0	9803.1/	4.0	9989.0/	4.0	9275.6/	8.0	0.1/	16.0	10000.0/Infinity	29.7
1192	1.4/	1.8	0.3/	2.2	9803.2/	3.1	9989.1/	4.0	9275.4/	5.2	0.0/	7.0	10000.0/Infinity	30.8
1193	1.4/	1.8	0.6/	4.0	9803.3/	4.0	9989.2/	4.0	9275.4/	8.0	0.1/	16.0	10000.0/Infinity	31.7
1194	1.4/	1.8	0.3/	2.0	9803.5/	4.0	9989.2/	6.0	9275.4/	8.0	0.0/	10.0	10000.0/Infinity	33.3
1195	1.4/	1.8	0.5/	4.0	9803.8/	4.0	9989.2/	4.0	9275.1/	8.0	0.1/	16.0	10000.0/Infinity	30.7
1196	1.4/	1.8	0.6/	4.0	9804.0/	4.0	9989.3/	4.0	9275.1/	8.0	0.1/	16.0	10000.0/Infinity	29.1
1197	1.4/	1.8	0.7/	3.0	9804.0/	4.8	9989.3/	6.0	9275.0/	6.9	0.2/	7.8	10000.0/Infinity	30.4
1198	1.4/	1.7	0.6/	2.0	9804.0/	4.0	9989.3/	6.0	9275.0/	8.0	0.1/	10.0	10000.0/Infinity	16.9
1199	1.4/	1.7	0.5/	2.0	9804.0/	3.0	9989.3/	5.0	9275.0/	8.0	0.2/	12.0	10000.0/Infinity	16.0
1200	1.4/	1.7	0.5/	2.0	9804.0/	3.0	9989.3/	5.0	9275.0/	8.0	0.2/	12.0	10000.0/Infinity	18.8
1201	1.3/	1.7	0.5/	2.0	9804.0/	3.0	9989.3/	5.0	9275.0/	8.0	0.2/	12.0	10000.0/Infinity	19.0
1202	1.3/	1.8	0.5/	2.0	9804.0/	3.0	9989.3/	5.0	9275.0/	8.0	0.3/	12.0	10000.0/Infinity	15.3
1203	1.4/	1.8	0.5/	2.0	9804.0/	3.0	9989.3/	5.0	9275.0/	8.0	0.3/	12.0	10000.0/Infinity	13.6
1204	1.4/	1.8	0.6/	2.0	9804.0/	3.0	9989.3/	5.0	9275.0/	8.0	0.3/	12.0	10000.0/Infinity	14.7
1205	1.4/	1.8	0.5/	2.0	9804.0/	3.0	9989.3/	5.0	9275.0/	8.0	0.3/	12.0	10000.0/Infinity	16.9
1206	1.4/	1.8	0.5/	2.0	9804.0/	3.0	9989.2/	5.0	9274.9/	8.0	0.2/	12.0	10000.0/Infinity	23.0
1207	1.4/	1.8	4.9/	4.0	10000.0/	4.0	10000.0/	4.0	10000.0/	8.0	70.1/	16.0	10000.0/Infinity	27.4
1208	1.4/	1.8	14.1/	2.0	9999.8/	3.0	10000.0/	5.0	10000.0/	8.0	0.0/	12.0	10000.0/Infinity	81.7

FID	Play1/ Tlay1	Play2/ Tlay2	Play3/ Tlay3	Play4/ Tlay4	Play5/ Tlay5	Play6/ Tlay6	Play7/Half	Spc Error
967	1.4/ 6.3	0.2/ 2.0	999.8/ 3.0	1000.0/ 5.0	10000.2/ 8.0	10000.1/ 12.0	9961.7/Infinity	65.2
968	1.4/ 6.6	0.1/ 2.0	15.7/ 4.0	479.8/ 6.0	6000.0/ 8.0	6900.0/ 12.0	9994.8/Infinity	31.3
969	1.4/ 5.8	0.1/ 2.0	19.7/ 4.0	479.8/ 6.0	6000.0/ 8.0	6900.0/ 12.0	9996.0/Infinity	34.1
970	1.4/ 5.5	0.1/ 2.0	26.5/ 4.0	480.0/ 6.0	6000.0/ 8.0	6900.0/ 12.0	9998.9/Infinity	34.1
971	1.4/ 5.0	0.1/ 2.0	1.2/ 3.0	479.7/ 5.0	6000.0/ 8.0	6900.0/ 12.0	9993.0/Infinity	29.5
972	1.4/ 4.2	0.1/ 2.0	10000.0/ 3.0	10000.0/ 5.0	10000.0/ 8.0	1000.0/ 12.0	1000.0/Infinity	14.3
973	1.4/ 4.3	0.1/ 2.0	10000.0/ 3.0	10000.0/ 5.0	10000.0/ 8.0	1000.0/ 12.0	1000.0/Infinity	18.1
974	1.4/ 4.4	0.2/ 4.0	10000.0/ 4.0	10000.0/ 4.0	10000.0/ 8.0	1000.0/ 16.0	1000.0/Infinity	16.7
975	1.4/ 4.6	0.2/ 4.0	10104.6/ 4.0	9786.9/ 4.0	9596.5/ 8.0	486.7/ 16.0	0.0/Infinity	17.1
976	1.4/ 4.2	0.2/ 4.0	10108.5/ 4.0	9409.1/ 4.0	9001.2/ 8.0	0.0/ 16.0	0.0/Infinity	10.0
977	1.4/ 3.4	0.2/ 4.0	10108.5/ 4.0	9409.1/ 4.0	9001.2/ 8.0	0.0/ 16.0	0.0/Infinity	14.4
978	1.4/ 2.7	0.2/ 4.0	10108.6/ 4.0	9409.7/ 4.0	9002.2/ 8.0	0.0/ 16.0	2.7/Infinity	25.9
979	1.4/ 2.5	0.3/ 4.0	10108.6/ 4.0	9409.8/ 4.0	9002.5/ 8.0	0.0/ 16.0	3.8/Infinity	39.3
980	1.4/ 2.4	0.3/ 4.0	10108.5/ 4.0	9409.9/ 4.0	9002.7/ 8.0	0.0/ 16.0	4.2/Infinity	38.1
981	1.4/ 2.0	0.3/ 4.0	10006.8/ 4.0	10014.8/ 4.0	10019.2/ 8.0	1021.4/ 16.0	1353.6/Infinity	36.4
982	1.4/ 1.8	0.2/ 2.0	10006.3/ 4.0	10013.1/ 6.0	10015.2/ 8.0	1020.3/ 12.0	1377.0/Infinity	39.2
983	1.4/ 1.5	0.4/ 3.0	10000.0/ 4.8	10000.0/ 6.0	10000.1/ 6.9	1000.1/ 7.8	1014.1/Infinity	33.0
984	1.4/ 1.4	0.8/ 4.0	151.3/ 4.0	0.0/ 4.0	7531.8/ 8.0	7541.7/ 16.0	18775.5/Infinity	15.3
985	1.4/ 1.5	1.1/ 3.0	6209.0/ 4.8	10557.3/ 6.0	0.0/ 6.9	0.0/ 7.8	2777.3/Infinity	5.2
986	1.4/ 1.5	0.9/ 3.0	6209.0/ 4.8	10557.3/ 6.0	0.1/ 6.9	0.1/ 7.8	2777.3/Infinity	15.3
987	1.4/ 1.5	0.4/ 2.2	10000.0/ 3.1	10000.0/ 4.0	10000.0/ 5.2	1000.0/ 7.0	999.9/Infinity	23.6
988	1.4/ 1.6	0.4/ 3.0	10000.0/ 4.8	10000.0/ 6.0	10000.0/ 6.9	1000.0/ 7.8	1000.0/Infinity	22.2
989	1.4/ 1.6	0.4/ 3.0	10000.0/ 4.8	10000.0/ 6.0	10000.0/ 6.9	1000.0/ 7.8	1000.0/Infinity	23.5
990	1.4/ 1.7	0.2/ 2.0	10001.2/ 3.0	10002.6/ 5.0	10002.9/ 8.0	1004.1/ 12.0	1130.1/Infinity	28.7
991	1.4/ 1.7	0.4/ 4.0	10003.9/ 4.0	10008.4/ 4.0	10010.8/ 8.0	1011.8/ 16.0	1263.7/Infinity	33.2
992	1.4/ 1.8	0.2/ 2.2	10000.0/ 3.1	10000.0/ 4.0	10000.0/ 5.2	1000.0/ 7.0	1000.2/Infinity	36.5
993	1.4/ 1.8	0.4/ 4.0	10000.0/ 4.0	10000.0/ 4.0	10000.0/ 8.0	1000.0/ 16.0	1000.0/Infinity	35.2
994	1.4/ 1.9	1.2/ 4.0	77.1/ 4.0	0.7/ 4.0	99999.0/ 8.0	99999.0/ 16.0	99999.0/Infinity	18.7
995	1.4/ 1.9	2.2/ 4.0	65.9/ 4.0	1.7/ 4.0	99999.0/ 8.0	99999.0/ 16.0	99999.0/Infinity	13.1
996	1.4/ 2.0	2.3/ 4.0	65.9/ 4.0	1.8/ 4.0	99999.0/ 8.0	99999.0/ 16.0	99999.0/Infinity	9.4
997	1.4/ 2.0	2.5/ 4.0	66.0/ 4.0	1.9/ 4.0	99999.0/ 8.0	99999.0/ 16.0	99999.0/Infinity	7.9
998	1.4/ 2.0	2.5/ 4.0	45.6/ 4.0	2.0/ 4.0	99999.0/ 8.0	99999.0/ 16.0	99999.0/Infinity	4.1
999	1.4/ 1.9	2.2/ 4.0	46.2/ 4.0	1.9/ 4.0	99999.0/ 8.0	99999.0/ 16.0	99999.0/Infinity	6.4
1000	1.4/ 1.8	1.9/ 4.0	46.8/ 4.0	1.7/ 4.0	99999.0/ 8.0	99999.0/ 16.0	99999.0/Infinity	5.3
1001	1.4/ 1.7	1.7/ 4.0	47.2/ 4.0	1.7/ 4.0	99999.0/ 8.0	99999.0/ 16.0	99999.0/Infinity	3.9
1002	1.4/ 1.8	2.0/ 4.0	27.6/ 4.0	1.6/ 4.0	99999.0/ 8.0	71620.2/ 16.0	85101.3/Infinity	4.9
1003	1.4/ 1.7	2.2/ 4.0	26.5/ 4.0	1.2/ 4.0	99999.0/ 8.0	99999.0/ 16.0	88988.0/Infinity	2.6
1004	1.4/ 1.8	2.1/ 4.0	26.8/ 4.0	1.0/ 4.0	99999.0/ 8.0	99999.0/ 16.0	94215.7/Infinity	4.9
1005	1.4/ 1.8	1.6/ 4.0	32.7/ 4.0	0.9/ 4.0	99999.0/ 8.0	99999.0/ 16.0	99510.4/Infinity	4.4
1006	1.4/ 1.9	2.0/ 4.0	32.9/ 4.0	1.4/ 4.0	99999.0/ 8.0	99999.0/ 16.0	99510.4/Infinity	12.1
1007	1.4/ 1.8	2.1/ 4.0	36.6/ 4.0	1.3/ 4.0	99999.0/ 8.0	99999.0/ 16.0	99510.5/Infinity	5.9
1008	1.4/ 1.7	1.5/ 4.0	139.6/ 4.0	0.8/ 4.0	99999.0/ 8.0	99999.0/ 16.0	99999.0/Infinity	8.2
1009	1.4/ 1.6	0.6/ 3.0	11020.3/ 4.8	12021.9/ 6.0	7521.0/ 6.9	0.0/ 7.8	5534.3/Infinity	5.2
1010	1.4/ 1.5	0.7/ 3.0	10000.5/ 4.8	10000.9/ 6.0	10001.1/ 6.9	1001.1/ 7.8	1046.3/Infinity	4.3
1011	1.4/ 1.4	1.0/ 4.0	160.7/ 4.0	0.0/ 4.0	8001.6/ 8.0	8080.5/ 16.0	17979.0/Infinity	10.7
1012	1.4/ 2.2	1.2/ 4.0	54.2/ 4.0	0.0/ 4.0	7858.1/ 8.0	7332.0/ 16.0	17750.3/Infinity	16.1
1013	1.4/ 3.9	1.4/ 3.0	10000.0/ 4.8	10000.0/ 6.0	10000.0/ 6.9	1000.0/ 7.8	999.7/Infinity	20.0
1014	1.4/ 3.2	1.4/ 4.0	10450.8/ 4.0	8628.4/ 4.0	8016.7/ 8.0	0.0/ 16.0	7316.0/Infinity	11.7
1015	1.4/ 2.8	0.3/ 2.0	9310.6/ 3.0	6370.1/ 5.0	3431.9/ 8.0	479.2/ 12.0	1097.0/Infinity	7.7
1016	1.4/ 1.3	0.3/ 4.0	10000.0/ 4.0	10000.1/ 4.0	10000.1/ 8.0	1000.2/ 16.0	1008.9/Infinity	21.7
1017	1.4/ 1.2	0.2/ 2.2	10000.0/ 3.1	10000.0/ 4.0	10000.0/ 5.2	1000.0/ 7.0	1000.0/Infinity	19.6
1018	1.4/ 1.1	0.2/ 2.2	10000.0/ 3.1	10000.0/ 4.0	10000.0/ 5.2	1000.0/ 7.0	1000.0/Infinity	25.0
1019	1.4/ 1.0	0.4/ 2.2	10000.0/ 3.1	10000.0/ 4.0	10000.0/ 5.2	1000.0/ 7.0	1000.0/Infinity	34.1
1020	1.4/ 1.8	1.6/ 3.0	83957.9/ 4.8	99999.0/ 6.0	99999.0/ 6.9	0.0/ 7.8	647.7/Infinity	34.3
1021	1.4/ 1.2	2.2/ 2.0	280.6/ 3.0	0.6/ 5.0	23109.2/ 8.0	99999.0/ 12.0	68196.2/Infinity	6.7
1022	1.4/ 1.1	0.7/ 2.0	321.4/ 3.0	0.2/ 5.0	23109.2/ 8.0	99999.0/ 12.0	68196.2/Infinity	4.9
1023	1.4/ 1.0	0.3/ 2.0	10000.0/ 4.0	10000.0/ 6.0	10000.0/ 8.0	1000.0/ 12.0	1000.0/Infinity	15.6
1024	1.4/ 1.0	0.2/ 2.0	10000.0/ 4.0	10000.0/ 6.0	10000.0/ 8.0	1000.0/ 12.0	1000.0/Infinity	22.6
1025	1.4/ 1.0	0.3/ 2.0	10000.0/ 4.0	10000.0/ 6.0	10000.0/ 8.0	1000.0/ 12.0	1000.0/Infinity	20.1
1026	1.4/ 1.0	0.5/ 2.0	10000.0/ 4.0	10000.0/ 6.0	10000.0/ 8.0	1000.0/ 12.0	1000.0/Infinity	27.6

1027	1.4/	1.0	1.9/	4.0	10000.1/	4.0	10000.1/	4.0	10000.0/	8.0	996.8/	16.0	933.5/Infinity	30.1
1028	1.4/	1.0	1.8/	2.0	368.6/	3.0	0.0/	5.0	10012.6/	8.0	10975.8/	12.0	10751.8/Infinity	5.0
1029	1.4/	1.0	2.2/	2.0	10351.3/	3.0	10593.9/	5.0	11470.1/	8.0	4718.3/	12.0	1154.6/Infinity	1.6
1030	1.4/	1.0	2.2/	2.2	10004.5/	3.1	10008.3/	4.0	10013.0/	5.2	1019.5/	7.0	1061.5/Infinity	1.6
1031	1.4/	1.0	1.9/	2.0	9997.0/	4.0	9995.2/	6.0	9994.1/	8.0	968.9/	12.0	974.2/Infinity	2.1
1032	1.4/	1.0	1.6/	2.2	10000.0/	3.1	10000.0/	4.0	10000.0/	5.2	999.9/	7.0	1007.4/Infinity	8.7
1033	1.4/	1.0	1.1/	2.0	99999.0/	3.0	0.0/	5.0	99999.0/	8.0	99999.0/	12.0	14718.2/Infinity	13.3
1034	1.4/	1.0	0.9/	2.0	17486.8/	4.0	25055.7/	6.0	37409.5/	8.0	47412.3/	12.0	1240.7/Infinity	14.9
1035	1.4/	1.0	0.8/	2.0	17486.8/	4.0	25055.7/	6.0	37409.5/	8.0	47412.3/	12.0	1240.7/Infinity	15.0
1036	1.4/	1.0	1.3/	4.0	10000.0/	4.0	10000.0/	4.0	10000.0/	8.0	1000.0/	16.0	999.9/Infinity	18.3
1037	1.4/	1.0	1.1/	4.0	10000.0/	4.0	10000.0/	4.0	10000.0/	8.0	1000.0/	16.0	999.9/Infinity	24.8
1038	1.4/	1.0	1.0/	4.0	10196.4/	4.0	10180.7/	4.0	9367.0/	8.0	0.0/	16.0	157.0/Infinity	26.4
1039	1.4/	1.0	0.7/	3.0	10045.7/	4.8	9996.1/	6.0	9742.6/	6.9	0.0/	7.8	471.0/Infinity	30.6
1040	1.4/	1.0	0.7/	4.0	10000.0/	4.0	10000.0/	4.0	10000.0/	8.0	1000.0/	16.0	1000.0/Infinity	27.3
1041	1.5/	1.0	0.7/	4.0	10000.0/	4.0	10000.0/	4.0	10000.0/	8.0	1000.0/	16.0	1000.0/Infinity	30.8
1042	1.5/	1.0	0.6/	4.0	10000.0/	4.0	10000.0/	4.0	10000.0/	8.0	1000.0/	16.0	1000.0/Infinity	24.6
1043	1.5/	1.0	0.6/	4.0	10000.0/	4.0	10000.0/	4.0	10000.0/	8.0	1000.0/	16.0	1000.0/Infinity	22.6
1044	1.5/	1.0	0.6/	4.0	10000.0/	4.0	10000.0/	4.0	10000.0/	8.0	1000.0/	16.0	1000.0/Infinity	25.3
1045	1.5/	1.0	0.3/	2.2	10000.0/	3.1	10000.0/	4.0	10000.0/	5.2	1000.0/	7.0	999.9/Infinity	24.1
1046	1.5/	1.0	0.3/	2.2	10000.0/	3.1	10000.0/	4.0	10000.0/	5.2	1000.0/	7.0	999.9/Infinity	29.1
1047	1.7/	1.0	0.3/	2.0	10000.0/	4.0	10000.0/	6.0	10000.0/	8.0	1000.0/	12.0	1000.0/Infinity	23.0
1048	1.7/	1.0	0.7/	4.0	10000.0/	4.0	10000.0/	4.0	10000.0/	8.0	1000.0/	16.0	1000.0/Infinity	22.4
1049	1.7/	1.0	1.2/	4.0	115.3/	4.0	0.1/	4.0	8570.3/	8.0	8365.4/	16.0	15342.7/Infinity	2.7
1050	1.8/	1.0	1.2/	4.0	10000.0/	4.0	10000.0/	4.0	10000.0/	8.0	1000.0/	16.0	1002.7/Infinity	1.0
1051	1.8/	1.0	1.2/	4.0	10032.3/	4.0	10001.5/	4.0	9857.4/	8.0	0.0/	16.0	861.5/Infinity	5.8
1052	1.8/	1.0	0.7/	2.0	99999.0/	3.0	99999.0/	5.0	99999.0/	8.0	0.0/	12.0	844.7/Infinity	5.8
1053	1.8/	1.0	1.0/	3.0	10000.0/	4.8	10000.0/	6.0	10000.0/	6.9	1000.0/	7.8	999.9/Infinity	2.3
1054	1.8/	1.0	0.7/	2.0	10000.0/	4.0	10000.0/	6.0	10000.0/	8.0	999.8/	12.0	1001.0/Infinity	1.8
1055	2.0/	1.0	0.8/	2.0	10000.0/	3.0	10000.0/	5.0	10000.0/	8.0	999.9/	12.0	1000.8/Infinity	1.7
1056	2.0/	1.0	1.0/	2.2	10000.0/	3.1	10000.0/	4.0	10000.0/	5.2	1000.0/	7.0	998.6/Infinity	1.6
1057	2.0/	1.0	1.1/	2.0	10001.0/	3.0	10001.7/	5.0	10005.2/	8.0	1023.1/	12.0	1044.4/Infinity	1.5
1058	1.9/	1.0	2.3/	2.0	6.3/	3.0	9949.2/	5.0	2225.1/	8.0	454.3/	12.0	14449.4/Infinity	3.2
1059	1.9/	1.0	4.4/	2.0	4.6/	3.0	9953.9/	5.0	2227.3/	8.0	360.1/	12.0	14451.2/Infinity	6.5
1060	1.9/	1.0	3.2/	4.0	9848.4/	4.0	9642.7/	4.0	9313.9/	8.0	0.0/	16.0	1141.1/Infinity	5.6
1061	1.9/	1.0	3.2/	4.0	233.0/	4.0	0.0/	4.0	9918.6/	8.0	10245.2/	16.0	11793.4/Infinity	5.2
1062	1.9/	1.0	2.6/	3.0	336.0/	4.8	0.0/	6.0	9921.6/	6.9	10051.0/	7.8	11153.4/Infinity	1.3
1063	1.9/	1.0	2.4/	3.0	335.9/	4.8	0.0/	6.0	9921.6/	6.9	10051.0/	7.8	11153.4/Infinity	3.0
1064	1.9/	1.0	1.3/	2.2	9998.5/	3.1	9998.0/	4.0	9997.6/	5.2	994.2/	7.0	982.6/Infinity	2.5
1065	1.7/	1.0	1.1/	2.2	99999.0/	3.1	0.0/	4.0	99999.0/	5.2	0.0/	7.0	1466.1/Infinity	7.3
1066	1.7/	1.0	1.5/	3.0	138.8/	4.8	0.0/	6.0	24655.9/	6.9	84997.0/	7.8	99999.0/Infinity	3.5
1067	1.7/	1.0	0.7/	2.0	3138.8/	4.0	6373.2/	6.0	90165.1/	8.0	58117.9/	12.0	1290.8/Infinity	4.8
1068	1.7/	1.0	0.7/	2.0	3138.8/	4.0	6373.2/	6.0	90165.1/	8.0	58117.9/	12.0	1290.8/Infinity	15.2
1069	1.7/	1.0	1.6/	4.0	10000.0/	4.0	10000.0/	4.0	10000.0/	8.0	1000.0/	16.0	999.8/Infinity	21.4
1070	1.7/	1.0	2.1/	4.0	125.6/	4.0	0.1/	4.0	7853.5/	8.0	8159.6/	16.0	19333.0/Infinity	3.2
1071	1.7/	1.0	2.4/	4.0	125.6/	4.0	0.1/	4.0	7853.5/	8.0	8159.6/	16.0	19333.0/Infinity	2.3
1072	1.7/	1.0	3.2/	4.0	125.8/	4.0	0.2/	4.0	7853.5/	8.0	8159.6/	16.0	19333.0/Infinity	3.5
1073	1.7/	1.0	2.8/	4.0	182.6/	4.0	0.1/	4.0	99999.0/	8.0	99999.0/	16.0	17017.2/Infinity	4.4
1074	1.7/	1.0	1.5/	2.0	254.5/	4.0	0.1/	6.0	6676.7/	8.0	99999.0/	12.0	99999.0/Infinity	3.0
1075	1.7/	1.0	1.5/	2.0	254.5/	4.0	0.1/	6.0	6676.7/	8.0	99999.0/	12.0	99999.0/Infinity	2.4
1076	1.7/	1.0	1.9/	3.0	168.8/	4.8	0.0/	6.0	9621.5/	6.9	9708.4/	7.8	13250.7/Infinity	2.3
1077	1.7/	1.0	1.8/	3.0	168.8/	4.8	0.0/	6.0	9621.5/	6.9	9708.4/	7.8	13250.7/Infinity	3.1
1078	1.7/	1.0	1.6/	3.0	164.0/	4.8	0.0/	6.0	9101.2/	6.9	9157.6/	7.8	14230.3/Infinity	1.9
1079	1.7/	1.0	1.4/	3.0	164.0/	4.8	0.0/	6.0	9101.2/	6.9	9157.6/	7.8	14230.3/Infinity	5.7
1080	1.7/	1.0	1.6/	3.0	145.7/	4.8	0.2/	6.0	7768.2/	6.9	7452.0/	7.8	11029.4/Infinity	6.9
1081	1.7/	1.0	1.9/	3.0	147.6/	4.8	0.9/	6.0	7768.2/	6.9	7452.0/	7.8	11029.4/Infinity	5.8
1082	1.7/	1.0	2.0/	3.0	149.6/	4.8	1.2/	6.0	7768.2/	6.9	7452.0/	7.8	11029.4/Infinity	4.2
1083	1.8/	1.0	1.7/	3.0	202.6/	4.8	0.0/	6.0	9559.2/	6.9	9596.7/	7.8	13635.7/Infinity	3.0
1084	1.8/	1.0	2.5/	4.0	270.0/	4.0	0.0/	4.0	9546.8/	8.0	10043.4/	16.0	13174.1/Infinity	2.1
1085	1.8/	1.0	2.6/	4.0	311.0/	4.0	0.0/	4.0	9673.3/	8.0	10181.5/	16.0	12557.1/Infinity	2.7
1086	1.8/	1.0	2.5/	4.0	310.9/	4.0	0.0/	4.0	9673.3/	8.0	10181.5/	16.0	12557.1/Infinity	2.4
1087	1.8/	1.0	2.3/	4.0	310.9/	4.0	0.0/	4.0	9673.3/	8.0	10181.5/	16.0	12557.1/Infinity	2.8
1088	1.8/	1.0	1.9/	4.0	310.9/	4.0	0.0/	4.0	9673.3/	8.0	10181.5/	16.0	12557.1/Infinity	6.3
1089	1.7/	1.0	1.9/	4.0	153.1/	4.0	0.0/	4.0	8781.1/	8.0	8814.6/	16.0	17560.0/Infinity	10.0
1090	1.7/	1.0	3.5/	4.0	157.3/	4.0	0.5/	4.0	8781.1/	8.0	8814.6/	16.0	17560.0/Infinity	8.5
1091	1.7/	1.0	2.0/	2.2	481.4/	3.1	0.0/	4.0	99999.0/	5.2	99999.0/	7.0	99999.0/Infinity	5.3
1092	1.7/	1.0	1.8/	2.2	481.3/	3.1	0.0/	4.0	99999.0/	5.2	99999.0/	7.0	99999.0/Infinity	2.4

1093	1.77	1.0	1.67	2.2	440.77	3.1	0.07	4.0	99999.07	5.2	99999.07	7.0	99999.07/Infinity	3.0
1094	1.77	1.0	1.37	2.0	205.57	4.0	0.07	6.0	99999.17	8.0	99999.17	12.0	14017.0/Infinity	2.7
1095	1.77	1.0	2.07	4.0	137.47	4.0	0.07	4.0	0.07	8.0	0.07	16.0	0.07/Infinity	8.1
1096	1.77	1.0	1.97	4.0	126.57	4.0	1.47	4.0	0.07	8.0	0.87	16.0	0.07/Infinity	7.1
1097	1.77	1.0	2.07	4.0	185.67	4.0	11.77	4.0	0.07	8.0	30695.27	16.0	0.07/Infinity	2.5
1098	1.77	1.0	2.07	4.0	185.67	4.0	11.77	4.0	0.07	8.0	30695.27	16.0	0.07/Infinity	5.6
1099	1.77	1.0	2.37	4.0	161.17	4.0	0.77	4.0	0.07	8.0	30700.27	16.0	16.57/Infinity	7.8
1100	1.77	1.0	1.77	2.0	97.27	4.0	1.27	6.0	0.07	8.0	99999.07	12.0	25540.97/Infinity	4.4
1101	1.87	1.0	1.47	2.0	98.97	4.0	5.07	8.0	0.07	8.0	99999.07	12.0	25540.97/Infinity	3.2
1102	1.87	1.0	1.57	2.0	96.67	4.0	8.47	6.0	0.07	8.0	99999.07	12.0	25540.97/Infinity	6.5
1103	1.87	1.0	1.37	2.0	96.77	4.0	8.77	6.0	0.07	8.0	99999.07	12.0	25540.97/Infinity	4.6
1104	1.87	1.1	1.97	4.0	247.07	4.0	0.07	4.0	8740.17	8.0	8735.57	16.0	17241.77/Infinity	11.5
1105	1.87	1.2	1.07	2.0	9884.37	3.0	5152.17	5.0	0.07	8.0	17.87	12.0	3478.17/Infinity	8.9
1106	1.87	1.3	1.67	3.0	201.47	4.8	0.17	6.0	17.87	6.9	0.07	7.8	0.07/Infinity	7.4
1107	1.87	1.4	2.87	3.0	29.97	4.8	480.07	6.0	6000.07	6.9	6900.07	7.8	10000.07/Infinity	2.5
1108	1.87	1.4	2.77	3.0	11259.37	4.8	1371.97	6.0	36573.17	6.9	0.07	7.8	1391.57/Infinity	3.9
1109	1.87	1.4	2.07	2.0	3462.57	4.0	113.57	6.0	4773.97	8.0	15725.27	12.0	7711.87/Infinity	2.5
1110	1.87	1.4	2.07	2.0	29.57	4.0	480.07	6.0	6000.07	8.0	6900.07	12.0	10000.07/Infinity	1.7
1111	1.87	1.5	4.07	2.0	4.47	4.0	2489.47	6.0	4010.97	8.0	96.17	12.0	18948.37/Infinity	4.4
1112	1.87	1.5	5.87	4.0	4.07	4.0	2110.17	4.0	4982.87	8.0	4494.27	16.0	22766.27/Infinity	4.6
1113	1.87	1.5	1.47	3.0	10000.07	4.8	10000.07	6.0	10000.07	6.9	1000.07	7.8	999.87/Infinity	9.6
1114	1.87	1.5	1.57	3.0	32017.57	4.8	58909.57	6.0	99999.07	6.9	0.07	7.8	1183.57/Infinity	3.1
1115	1.87	1.5	1.57	3.0	99999.07	4.8	99033.57	6.0	0.07	6.9	32249.57	7.8	984.97/Infinity	5.4
1116	1.47	1.5	1.67	3.0	9998.57	4.8	9998.07	6.0	9998.97	6.9	994.27	7.8	967.37/Infinity	2.5
1117	1.47	1.5	0.97	2.0	50.57	4.0	480.47	6.0	6000.07	8.0	6900.07	12.0	10000.07/Infinity	5.7
1118	1.47	1.4	0.67	2.0	11718.07	3.0	5849.67	5.0	2712.57	8.0	0.07	12.0	6071.17/Infinity	6.1
1119	1.47	1.4	0.67	2.0	11718.07	3.0	5849.67	5.0	2712.57	8.0	0.07	12.0	6071.17/Infinity	8.9
1120	1.47	1.3	0.67	2.0	11718.07	3.0	5849.67	5.0	2712.57	8.0	0.07	12.0	6071.17/Infinity	11.8
1121	1.47	1.3	0.77	2.2	10000.07	3.1	10000.07	4.0	10000.07	5.2	1000.07	7.0	999.97/Infinity	13.5
1122	1.57	1.3	0.97	2.2	69272.47	3.1	99999.07	4.0	99999.07	5.2	0.07	7.0	803.97/Infinity	13.6
1123	1.57	1.2	1.07	2.0	22944.47	4.0	99999.07	6.0	99999.07	8.0	0.07	12.0	1283.47/Infinity	11.1
1124	1.57	1.2	1.17	2.0	22952.47	4.0	99999.07	6.0	99999.07	8.0	0.07	12.0	1283.17/Infinity	8.1
1125	1.57	1.2	2.37	4.0	280.97	4.0	0.07	4.0	9082.67	8.0	9139.97	16.0	15813.77/Infinity	5.7
1126	1.57	1.2	1.97	3.0	186.57	4.8	0.07	6.0	44829.87	6.9	34078.97	7.8	99999.07/Infinity	2.9
1127	1.47	1.2	2.37	4.0	10000.07	4.0	10000.07	4.0	10000.07	8.0	1000.07	16.0	999.97/Infinity	2.2
1128	1.47	1.2	2.37	4.0	10000.07	4.0	10000.07	4.0	10000.07	8.0	1000.07	16.0	999.97/Infinity	1.7
1129	1.47	1.2	1.17	2.0	1600.57	3.0	0.07	5.0	5882.37	8.0	4006.67	12.0	17409.87/Infinity	2.0
1130	1.47	1.2	1.17	2.0	1600.57	3.0	0.07	5.0	5882.37	8.0	4006.67	12.0	17409.87/Infinity	2.1
1131	1.47	1.4	1.77	2.2	46.07	3.1	480.27	4.0	6000.07	5.2	6900.07	7.0	10000.07/Infinity	1.6
1132	1.47	1.5	1.57	2.2	9901.07	3.1	9999.97	4.0	10118.57	5.2	0.07	7.0	1472.67/Infinity	2.8
1133	1.47	1.6	1.27	2.0	10095.77	4.0	10147.57	6.0	10408.37	8.0	2963.07	12.0	1127.97/Infinity	2.8
1134	1.47	1.6	1.97	4.0	21699.27	4.0	64606.57	4.0	99999.07	8.0	6664.47	16.0	909.57/Infinity	4.8
1135	1.47	1.6	0.67	2.2	10069.77	3.1	10371.27	4.0	8837.27	5.2	0.07	7.0	2460.17/Infinity	4.8
1136	1.47	1.5	0.77	3.0	10000.07	4.8	10000.07	6.0	10000.07	6.9	1000.07	7.8	1001.87/Infinity	8.1
1137	1.47	1.5	0.67	3.0	10000.07	4.8	10000.07	6.0	10000.07	6.9	1000.07	7.8	1001.87/Infinity	7.0
1138	1.47	1.5	0.47	2.0	174.57	4.0	0.17	6.0	17022.97	8.0	18159.47	12.0	0.07/Infinity	5.7
1139	1.27	1.5	0.57	2.0	255.77	4.0	0.57	6.0	17022.97	8.0	18159.47	12.0	0.97/Infinity	5.1

FID	Play1/	Tplay1	Play2/	Tplay2	Play3/	Tplay3	Play4/	Tplay4	Play5/	Tplay5	Play6/	Tplay6	Play7/Half	Spc Error
967	1.4/	6.3	0.1/	2.0	43.5/	2.0	37.4/	3.0	33.1/	5.0	0.0/	10.0	0.3/Infinity	112.0
968	1.4/	6.6	0.1/	2.0	40.0/	2.0	33.7/	3.0	29.1/	5.0	0.0/	10.0	0.0/Infinity	53.2
969	1.4/	5.8	0.1/	3.0	9.3/	3.0	19.9/	3.0	40.0/	5.0	80.1/	15.0	159.9/Infinity	51.0
970	1.4/	5.5	0.1/	2.0	7.2/	2.0	6.3/	3.0	11.4/	5.0	20.3/	10.0	21.4/Infinity	48.8
971	1.4/	5.0	0.1/	2.0	6.4/	2.0	8.3/	2.0	11.3/	2.0	13.3/	2.0	27.9/Infinity	40.3
972	1.4/	4.2	0.1/	2.0	6.4/	2.0	8.3/	2.0	11.3/	2.0	13.3/	2.0	27.9/Infinity	15.1
973	1.4/	4.3	0.1/	3.0	16.4/	3.0	0.0/	3.0	0.0/	5.0	216.0/	15.0	0.0/Infinity	12.0
974	1.4/	4.4	0.2/	3.0	16.3/	3.0	0.0/	3.0	0.0/	5.0	216.0/	15.0	0.0/Infinity	7.9
975	1.4/	4.6	0.2/	3.0	16.3/	3.0	0.0/	3.0	0.0/	5.0	216.0/	15.0	0.0/Infinity	13.0
976	1.4/	4.2	0.1/	2.0	1.1/	2.0	12.0/	2.0	31.4/	4.0	75.4/	8.0	156.1/Infinity	9.1
977	1.4/	3.4	0.1/	2.0	14.1/	2.0	7.4/	3.0	0.3/	5.0	111.3/	10.0	26.1/Infinity	3.4
978	1.4/	2.7	0.2/	2.0	14.1/	2.0	7.4/	3.0	0.4/	5.0	111.3/	10.0	26.1/Infinity	14.8
979	1.4/	2.5	0.6/	4.0	11.5/	4.0	0.3/	4.0	80.3/	4.0	105.2/	4.0	127.0/Infinity	26.2
980	1.4/	2.4	0.6/	4.0	11.4/	4.0	0.3/	4.0	80.3/	4.0	105.2/	4.0	127.0/Infinity	16.6
981	1.4/	2.0	0.6/	4.0	11.4/	4.0	0.3/	4.0	80.3/	4.0	105.2/	4.0	127.0/Infinity	14.2
982	1.4/	1.8	0.7/	4.0	11.2/	4.0	0.3/	4.0	80.3/	4.0	105.2/	4.0	127.0/Infinity	17.0
983	1.4/	1.5	1.0/	4.0	10.3/	4.0	0.5/	4.0	9.9/	4.0	31.4/	4.0	117.2/Infinity	14.4
984	1.4/	1.4	1.2/	4.0	33.7/	4.0	1.0/	4.0	8.4/	4.0	2.9/	4.0	125.3/Infinity	5.5
985	1.4/	1.5	0.8/	2.0	9.8/	2.0	20.1/	2.0	40.0/	2.0	80.0/	2.0	160.0/Infinity	5.7
986	1.4/	1.5	1.5/	4.0	9.8/	4.0	20.2/	4.0	40.1/	4.0	80.0/	4.0	160.1/Infinity	14.5
987	1.4/	1.5	2.3/	4.0	0.9/	4.0	10.9/	4.0	14.6/	4.0	16.1/	4.0	15.8/Infinity	18.7
988	1.4/	1.6	2.1/	4.0	0.8/	4.0	10.9/	4.0	14.6/	4.0	16.1/	4.0	16.2/Infinity	8.1
989	1.4/	1.6	2.8/	4.0	0.5/	4.0	16.6/	4.0	21.5/	4.0	20.3/	4.0	16.4/Infinity	8.6
990	1.4/	1.7	3.0/	4.0	0.4/	4.0	16.6/	4.0	21.5/	4.0	20.3/	4.0	16.4/Infinity	11.2
991	1.4/	1.7	3.5/	4.0	0.4/	4.0	16.6/	4.0	21.5/	4.0	20.3/	4.0	16.4/Infinity	17.3
992	1.4/	1.8	4.1/	4.0	0.4/	4.0	16.6/	4.0	21.5/	4.0	20.3/	4.0	16.3/Infinity	21.9
993	1.4/	1.8	0.4/	2.0	38.6/	2.0	0.0/	2.0	0.0/	4.0	0.0/	8.0	3528.7/Infinity	8.5
994	1.4/	1.9	0.4/	2.0	38.6/	2.0	0.0/	2.0	0.0/	4.0	0.0/	8.0	3528.7/Infinity	8.6
995	1.4/	1.9	0.4/	2.0	38.6/	2.0	0.0/	2.0	0.0/	4.0	0.0/	8.0	3528.7/Infinity	6.0
996	1.4/	2.0	0.4/	2.0	38.6/	2.0	0.0/	2.0	0.0/	4.0	0.0/	8.0	3528.7/Infinity	5.6
997	1.4/	2.0	0.4/	2.0	38.6/	2.0	0.0/	2.0	0.0/	4.0	0.0/	8.0	3528.7/Infinity	6.2
998	1.4/	2.0	0.3/	2.0	38.5/	2.0	0.0/	2.0	0.1/	4.0	0.0/	8.0	3528.7/Infinity	6.2
999	1.4/	1.9	0.3/	2.0	38.5/	2.0	0.0/	2.0	0.1/	4.0	0.0/	8.0	3528.7/Infinity	7.0
1000	1.4/	1.8	0.3/	2.0	38.5/	2.0	0.0/	2.0	0.1/	4.0	0.0/	8.0	3528.7/Infinity	7.4
1001	1.4/	1.7	0.3/	2.0	38.5/	2.0	0.0/	2.0	0.1/	4.0	0.0/	8.0	3528.7/Infinity	8.4
1002	1.4/	1.8	0.3/	2.0	38.5/	2.0	0.0/	2.0	0.1/	4.0	0.0/	8.0	3528.7/Infinity	9.0
1003	1.4/	1.7	0.3/	2.0	38.5/	2.0	0.1/	2.0	0.2/	4.0	0.2/	8.0	3528.7/Infinity	10.9
1004	1.4/	1.8	0.3/	2.0	38.5/	2.0	0.1/	2.0	0.2/	4.0	0.2/	8.0	3528.7/Infinity	13.3
1005	1.4/	1.8	0.3/	2.0	9.8/	2.0	19.7/	2.0	0.0/	4.0	0.0/	8.0	0.0/Infinity	8.4
1006	1.4/	1.9	0.4/	2.0	9.8/	2.0	19.7/	2.0	0.0/	4.0	0.3/	8.0	0.0/Infinity	14.8
1007	1.4/	1.8	0.3/	2.0	9.7/	2.0	20.5/	2.0	1.1/	4.0	1.1/	8.0	0.0/Infinity	11.7
1008	1.4/	1.7	0.8/	4.0	8.8/	4.0	11.9/	4.0	12.7/	4.0	12.4/	4.0	13.2/Infinity	4.0
1009	1.4/	1.6	0.8/	4.0	12.7/	4.0	24.9/	4.0	41.1/	4.0	79.7/	4.0	158.1/Infinity	5.1
1010	1.4/	1.5	1.5/	4.0	2.3/	4.0	43.1/	4.0	33.7/	4.0	75.8/	4.0	149.1/Infinity	2.4
1011	1.4/	1.4	1.5/	4.0	6.7/	4.0	10.4/	4.0	18.2/	4.0	20.2/	4.0	13.0/Infinity	5.1
1012	1.4/	2.2	4.4/	4.0	2.8/	4.0	3.6/	4.0	11.7/	4.0	30.0/	4.0	9.8/Infinity	5.3
1013	1.4/	3.9	13.0/	4.0	1.7/	4.0	5.3/	4.0	21.3/	4.0	0.0/	4.0	0.0/Infinity	3.0
1014	1.4/	3.2	3.8/	4.0	1.5/	4.0	30.0/	4.0	39.6/	4.0	0.0/	4.0	11.1/Infinity	3.9
1015	1.4/	2.8	0.4/	3.0	86.4/	3.0	239.0/	3.0	0.0/	5.0	0.0/	15.0	0.0/Infinity	7.8
1016	1.4/	1.3	0.3/	4.0	9.8/	4.0	20.1/	4.0	40.1/	4.0	80.0/	4.0	160.0/Infinity	21.1
1017	1.4/	1.2	0.3/	4.0	6.7/	4.0	9.4/	4.0	10.4/	4.0	10.7/	4.0	15.9/Infinity	16.9
1018	1.4/	1.1	0.9/	4.0	0.5/	4.0	17.4/	4.0	20.1/	4.0	21.8/	4.0	24.4/Infinity	20.8
1019	1.4/	1.0	6.5/	4.0	0.6/	4.0	6.9/	4.0	38.3/	4.0	0.0/	4.0	82.1/Infinity	16.9
1020	1.4/	1.8	15.1/	2.0	12.3/	2.0	4.4/	2.0	7.7/	4.0	6.0/	8.0	18.4/Infinity	12.1
1021	1.4/	1.2	3.7/	2.0	9.4/	2.0	31.9/	2.0	4.9/	4.0	111.5/	8.0	70.8/Infinity	13.9
1022	1.4/	1.1	1.7/	4.0	4.1/	4.0	19.0/	4.0	39.9/	4.0	80.2/	4.0	161.6/Infinity	3.3
1023	1.4/	1.0	0.6/	4.0	9.7/	4.0	20.2/	4.0	40.1/	4.0	80.0/	4.0	160.1/Infinity	14.8
1024	1.4/	1.0	0.4/	4.0	9.6/	4.0	20.2/	4.0	40.1/	4.0	80.0/	4.0	160.1/Infinity	21.6
1025	1.4/	1.0	0.4/	2.0	3.7/	2.0	5.7/	3.0	8.6/	5.0	10.9/	10.0	13.8/Infinity	16.8
1026	1.4/	1.0	1.8/	4.0	6.0/	4.0	9.0/	4.0	10.1/	4.0	10.6/	4.0	12.1/Infinity	18.8

1027	1.4/	1.0	6.0/	4.0	8.5/	4.0	8.9/	4.0	9.3/	4.0	9.2/	4.0	9.9/Infinity	14.4
1028	1.4/	1.0	2.2/	2.0	23.1/	2.0	63.6/	2.0	57.1/	2.0	32.0/	2.0	61.0/Infinity	7.3
1029	1.4/	1.0	3.7/	2.0	11.7/	2.0	21.1/	2.0	40.6/	2.0	80.3/	2.0	160.1/Infinity	2.9
1030	1.4/	1.0	3.6/	2.0	8.0/	2.0	25.5/	2.0	43.5/	2.0	82.4/	2.0	160.0/Infinity	2.5
1031	1.4/	1.0	2.9/	2.0	7.7/	2.0	26.2/	2.0	44.0/	2.0	82.5/	2.0	159.4/Infinity	2.2
1032	1.4/	1.0	6.5/	4.0	7.4/	4.0	20.4/	4.0	40.4/	4.0	80.1/	4.0	159.3/Infinity	4.3
1033	1.4/	1.0	6.3/	4.0	4.0/	4.0	20.8/	4.0	41.3/	4.0	80.8/	4.0	163.0/Infinity	7.5
1034	1.4/	1.0	5.6/	4.0	3.3/	4.0	21.8/	4.0	42.0/	4.0	81.1/	4.0	164.0/Infinity	7.8
1035	1.4/	1.0	4.8/	4.0	2.4/	4.0	25.4/	4.0	45.5/	4.0	83.0/	4.0	167.4/Infinity	8.2
1036	1.4/	1.0	4.4/	4.0	1.6/	4.0	31.3/	4.0	52.2/	4.0	86.7/	4.0	172.0/Infinity	9.0
1037	1.4/	1.0	4.6/	4.0	2.8/	4.0	7.3/	4.0	9.6/	4.0	10.7/	4.0	12.9/Infinity	6.7
1038	1.4/	1.0	5.4/	4.0	2.3/	4.0	7.1/	4.0	9.5/	4.0	10.6/	4.0	13.2/Infinity	10.0
1039	1.4/	1.0	6.1/	4.0	1.3/	4.0	7.0/	4.0	9.4/	4.0	10.6/	4.0	13.9/Infinity	14.4
1040	1.4/	1.0	5.6/	4.0	1.0/	4.0	2.9/	4.0	7.2/	4.0	13.5/	4.0	12.0/Infinity	11.3
1041	1.5/	1.0	5.6/	4.0	0.9/	4.0	2.9/	4.0	7.2/	4.0	13.5/	4.0	12.1/Infinity	13.6
1042	1.5/	1.0	4.3/	4.0	1.0/	4.0	1.5/	4.0	5.1/	4.0	32.3/	4.0	11.3/Infinity	12.6
1043	1.5/	1.0	4.3/	4.0	0.8/	4.0	2.0/	4.0	5.3/	4.0	32.4/	4.0	10.7/Infinity	13.1
1044	1.5/	1.0	4.4/	4.0	0.8/	4.0	2.0/	4.0	5.3/	4.0	32.4/	4.0	10.7/Infinity	10.9
1045	1.5/	1.0	4.2/	4.0	0.6/	4.0	3.1/	4.0	5.4/	4.0	32.9/	4.0	10.8/Infinity	14.0
1046	1.5/	1.0	4.2/	4.0	0.6/	4.0	3.1/	4.0	5.4/	4.0	32.9/	4.0	10.8/Infinity	9.5
1047	1.7/	1.0	4.8/	4.0	0.7/	4.0	3.1/	4.0	5.4/	4.0	32.8/	4.0	10.4/Infinity	16.4
1048	1.7/	1.0	1.1/	4.0	4.9/	4.0	6.3/	4.0	9.4/	4.0	12.0/	4.0	12.4/Infinity	11.9
1049	1.7/	1.0	0.8/	3.0	80.0/	3.0	50.2/	3.0	0.0/	5.0	2.8/	15.0	0.0/Infinity	3.3
1050	1.8/	1.0	0.6/	2.0	36.4/	2.0	53.4/	2.0	64.4/	2.0	66.6/	2.0	81.4/Infinity	2.1
1051	1.8/	1.0	1.3/	3.0	6.0/	3.0	19.0/	3.0	40.0/	5.0	80.9/	15.0	160.3/Infinity	3.7
1052	1.8/	1.0	1.4/	4.0	51.7/	4.0	64.2/	4.0	62.8/	4.0	58.8/	4.0	65.7/Infinity	3.9
1053	1.8/	1.0	0.8/	2.0	6.3/	2.0	18.2/	2.0	39.6/	2.0	80.0/	2.0	161.6/Infinity	2.0
1054	1.8/	1.0	1.0/	2.0	3.6/	2.0	19.9/	2.0	40.5/	2.0	80.7/	2.0	163.2/Infinity	2.3
1055	2.0/	1.0	0.9/	2.0	9.5/	2.0	19.9/	2.0	40.0/	2.0	80.0/	2.0	160.3/Infinity	1.8
1056	2.0/	1.0	1.1/	2.0	9.4/	2.0	19.9/	2.0	40.0/	2.0	80.0/	2.0	160.3/Infinity	2.2
1057	2.0/	1.0	1.3/	2.0	8.6/	2.0	44.8/	2.0	34.8/	2.0	66.6/	2.0	159.6/Infinity	2.7
1058	1.9/	1.0	1.3/	2.0	1930.2/	2.0	90.2/	2.0	0.0/	2.0	0.0/	2.0	0.0/Infinity	5.0
1059	1.9/	1.0	1.6/	2.0	1925.5/	2.0	92.2/	2.0	0.0/	2.0	0.0/	2.0	3.0/Infinity	8.1
1060	1.9/	1.0	5.2/	2.0	3.1/	2.0	12.9/	2.0	44.2/	2.0	136.0/	2.0	153.2/Infinity	6.4
1061	1.9/	1.0	2.7/	2.0	5.4/	2.0	37.5/	2.0	55.3/	2.0	66.0/	2.0	63.8/Infinity	3.4
1062	1.9/	1.0	2.1/	2.0	35.8/	2.0	56.4/	3.0	66.4/	5.0	59.6/	10.0	56.2/Infinity	2.3
1063	1.9/	1.0	2.7/	2.0	7.0/	2.0	19.0/	2.0	39.9/	2.0	80.1/	2.0	161.4/Infinity	2.7
1064	1.9/	1.0	1.5/	2.0	8.8/	2.0	38.0/	2.0	52.8/	2.0	79.3/	2.0	156.8/Infinity	3.1
1065	1.7/	1.0	3.7/	4.0	5.2/	4.0	29.5/	4.0	45.5/	4.0	82.4/	4.0	162.9/Infinity	4.0
1066	1.7/	1.0	2.4/	4.0	12.9/	4.0	33.7/	4.0	58.2/	4.0	91.3/	4.0	61.1/Infinity	6.3
1067	1.7/	1.0	1.3/	3.0	9.5/	3.0	20.0/	3.0	40.2/	5.0	80.2/	15.0	160.2/Infinity	2.7
1068	1.7/	1.0	2.6/	3.0	2.0/	3.0	16.2/	3.0	39.2/	5.0	84.1/	15.0	162.3/Infinity	11.5
1069	1.7/	1.0	3.6/	3.0	7.4/	3.0	9.5/	3.0	9.5/	5.0	8.2/	15.0	9.3/Infinity	13.0
1070	1.7/	1.0	8.1/	3.0	1.5/	3.0	230.4/	3.0	0.0/	5.0	790.2/	15.0	10000.0/Infinity	11.5
1071	1.7/	1.0	8.1/	3.0	1.5/	3.0	230.4/	3.0	0.0/	5.0	790.2/	15.0	10000.0/Infinity	10.5
1072	1.7/	1.0	3.6/	4.0	11.7/	4.0	14.7/	4.0	54.7/	4.0	94.8/	4.0	67.0/Infinity	10.1
1073	1.7/	1.0	2.2/	2.0	8.0/	2.0	24.6/	2.0	8.1/	4.0	91.7/	8.0	73.1/Infinity	9.9
1074	1.7/	1.0	2.4/	3.0	24.4/	3.0	52.9/	3.0	42.2/	5.0	71.2/	15.0	56.7/Infinity	6.6
1075	1.7/	1.0	2.5/	3.0	24.4/	3.0	52.9/	3.0	42.2/	5.0	71.2/	15.0	56.7/Infinity	4.0
1076	1.7/	1.0	2.2/	3.0	17.4/	3.0	52.6/	3.0	37.5/	5.0	78.0/	15.0	57.5/Infinity	5.0
1077	1.7/	1.0	2.2/	3.0	17.4/	3.0	52.6/	3.0	37.5/	5.0	78.0/	15.0	57.5/Infinity	5.4
1078	1.7/	1.0	2.6/	4.0	17.5/	4.0	37.5/	4.0	58.0/	4.0	82.5/	4.0	65.3/Infinity	4.7
1079	1.7/	1.0	4.3/	4.0	4.2/	4.0	26.7/	4.0	44.1/	4.0	82.3/	4.0	165.2/Infinity	4.7
1080	1.7/	1.0	4.5/	4.0	3.8/	4.0	26.7/	4.0	44.1/	4.0	82.3/	4.0	165.2/Infinity	8.7
1081	1.7/	1.0	3.4/	4.0	7.0/	4.0	31.3/	4.0	61.8/	4.0	97.8/	4.0	72.5/Infinity	8.1
1082	1.7/	1.0	3.4/	4.0	9.4/	4.0	25.1/	4.0	54.6/	4.0	96.8/	4.0	69.0/Infinity	6.4
1083	1.8/	1.0	2.7/	4.0	31.0/	4.0	54.5/	4.0	61.1/	4.0	74.6/	4.0	63.9/Infinity	3.7
1084	1.8/	1.0	2.5/	3.0	13.9/	3.0	35.0/	3.0	41.7/	5.0	74.9/	15.0	55.1/Infinity	3.6
1085	1.8/	1.0	1.7/	2.0	11.9/	2.0	40.2/	2.0	36.0/	2.0	59.0/	2.0	68.2/Infinity	3.3
1086	1.8/	1.0	1.4/	2.0	36.1/	2.0	55.3/	2.0	66.3/	2.0	67.5/	2.0	65.0/Infinity	2.5
1087	1.8/	1.0	1.3/	2.0	35.9/	2.0	55.1/	2.0	66.3/	2.0	68.4/	2.0	65.1/Infinity	1.9
1088	1.8/	1.0	3.5/	4.0	5.5/	4.0	29.0/	4.0	45.8/	4.0	83.4/	4.0	164.7/Infinity	4.6
1089	1.7/	1.0	5.8/	4.0	2.5/	4.0	28.9/	4.0	45.8/	4.0	83.4/	4.0	164.9/Infinity	10.7
1090	1.7/	1.0	4.4/	3.0	15.2/	3.0	11.0/	3.0	7.4/	5.0	137.2/	15.0	66.9/Infinity	14.1
1091	1.7/	1.0	2.0/	2.0	39.6/	2.0	57.5/	2.0	70.0/	4.0	63.2/	8.0	60.8/Infinity	6.0
1092	1.7/	1.0	2.7/	2.0	7.2/	2.0	18.7/	2.0	39.7/	2.0	80.0/	2.0	161.5/Infinity	2.6

1093	1.77/	1.0	2.57/	3.0	42.37/	3.0	54.97/	3.0	59.37/	5.0	64.47/	15.0	56.47/Infinity	3.5
1094	1.77/	1.0	2.57/	3.0	19.97/	3.0	26.07/	3.0	29.17/	5.0	95.87/	15.0	57.77/Infinity	5.3
1095	1.77/	1.0	5.47/	4.0	2.87/	4.0	21.87/	4.0	41.97/	4.0	81.17/	4.0	165.07/Infinity	11.5
1096	1.77/	1.0	4.97/	4.0	2.97/	4.0	21.67/	4.0	41.87/	4.0	81.17/	4.0	165.87/Infinity	12.9
1097	1.77/	1.0	1.17/	2.0	36.57/	2.0	56.97/	2.0	69.87/	2.0	71.27/	2.0	68.37/Infinity	3.0
1098	1.77/	1.0	4.27/	4.0	4.47/	4.0	27.07/	4.0	44.27/	4.0	82.17/	4.0	164.37/Infinity	3.5
1099	1.77/	1.0	6.27/	4.0	3.67/	4.0	21.27/	4.0	41.57/	4.0	80.97/	4.0	163.67/Infinity	8.9
1100	1.77/	1.0	6.97/	3.0	9.57/	3.0	10.77/	3.0	10.67/	5.0	10.37/	15.0	6.87/Infinity	13.2
1101	1.87/	1.0	6.37/	4.0	3.67/	4.0	19.77/	4.0	41.07/	4.0	80.87/	4.0	164.57/Infinity	12.5
1102	1.87/	1.0	8.27/	4.0	3.17/	4.0	17.47/	4.0	42.87/	4.0	81.97/	4.0	165.27/Infinity	13.4
1103	1.87/	1.0	8.27/	4.0	3.07/	4.0	17.47/	4.0	42.87/	4.0	81.97/	4.0	165.27/Infinity	12.8
1104	1.87/	1.1	6.47/	4.0	2.67/	4.0	18.17/	4.0	43.17/	4.0	82.07/	4.0	165.67/Infinity	6.9
1105	1.87/	1.2	4.57/	4.0	4.37/	4.0	31.57/	4.0	46.97/	4.0	83.07/	4.0	162.47/Infinity	4.8
1106	1.87/	1.3	2.27/	2.0	8.27/	2.0	12.67/	2.0	9.27/	4.0	57.97/	8.0	62.67/Infinity	7.4
1107	1.87/	1.4	1.97/	2.0	18.07/	2.0	37.57/	2.0	37.37/	2.0	66.07/	2.0	159.07/Infinity	5.1
1108	1.87/	1.4	2.37/	2.0	18.07/	2.0	37.57/	2.0	37.37/	2.0	66.07/	2.0	158.97/Infinity	4.0
1109	1.87/	1.4	2.77/	2.0	8.67/	2.0	167.87/	3.0	66.77/	5.0	77.37/	10.0	161.67/Infinity	3.3
1110	1.87/	1.4	2.57/	3.0	1204.07/	3.0	212.27/	3.0	69.97/	5.0	54.67/	15.0	51.97/Infinity	5.0
1111	1.87/	1.5	1.87/	3.0	309.47/	3.0	1387.37/	3.0	79.87/	5.0	19.77/	15.0	49.37/Infinity	6.4
1112	1.87/	1.5	1.47/	3.0	150.37/	3.0	1238.27/	3.0	0.07/	5.0	6.57/	15.0	44.27/Infinity	5.0
1113	1.87/	1.5	4.37/	4.0	3.77/	4.0	23.97/	4.0	43.07/	4.0	81.57/	4.0	164.67/Infinity	5.1
1114	1.87/	1.5	1.67/	2.0	4.07/	2.0	18.17/	2.0	38.87/	4.0	79.17/	8.0	160.67/Infinity	2.5
1115	1.87/	1.5	1.97/	2.0	3.17/	2.0	31.77/	2.0	36.17/	2.0	30.17/	2.0	63.27/Infinity	3.0
1116	1.47/	1.5	1.37/	2.0	8.67/	2.0	19.57/	2.0	39.97/	2.0	79.97/	2.0	160.17/Infinity	2.9
1117	1.47/	1.5	1.17/	3.0	312.57/	3.0	186.17/	3.0	0.17/	5.0	240.37/	15.0	0.17/Infinity	7.1
1118	1.47/	1.4	0.77/	2.0	9.47/	2.0	20.07/	3.0	40.27/	5.0	80.27/	10.0	160.17/Infinity	5.3
1119	1.47/	1.4	3.27/	4.0	1.77/	4.0	34.47/	4.0	52.97/	4.0	83.37/	4.0	151.47/Infinity	5.8
1120	1.47/	1.3	0.97/	2.0	5.07/	2.0	10.77/	2.0	14.07/	2.0	18.47/	2.0	12.77/Infinity	4.7
1121	1.47/	1.3	1.57/	2.0	2.37/	2.0	10.17/	2.0	14.37/	2.0	19.27/	2.0	12.97/Infinity	3.9
1122	1.57/	1.3	2.17/	2.0	6.37/	2.0	8.67/	2.0	9.67/	2.0	10.07/	2.0	10.07/Infinity	8.7
1123	1.57/	1.2	5.17/	4.0	3.67/	4.0	20.47/	4.0	41.07/	4.0	80.97/	4.0	164.77/Infinity	6.1
1124	1.57/	1.2	2.77/	2.0	3.87/	2.0	8.77/	3.0	31.67/	5.0	83.27/	10.0	169.17/Infinity	5.6
1125	1.57/	1.2	4.67/	3.0	4.37/	3.0	22.47/	3.0	39.27/	5.0	85.07/	15.0	161.57/Infinity	3.2
1126	1.57/	1.2	2.87/	4.0	51.27/	4.0	55.07/	4.0	12.27/	4.0	178.27/	4.0	57.87/Infinity	5.1
1127	1.47/	1.2	1.67/	2.0	5.87/	2.0	26.97/	2.0	46.07/	2.0	82.27/	2.0	159.17/Infinity	3.1
1128	1.47/	1.2	1.67/	2.0	5.87/	2.0	26.97/	2.0	46.07/	2.0	82.27/	2.0	159.17/Infinity	2.4
1129	1.47/	1.2	1.97/	2.0	4.87/	2.0	27.07/	2.0	45.87/	2.0	82.87/	2.0	158.67/Infinity	3.4
1130	1.47/	1.2	1.77/	2.0	5.47/	2.0	22.57/	2.0	47.27/	2.0	84.37/	2.0	159.67/Infinity	3.3
1131	1.47/	1.4	1.27/	2.0	649.87/	2.0	317.87/	3.0	0.07/	5.0	0.07/	10.0	0.07/Infinity	3.9
1132	1.47/	1.5	1.27/	2.0	649.87/	2.0	317.87/	3.0	0.07/	5.0	0.07/	10.0	0.07/Infinity	3.1
1133	1.47/	1.6	1.67/	2.0	10.87/	2.0	21.37/	2.0	41.07/	4.0	81.37/	8.0	160.27/Infinity	2.1
1134	1.47/	1.6	1.77/	2.0	3.27/	2.0	15.97/	3.0	38.07/	5.0	80.57/	10.0	161.47/Infinity	2.9
1135	1.47/	1.6	1.17/	4.0	600.17/	4.0	565.57/	4.0	69.47/	4.0	0.07/	4.0	57.37/Infinity	4.2
1136	1.47/	1.5	2.57/	4.0	1.37/	4.0	36.77/	4.0	57.97/	4.0	83.17/	4.0	142.57/Infinity	7.0
1137	1.47/	1.5	0.97/	3.0	3.07/	3.0	13.77/	3.0	19.77/	5.0	13.27/	15.0	11.37/Infinity	3.3
1138	1.47/	1.5	1.87/	4.0	1.87/	4.0	27.17/	4.0	46.57/	4.0	82.47/	4.0	159.27/Infinity	3.4
1139	1.27/	1.5	1.37/	4.0	9.57/	4.0	20.17/	4.0	40.27/	4.0	80.17/	4.0	160.27/Infinity	2.8
1140	1.27/	1.4	1.67/	4.0	9.47/	4.0	20.17/	4.0	40.27/	4.0	80.17/	4.0	160.27/Infinity	2.0
1141	1.27/	1.4	2.17/	4.0	9.27/	4.0	20.07/	4.0	40.27/	4.0	80.17/	4.0	160.27/Infinity	2.8
1142	1.27/	1.4	1.27/	2.0	5.47/	2.0	16.37/	3.0	38.37/	5.0	80.77/	10.0	161.37/Infinity	2.2
1143	1.27/	1.4	1.07/	2.0	9.87/	2.0	20.17/	2.0	40.07/	2.0	80.07/	2.0	160.17/Infinity	3.7
1144	1.27/	1.4	0.97/	2.0	9.57/	2.0	19.97/	2.0	40.07/	2.0	80.07/	2.0	160.17/Infinity	3.3
1145	1.27/	1.4	0.87/	2.0	9.17/	2.0	19.77/	2.0	40.07/	2.0	80.07/	2.0	160.17/Infinity	2.5
1146	1.27/	1.3	1.37/	4.0	10.57/	4.0	20.77/	4.0	40.37/	4.0	80.17/	4.0	160.07/Infinity	1.3

APPENDIX B

Table B-1: Eleven inversions with ResixIP at fids selected in Table III of report.

Line 10D - 10 m Dipoles

<u>Fid 976</u>		ResixIP (7 layer) (5.4%)		ResixIP (3 layer) (8.3%)	
Layer	Thick (m)	Resistivity (ohm-m)	Thick. (m)	Resistivity (ohm-m)	
1	4.2	1.4	4.2	1.4	
2	2.0	0.1	0.1 - 3.4	0.0 - 0.2	
3	3.0	13.6k		2.6 - 6.5	
4	5.0	12.8k			
5	8.0	15M			
6	12.0	21.0			
7		11.4			

<u>Fid 985</u>		ResixIP (7 layer) (5.1%)		ResixIP (3 layer) (1.7%)	
Layer	Thick (m)	Resistivity (ohm-m)	Thick. (m)	Resistivity (ohm-m)	
1	1.5	1.5	1.5	1.5	
2	2.0	0.8	9.2 - 9.7	4.1 - 4.4	
3	3.0	39.6		17.8k - 19.2k	
4	5.0	333.0			
5	8.0	1055			
6	12.0	1180			
7		3.9k			

<u>Fid 1012</u>		ResixIP (7 layer) (21.7%)		ResixIP (3 layer) (1.7%)	
Layer	Thick (m)	Resistivity (ohm-m)	Thick. (m)	Resistivity (ohm-m)	
1	2.2	1.4	2.2	1.4	
2	2.0	0.7	21.2 - 22.3	5.9 - 6.1	
3	3.0	70.5		11.4k - 13.0k	
4	5.0	385			
5	8.0	606			
6	12.0	857			
7		1210			

Fid 1029ResixIP (7 layer)
(1.3%)

Layer	Thick (m)	Resistivity (ohm-m)
1	1.0	1.4
2	2.0	2.4
3	3.0	81.7
4	5.0	488
5	8.0	671
6	12.0	848
7		5.17k

ResixIP (3 layer)
(3.6%)

Thick (m)	Resistivity (ohm-m)
1.0	1.4
13.3 - 16.3	17.6 - 25.3
	45k - 73k

Fid 1044ResixIP (7 layer)
(36.2%)

Layer	Thick (m)	Resistivity (ohm-m)
1	1.0	1.5
2	2.0	0.2
3	3.0	57.7
4	5.0	424
5	8.0	686
6	12.0	1020
7		891

ResixIP (3 layer)
(3.6%)

Thick. (m)	Resistivity (ohm-m)
1.0	1.5
21.2 - 23.2	3.0 - 3.6
	12k - 23.6k

Fid 1059ResixIP (7 layer)
(6.6%)

Layer	Thick (m)	Resistivity (ohm-m)
1	1.0	1.9
2	2.0	1.8
3	3.0	4.42k
4	5.0	0.3
5	8.0	11.6k
6	12.0	24.4
7		18.3k

ResixIP (3 layer)
(4.3%)

Thick. (m)	Resistivity (ohm-m)
1.0	1.9
10.2 - 11.7	13.9 - 16.8
	77.2k - 100k

Fid 1084ResixIP (7 layer)
(1.3%)

Layer	Thick (m)	Resistivity (ohm-m)
1	1.0	1.8
2	2.0	1.5
3	3.0	39.5
4	5.0	159
5	8.0	7.7
6	12.0	36.8
7		6.54k

ResixIP (3 layer)
(6.4%)

Thick. (m)	Resistivity (ohm-m)
1.0	1.8
4.6 - 9.0	2.8 - 5.6
	95.9 - 10.7k

Fid 1137

ResixIP (7 layer)

(1.1%)

Layer	Thick (m)	Resistivity (ohm-m)
1	1.5	1.4
2	2.0	0.6
3	3.0	10.5
4	5.0	7.3
5	8.0	12.0
6	12.0	309
7		333

ResixIP (3 layer)

(5.3%)

Thick. (m)	Resistivity (ohm-m)
1.5	1.4
9.2 - 12.4	1.9 - 2.8
	3.0k - 9.5k

Fid 1164

ResixIP (7 layer)

(392%)

Layer	Thick (m)	Resistivity (ohm-m)
1	1.6	1.5
2	2.0	10
3	3.0	100
4	5.0	500
5	8.0	750
6	12.0	1000
7		5000

ResixIP (3 layer)

(5.9%)

Thick. (m)	Resistivity (ohm-m)
1.6	1.5
25.5 - 31.5	3.9 - 4.3
	6.9k - 15.4k

Fid 1185

ResixIP (7 layer)

(23.4%)

Layer	Thick (m)	Resistivity (ohm-m)
1	1.7	1.6
2	2.0	0.5
3	3.0	65.8
4	5.0	346
5	8.0	562
6	12.0	861
7		1120

ResixIP (3 layer)

(3.1%)

Thick. (m)	Resistivity (ohm-m)
1.7	1.6
19.0 - 20.8	4.5 - 5.7
	15.9k - 28.7k

Fid 1192

ResixIP (7 layer)

(415%)

Layer	Thick (m)	Resistivity (ohm-m)
1	1.8	1.4
2	2.0	10
3	3.0	100
4	5.0	50
5	8.0	750
6	12.0	1000
7		5000

ResixIP (3 layer)

(5.7%)

Thick. (m)	Resistivity (ohm-m)
1.8	1.4
24.9 - 32.5	2.5 - 3.2
	2.3k - 10.0k

Table B-2: Eight inversions with ResixIP, using as starting models the final model from the inversions of Test 3. The three-layer models for these fids are shown in Table B-1 above.

Line 10D - 10 m Dipoles

Fid 976

Layer (error)	Thick.	Davis (24.2%) Resistivity	ResixIP (7layer) (9.9%) Resistivity
1	4.2	1.4	1.4
2	2.0	0.9	0.1 - 0.2
3	3.0	0.2	0.3 - 1.0
4	5.0	1.9	1.2 - 39.0
5	8.0	3.9	1.6 - 49.7
6	12.0	10.2	0.9 - 86.0
7		100.0	1.0 - 1024

Fid 985

Layer (error)	Thick.	Davis (14.5%) Resistivity	ResixIP (7layer) (6.6%) Resistivity
1	1.5	1.5	1.5
2	2.2	0.7	0.9
3	3.1	129	412
4	4.0	1.5	1.6
5	5.2	0.0	12.1
6	7.0	0.0	6.0
7		10.0k	7.0k

Fid 1012

Layer (error)	Thick.	Davis (12.1%) Resistivity	ResixIP (7layer) (1.5%) Resistivity
1	2.2	1.4	1.4
2	2.0	1.0	1.6 - 4.3
3	4.0	3.8	3.3 - 10.7
4	6.0	40.3	3.2 - 11.6
5	8.0	0.0	3.5 - 9.7
6	10.0	10.0k	1.1k - 1.1M
7		10.0k	873 - 8.7k

Fid 1029

Layer (error)	Thick.	Davis (13.4%) Resistivity	ResixIP (7layer) (1.5%) Resistivity
1	1.0	1.4	1.4
2	3.0	4.0	3.0 - 3.8
3	4.8	165.1	759 - 8.6k
4	6.0	0.0	16.7 - 4.2k
5	6.9	0.0	27.8 - 27.8k
6	7.8	0.0	7.7 - 7.7k
7		10.0k	37.7 - 17.9k

Fid 1044

Layer (error)	Thick.	Davis (24.7%) Resistivity	ResixIP (7layer) (29.9%) Resistivity
1	1.0	1.5	1.5
2	2.2	0.3	0.3
3	3.1	10.0k	5.4M
4	4.0	10.0k	10.3M
5	5.2	9.9k	10.7M
6	7.0	1.9	37.3
7		0.1	0.0002

Fid 1059

Layer (error)	Thick.	Davis (8.0%) Resistivity	ResixIP (7layer) (7.8%) Resistivity
1	1.0	1.9	1.9
2	2.2	1.9	1.6 - 2.0
3	3.1	10.0k	203 - 20.3k
4	4.0	10.0k	457 - 13.4k
5	5.2	10.0k	4.6 - 4.6k
6	7.0	56.7	1.0 - 976
7		12.6	5.9 - 74.7

Fid 1084

Layer (error)	Thick.	Davis (6.8%) Resistivity	ResixIP (7layer) (6.9%) Resistivity
1	1.0	1.8	1.8
2	4.0	2.5	2.3 - 2.9
3	4.0	10.0k	28.5 - 112k
4	4.0	10.0k	9.2k - 113k
5	8.0	10.0k	22.0 - 23.8k
6	16.0	0.1	0 - 2.1
7		10.0k	9.4k - 107k

Fid 1137Layer
(error)

Thick.

Davis
(6.7%)

Resistivity

ResixIP (7layer)
(2.6%)

Resistivity

1	1.5	1.4	1.4
2	2.2	0.5	0.4
3	3.1	9.8k	10.0M
4	4.0	10.0k	14.0k - 1.5M
5	5.2	9.2k	11.1M
6	7.0	0.0	0.1 - 72.1
7		10.0k	0.0 - 11.1

Table B-3: Eight inversions with ResixIP, using as starting models the final model from the inversions of Test 4a. The three-layer models for these fids are shown in Table B-1 above.

Line 10D - 10 m Dipoles

Fid 976

Layer (error)	Thick.	Davis (10.0%) Resistivity	ResixIP (7layer) (10.7%) Resistivity
1	4.2	1.4	1.4
2	4.0	0.2	0.2
3	4.0	10.1k	10k
4	4.0	9.4k	9.4k
5	8.0	9.0k	9.0k
6	16.0	0.0	0.0
7		0.0	0.0

Fid 985

Layer (error)	Thick.	Davis (5.2%) Resistivity	ResixIP (7layer) (5.1%) Resistivity
1	1.5	1.5	1.5
2	3.0	1.1	1.0 - 1.1
3	4.8	6.2k	43.9 - 47k
4	6.0	10.5k	4.0k - 66k
5	6.9	0.0	0.0 - 15.5
6	7.8	0.0	0.0 - 15.5
7		2.8k	15.5 - 3.0k

Fid 1012

Layer (error)	Thick.	Davis (16.1%) Resistivity	ResixIP (7layer) (11.0%) Resistivity
1	2.2	1.4	1.4
2	4.0	1.2	1.4 - 1.7
3	4.0	54.2	45.9 - 63.8
4	4.0	0.0	0.0 - 0.1
5	8.0	7.9k	7.9k - 79k
6	16.0	7.3k	40.3 - 7.6k
7		18k	40.3 - 10.3k

Fid 1029

Layer (error)	Thick.	Davis (1.6%) Resistivity	ResixIP (7layer) (1.4%) Resistivity
1	1.0	1.4	1.4
2	2.0	2.2	2.2 - 2.3
3	3.0	10.3k	1k - 101k
4	5.0	10.6k	9.2k - 100k
5	8.0	11.4k	102 - 102k
6	12.0	4.7k	47.5 - 47.5k
7		1.16k	121 - 3.8k

Fid 1044

Layer (error)	Thick.	Davis (25.3%) Resistivity	ResixIP (7layer) (35.9%) Resistivity
1	1.0	1.5	1.5
2	4.0	0.6	0.5 - 0.7
3	4.0	10k	101 - 101k
4	4.0	10k	101 - 101k
5	8.0	10k	101 - 101k
6	16.0	1000	757 - 10k
7		1000	11.9 - 4.4k

Fid 1059

Layer (error)	Thick.	Davis (6.5%) Resistivity	ResixIP (7layer) (5.8%) Resistivity
1	1.0	1.9	1.9
2	2.0	3.2	3.7 - 8.8
3	3.0	9.8k	3.6 - 5.3
4	5.0	9.6k	7.9k - 348k
5	8.0	9.3k	258 - 3.4k
6	12.0	0.0	110 - 12k
7		1.1k	16k - 28k

Fid 1084

Layer (error)	Thick.	Davis (2.1%) Resistivity	ResixIP (7layer) (5.9%) Resistivity
1	1.0	1.8	1.8
2	4.0	2.5	2.5
3	4.0	270	240
4	4.0	0.0	0.0
5	8.0	9.5k	10k
6	16.0	10k	10k
7		13k	10k

Fid 1137Layer
(error)

Thick.

Davis
(7.0%)

Resistivity

ResixIP (7layer)
(7.1%)

Resistivity

1	1.5	1.4	1.4
2	3.0	0.6	0.6 - 0.7
3	4.8	10k	201 - 643k
4	6.0	10k	3.1k - 549k
5	6.9	10k	871 - 176k
6	7.8	1000	65.5 - 47k
7		1000	0.0 - 412

Table B-4: Eight inversions with ResixIP, using as starting models the final model from the inversions of Test 4b. The three-layer models for these fids are shown in Table B-1 above.

Line 10D - 10 m Dipoles

Fid 976

Layer (error)	Thick.	Davis (9.1%) Resistivity	ResixIP (7layer) (9.9%) Resistivity
1	4.2	1.4	1.4
2	2.0	0.1	0.1
3	2.0	1.1	0.4 - 5.4
4	2.0	12.0	0.9 - 121
5	4.0	31.4	1.4 - 317
6	8.0	75.4	71.4 - 760
7		156	1.6 - 491

Fid 985

Layer (error)	Thick.	Davis (5.7%) Resistivity	ResixIP (7layer) (5.0%) Resistivity
1	1.5	1.5	1.5
2	2.0	0.8	0.8 - 1.0
3	2.0	9.8	4.2 - 31.2
4	2.0	20.1	5.3 - 78.5
5	2.0	40.0	8.3 - 872
6	2.0	80.0	11.4 - 914
7		160	899 - 5.2k

Fid 1012

Layer (error)	Thick.	Davis (5.8%) Resistivity	ResixIP (7layer) (2.3%) Resistivity
1	2.2	1.4	1.4
2	4.0	4.4	2.9 - 3.9
3	4.0	2.8	4.6 - 8.4
4	4.0	3.6	2.5 - 4.0
5	4.0	11.7	5.0 - 26.4
6	4.0	30.0	6.5 - 107
7		9.8	10.4 - 57.2

Fid 1029

Layer (error)	Thick.	Davis (2.9%) Resistivity	ResixIP (7layer) (1.5%) Resistivity
1	1.0	1.4	1.4
2	2.0	3.7	2.9 - 3.5
3	2.0	11.7	9.2 - 21.2
4	2.0	21.1	24.5 - 154
5	2.0	40.6	38.7 - 721
6	2.0	80.3	50.9 - 6.0k
7		160	235 - 5.2k

Fid 1044

Layer (error)	Thick.	Davis (10.9%) Resistivity	ResixIP (7layer) (4.8%) Resistivity
1	1.0	1.5	1.5
2	4.0	4.4	1.6 - 2.7
3	4.0	0.8	2.1 - 4.6
4	4.0	2.0	0.8 - 1.8
5	4.0	5.3	1.3 - 4.6
6	4.0	32.4	4.5 - 223
7		10.7	12.4 - 1.2k

Fid 1059

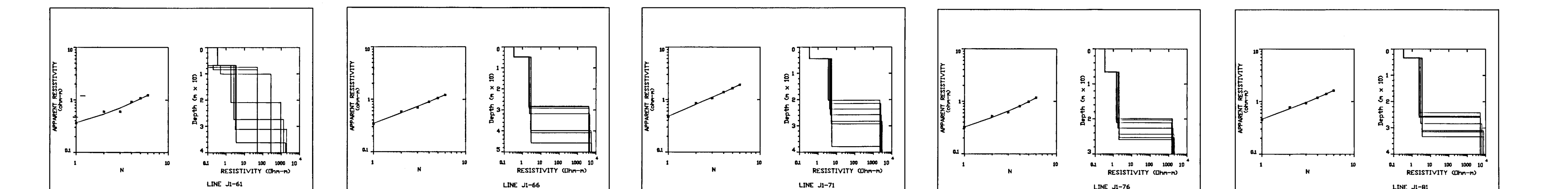
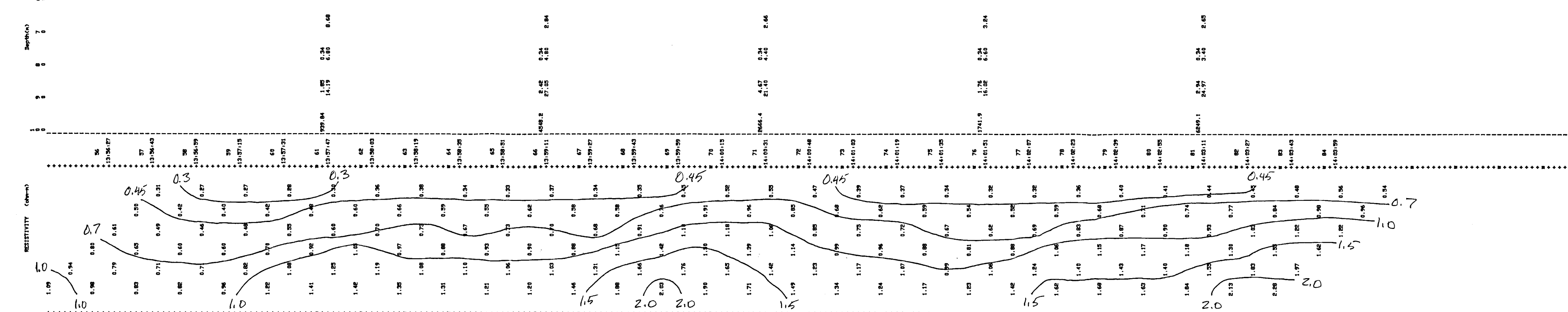
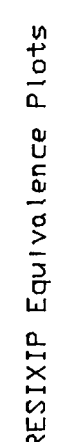
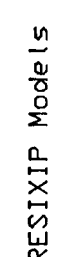
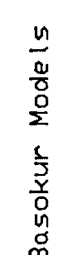
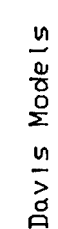
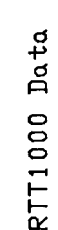
Layer (error)	Thick.	Davis (8.1%) Resistivity	ResixIP (7layer) (8.2%) Resistivity
1	1.0	1.9	1.9
2	2.0	1.6	1.5 - 1.7
3	2.0	1.9k	1.4k - 25k
4	2.0	92.2	93.1 - 934
5	2.0	0.0	0.0
6	2.0	0.0	0.0
7		3.0	0.0 - 30.1

Fid 1084

Layer (error)	Thick.	Davis (3.6%) Resistivity	ResixIP (7layer) (1.7%) Resistivity
1	1.0	1.8	1.8
2	3.0	2.5	1.9 - 2.2
3	3.0	13.9	14.0 - 73.0
4	3.0	35.0	50.9 - 197
5	5.0	41.7	44.9 - 139
6	15.0	75.0	4.4 - 30.1
7		55.1	2.8 - 65.6

Fid 1137

Layer (error)	Thick.	Davis (3.3%) Resistivity	ResixIP (7layer) (1.2%) Resistivity
1	1.5	1.4	1.4
2	3.0	0.9	1.0 - 1.2
3	3.0	3.0	2.5 - 4.3
4	3.0	13.7	6.1 - 19.3
5	5.0	19.7	5.1 - 10.4
6	15.0	13.2	25.0 - 57.5
7		11.3	4.5 - 386



LEGEND:

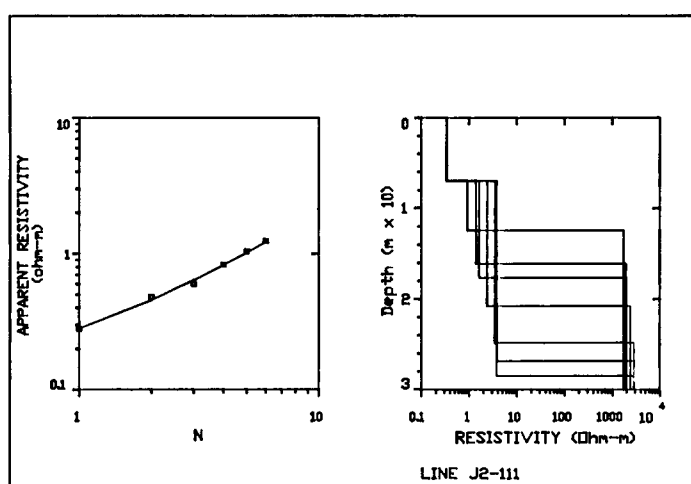
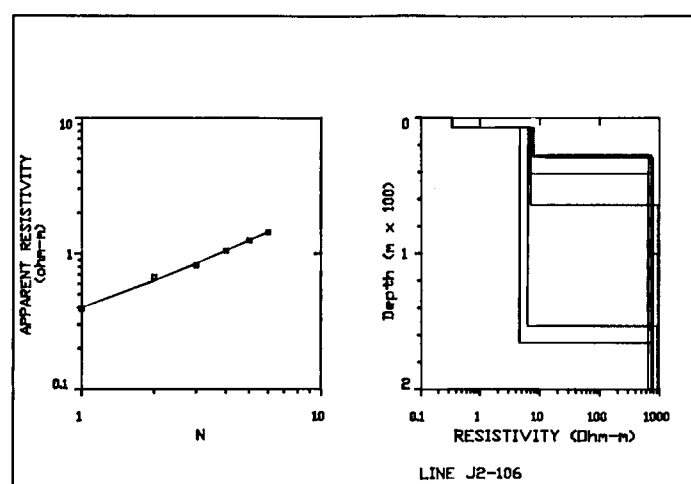
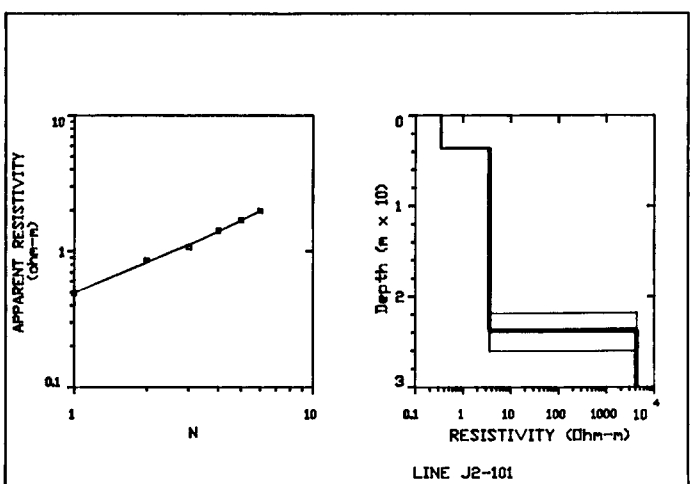
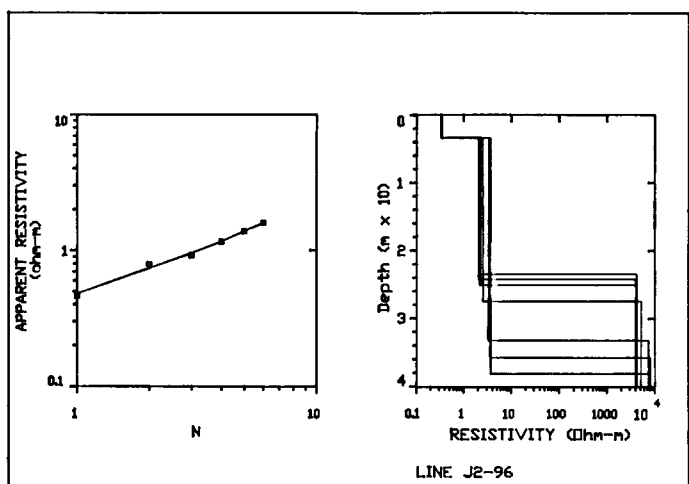
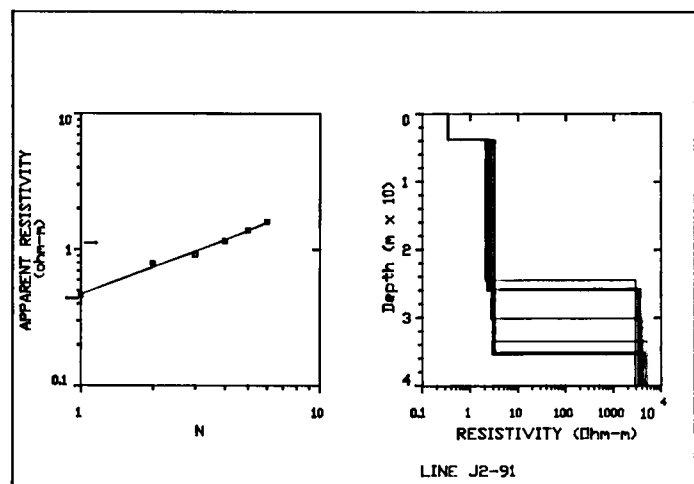
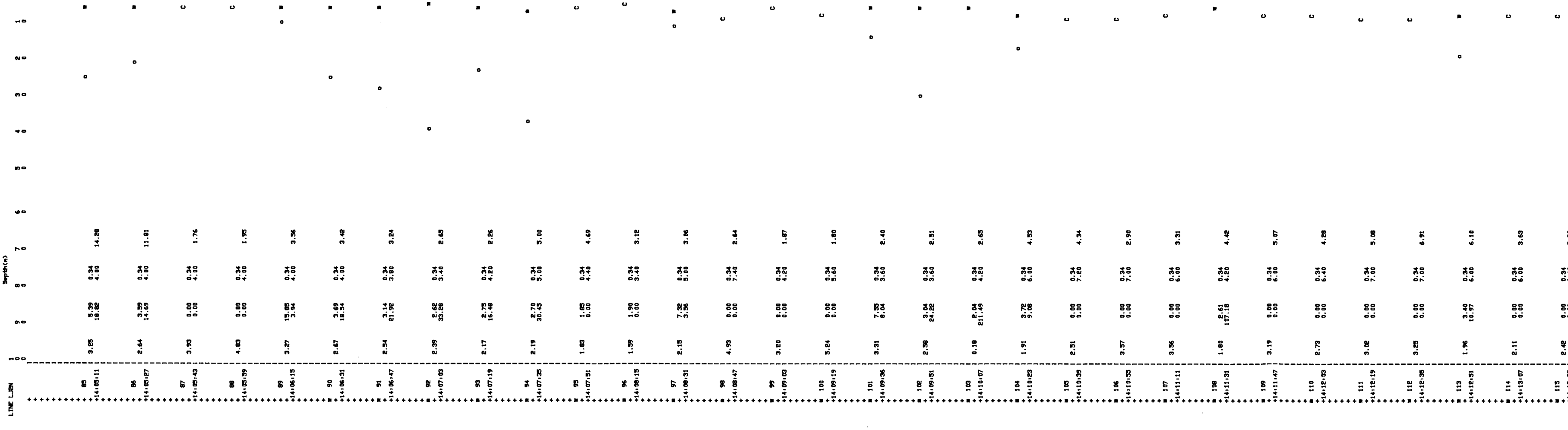
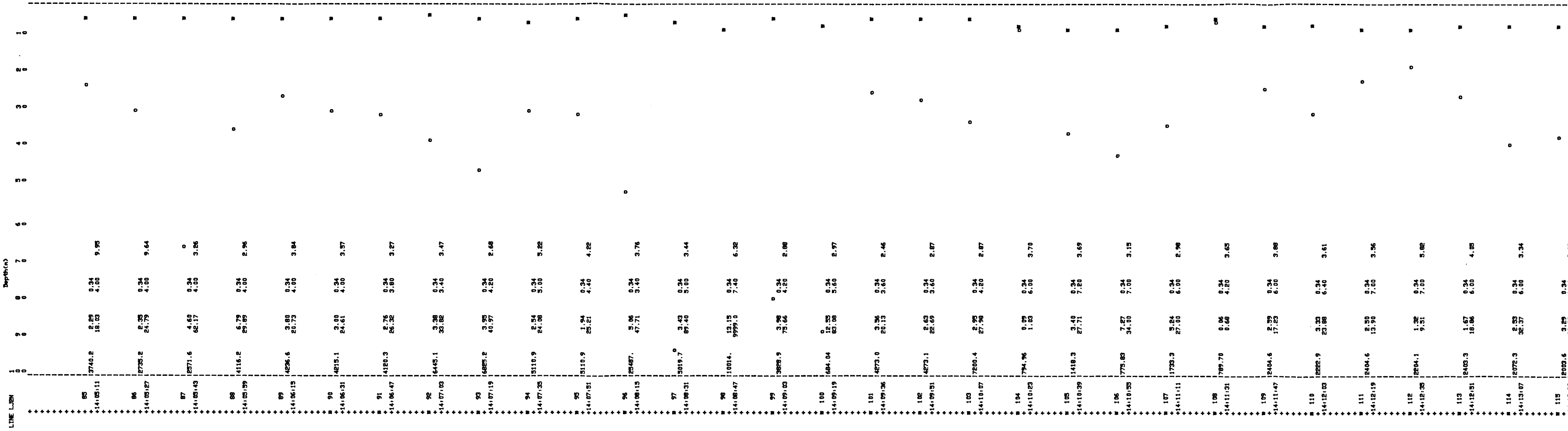
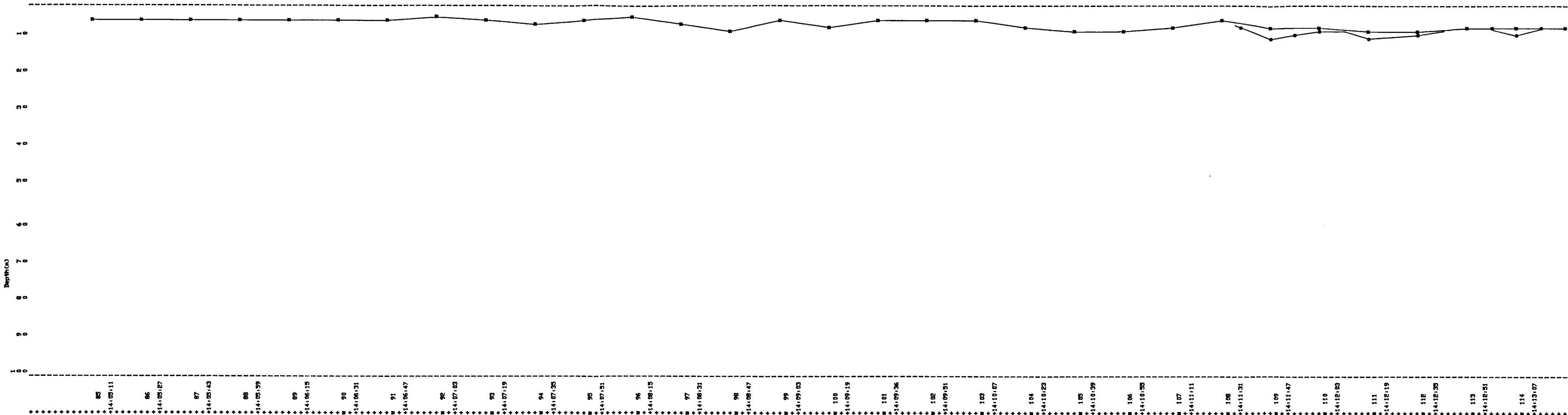
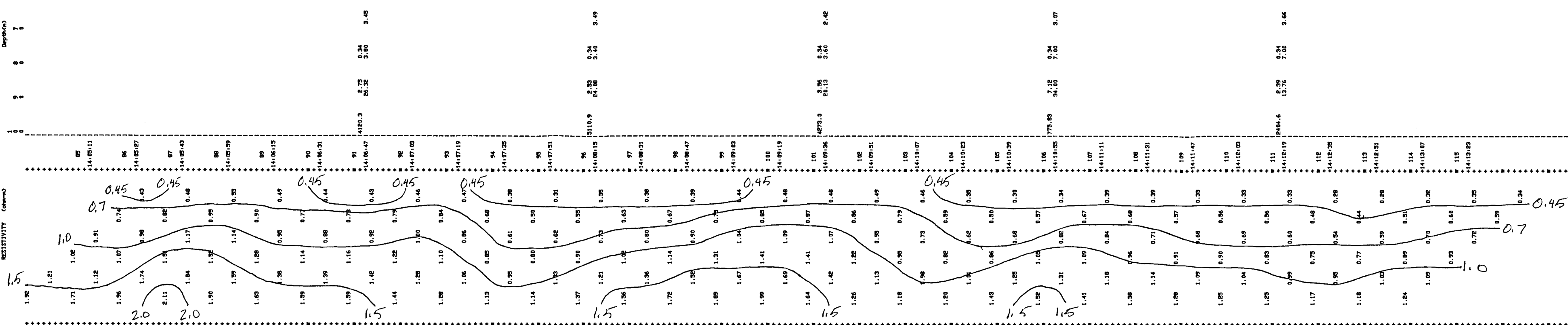
SECTION:

- seabed boundary
- base of second interpreted boundary
- △ coincident seabed and second boundaries

SOUNDING:

percent fitting error	0.00
layer 1 resistivity	0.08
	0.08
	layer 1 thickness
layer 2 resistivity	0.09
	0.09
	layer 2 thickness
half-space resistivity	09.84

FIGURE 12
CLIENT: INAC
PROJECT: Bay of Fundy
LOCATION: New Brunswick
10 m DIPOLES
LINE LJ1S



LEGEND:
SECTION:
■ sealed boundary
○ base of second interpreted boundary
u coincident sealed and second boundaries

SOUNDING:
percent fitting error
0.68

layer 1 resistivity 0.45
layer 1 thickness 10.0

layer 2 resistivity 1.5
layer 2 thickness 10.0

half-space resistivity 999.84

FIGURE 14
CLIENT: INAC
PROJECT: Bay of Fundy
LOCATION: New Brunswick
10 m DIPOLES
LINE LJ2N

RTTI000 Data

Davis Models

Basokur Models

RESIXIP Models

RESIXIP Equivalence Plots

LEGEND:

SECTION:

■ seabed boundary
○ base of second interpreted boundary
u coincident seabed and second boundaries

SOUNDING:

percent
fitting
error

layer 1
resistivity 0.24 layer 1
thickness 6.68

layer 2
resistivity 1.85 layer 2
thickness 14.19

half-space
resistivity 929.84

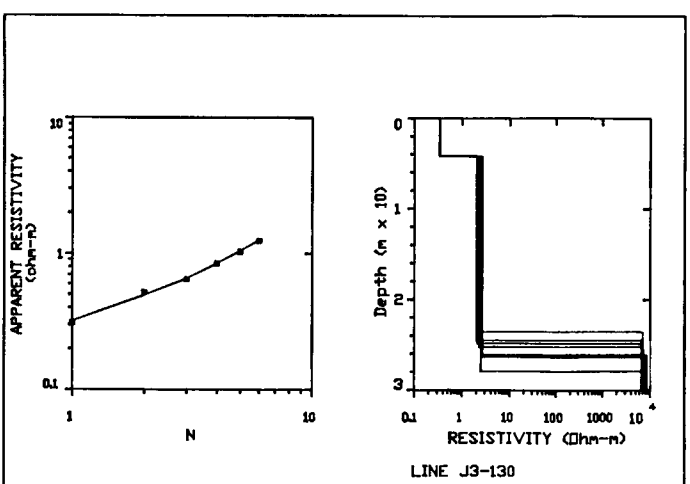
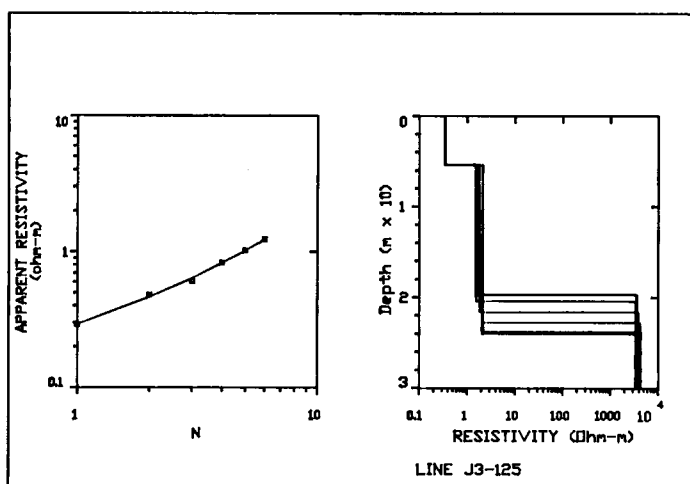
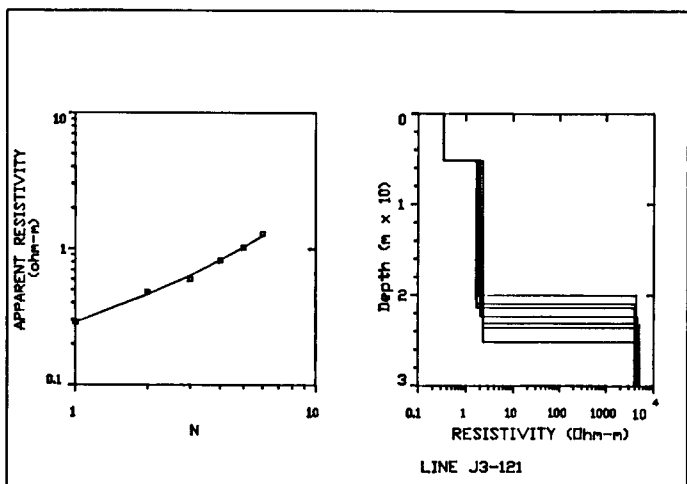
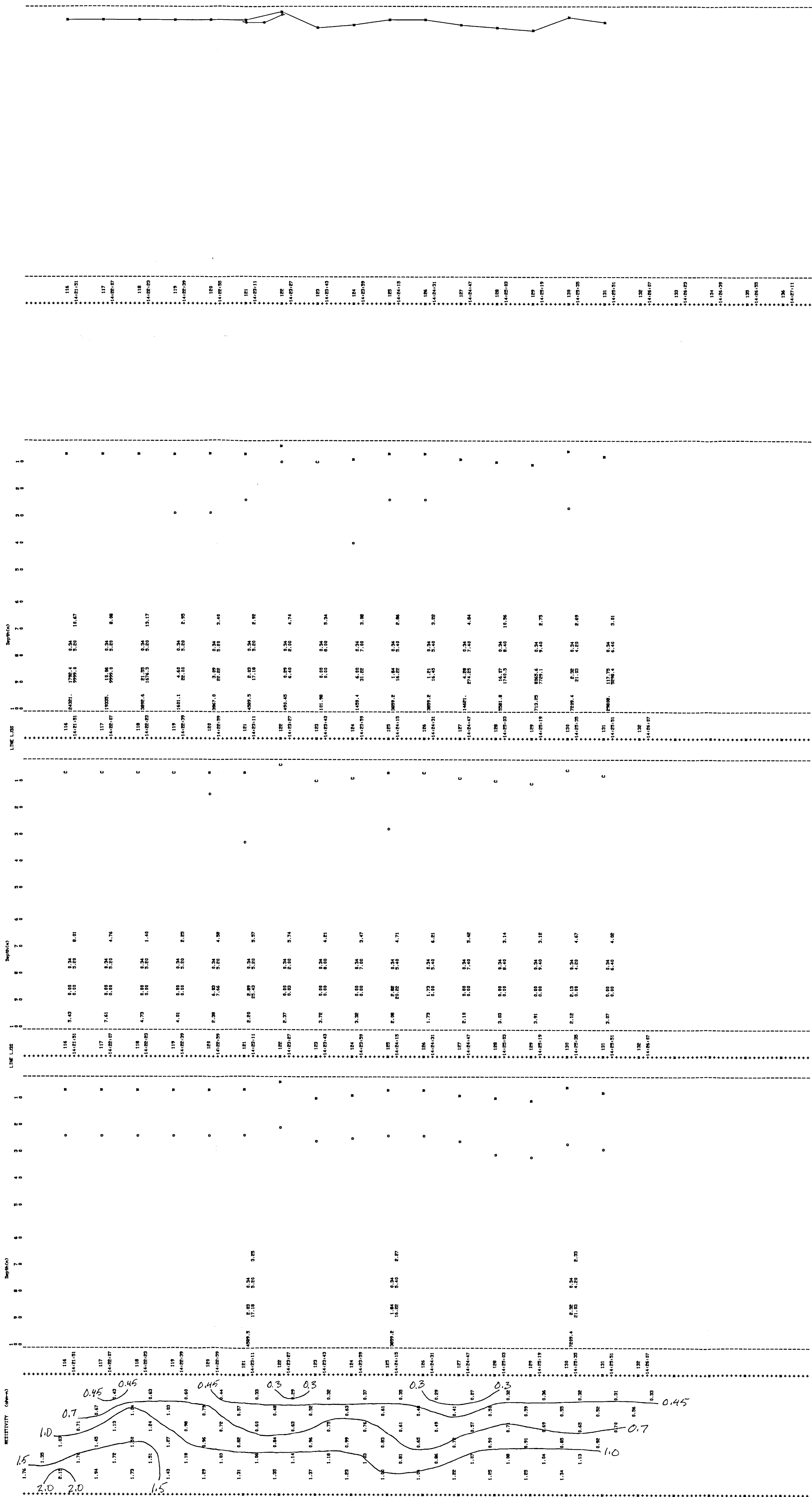
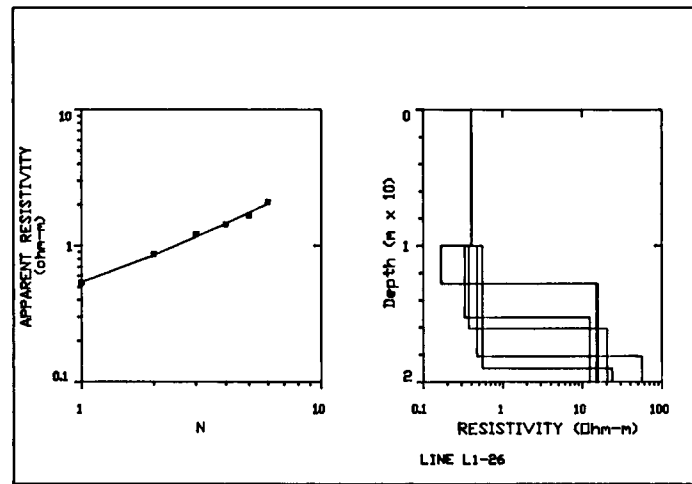
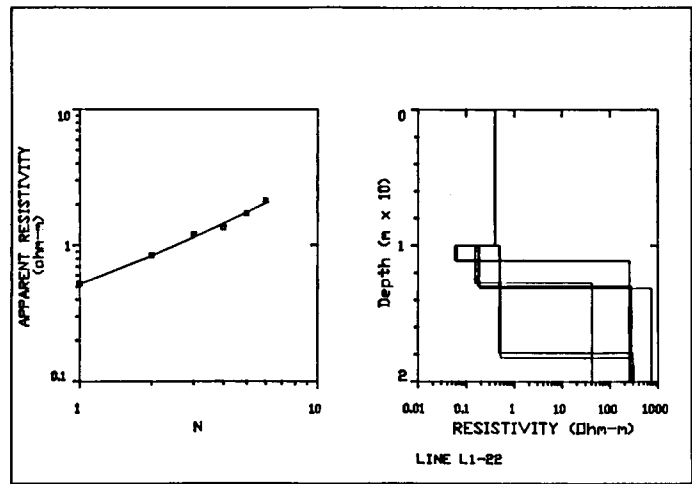
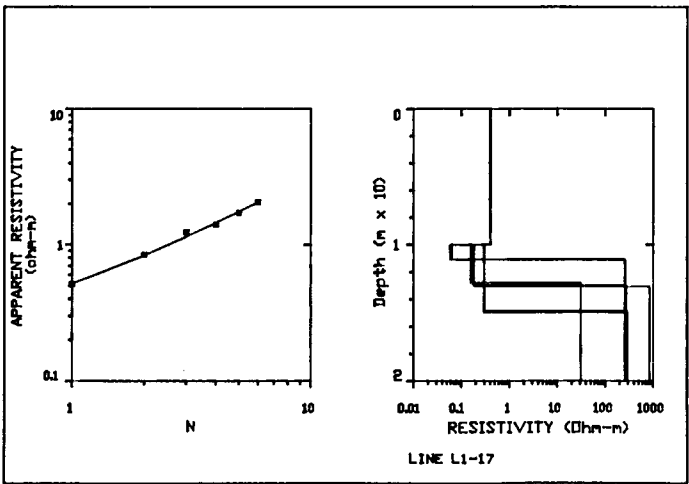
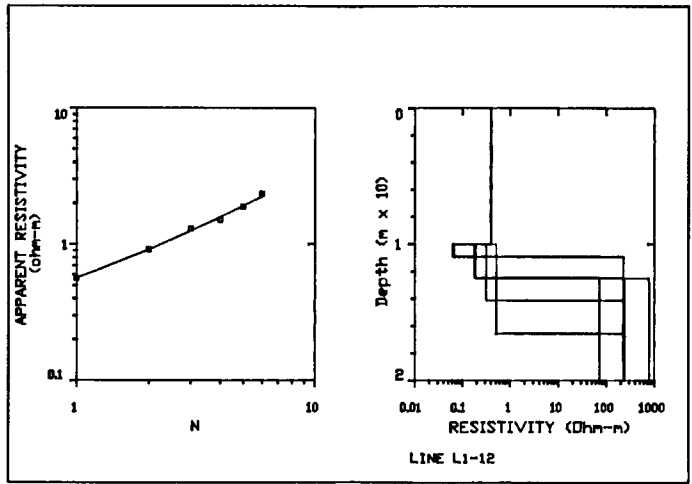
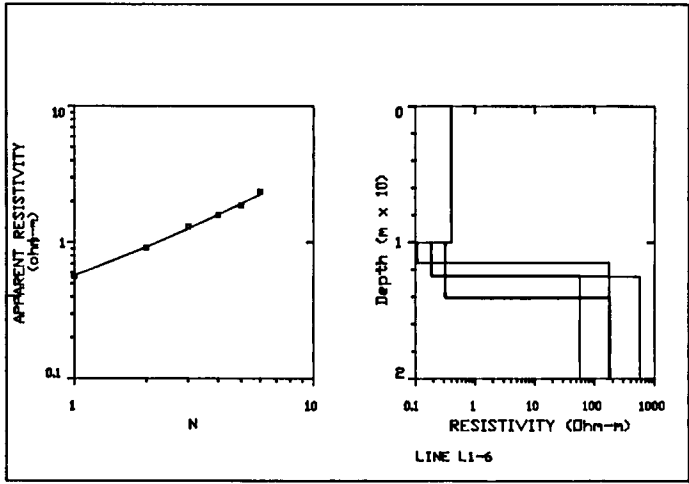


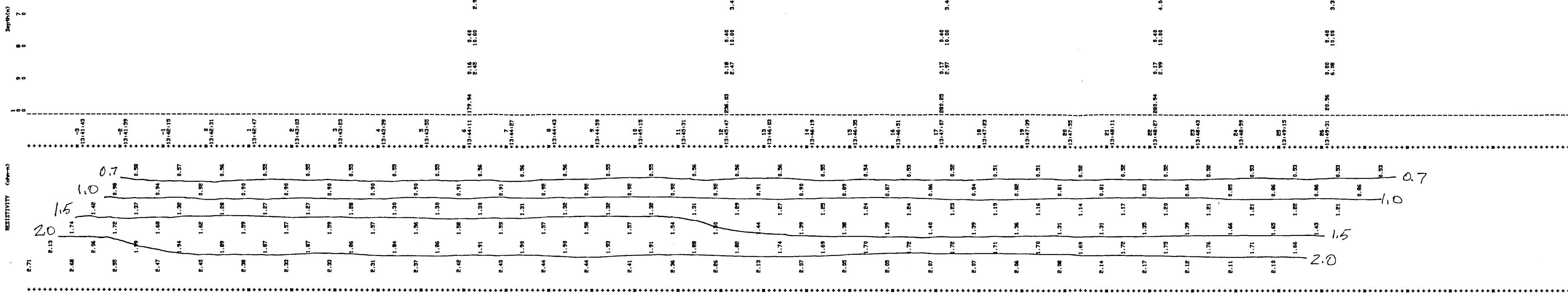
FIGURE 16
CLIENT: INAC
PROJECT: Bay of Fundy
LOCATION: New Brunswick
10 m DIPOLES
LINE LJ3S

RESISTIP Equivalence Plots

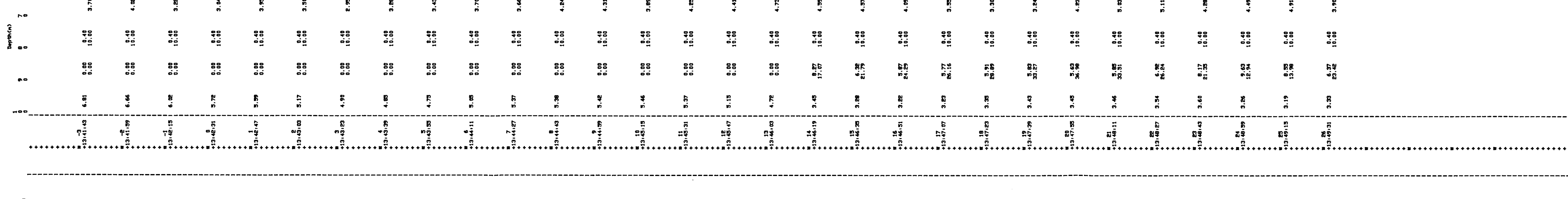
LEGEND:
SECTION:
■ Sealed boundary
○ Base of second interpreted boundary
u Coincident sealed and second boundaries
SOUNDING:
percent
Fitting
error
0.68
layer 1
resistivity
0.08
layer 1
thickness
0.08
layer 2
resistivity
1.10
layer 2
thickness
1.10
half-space
resistivity
929.84



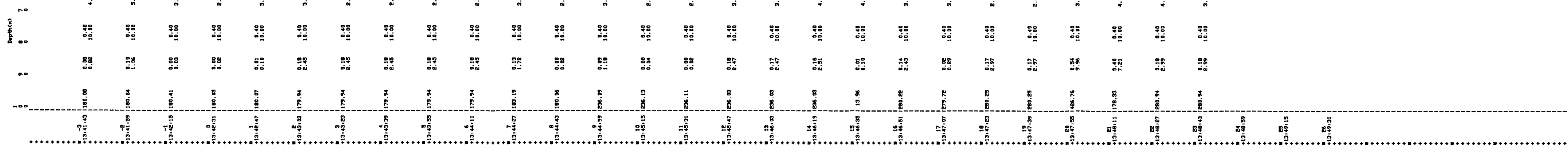
RESISTIP Models



Basokur Models



Davis Models



Hardy Log Data

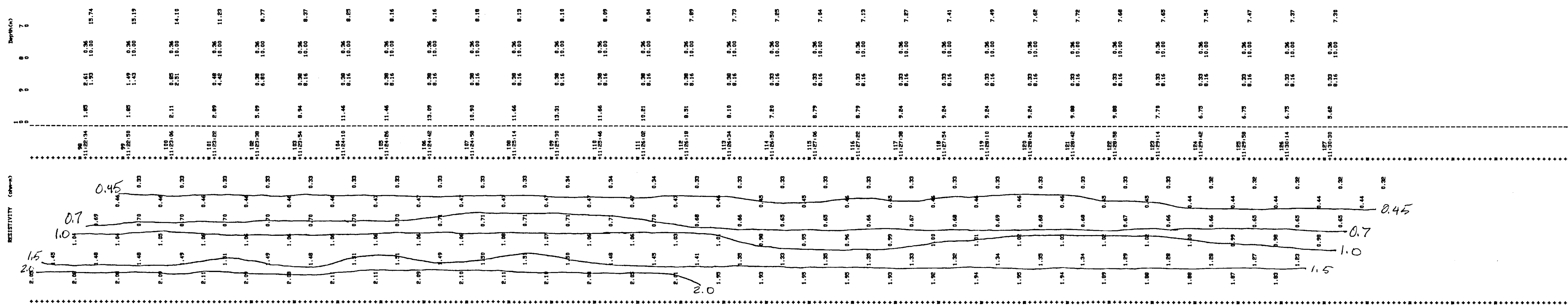


FIGURE 19
CLIENT: INAC
PROJECT: Inversion Study
LOCATION: Conception Bay
25 m DIPOLES LINE L1
Log DIPOLES LINE L5